UNIVERSITÉ DE STRASBOURG

ÉCOLE DOCTORALE DES SCIENCES DE LA VIE ET DE LA SANTE (ED414)

Laboratoire de Neurosciences Cognitives et Adaptatives - UMR7364

THÈSE présentée par :

Matthieu AGUILERA

soutenue le : 13 décembre 2024

pour obtenir le grade de : **Docteur de l'université de Strasbourg**

Discipline/ Spécialité : **Neurosciences**

La lumière au bout du tunnel : étude des altérations de la dynamique cérébrale aux stades précoces de la maladie d'Alzheimer et des effets bénéfiques d'un protocole de stimulations lumineuses dans le modèle murin App^{NL-F}/MAPT.

The Light at the End of the Tunnel: Study of Early-Stage Brain Dynamics Alterations in Alzheimer's Disease and Beneficial Effects of Light Stimulation in the App^{NL-F}/MAPT Mouse Model.

THÈSE dirigée par :

Dr. GOUTAGNY Romain — Directeur de Recherche, Université de Strasbourg

RAPPORTEURS :

Pr. BETHUS Ingrid — Professeure, Université Côte d'Azur, Nice

Pr. DECO Gustavo — Professeur, Universitat Pompeu Fabra, Barcelone

AUTRES MEMBRES DU JURY :

Dr. HARSAN Laura-Adela — Maître de Conférences, Université de Strasbourg

Acknowledgments

This thesis marks the end of a long journey that has brought me here, a journey accompanied by many wonderful people whom I will try to acknowledge here.

First of all, I want to deeply thanks my jury, Pr. **Ingrid Bethus**, Pr. **Gustavo Deco** and Dr. **Laura Adela Harsan** for accepting my invitation. Thank you for taking the times to evaluate my work and for all the insight you will give me to improve it. I'm really honored to have you in my jury and I'm really looking forward to discuss this manuscript with you.

J'aimerais aussi remercier **Aline Stephan** et **Lionel Dahan**, qui m'ont accompagné pendant ces 4 années en tant que membres de mon Comité de suivi de thèse. En plus de vos précieux conseils scientifiques, vous avez su me conseiller personnellement et me faire relativiser à des moments où j'étais un peu perdu dans mon projet ce qui m'a été d'une aide précieuse. Je ne pouvais pas avoir meilleur comité pour m'accompagner ces 4 années.

Je ne peux pas aller plus loin sans remercier mon directeur de thèse **Romain Goutagny**, sans qui je ne serais là où j'en suis aujourd'hui et sans qui le document sur lequel j'écris ces lignes n'existerait pas. Merci pour tout, depuis ma première venue au LNCA en 2019 jusqu'à maintenant. Merci de m'avoir fait confiance, surement à des moments où vous étiez le seul à avoir confiance en moi. Merci pour la science, merci de m'avoir poussé à creuser ces données pendant 4 ans. Je m'attends toujours à avoir quelqu'un s'asseoir derrière moi dès que je m'assois à un bureau désormais mais au final ça m'a permis de me poser beaucoup plus de question et de réflexions, de me développer plus que dans d'autres conditions. Merci pour tout, les conseils, les congrès, les rencontres, les bières, les bbq au jardin, les soirées de noël, les five, je n'aurais pu demander meilleur directeur de thèse.
Merci aussi à mon co-superviseur officieux **Demian Battaglia**. Merci de m'avoir amené dans ton domaine que sont les neurosciences physiques et computationnelles. Merci d'avoir pris le temps de m'expliquer les concepts, demandant parfois de grandes capacités de vulgarisation ! Merci de m'avoir guidé dans ce projet avec tes idées parfois farfelues au premier abord comme utiliser des métriques de climatologie dans le cerveau. Merci de m'avoir emmené en congrès et de m'avoir fait rencontrer plein de monde. Merci aussi pour toutes tes anecdotes et fun facts sur tout, prodigués lors des voyages en train ou en voiture pour aller en congrès, je ressors de ces 4 années de thèse avec des connaissances scientifiques certes mais avec une progression en culture générale pour sûr !
Pour poursuivre avec l'équipe FunSy, j'aimerais particulièrement remercier **Vincent Douchamps**. Merci de m'avoir aidé et accompagné à mon arrivée dans les manips et le code. Merci pour toutes les discussions qu'on a pu avoir dans la mezzanine ou au bar et surtout merci pour les bières belges !

Je ne peux pas parler de la mezzanine sans enchainer sur les personnes qui la partage avec moi, dans l'obscurité de l'hiver comme dans la fournaise de l'été, cette mezzanine qui fait que personne ne sait où on se trouve.
Merci **Coline**, je ne pouvais espérer meilleure collègue et amie pour partager le bureau pendant quasiment toute ma thèse, depuis ce jour où tu t'es pointée en gueule de bois de l'espace un deuxième jour de stage. Merci d'avoir toujours été là pour m'aider, de m'avoir appris à faire des électrodes et des fibres optiques ^^ Nous avons su monter au cours de ces années un duo aussi terrible qu'efficace, les tapeurs de nachos, les dégommeurs de buffets, 3 années de pratique qui font de nous des pros quand il s'agit de manger, bien meilleur à ça qu'à voyager en passant par Montréal. Merci pour tous ces moments passés, merci d'avoir été la bunnysitter de Titou et Pamou. Allez, c'est toi la doyenne de la mezzanine maintenant ! (Plus pour très longtemps :P).
Merci **Flora** pour ta joie de vivre et ton insouciance qui font de toi une source inépuisable de bonne humeur. S'il te plait ne change pas. Merci également de ramener de l'ordre dans la mézzanine qui en avait grandement besoin !
Je tiens aussi à vous remercier collectivement toutes les deux pour l'inventivité dont vous faites preuve lorsqu'il s'agit d'emballer tout mon bureau et mes affaires dans du papier bulle.
Après le coté expérimental de l'équipe je peux remercier le côté computationnel.
Samy I want to deeply thank you for all the moments spent together, from this first beer on a bench during Covid curfew to moving you with your new family to Austria through our congress adventures and all the after work beers which ended up discussing sciences until dawn. I'm glad to have won a great friend who is brilliant and dance like no one (even when the music is from "dj stop").
Jyotika thanks you for being always happy and ready to help for everything. I deeply thank you for feeding the students in the mezzanine with chocolate!
Anagh and **Sima** thanks for all the discussions and advice you gave me while I was annoying you in your office going to seek my 5th coffee of the day.
I also want to thank **Vinicius**, **Laura**, and **Jungyoung** for all the moments spent together either in Strasbourg when you came visiting or in congress. Special mention to Vinicius incredible impression talents.
I also want to thank our Canadians collaborators, thank you **Jesse Jackson** for all the good advices and the interesting discussion we had the different times we met. Thank you for welcoming me in your house to make a bbq by -10 degrees outside which is by far the most Canadian experience I hever had. **Alisson** merci pour tes super reco resto à Edmonton et pour être montée avec moi sur la scène du DJ à la soirée de la SFN !

J'aimerais maintenant remercier 3 personnes que j'ai quotidiennement embêté pendant ces 4 années et sans qui le labo ne fonctionnerait pas.
Karin, merci pour tout, merci malgré tout, d'être toujours de bonne humeur, d'être toujours prête à aider, tu es une personne incroyable et sans toi on serait tous perdu.
Catherine, j'ai dû être un enfer pour toi entre les papiers au dernier moment et les problèmes d'ordre de mission (et le fait que je claquais la porte d'entrée aussi).

Néanmoins, tu as toujours réglé tous les problèmes super rapidement avec sourire, merci pour tout le travail que tu fais pour rendre nos vies plus faciles.
Aminé, merci de gérer toutes les souris comme tu fais, merci d'avoir toujours été dispo pour mes questions mais aussi lors des urgences que j'ai eu le weekend à l'animalerie.

Au sein du LNCA j'aimerais également remercier **Jean Christophe** qui était directeur du laboratoire au moment où je suis arrivé, merci de m'avoir accueilli au labo. Également, **Chantal**, qui a pris le relais mais surtout qui a suivi mon projet au long de ces 4 années, merci pour ces longues discussions intéressantes et les conseils sur les expériences de comportement. Merci également d'avoir lu mon mail de demande de stage il y a 5 ans et de l'avoir transféré à Romain.
J'aimerais également remercier tous les étudiants qui ont partagés le LNCA avec moi pendant ces années.
Florian merci d'avoir été mon compagnon de galère quand on venait tous les weekends au labo notre première année de thèse, mais également le partenaire d'humour « spécial », notamment pendant nos super cours d'allemand (mes connaissances d'allemands restent limitées à « Mitte karte bitte »).
Laurine merci pour ta bonne humeur, les soirées étoiles au Champs du feu, et de tous nous faire peur quand tu joues à Mario Kart. Tu aurais adoré écrire ta thèse en même temps que moi car pour le coup tu ne te serais pas sentie en retard.
Anne Sophie merci pour la quantité infinie de cannelés que tu as ramené de Bordeaux au labo, as-tu préféré faire du sucrose binging sur tes souris ou sur nous tous ?
Baptiste merci de m'avoir embrigadé dans Doctoneuro dont tu as été le super président, je veux continuer de te voir avec différentes perruques ou chapeau pendant encore plein d'années.
Iris thank you for all the discussion we had when we were both pissed about everything. And to be THE one with who I was able to make some of the office jokes. I will always regret to not have put some of your stuff in jello. I'm really glad we met and I'm really glad you didn't slap that bouncer in front of "the living".
Elodie merci d'être notre maman à tous les doctorants. **Noémie** merci de nous avoir fait découvrir que les M&Ms carrefour ne valent pas les vrais. **Cécile** merci pour tes imitations incroyables.
Ainsi que tous les autres étudiants de labo **Jil, Anaelle, Vincent, Adrien, Henry, Johanne, Lisa, Coline M** (tu n'es plus étudiante je sais). Et tous les anciens doctorants du labo qui nous ont accueillis au début de nos thèse **Chris, Laura T, Caroline, Laura D, Gaelle**.

J'aimerai finalement remercier toutes les autres personnes du LNCA qui m'ont accompagné pendant ces 4 années et toutes les souris sans qui les projets comme le mien ne pourraient pas se faire.

Je remercie aussi **Elise** et **Emeline** du Jardin des Sciences, qui m'ont accompagné dans mon aventure MT180 avec **Noëmi**. Je tiens aussi à remercier toutes les super personnes que j'ai pu rencontrer pendant cette aventure.

Je remercie également Dr. **Sakina Torch**, Dr. **Chantal Thibert** et Dr. **Fabien Lanté**, qui m'ont permis de faire mes premiers stages en laboratoire de recherche à Grenoble

I want now to thank the "Arriba Abajo" group. Thanks **Wilf**, **Ari**, **Marine** (and Lunita) and **Jad** for all the moments spent together in Strasbourg, Rome, Freiburg, Innsbruck and surely more places to come. I'm really glad to count you among my closest friends.

J'aimerais également remercier toute l'équipe de Doctoneuro dont j'ai pu faire partie et avec qui j'ai pu passer de super moments, **Karim, Valentin, Valod, Sarah, Etienne, Robin, Marion, Henrico, Enora, Pierre, Jeanne, Charlotte** et tous ceux que j'oublie.

Merci aussi à ma bande d'amis depuis des années, **IMODOS**, avec qui on arrive toujours à se retrouver et reprendre toute nos discussions là où on les avait laissés. Merci pour tous les Among Us et les apéros zoom pendant les confinements.

Merci à mes compagnons de fac à Grenoble **Naël, Pierre Vincent**, **Sarah, Mélodie, Agathe, Léa, Anthony** pour tous les moments passés ensemble.

Merci à la bande de Grenoble **Emeline, Robin, Stef, Juliette, Vaida.**

Merci aussi aux nouveaux amis que j'ai pu me faire pendant ces années de thèse lors de mes multiples allers-retours au Quebec, **Philippe, Laura, Mikael** et **Thomas.**

Merci à ma belle-famille, **Valérie**, **Michel**, **Madeline** et **Rémi** pour votre accueil et d'avoir toujours été là pendant ces années.

Merci à ma famille, et notamment à **Ma mère**, **Seb** et **Cannelle** pour m'avoir supporté pendant tant d'années, de m'avoir soutenue pendant toutes ces années d'études et m'avoir permis d'arriver où j'en suis aujourd'hui.

Enfin, last but not least, merci **Ophélie**, merci d'être dans ma vie depuis 13 ans, de me soutenir, de me supporter, de me faire rire, de m'encourager, de me faire vivre des moments incroyables, et de me pousser pour que je sois une meilleure version de moi-même, sans toi je ne serais pas là où j'en suis aujourd'hui.

À mon père…

Table of content

List of figures

List of abbreviations

Aβ: Amyloid-beta

ACh: Acetylcholine

AD: Alzheimer's Disease

AICD: APP Intracellular Domain

aMCI: amnestic Mild Cognitive Impairment

APP: Amyloid Precursor Protein

ARs: Adrenergic Receptors

BACE1: Beta-site APP Cleaving Enzyme 1

CLA: Claustrum

CSF: Cerebrospinal Fluid

CTF: C-Terminal Fragment

dFC: dynamic Functional Connectivity

dKI: double Knock-In

DMN: Default Mode Network

EC: Entorhinal Cortex

EEG: Electroencephalography

fMRI: functional Magnetic Resonance Imaging

GENUS: Gamma ENtrainment Using Sensory stimuli

GPD: Generalized Pareto Distribution

hdEEG: high-density EEG

HPC: Hippocampus

ICA: Independent Component Analysis

ITI: Inter-Trial Interval

KI: Knock-In

LC: Locus Coeruleus

LEC: Lateral Entorhinal Cortex

LFP: Local Field Potential

LTP: Long-Term Potentiation

MA: Maladie d'Alzheimer

mAChRs: muscarinic Acetylcholine Receptors

MCI: Mild Cognitive Impairment

MEG: Magnetoencephalography

MI: Memory Index

MI: Mutual information (in Results Part1 Complementary Results)

MOC: Motor Cortex

ModInd: Modulation Index

MS-DBB: Medial Septum-Diagonal Band of Broca

MTL: Medial Temporal Lobe

NA: Noradrenaline

nAChRs: nicotinic Acetylcholine Receptors

NFTs: Neurofibrillary Tangles

NOR: Novel Object Recognition

OiP: Object in Place

PAC: Phase-Amplitude Coupling

PAR: Parietal Cortex

PET: Positron Emission Tomography

PFC: Prefrontal Cortex

PPN: Pedunculopontine Nucleus

PRC: Perirhinal Cortex

PSEN: Presenilin

PV: Parvalbumin

REM: Rapid Eye Movement

RSC: Retrosplenial Cortex

SCD: Subjective Cognitive Decline / Deficit Cognitif Subjectif

SSC: Somatosensory Cortex

SWS: Slow-Wave Sleep

TBI: Traumatic Brain Injury

Tg: Transgenic

VIS: Visual Cortex

vGENUS: visual GENUS

WT: Wild-Type

Introduction

1. Alzheimer's disease

In 1906, Dr. Alois Alzheimer, a German physician, described for the first time a case of a patient, Mrs. Auguste Deter, a 51-year-old woman, who exhibited cognitive impairments, hallucinations, delusions, focal symptoms and psychosocial incompetence, symptoms collectively recognized as senile dementia. Dr Alzheimer described after postmortem histological analysis of Auguste Deter brain extracellular plaques accumulation and neurofibrillary tangles (Maurer et al., 1997). In 1910, E. Kraepelin officially named this condition "Alzheimer's disease". Over a century later, Alzheimer's disease has grown into one of the most significant medical challenges facing our society. It is now recognized as a neurodegenerative disorder marked by the accumulation of amyloid plaques, resulting from β-amyloid (Aβ) peptide aggregation, and neurofibrillary tangles, which are caused by the aggregation of hyperphosphorylated Tau. These pathological changes would ultimately lead to neuronal death and dementia.

1.1. Alzheimer's disease in numbers

Alzheimer's disease (AD) is the leading cause of dementia worldwide, accounting for over 60-70% of the 55 million people with dementia worldwide (Alzheimer's disease international, 2023), and this number is set to almost double every 20 years with estimates of 139 million by 2050, with the increase mainly affecting low- and middle-income countries (Alzheimer's disease international, 2015). In France, 3 million people are directly (patients) or indirectly (caregivers, family) concerned by AD (France Alzheimer, FRM). Based on a French epidemiologic study on people older than 65 years old (*PAQUID* cohort, Ramaroson et al. 2003) and data form French healthcare, the number of people over 65 years old with AD has been evaluated to 1 million in 2018 and estimated to reach 1,8 million in 2050 (Vaincre Alzheimer). The incidence (e.g. the number of new cases of the disease over a given period) is estimated to 225 000 persons per year. This latter depends on age, evolving from 2‰ for individuals between 65 and 69 years old to 70‰ for those over 90, consistent with age being the principal risk factor for the disease. However, these numbers mostly account for the final stages of the disease, while Alzheimer's pathology begins years before symptoms appear. As a result, the number of affected individuals is likely underestimated. Indeed,

a recent study estimated that considering all the different stage of the disease, from asymptomatic prodromal to dementia, 416 million persons would be in the AD continuum worldwide, representing 22% of the people aged 50 and above (Gustavsson et al., 2023), emphasizing the importance of the research on the pathology.

1.2. Risk Factors of the disease

The major risk factor for AD remains ageing. This could be explained first by influence of unspecific ageing factors as increase of oxygen free radicals (M. A. Smith et al., 1995), or hormone dysregulation notably through menopause (Mosconi et al., 2021). In addition, common proteinopathies associated with AD—such as amyloid plaques formed by the accumulation of Aβ peptides or neurofibrillary tangles resulting from the aggregation of hyper-phosphorylated Tau proteins—have been linked to aging (Arriagada et al., 1992) and are even found in non-pathologic or asymptomatic elderly individuals (Iacono et al., 2014; Monsell et al., 2013; Rowe et al., 2010). Besides aging, other risk factors were identified notably depending on the type of AD pathology. The familial form, representing less than 2% of AD cases (Bekris et al., 2010), is related to hereditary genetic mutations. In contrast, sporadic AD, representing 98% of AD cases, may be linked to environmental risk factors.

1.2.1. Genetic factors

1.2.1.1. Autosomal Dominant mutation

Familial forms of AD, which account for the vast majority of early-onset cases, result from autosomal dominant mutations in three genes: amyloid precursor protein (APP), presenilin 1 (PSEN1), and presenilin 2 (PSEN2). These genes are all involved in the production of Aβ peptides. Mutations in APP account for 10% to 15% of familial AD, with 32 different missense mutations identified across 85 families (Bekris et al., 2010). Most of these mutations are located at the secretase cleavage site. PSEN1 missense mutations represent 18% to 50% of early-onset familial AD, with 176 mutations identified in 390 families, making it the most common genetic cause of familial early-onset AD (Bekris et al., 2010). PSEN2 missense mutations, on the other hand, are rare causes of early-onset familial AD. Both PSEN1 and PSEN2 encode proteins that form part of the γ-secretase complex. Mutations in these genes affect the γ-secretase cleavage of APP, resulting in increased production of pathological $A\beta_{42}$ peptides.

Familial AD caused by these autosomal dominant mutations usually develops early, and is therefore referred to as early-onset AD. Individuals with APP mutations typically develop symptoms in their mid-40s to 50s, while those with PSEN1 mutations may experience onset as early as their 30s, making these the most severe forms of AD. APP and PSEN1 mutations are associated with complete penetrance, meaning that every carrier of one of these mutations will develop AD during their lifetime, whereas PSEN2 mutations show a 95% penetrance (J. S. Goldman et al., 2011). Despite accounting for only 2% of all AD cases, these known genetic mutations have been used to design the vast majority of animal models of AD. The use of familial AD animal models to study AD assumes a pathological similarity between different forms of the disease, based on the amyloid hypothesis. These assumptions may partly explain the failures encountered when treatments effective in animal models do not translate to Human patients. However, new genetic polymorphisms, such as those in the APOE gene, have been identified in sporadic forms of AD, offering a basis for the development of new animal models.

1.2.1.2. APOE polymorphism

The APOE gene encodes apolipoprotein E (ApoE), a protein involved in the transport and metabolism of cholesterol and triglycerides in both the bloodstream and the brain. While this protein is primarily synthesized in the liver, astroglia and microglia are the main producers of apolipoprotein E in the brain. Cholesterol plays a crucial role in maintaining cell membrane plasticity, cellular homeostasis, synaptogenesis, and neuronal function (J.-P. Liu et al., 2010). The APOE gene exists in three different alleles: e2, e3, and e4, with each individual inheriting one allele from each parent, resulting in six possible APOE genotypes. The presence of a single APOE e4 allele increases the risk of AD by 2 to 3 times, while having two copies of the e4 allele increases the risk by 5 (Reitz et al., 2011). Despite the strong association between APOE e4 and AD, particularly in relation to memory impairment, mild cognitive impairment (MCI), and the progression from MCI to dementia, the presence of the e4 allele is neither sufficient nor necessary for the development of the disease.

1.2.1.3. Down's Syndrome

People with Down's syndrome have an extra copy of the 21st chromosome, the one including the gene responsible to produce the APP protein. Thus, this extra copy of the

chromosome 21 can increase the production of pathologic Aβ fragments, which then aggregates into amyloid plaques. People with Down's syndrome thus develop earlier AD and by the age of 40, almost all individuals with Down's syndrome have characteristics of AD like plaques and tangles. However, despite presence of AD characteristics, not all adults with Down's syndrome display clinical signs of dementia. Nevertheless, the prevalence of dementia significantly increases with age in this population, reaching up to 75% in those over 45 years old (Lott & Dierssen, 2010).

1.2.1.4. Genetic protective factors

While genetic mutations can increase the risk of developing AD, some mutations serve as protective factors. In the APP gene, the A673T mutation, also known as the Icelandic mutation, reduces Aβ peptide formation and protects elderly individuals without AD from cognitive decline (Jonsson et al., 2012). Beyond APP mutations, the effect of APOE alleles can vary greatly. As discussed earlier, while APOE e4 is a significant risk factor for AD, the expression of APOE e2, conversely, acts as a protective factor against AD (Corder et al., 1994) and against dementia in individuals with Down's syndrome (Royston et al., 1994).

1.2.2. Non genetic risk factors

Besides genetic alterations involved in familiar and sporadic forms of the disease, the apparition of late onset sporadic AD, usually manifesting around ages 60 to 70, can be influenced by several environmental factors.

1.2.2.1. Traumatic Brain Injury (TBI)

TBI are defined as a disruption of normal brain function caused by a bump, a blow, or a jolt to the head, or an object entering the head (NIH). Depending on their severity, TBI can be classified in different category as mild, moderate or severe. Moderate and severe TBI has been associated to increase risks of AD and other dementia in late life (Barnes et al., 2018; Plassman et al., 2000). Several factors following TBI seem to contribute to this elevated risk, including axonal damage, dysregulation of key proteins such as APP, beta-site APP cleaving enzyme 1 (BACE1), α-synuclein, tau, and ApoE (for which the secretion is increased after TBI which could be deleterious in the case of an ApoE e4 expression), as well as the activation of Caspase-3, a key mediator of apoptosis (for review see Sivanandam and Thakur 2012). In addition to the severity of

the injury, the frequency of TBIs also appears to be a significant risk factor. Repeated head trauma can lead to chronic traumatic encephalopathy (CTE), a neurodegenerative condition commonly observed in contact sports (Zuckerman et al., 2018). CTE is characterized by the accumulation of abnormal tau protein tangles around small blood vessels in the brain. While CTE and AD are distinct pathologies, repetitive head trauma increase the risk of developing AD later in life (Batty et al., 2022).

1.2.2.2. Cardiovascular diseases

Despite its relatively small size, the brain is one of the body's largest consumers of oxygen and energy. Since oxygen is delivered to the brain via the cardiovascular system, it is logical that cardiovascular conditions can impact brain function. Common cardiovascular disease risk factors such as smoking, diabetes, hypertension, obesity, and high cholesterol levels have been linked to an increased risk of developing AD (Rusanen et al., 2011; Saeed et al., 2023). Beyond affecting blood vessels, disruptions in cholesterol metabolism can influence proteins involved in cholesterol processing, such as ApoE, which is directly implicated in AD. As cholesterol is essential for maintaining the structural integrity of cell membranes, a disruption in its trafficking can compromise membrane stability and, consequently, cell viability. The relationship between cardiovascular disease and AD is further supported by evidence that early treatment for hypertension reduces the incidence of MCI (Williamson, 2023; L. Wu et al., 2016). Strokes are also associated with an increased risk of dementia, as stroke-induced lesions can trigger neuronal death and neuroinflammation, creating conditions conducive to the development of dementia (Zhou et al., 2015). Given the established link between cardiovascular disease and AD, protective factors like regular physical exercise have also been shown to reduce AD risk (De la Rosa et al., 2020).

1.2.2.3. Education, socialisation and Cognitive reserve

More of a protective factor than a risk factor, education has been shown to be positively correlated with intracranial volume, meaning that people with longer education tend to have larger brains with more connections, which may allow them to endure greater degeneration before exhibiting symptoms. Additionally, it has been demonstrated that, with the same levels of Aβ and neurodegeneration, individuals with higher education show better resilience and fewer cognitive symptoms of dementia (Negash et al.,

2013). Other factors, such as social interactions in later life, may also help maintain cognitive function (Evans et al., 2018). Conversely, loneliness is associated with an increased risk of dementia (R. S. Wilson et al., 2007) and increased amyloid burden (Donovan et al., 2016). This introduces the concept of cognitive reserve, which refers to the brain's ability to adapt or compensate for neurological damage through a lifetime of intellectual and social activities. This reserve helps explain why some individuals are more resilient to functional impairment despite the presence of neurological pathology or other disorders (Figure 1; Barulli and Stern 2013).

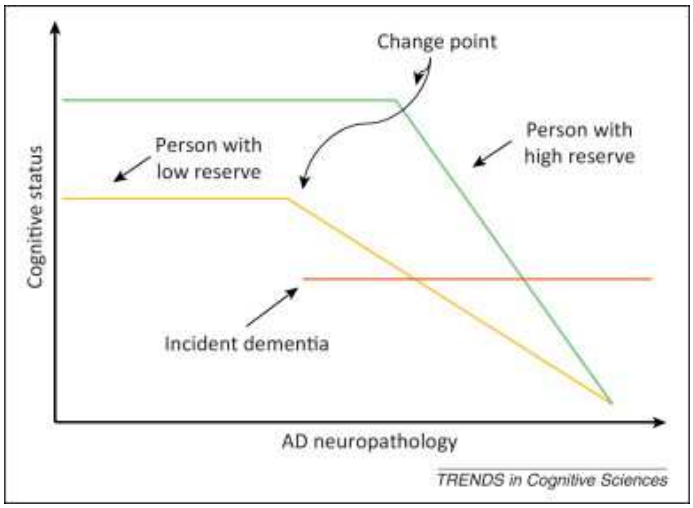

Figure 1. Impact of cognitive reserve on AD pathology.

From Barulli & Stern, 2013

1.2.2.4. Covid 19 and viral infections

In the last five years, COVID-19, caused by the SARS-CoV-2 virus has emerged as a new risk factor (Furman et al., 2024; Nawaz et al., 2024). During the outbreak, the isolation of elderly individuals, intended to protect them from infection, led to an increased risk of developing dementia within this population (Lazzari & Rabottini, 2022). Prolonged social isolation resulted in reduced cognitive stimulation and physical activity, exacerbating cognitive decline. While these effects are not directly caused by the virus itself, COVID-19 infection has also demonstrated significant long-term effects on the brain. One of the hallmark symptoms of SARS-CoV-2 infection was the loss of taste and smell, likely caused by tissue damage in the olfactory regions of the brain (Douaud et al., 2022). However, these damages were not restricted to these areas as

reductions in gray matter thickness were shown not only in the olfactory regions but also in areas critical for cognition, such as the parahippocampal gyrus and orbitofrontal cortex. This widespread tissue damage has been associated with increased cognitive decline following infection (Douaud et al., 2022). Beyond structural brain damage, the virus may also contribute directly to AD-related molecular mechanisms. SARS-CoV-2 viral proteins have been shown to form amyloid aggregates (Bhardwaj et al., 2023) and infection has been linked to the hyperphosphorylation of tau proteins (Ramani et al., 2020), increased Aβ neurotoxicity (Chiricosta et al., 2021) and amyloid aggregation in cerebrospinal fluid (Christ et al., 2024). Furthermore, research has reported neuronal degeneration, reduced neurogenesis, and changes in glial cells within the hippocampus (HPC) of infected individuals (Bayat et al., 2022). These AD-related pathological changes following COVID-19 infection may explain why infection significantly increases the risk of developing AD within a year post-infection (L. Wang et al., 2022), positioning COVID-19 as a newly recognized risk factor for AD.

COVID-19 is not the only viral infection linked to AD; other viral or bacterial agents, such as herpes simplex virus type 1, picornavirus, Borna disease virus, *Chlamydia pneumoniae*, and *Helicobacter pylori*, have also been shown to be associated with AD pathology (Honjo et al., 2009).

1.3. Evolution of the disease

1.3.1. Clinical evolution of the disease

Even if impaired sense of smell or hyposmia is one of the earliest clinical features in AD (J. M. Peters et al., 2003), consensus exists that the disease starts clinically with memory complaints. Neuropsychological test batteries, such as the CERAD (Consortium to Establish a Registry for Alzheimer's Disease) examination, the Mini-Mental State Examination, and the Clinical Dementia Rating scale, are commonly used to assess various cognitive domains (Folstein et al., 1975; J. C. Morris, 1993). AD patients present a cognitive profile marked by deficits across multiple domains, which progressively worsen over time (for review, see Peña-Casanova et al. 2012; Tromp et al. 2015). Early on, working memory shows a gradual decline, with patients becoming increasingly sensitive to distraction during memory tasks. Alterations in spatial memory and wayfinding are also often observed as early cognitive deficits. Patients may

experience significant challenges in navigating familiar environments and remembering spatial relationships, which can lead to increased disorientation. As the disease advances, deficits in executive functions become more pronounced. Patients begin to struggle with tasks requiring planning, problem-solving, or cognitive flexibility. Importantly, the disease is now understood to have a prolonged preclinical phase, often beginning years or even decades before symptoms become noticeable. This extended progression has led to the identification of multiple stages of AD, including subjective cognitive decline, MCI), and eventual dementia. As research continues, an increasing focus on these early stages is helping to map the trajectory of cognitive decline and refine our understanding of AD pathology.

1.3.1.1. Subjective Cognitive Decline

Subjective Cognitive Decline (SCD) refers to individuals who report experiencing memory or cognitive difficulties despite showing no objective deficits on neuropsychological tests (Jessen, Amariglio, et al., 2014). Although clinical assessments may not reveal impairments, people with SCD often exhibit pathological changes, such as disrupted brain functional connectivity similar to those observed in MCI (López-Sanz et al., 2017), altered resting-state phase-amplitude coupling (C.-H. Cheng et al., 2023), and structural changes in both gray and white matter (X. Wang et al., 2020). These alterations, along with the fact that individuals with SCD are at a higher risk of developing AD dementia (Jessen, Wolfsgruber, et al., 2014; Reisberg et al., 2010; Rönnlund et al., 2015), position SCD as a potential early clinical manifestation of AD. Correctly detecting this stage in clinic might thus represent a way to diagnose AD earlier.

1.3.1.2. Mild Cognitive Impairment

MCI is a transitional state between normal aging and dementia, characterized by memory loss that exceeds what is expected for matching age but does not meet the criteria for AD (Petersen et al., 2001). Due to its broad definition and underlying heterogeneity, MCI is classified into two subtypes: amnestic MCI (aMCI), where memory loss is predominant, and non-amnestic MCI (naMCI), which involves impairments in cognitive domains other than memory. Individuals with aMCI have a higher likelihood of developing AD, with a conversion rate of approximately 12% per year (Campbell et al., 2013). This increased risk may be linked to the presence, in

aMCI patients, of neurofibrillary tangles observed in regions critical for memory, such as the HPC, entorhinal cortex, and amygdala (Markesbery, 2010). The high conversion rate to AD and the similarities in pathophysiology have led to the suggestion that aMCI could be considered a prodromal stage of AD. However, it is to remember that MCI does not always progress to AD and can also precede other neurodegenerative diseases, such as dementia with Lewy bodies (Ferman et al., 2013) or Parkinson's disease (J. G. Goldman et al., 2015) and can even reverse to normal cognitive state (Koepsell & Monsell, 2012).

1.3.1.3. Dementia

As previously mentioned, approximately 10% of individuals with MCI will progress to AD dementia, which can be considered the final stage of the disease. Patients experience a significant worsening of symptoms, including severe neuropsychiatric manifestations such as aggression, psychotic episodes, and hallucinations. As cognitive and motor functions deteriorate, individuals increasingly lose the ability to navigate their environment and perform basic movements, often becoming mute and incontinent. This profound physical immobility heightens the risk of complications such as deep vein thrombosis, malnutrition, aspiration pneumonia, and infections, which are frequently the primary causes of death in AD patients (Zvěřová, 2019).

1.3.2. Neuropathological evolution of the disease

The neuropathological evolution of AD is all but random, it follows a specific pattern, as first characterized by Eva and Heiko Braak through histological analysis of postmortem AD patient brains. The Braak stages (Braak & Braak, 1991) describe the spread of Tau neurofibrillary tangles (NFTs). In stages I and II, referred to as "transentorhinal stages," NFTs appear in the transentorhinal cortex and hippocampal CA1 region. Stages III and IV, known as "limbic stages," show significant involvement of the entorhinal and transentorhinal cortices, with further spread to the HPC, amygdala, thalamus, nucleus accumbens, and claustrum. By stages V and VI, termed "isocortical stages," the isocortex is heavily affected, with increasing involvement of all previously mentioned regions. Later, Dietmar Thal, a student in Braak group, mapped out the progression of Aβ deposition (Thal et al., 2002). Phase I is marked by focal diffuse plaques in cortical layers II, III, IV and V of the frontal, temporal, parietal, and occipital cortices. In phase II, Aβ spreads to the entorhinal cortex, HPC, and insular

cortex. Phase III involves subcortical regions such as the amygdala, thalamus, striatum, and hypothalamus. In phase IV, Aβ deposits appear in areas like the substantia nigra, superior colliculus, red nucleus, and CA4. Finally, phase V shows involvement of the cerebellum, locus coeruleus, and other brainstem regions. Following these classifications, Aβ and Tau deposition would thus follow two distincts progression patterns (Figure 2).

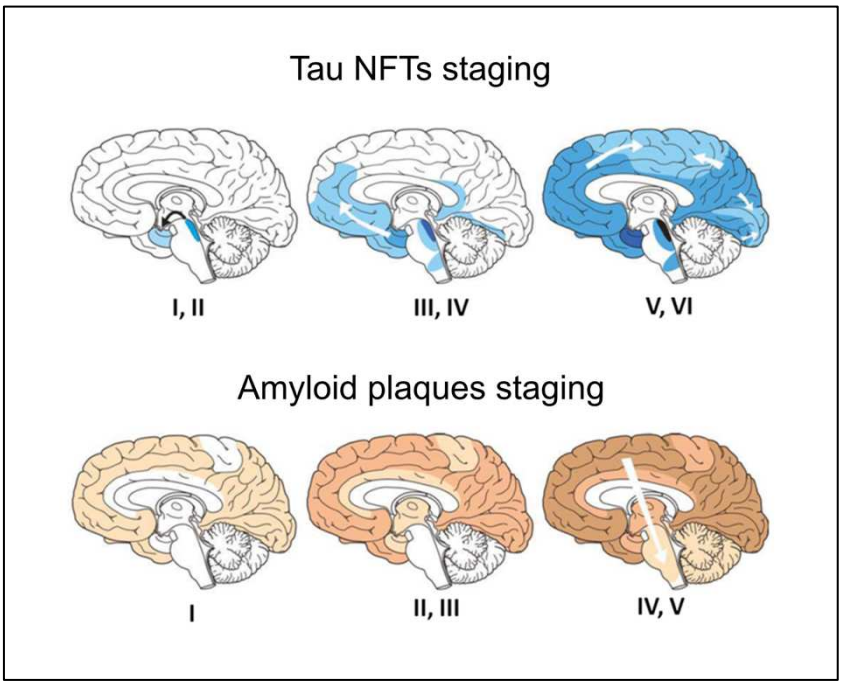

Figure 2. NFTs and amyloid plaques staging

Braak stages of Tau NFT deposition (Top) and Thal phases of Amyloid plaques deposition (Bottom). Adapted from Jouanne et al., 2017

The development of neuroimaging techniques, particularly PET scans (Ametamey et al., 2008), has enabled the study of these stages in living patients. PET allows for the visualization of specific molecules labeled with radioactive tracers, facilitating the study of metabolic and physiological processes. Longitudinal Aβ labelling has refined Thal's early stages, revealing that Aβ accumulation actually begins in the precuneus, medial orbitofrontal cortex, and posterior cingulate cortex, regions integral to the Default Mode Network (DMN; Palmqvist et al. 2017). Similarly, Tau imaging has confirmed Braak's hierarchical staging of Tau aggregation, showing that progression through Braak stages correlates with the evolution of hyperphosphorylated Tau and Aβ levels in the CSF (Therriault et al., 2022). Interestingly, while Braak stages I and II can occur without

Aβ deposition, progression beyond stage III is exclusively associated with the presence of Aβ (Therriault et al., 2022). Additionally, cognitive alterations align with Braak staging: subtle memory impairments are observed in stage II, consistent with Tau accumulation in the medial temporal regions critical for memory, while Braak stages IV and V are incompatible with normal cognition (Therriault et al., 2022). Overall, Braak's classification of tau pathology and the different phases of amyloid deposition provide a solid framework for understanding the neuropathological progression of AD, helping to track how the disease advances in both molecular markers and cognitive decline (Figure 3).

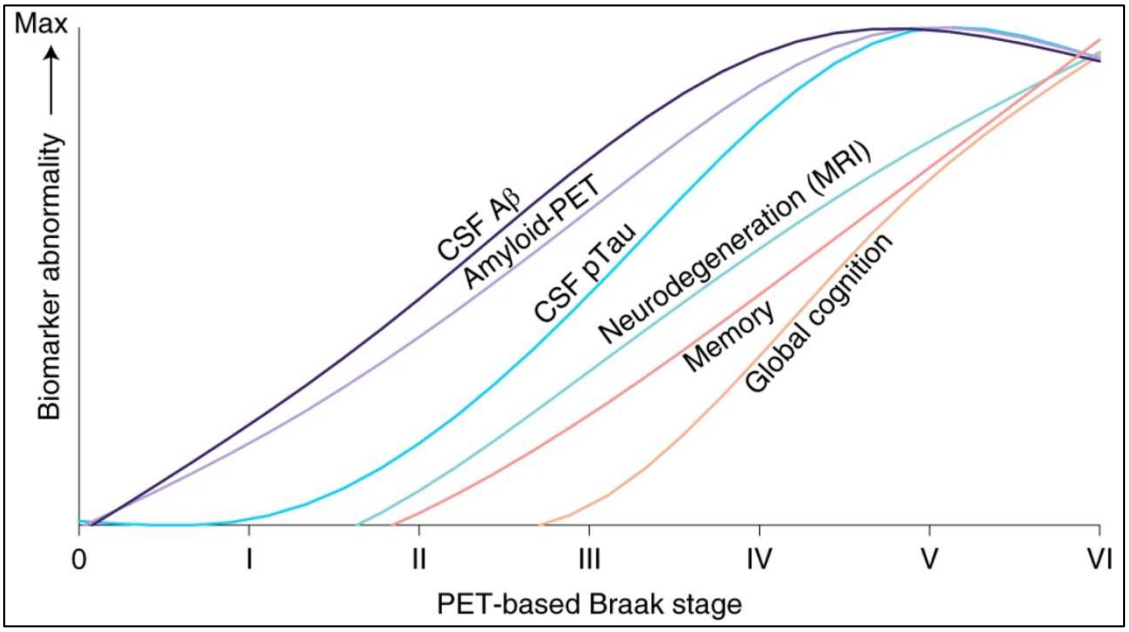

Figure 3. Biomarkers evolution follows Braak staging.

Adapted from Thierrault et al., 2022

1.4. Diagnosis and treatment

1.4.1. The major challenge of diagnosis

For decades, the criterion for classifying a group of symptoms as "definite AD" was post-mortem histological analysis, which can certainly be considered as a late diagnosis. At that time, earlier stages were classified as "probable AD" or "possible AD" and and linked mainly to a progressive amnestic disorder with dementia affecting cognitive and executive functions and by rejecting other diagnosis (G. McKhann et al.,

1984). Diagnostic criteria have therefore undergone a necessary evolution. A recent reappraisal by the International Working Group established criteria for the clinical phenotyping of AD, as well as for both the asymptomatic and presymptomatic stages of the disease. These criteria have been predominantly used in clinical practice over the past decade (Dubois et al., 2014). Typical AD would thus be described as presence of an early and significant episodic memory impairment that occurred gradually and progressively and was reported by the patient or the informant as having persisted for more than 6 months. The patient must also display an amnestic syndrome of the hippocampal type, assessed via significantly impaired performances on an episodic memory test. Additionally, the patient should present at least one of the following in-vivo evidence such as decreased $A\beta_{42}$ with increased Tau in the CSF, an increased tracer retention on amyloid PET, or an AD autosomal dominant mutation in PSEN1, PSEN2 or APP (as explained in the genetic risk factor chapter). Criterion for asymptomatic or presymptomatic AD mainly reside into presenting one of the in vivo biomarkers or a proven AD autosomal dominant mutation, respectively, without presenting any cognitive impairments. Despite being resolutely better than the former classification this latter still displays some shortcomings. Indeed, as we stated in the previous chapter, memory impairments are arising after an already long progression of the disease, waiting for memory impairments and furthermore the ones that last for already 6 months means to detect the disease at an already highly developed stage. On the other side, we saw previously that PET imaging of some biomarker and CSF dosage can show pathological hallmarks before cognitive impairments and thus could appear as a viable solution to detect earlier stages of the disease. However, these techniques are invasive procedures - intravenous injection of a radioactive tracer for PET scans and lumbar puncture for CSF analysis - which can be traumatic for the patient. Therefore, the invasive nature of these procedures limits their use in the absence of clinical symptoms, leading to delayed diagnoses. As a result, efforts have shifted towards earlier detection through less invasive techniques. One approach gaining attention is refining cognitive examinations, which could allow for earlier diagnosis by creating more sensitive tests and accounting for patients' cognitive complaints, even when no objective impairments are detected (as in SCD; Sabbagh et al. 2017). Besides these refined cognitive examinations, finding a reliable non-invasive biomarker for early stages such as SCD would represent a major step forward in AD

diagnosis and management, as this would facilitate clinical implementation and enable diagnosis before significant symptoms appearance.

1.4.2. AD treatment attempts

For now, there is still no treatment for AD, the actual treatment protocol mainly aims to retain the quality of life, mitigating the burden of illness and slowing down the progression of cognitive impairment by combining cholinesterase inhibitors and NMDA antagonist such as memantine (Atri, 2019). This combination indeed shows some benefits in cognitive performances in AD patient notably by increasing acetylcholine (ACh) levels at the central synapses (Grutzendler & Morris, 2001; Hampel et al., 2018). However, these treatments target the symptoms rather than addressing the underlying pathology of AD. Over the past few decades, numerous clinical trials have been conducted for various compounds, but most have ended in failure. Between 2002 and 2012, 244 compounds were tested across 413 trials, with a success rate for Food and Drug Administration (FDA) approval of only 0.4% (J. L. Cummings et al., 2014). Recent efforts have focused on new pharmacological approaches, such as antibodies that bind soluble forms of Aβ (Solanezumab) or γ-secretase inhibitors (Semagacestat), which aim to reduce the production of Aβ. Unfortunately, neither approach has demonstrated cognitive improvements (Doody et al., 2013, 2014), and in some cases, γ-secretase inhibitors have even worsened AD symptoms (Strooper, 2014). Given the challenges of pharmacological interventions and the side effects associated with these treatments, there is growing interest in exploring alternative, non-invasive approaches which may offer a promising avenue for future therapeutic development.

1.5. Pathology

Since the beginning of this manuscript, we talked a lot about amyloid plaques, Aβ, Tau, neurofibrillary tangles and others but we haven’t really seen what the origins of these classical pathological biomarkers of AD are, we will thus now go through these concepts.

1.5.1. Amyloidopathy

1.5.1.1. The Amyloid precursor protein (APP) and its non-amyloidogenic cleavage

APP is a transmembrane glycoprotein that consists of a large extracellular N-terminal domain, a single transmembrane domain, and a small intracellular C-terminal tail. It belongs to a family of proteins, which also includes Amyloid Precursor Like Protein 1 (APLP1) and APLP2, sharing a high sequence homology. This family plays a crucial role in development, as double knockouts of APP/APLP1 or APP/APLP2 are non-viable (Barbagallo et al., 2011; Matrone et al., 2012). Further, App mRNA is expressed in the embryonic neural tube during key periods of neural differentiation (Salbaum & Ruddle, 1994), and it has been detected in radial glial cells in the fetal mouse brain (Trapp & Hauer, 1994).

In the adult brain, APP is highly expressed in regions undergoing synaptic modifications, suggesting a role in memory processes (Löffler & Huber, 1992; Ouimet et al., 1994). Memory deficits observed in APP knockout animals further support this hypothesis (Dawson et al., 1999).

At the membrane, APP undergoes cleavage through different secretase actions, leading to three distinct pathways, depending on which secretase cleaves the extracellular part of the protein (Figure 4). The α-secretase pathway, also called the non-amyloidogenic pathway, involves cleavage at the α-secretase site, releasing a peptide known as soluble Amyloid Precursor Protein α (sAPPα) and leaving an α-C Terminal Fragment (αCTF) at the membrane. sAPPα plays an important role in neuronal plasticity, stem cell proliferation, and CNS development, and it offers protection against excitotoxicity (Caillé et al., 2004; Furukawa et al., 1996; Mattson, 1997; Ohsawa et al., 1999; Y. Zhang et al., 2011). sAPPα also exhibits benefits against AD pathology, as it can directly inhibit β-secretase cleavage (Peters-Libeu et al., 2015), and its overexpression in transgenic AD-like mice reduces both amyloid plaques and soluble Aβ (Obregon et al., 2012).

The remaining αCTF is subsequently cleaved by γ-secretase, a complex composed of four proteins: PSEN1 or PSEN2 (both linked to familial AD mutations), Anterior Pharynx-Defective 1 (APH-1), Nicastrin, and Presenilin Enhancer 2 (PEN-2). This γ-secretase activity results in the release of a small P3 peptide extracellularly and an

APP intracellular domain (AICD). The P3 peptide has been associated with neurotoxicity, such as inducing apoptosis in vitro (Wei et al., 2002) and increasing cytokine production in mouse microglial cells, which exacerbates inflammatory responses (Szczepanik et al., 2001). However, due to its instability, P3 does not form oligomers like Aβ and is therefore considered relatively harmless (Dulin et al., 2008), further supported by its lack of impact on synaptic function (Walsh et al., 2002). The AICD, on the other hand, has been linked to various processes, including nuclear signaling (Gao & Pimplikar, 2001), transcriptional regulation (Hébert et al., 2006), and apoptosis (Nakayama et al., 2008).

In addition, a less prominent non-amyloidogenic cleavage involves the η-secretase pathway, which produces η-CTF and sAPPη fragments. Subsequent cleavage of η-CTF by α-secretase gives rise to Aη fragments, which have been shown to impair neuronal activity in the HPC (Dunot et al., 2024; Willem et al., 2015).

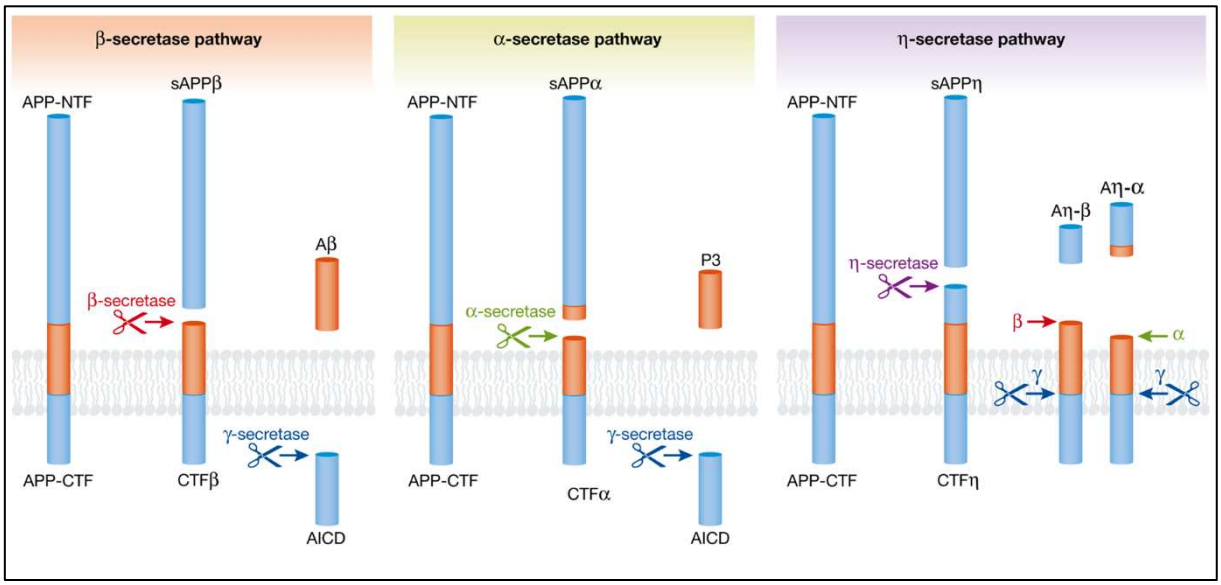

Figure 4. Different cleavage pathways of APP protein.

Amyloidogenic β-secretase pathway (Left) and non-amyloidogenic α and η-secretase pathways (Middle, Right). Adapted from Sasaguri et al., 2017

1.5.1.2. Amyloidogenic cleavage of APP and Aβ peptide

The amyloidogenic pathway, central to AD pathology, begins with the cleavage of APP by β-secretase, which the most common one is Beta-site APP-cleaving enzyme 1 (BACE1). This cleavage produces two proteins: sAPPβ and β-CTF. While sAPPβ

shares much of its sequence with sAPPα, it differs in the last 16 C-terminal amino acids, a difference that has significant consequences. Unlike sAPPα, sAPPβ lacks neuroprotective properties, does not reduce cell death, and is not involved in long-term potentiation (LTP; Chasseigneaux and Allinquant 2012).

The β-CTF protein, the direct precursor of Aβ peptide, is also considered neurotoxic even before its cleavage. It may play a critical role in AD genesis. In AD mouse models, β-CTF accumulates intracellularly in the HPC months before Aβ peptides appear, with this accumulation increasing when γ-secretase activity is inhibited (Lauritzen et al., 2012). This accumulation has detrimental effects on synaptic function, as β-CTF-expressing mice show an absence of LTP in the subiculum (Lauritzen et al., 2016). Recent studies suggest β-CTF might induce synaptic toxicity by promoting synaptic loss through endosome-related pathways (Luo et al., 2024). These harmful effects may explain why AD treatment strategies focused on γ-secretase inhibition have largely failed (Doody et al., 2013; Hamm et al., 2017).

Further cleavage of β-CTF releases both Aβ peptide and AICD. Aβ has been extensively studied for its pathological role in AD. However, it is essential to recognize that the cleavage of APP and the presence of Aβ in the brain are initially part of a physiological process. The switch between physiological and pathological effects is largely driven by the concentration of Aβ, with low levels favoring monomeric forms and preventing the formation of harmful oligomers. At low concentrations, Aβ monomers may have beneficial roles, such as sealing leaks in the blood-brain barrier, aiding recovery from brain injury, and even regulating synaptic function (Brothers et al., 2018). Aβ also appears to play a role in memory, as low doses enhance memory retention and ACh levels in the HPC, whereas depletion of Aβ impairs learning, and anti-Aβ antibodies inhibit hippocampal LTP (Morley et al., 2010).

Aβ monomers can range in size from 36 to 43 amino acid residues, but the most common forms are $A\beta_{40}$ and $A\beta_{42}$, with their size differences primarily determined by γ-secretase activity (Kuperstein et al., 2010). In physiological conditions, the ratio is roughly 90% $A\beta_{40}$ and 10% $A\beta_{42}$ (Pauwels et al., 2012). $A\beta_{42}$ is more hydrophobic than $A\beta_{40}$ and more prone to forming fibrils and oligomers (W. Kim & Hecht, 2005), which makes it the primary component of amyloid plaques in AD (B. J. Cummings et al., 1996). Mutations linked to familial forms of AD often increase $A\beta_{42}$ production, and this elevated $A\beta_{42}/A\beta_{40}$ ratio negatively affects synaptic activity, neuronal viability, and memory formation in animal models (Citron et al., 1997; Duff et al., 1996; Mann et al.,

1996; Scheuner et al., 1996; R. Wang et al., 2006). Even a slight shift in the $A\beta_{42}/A\beta_{40}$ ratio significantly influences the formation of neurotoxic oligomers (Kuperstein et al., 2010). Consequently, the $A\beta_{42}/A\beta_{40}$ ratio has become a key biomarker for assessing the progression of AD pathology.

1.5.1.3. Aβ oligomers and amyloid plaques

Aβ oligomers are soluble aggregates of Aβ that vary in size, ranging from less than 10 kDa to over 100 kDa, and exhibit structural polymorphism. These oligomers can be found both intra- and extracellularly (Sakono & Zako, 2010) and are believed to be the most toxic form of Aβ (Kayed and Lasagna-Reeves 2013; Figure 5). Extracellular Aβ oligomers can disrupt cellular integrity through various mechanisms. For example, their binding to nerve growth factor (NGF) receptors can induce neuronal death (Yamamoto et al., 2007), while their interaction with NMDA glutamate receptors disrupts calcium homeostasis, leading to increased oxidative stress and synapse loss (Felice et al., 2007; Shankar et al., 2007). Additionally, Aβ oligomers can destabilize cell membranes (Valincius et al., 2008), with the formation of membrane pores causing abnormal ion flow, which further contributes to cellular toxicity (Kawahara & Kuroda, 2000; Soto, 2003). Together, these mechanisms increase toxicity and ultimately lead to cell death. Intracellular Aβ oligomers can form through the aggregation of Aβ monomers, either endocytosed from the extracellular space or synthesized at the membranes of the endoplasmic reticulum or Golgi system (Sakono & Zako, 2010). While their toxic mechanisms differ from those of extracellular oligomers, intracellular Aβ oligomers are also harmful. They can bind to the proteasome, inhibiting its protein degradation function, which leads to the accumulation of proteins, including Aβ and Tau, inside the cell (Tseng et al., 2008). This disruption of cellular processes contributes to intracellular protein aggregation and ultimately results in cell death (Chui et al., 2001; Y. Zhang et al., 2002).

On the other hand, amyloid plaques are insoluble fibrillar aggregates of Aβ located in the extracellular space. While the role of these plaques in AD pathogenesis remains unclear, they have long been considered a primary pathogenic marker. Neural elements around amyloid plaques often show dystrophy (Wong et al., 1999) and destruction (Zempel et al., 2010). However, with recent research suggesting that soluble oligomers, rather than plaques, are the most toxic form of Aβ and the poor correlation between amyloid plaque load and cognitive decline or neurodegeneration

(Benilova et al., 2012), the view that plaques are the main cause of AD pathology is now being reconsidered. Some studies even propose that plaques may initially act as protective factors by sequestering toxic soluble oligomers (Selkoe & Hardy, 2016). Supporting this, research has shown that soluble Aβ accumulates within amyloid plaques (Gureviciene et al., 2017). However, this sequestration would have physical limits, beyond which plaques may release the toxic Aβ they contain (Selkoe & Hardy, 2016).

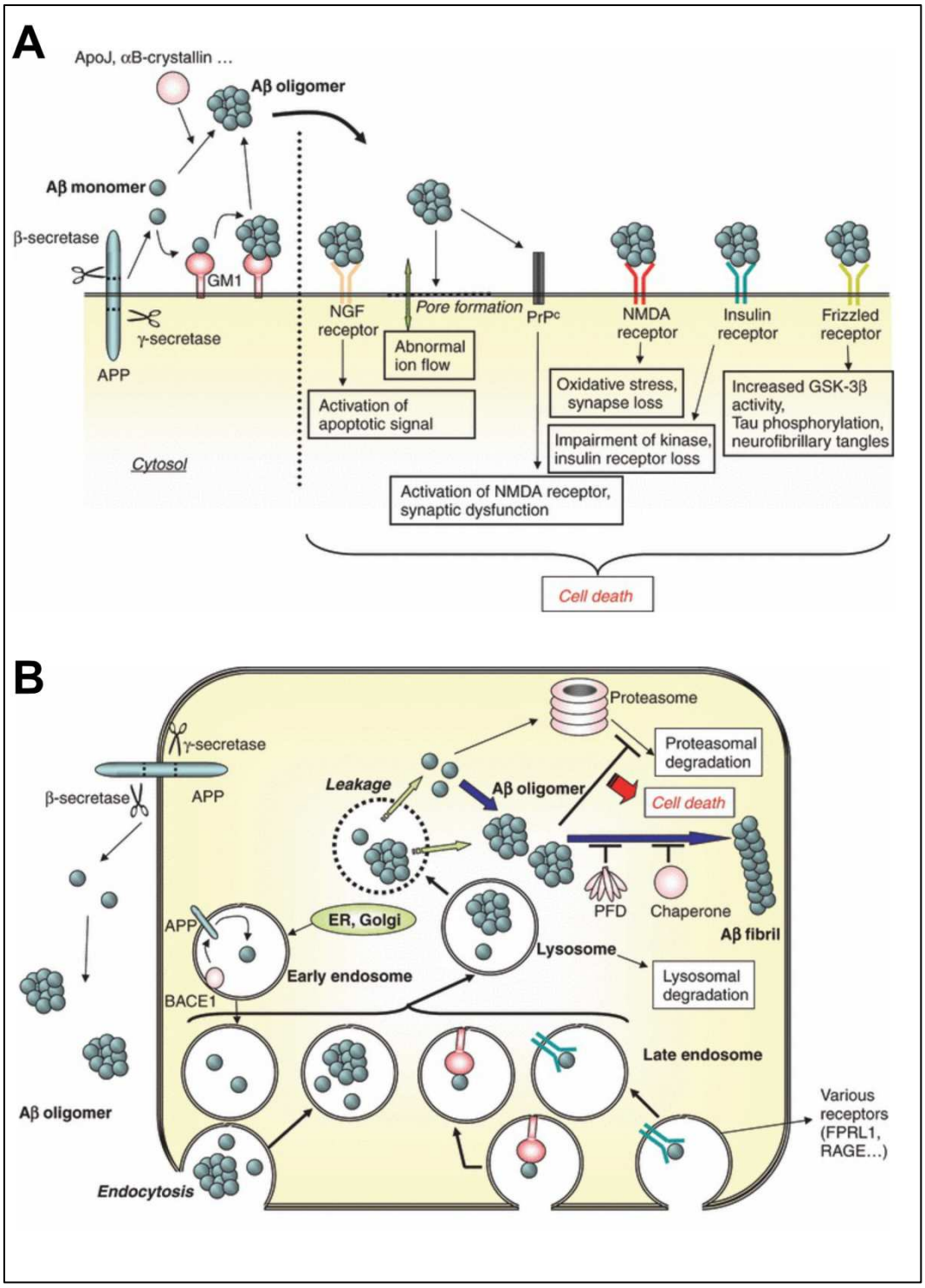

Figure 5. Aβ oligomers formation and toxicity

Formation and toxicity of extracellular (A) and intracellular (B) Aβ oligomers. Adapted from Sakono & Zako, 2011.

1.5.1.4. The Amyloid hypothesis and its limits

All of these pathological mechanisms driven by Aβ in AD have, over the decades, contributed to the development of the amyloid hypothesis. This hypothesis posits that Aβ-related processes are the main drivers of AD pathology (Selkoe & Hardy, 2016). Over time, it has established itself as the dominant conceptual framework for understanding AD, guiding much of the research focus and funding in the field. However, despite the clear role of Aβ in AD, the complexity of the disease—particularly the differences between familial forms, where amyloid pathway mutations are identified, and the more common sporadic forms, where the underlying causes remain unclear—highlights the need to remain open to alternative pathological hypotheses that may answer key unresolved questions.

The strength of the amyloid hypothesis has also been called into question by the incredibly high failure rate of therapies targeting the amyloid cascade (J. L. Cummings et al., 2014). Furthermore, recent concerns about scientific misconduct have cast doubt on some foundational studies supporting this hypothesis. For instance, an investigation led by *Science* Magazine (Piller, 2022) revealed that a key paper published in *Nature*, which claimed that a specific Aβ oligomer, the Aβ*56, caused memory impairments in AD models independent of plaques (Lesné et al., 2006), contained fraudulent results impacting the veracity of the scientific outcome of this paper, and this led to its recent retractation. At the time, this study was considered groundbreaking and contributed significantly to the momentum behind the amyloid hypothesis, influencing drug development efforts that eventually failed in clinical trials. This controversy underscores the importance of exploring other avenues beyond the amyloid cascade to fully understand AD pathophysiology and develop effective treatments and biomarkers.

1.5.2. Tauopathy

1.5.2.1. The Tau protein

The Tau protein, encoded by the *Microtubule-Associated Protein Tau* (MAPT) gene, is a microtubule-associated protein that plays a vital role in maintaining the cell cytoskeleton. In the human CNS, Tau is translated into six isoforms ranging from 37 to 46 kDa (Guo et al., 2017). The expression of these isoforms is developmentally regulated: while the adult brain expresses all six isoforms, only the shortest isoform is

present in the fetal brain (Goedert et al., 1989). Tau performs several key functions within cells, especially neurons. It regulates microtubule dynamics, affecting the spacing between microtubules and other cellular components (J. Chen et al., 1992), and is involved in associating the microtubule motor dynein with membranous cargoes (Magnani et al., 2007). Additionally, Tau contributes to neuronal signaling, nuclear function, and cytoskeletal maintenance by regulating microtubule assembly (Eidenmüller et al., 2001; Goode et al., 1997) and binding to actin (H. J. He et al., 2009).

Under physiological conditions, Tau is predominantly expressed in neurons, with lower levels observed in oligodendrocytes and astrocytes (Müller et al., 1997; Papasozomenos & Binder, 1987). In neurons, it is mainly localized in axons, where it stabilizes microtubules essential for the transport of vesicles between the cell body and the synapse (Aamodt & Williams, 1984). Furthermore, animal models of Tau depletion have revealed its broader role in neurophysiological processes. Mice lacking Tau exhibit deficits in long-term depression (LTD) in the hippocampal CA1 region, which indicates Tau's involvement in synaptic plasticity. Additionally, Tau influences neuronal activity, neurogenesis, migration, and adult hippocampal neurogenesis (Fuster-Matanzo et al., 2009; Hong et al., 2010; Kimura et al., 2014).

In summary, Tau protein is essential for maintaining neuronal structure and function, playing a key role in microtubule stabilization, intracellular transport, and synaptic plasticity. Its involvement in these cellular processes underlines the importance of Tau in supporting overall brain function and neuronal communication.

1.5.2.2. Pathological Tau hyperphosophrylation and aggregation leading to NFTs

One of the main modifications that Tau protein can undergo is phosphorylation by the addition of a phosphate on one of its many phosphorylation sites. In pathological conditions, Tau protein appears to be abnormally hyperphosphorylated, which leads to a loss of its ability to bind to microtubule (Cowan et al., 2010). Given Tau's critical role in maintaining microtubule stability, this loss of binding due to hyperphosphorylation can result in the destabilization of the cell's microtubule network (Cowan et al., 2010). The pathological hyperphosphorylation results from an imbalance between protein kinase, which phosphorylate Tau, and phosphatases, responsible of dephosphorylation (F. Liu et al., 2006; Medeiros et al., 2011). In AD, one potential

trigger for this imbalance is Aβ, which appears to overactivate the GSK3 kinase. Under normal conditions, GSK3 phosphorylates Tau, but in AD, its overactivation leads to Tau hyperphosphorylation (Hernández et al., 2010). Hyperphosphorylated Tau not only detaches from microtubules but also gains toxic properties, sequestering normal Tau and other microtubule-associated proteins. More critically, hyperphosphorylated Tau begins to aggregate and form NFTs (Iqbal et al., 2010). As previously mentioned, the spread of NFTs in AD is progressive, following the hierarchical progression of both the disease and cognitive impairments (Braak & Braak, 1991; Therriault et al., 2022). However, as for Aβ aggregates and amyloid plaques, despite showing correlation between NFTs and neurodegeneration or neuronal death (Gómez-Isla et al., 1997), some hypotheses as emerged proposing that hyperphosphorylated Tau soluble monomers or oligomers would be more toxic than the NFTs (Cowan & Mudher, 2013). While being discussed here for its implication in AD, disruption of Tau and formation of NFTs is observed in other neurodegenerative diseases such as Dementia with Lewy body (Armstrong et al., 1997) or Parkinson's disease (Rajput et al., 1989).

1.5.3. Neuromodulatory systems

During the development of AD pathology different neuromodulatory systems are affected, we will discuss some of the principal ones here.

1.5.3.1. Cholinergic system

One of the main neuromodulatory systems affected in AD is the cholinergic system. This system is composed of cholinergic neurons synthesizing ACh as their main neurotransmitter. ACh displays different functions in neuronal signaling depending on the site of its release and on which cholinergic receptor it binds. In the brain, two types of cholinergic receptors are present: nicotinic receptors (nAChRs) and muscarinic receptors (mAChRs). The main sources of cholinergic neurons are the medial septum-diagonal band of Broca (MS-DBB), basal forebrain, and pedunculopontine nucleus (PPN) (Bekdash, 2021; Hasselmo & Sarter, 2011; Picciotto et al., 2012). Different brain regions, such as the HPC, thalamus, striatum, and neocortex, are innervated by cholinergic neurons and show high densities of cholinergic receptors (Hasselmo & Sarter, 2011; Picciotto et al., 2012). The cholinergic system is mainly active during wakefulness and REM sleep (REM), while its activity is reduced during slow-wave sleep (SWS) (at least for basal forebrain: Lee et al. 2005).

The cholinergic system is crucial for several cognitive functions, including attention, thinking, learning, and memory (Hasselmo, 2006; Hasselmo & Sarter, 2011; Picciotto et al., 2012). ACh enhances memory encoding through various mechanisms, including increasing sensory input influence during memory encoding by modulating excitatory synaptic transmission via nicotinic receptors, while inhibiting excitatory feedback through muscarinic receptors (Hasselmo, 2006). This modulation helps reduce interference during encoding. Additionally, ACh influences hippocampal activity by enhancing theta oscillations, which are critical for memory (Siok et al., 2006).
The still widely accepted cholinergic hypothesis of AD state that cholinergic neurons from basal forebrain and MS-DBB degenerate early, thus reducing Ach concentration in key regions for memory as the HPC and the entorhinal cortex (Ballinger et al., 2016). This reduced Ach concentration is associated with reduced concentration of muscarinic and nicotinic receptor and his followed by cognitive and memory impairments (Ballinger et al., 2016). These cognitive impairments associated with reduced Ach levels have paved the way to treatment using Ach-esterase inhibitors, thus reducing the degradation of Ach in the synapse. These treatments have shown some beneficial effects on cognitive symptoms of AD and as previously described is still mainly used as treatments to mitigate AD symptoms (Vecchio et al., 2021).

1.5.3.2. Noradrenergic system

The noradrenergic system functions through noradrenergic transmission, involving the release of noradrenaline (NA), which is synthesized from dopamine, at the synapse. The primary source of noradrenaline in the brain is the Locus Coeruleus (LC), which projects to various brain regions, including the cortex, HPC, striatum, amygdala, cerebellum, basal forebrain, and hypothalamus (Perez, 2020). In the brain, NA acts by binding to adrenergic receptors (ARs), which are part of the G-protein coupled receptor (GPCR) family. There are three main types of ARs: α1, α2, and β, with α2 showing the highest affinity for NA, followed by α1 and then β (Gannon et al., 2015). The noradrenergic system, driven by LC activity, is most active during wakefulness, where it plays a key role in modulating arousal and alertness (Berridge et al., 2012). The LC is activated in response to salient stimuli, promoting sensory processing, cognitive flexibility, and memory consolidation (Sara & Bouret, 2012). In addition to these functions, NA is crucial in modulating hippocampal synaptic plasticity, LTP, and learning

processes (Gelinas & Nguyen, 2007; Hansen & Manahan-Vaughan, 2015), and plays an essential role in memory consolidation (Kobayashi & Yasoshima, 2001).

In AD, the LC is one of the first brain regions to show pre-tangle Tau alterations, making it a significant early site of Tau pathology (Braak et al., 2011). The progressive neurodegeneration of the LC follows the Braak staging of AD (Theofilas et al., 2017) and correlates with disease severity (Zarow et al., 2003). As LC neurons degenerate, NA levels in many brain regions drop significantly by up to 50% within just two years after the onset of dementia (German et al., 1992). This decline in NA, along with the loss of LC fibers, disrupts several crucial functions, including sleep-wake cycles, alertness, synaptic plasticity, and memory (Giorgi et al., 2017). Given the relationship between these adrenergic changes and Tauopathy, similar alterations are also observed in other neurodegenerative diseases involving Tau pathology, such as dementia with Lewy bodies and Parkinson's disease (Brunnström et al., 2011).

1.6. Models of the Pathology

Research on AD has heavily relied on animal models to investigate various pathological processes, identify potential biomarkers, and explore treatments, all aimed at gaining a deeper understanding of the disease. While rodent models represent the majority of animal models used in AD research, they do not naturally develop the disease. Therefore, specific models had to be engineered using molecular biological techniques.

1.6.1. Spontaneous models of AD

Before describing rodent models genetically designed for the study of AD, it is important to note that some animal species can spontaneously develop, as they age, pathologies associated with those observed in AD. These species are increasingly considered for study because they can provide a better representation of the sporadic forms of the disease, which remain poorly understood.

One of the most relevant spontaneous animal models for studying aging and neurodegenerative diseases is the common marmoset (Perez-Cruz & Rodriguez-Callejas, 2023). This model is used for several reasons, including its ability to live for an extended period after reaching adulthood, which closely resembles aging, as well as its age-dependent changes in executive functions and spatial working memory.

Interestingly, marmosets exhibit the spontaneous appearance of Aβ aggregates as they age, along with Tau hyperphosphorylation in both young and old individuals, but do not develop NFTs (Perez-Cruz & Rodriguez-Callejas, 2023). These characteristics make them suitable models for AD. Other non-human primates, such as *Macaca mulatta*, *Macaca arctoides*, or *Macaca fascicularis*, can also display functional and morphological changes related to AD.

Another spontaneous model, the Octodon degus, a rodent native to South America, exhibits intracellular and extracellular Aβ deposits, as well as intracellular Tau accumulation and memory impairments in aged wild-type individuals (Ardiles et al., 2012; Inestrosa et al., 2005). However, recent studies have shown that captive-bred Octodon degus do not automatically develop this pathological phenotype with age (Steffen et al., 2016).

Finally, dogs may serve as another spontaneous model, as they can develop Canine Cognitive Dysfunction or canine dementia, a neurodegenerative condition characterized by Aβ deposits that correlate with memory impairments as they age (Z.-Y. Chen & Zhang, 2022).

Despite offering promising opportunities to study the sporadic form of the disease, most AD research has been conducted using genetically modified rodent models of the familial form of AD.

1.6.2. Transgenic mice models

The development of transgenic (Tg) mice models was one of the first major approaches to studying AD. Here the term “transgenic” not only refers to “genetically modified animals” but to animals for which a transgene is inserted in single or multicopy in the genome.

1.6.2.1. Single Transgenic models

Given that APP is the main precursor of Aβ peptides, which lead to the formation of pathological oligomers and amyloid plaques, and that mutations in APP are associated with certain familial forms of AD, it was logical to first develop mouse models carrying mutated human APP. Several models were created based on this approach, differing by the APP mutation and the promoter used for the transgene. Among the most well-known are the Tg2576 mice (Hsiao et al., 1996), which carry the Swedish mutation (K670N/M671L; Citron et al. 1992), the J20 mice (Mucke et al., 2000), and the

TgCRND8 mice (Chishti et al., 2001). Both J20 and TgCRND8 models carry two APP mutations: Swedish and Indiana (V717F; Murrell et al. 1991), though they differ in the promoter used. All three models show pathological accumulation of Aβ, amyloid plaques, and cognitive impairments (I. H. Cheng et al., 2007; Wright et al., 2013). However, despite displaying these pathological signs, they show little or no neuronal loss and do not develop NFTs.

1.6.2.2. Double Transgenic models

To improve upon earlier models, double Tg mice were developed. These mice carry both an APP transgene with human mutations and a PSEN1 transgene, given that mutations in PSEN1 account for up to 50% of familial AD cases. The two principal models in this category are the APP/PS1 mice (Radde et al., 2006), which overexpress human APP with the Swedish mutation and human PSEN1 with the L166P mutation (Moehlmann et al., 2002), and the 5XFAD mice (Oakley et al., 2006), which overexpress human APP with three mutations: Swedish, Florida (I716V; Eckman et al. 1997), and London (V717I; Goate et al. 1991), along with human PSEN1 carrying two mutations, M146L and L286V (Sherrington et al., 1995). Both models exhibit pathological Aβ accumulation, amyloid plaques, synaptic degradation, cognitive deficits, and neuronal loss. The 5XFAD model, in particular, is known for its degree of aggressiveness, showing amyloid deposition by two months of age, elevated $A\beta_{42}$ levels by 1.5 months, and cognitive deficits by four months (Oakley et al., 2006). However, like the single Tg models, no NFTs are observed.

1.6.2.3. Triple Transgenic models

To incorporate both Tau and amyloid pathologies into a single model, triple Tg mice were developed. These models carry human APP, PSEN1, and MAPT transgenes. The most widely known model is the 3xTg mouse (Oddo et al., 2003), which overexpresses human APP with the Swedish mutation, human PSEN1 with the M146V mutation (Clark et al., 1995), and human MAPT with the P301L mutation (Dumanchin et al., 1998). This model exhibits extracellular Aβ deposition that progresses with age, cognitive impairments (Billings et al., 2005), and the formation of NFTs.

1.6.2.4. Limits of transgenic models

While Tg models offer significant insights into AD, they have important limitations. The random integration and overexpression of the transgene, along with potential conflicts between the human transgene and the murine version of the gene, can result in models that do not fully replicate the physiological features of the disease. These interactions may cause artificial results unrelated to actual disease mechanisms. To address these shortcomings, knock-in models have been developed, which aim to produce more physiologically relevant phenotypes.

1.6.3. Knock-in mice models

To address the limitations of APP overexpression, knock-in (KI) models were developed. With knock-in technology, the gene of interest is inserted into the genome, replacing the endogenous murine version of the gene without being overexpressed. This results in a physiological expression of the humanized gene further eliminating potential interactions between the human transgene and the murine counterpart.

1.6.3.1. Single Knock-In

The first knock-in models focused on humanizing the Aβ sequence in the murine genome by changing three amino acids that differ between mice and humans and introducing two familial AD mutations (KM670/671NL: Swedish and I716F: Beyreuther/Iberian mutations; Lichtenthaler et al. 1999) into the endogenous mouse App gene (Saito et al., 2014). This model, called App^{NL-F}, showed an increase in $Aβ_{42}$ production and a higher $Aβ_{42}/Aβ_{40}$ ratio without altering APP expression. Homozygous mice began to exhibit amyloid plaques at 6 months of age, while heterozygotes showed plaques by 24 months. Cognitive deficits, particularly in the Y-maze task, were observed at 18 months. However, this model did not exhibit neuronal loss or the presence of NFTs.

1.6.3.2. Double Knock-In

To extend the model to include Tau pathology, another single knock-in model was developed: the MAPT KI. In this model, the entire murine Mapt gene was replaced with the human ortholog without any mutations, allowing the expression of all six human Tau isoforms, as opposed to the three found in the murine gene (Saito et al., 2019).

This MAPT KI model was then crossed with the App^{NL-F} model to create a double knock-in (dKI) mouse, denoted App^{NL-F}/MAPT (Saito et al., 2019). These mice showed mild memory deficits at 4 months in a specific object-in-place memory task, coinciding with an increased production of $A\beta_{42}$ and subtle changes in Tau phosphorylation. However, at this stage, they did not exhibit amyloid plaques, NFTs, or cognitive impairments in more traditional behavioral tasks (Borcuk et al., 2022).
Given its ability to model early-stage pathology in a more physiological context, the App^{NL-F}/MAPT double knock-in model represents a promising candidate for studying the initial stages of AD. This model was used in the present thesis work.

1.6.4. Evaluating memory in rodent

As mentionned earlier, AD patients exhibit early alterations across multiple cognitive domains, including working memory, cognitive flexibility, and spatial memory. In rodent models of the disease, various types of memory can also be assessed, providing valuable insights into the underlying mechanisms of initial cognitive impairments. Here, we will review relevant tests (some of which were used in our work) and discuss how they are evaluated and affected by the disease

1.6.4.1. Recognition memory

Rodents are naturally curious and tend to explore novel objects in their environment, a behavior that forms the basis of the spontaneous object recognition paradigm (Ennaceur & Delacour, 1988). In this task, rodents are first exposed to two identical objects. After a specified inter-trial interval (ITI), they are presented with one familiar and one novel object. Most rodents can distinguish between the two, typically spending more time exploring the novel object, with short- and long-term recognition memory assessed by varying the ITI from a few minutes to several hours or even days.
The perirhinal cortex (PRC) is a key brain region involved in recognition memory across ITIs ranging from 5 minutes to 24 hours (Barker et al., 2007; Wan et al., 1999; Winters et al., 2004; Winters & Bussey, 2005a, 2005c, 2005b). However, the role of the HPC in object recognition remains debated; some studies suggest hippocampal lesions do not affect recognition memory (Winters et al., 2004), while others indicate they do (Cohen et al., 2013). Task complexity may influence the contributions of the PRC and HPC, with both regions potentially serving complementary functions (Cinalli Jr. et al., 2020; Squire et al., 2007). Additionally, the HPC, prefrontal cortex (PFC), and

retrosplenial cortex (RSC) are involved in long-term object recognition when the ITI extends to 24 hours (de Landeta et al., 2020; Preston & Eichenbaum, 2013; Warburton & Brown, 2015).

Object recognition deficits are progressively observed in various AD mouse models. Different single-Tg APP models display deficits at different ages: tgCRND8 mice show long-term object recognition deficits by 8 weeks (Francis et al., 2012), tg2576 mice by 13 weeks (Huang et al., 2006), and J20 mice by 3 months (Ameen-Ali et al., 2019). In double-Tg APP/PS1 models, deficits emerge around 6 months (Howlett et al., 2004), and in 5XFAD mice, at 4 months, both with a 4-hour ITI (D.-H. Kim et al., 2020). These findings suggest that Tg mouse models generally exhibit object recognition deficits around 4 months, with a greater sensitivity to long-term recognition memory. Interestingly, dKI App^{NL-F}/MAPT mice show no impairment in object recognition at 6 months, regardless of whether the ITI is 5 minutes or 24 hours (Borcuk et al., 2022).

1.6.4.2. Spatial memory

Spatial memory is one of the most commonly assessed forms of memory in rodent models. In addition to its translational significance, this focus on spatial testing reflects its ecological importance, as animals rely on spatial memory to remember critical locations for food, shelter, and other survival needs. One of the most well-known tasks for assessing spatial memory is the Morris Water Maze (MWM; R. G. M. Morris 1981), in which rodents must locate a hidden platform in a pool. However, since swimming can be highly stressful for mice, alternative dry mazes, such as the Barnes maze and star maze, are increasingly used to minimize stress. A network comprising the HPC, EC, and RSC is crucial for spatial memory, as it plays a major role in allocentric navigation, spatial working memory, and recognizing novel spatial features (Assini et al., 2009; R. G. M. Morris et al., 1982, 1990; Mumby et al., 2002). This role is likely facilitated by spatially modulated cells in these regions, including place cells and grid cells (Hafting et al., 2005; Jacob et al., 2017; Mao et al., 2017; O'Keefe & Dostrovsky, 1971; Van Cauter et al., 2013).

Additionally, spatial memory can also be assessed using spontaneous object exploration tasks, such as the novel object location task (NOL). Like the classical maze tests, this task provides a measure of HPC-dependent spatial memory in mice (Vogel-Ciernia & Wood, 2014) and involves a distributed network that includes the EC and the RSC (see Chao et al. 2022 for review).

Spatial memory is impaired in several AD mouse models. For example, single-Tg APP mice, such as tgCRND8, exhibit object location memory deficits with three objects by 2 months of age (Hamm et al., 2017) and MWM impairments by 4 months (Doggui et al., 2010). Tg2576 mice display spatial memory issues from 8 months (Stewart et al., 2011), and J20 mice show their first radial maze deficits at 4 months (Wright et al., 2013). Double-Tg APP/PS1 mice exhibit subtle MWM deficits starting at 3.5 months (W. Zhang et al., 2012), while 5XFAD mice begin to show spatial learning and memory impairments around 6 months (Kanno et al., 2014). In knock-in AD models, single KI mice with three App mutations (AppNL-G-F) present spatial memory deficits by 8 months (Sakakibara et al., 2018), whereas no spatial memory impairments have been observed in dKI AppNL-F/MAPT mice to date (Borcuk et al., 2022).

1.6.4.3. Associative memory

Spontaneous object exploration can be adapted to assess more complex memory paradigms beyond simple object recognition, such as associative memory. In associative memory tasks, animals must remember the association between different elements of the task. One such paradigm is the Object-in-Place (OiP) task, where animals first encounter two distinct objects. After a defined, typically short, inter-trial interval (ITI), one of the original objects is replaced by a duplicate of the other familiar object. This test the ability of the animal to detect the intrusion of a familiar object in the position previously occupied by a different familiar object (Dix & Aggleton, 1999). Different brain networks and regions are implicated depending on the difficulty of the task. While the version of the task with four objects requires a complex network that includes, but is not limited to, the PRC, PFC, HPC, and RSC (Chao et al., 2022), the two-object version primarily involves the lateral entorhinal cortex (LEC) and the PFC (Chao et al., 2016; Kuruvilla et al., 2020).

Associative memory is notably affected early on in several AD mouse models. Single-Tg tgCRND8 mice show deficits in two-object OiP tasks as early as 2 months, even before displaying object recognition impairments or amyloid plaque formation (Hamm et al., 2017). Similarly, double-Tg APP/PS1 mice exhibit deficits in two-object OiP tasks around 4 months (Bonardi et al., 2021, p. 20). Finally, deficits in the two-object OiP task appear to be the first detectable memory impairments in the dKI AppNL-F/MAPT mouse model, starting at 4 months of age (Borcuk et al., 2022).

In this thesis work, we focused on two tasks based on spontaneous object exploration using the AppNL-F/MAPT mouse model. The object-in-place (OiP) task, which tests associative memory, appears to be the first detectable memory alteration in this model. The 24-hour novel object recognition (NOR) task was also included, as no memory deficits have been observed in this task in the AppNL-F/MAPT model.

1.7. Take-home message

After going through several key aspects of AD here is some important points to summarize this first chapter:

- **AD is a neurodegenerative disease affecting an increasing number of elderly individuals worldwide.**
- **Both genetic and environmental factors can influence the development of AD.**
- **The evolution of the symptoms is slow and follows the progression of several biomarkers as Tau NFTs deposition.**
- **There are still no effective treatments for AD.**
- **Despites recent progress, AD diagnosis often occurs too late due to the lack of reliable, non-invasive biomarkers for the disease.**

One of the major challenges is the need for a reliable early biomarker that can be easily assessed at the onset of subjective cognitive complaints. To be practically implemented in clinical settings, this biomarker should be as non-invasive as possible, which limits the potential for molecular markers. Recent advancements in non-invasive neuroimaging techniques, such as functional Magnetic Resonance Imaging (fMRI) and Electroencephalography (EEG), have opened new avenues to investigate a potential early indicator of pathology: brain dynamics.

2. Brain Dynamics

The brain processes information through dynamic patterns of neural activity that continuously shift and reorganize. These dynamics are fundamental to brain function, determining how information is encoded, transformed, and transmitted across neural circuits. Recent advances in biology, physics, techniques and more globally neurosciences have allowed to record brain activity across different brain states, performance of different tasks or during pathological processes, providing a better understanding of how the brain functions under various circumstances. These studies have revealed that brain activity changes according to different brain states and cognitive demands, with even subtle alterations in dynamics potentially disrupting information processing. This underscores the significance of studying brain dynamics to understand both healthy cognitive function and its impairment in neurological conditions.

2.1. Brain dynamics or the difference between structural and functional networks

It is widely accepted that the brain's functional networks are influenced by the underlying structural networks. However, even if functional networks mainly emerge from structural networks, this relation is not always one to one (Mišić et al., 2016). Structural networks can be mapped using diffusion MRI, which tracks white matter tracts in the brain and helps construct the brain's underlying anatomical network (Basser et al., 1994; Hagmann et al., 2007). Functional networks, on the other hand, can be examined using techniques like EEG, Magnetoencephalography (MEG) or more commonly functional MRI (fMRI), which measures the Blood-Oxygen-Level-Dependent (BOLD) signal, a proxy for neuronal activity based on oxygen usage in brain regions (H.-J. Park & Friston, 2013). Correlations between BOLD signals across different regions allows to compute functional connectivity.

By combining structural and functional MRI, these two networks can be compared in the same individual, revealing interesting results. Functional connectivity patterns do not always mirror the brain's structural organization and can vary depending on the cognitive task or state of consciousness. For example, during states of reduced consciousness, functional connectivity more closely aligns with the brain's structural

connectivity (Barttfeld et al., 2015). These differences become more pronounced when analyzing functional connectivity over shorter timescales, which capture moment-to-moment brain state fluctuations and avoid the statistical averaging of the activity over time. Therefore, while structural networks provide the scaffolding for brain activity, several functional networks can emerge from this fixed structural topology, phenomenon referred as *functional multiplicity* (Battaglia, 2014). These functional networks will adapt dynamically to meet cognitive demands, with higher levels of consciousness or engagement leading to increase dynamic of functional patterns (Deco et al., 2015; Sarasso et al., 2015).

This underscores the importance of studying brain dynamics. In neurodegenerative diseases, disruptions in dynamic functional patterns may precede detectable changes in structural networks. Conversely, restoring healthy functional dynamics could help compensate for structural damage, offering a potential avenue for therapeutic interventions (Stulz et al., 2024).

2.2. Dynamics at different scales

Brain dynamics appears to organize, store or transfer information at different scales of brain systems from the intracellular protein plasticity to the whole brain functional networks, here we will see some dynamical properties of the main different brain scales.

2.2.1. Neuronal dynamics

One of the fundamental processes of brain dynamics is the action potential, or spike, fired by neurons. These electrical pulses are thought to convey information between connected neurons (Hodgkin & Huxley, 1952). While neuronal spikes tend to follow a uniform electrical pattern, they are dynamically modulated to encode different types of information.

2.2.1.1. Time, Space and neuronal tuning

Neurons do not fire randomly. Instead, their activity is typically tuned to specific stimuli or conditions. A key example of this is stimulus-driven firing, where neurons respond to sensory input in a highly organized manner. In the visual cortex, for instance, neurons are not only responsive to visual stimuli, but they are also specifically tuned

to particular patterns, such as orientation or movement direction (Hubel & Wiesel, 1962). This suggests that neuronal firing does more than just indicate the presence of a stimulus, it also encodes details about the stimulus itself.

Another form of neuronal tuning relates to spatial coding, which was central to the 2014 Nobel Prize in Physiology and Medicine. Place cells, discovered by O'Keefe and Dostrovsky (1971) in the HPC, fire in specific locations within an environment, allowing the brain to encode spatial information. Similarly, grid cells in the EC fire in a grid-like pattern that spans the environment, providing a unique map of the space (Hafting et al., 2005). These cells complement the role of place cells in spatial navigation.

In addition to spatial coding, neurons also display temporal tuning. Some hippocampal neurons, known as time cells, fire in sequence during tasks to represent the flow of time. This form of coding links specific neuronal firing to the temporal order of events, allowing the brain to track time intervals and organize information accordingly (Eichenbaum, 2014).

Thus, the dynamic tuning of neuronal firing allows the brain to encode a wide range of information, from the characteristics of sensory stimuli to spatial location and the passage of time. This flexibility in firing patterns highlights the importance of studying how neuronal dynamics support cognitive processes.

2.2.1.2. Cell assemblies

In the brain, neurons rarely fire alone and are more commonly firing in groups. These groups of interconnected neurons firing together are called cell assemblies and has been hypothesized to represent a distinct cognitive entity (Hebb, 1949). Their strong interconnectivity allows the activation of the entire assembly when only a portion is triggered (Legendy, 1967; Palm, 1982, 1987). These assemblies are believed to emerge from dynamic interactions within neural circuits and their hierarchical organization would serve as a neural syntax allowing to encode different pieces of information depending on the task, context, or brain state (Buzsáki, 2010).

A key feature of cell assemblies is their flexibility. Neurons can participate in different assemblies at different times, demonstrating the brain's capacity for dynamic reconfiguration (Cossart et al., 2003; Harris, 2005). This flexibility is crucial, enabling the rapid formation and dissolution of functional networks that are needed for the constantly changing demands of cognition.

Thus, these dynamics, flexible, and transient assemblies enable the brain to shift between tasks and states, supporting both basic sensory processing and more complex cognitive functions. This highlights the importance of dynamic networks in sustaining these processes.

2.2.2. Larger brain fields and oscillations

2.2.2.1. Brain oscillations

When neurons are firing together, their variation of membrane polarization will lead to fluctuation of voltage potential in the extracellular medium. The sum of all the current in the field will thus be recorded through local field potential (LFP) or further through electroencephalogram (EEG, Buzsáki, Anastassiou, and Koch 2012). Rhythmic variation of the LFP give rise to brain oscillations. These oscillations emerge from two main mechanisms: the intrinsic properties of neurons capable of generating rhythmic activity through their membrane properties, and the coordinated activity of neural networks, particularly through interactions between excitatory and inhibitory neurons (Buzsáki & Draguhn, 2004). Different types of oscillations are characterized by their frequency ranges, each associated with specific brain states and functions. Delta oscillations (1-4 Hz) are primarily generated in the thalamus and cortex during deep sleep, involving specialized thalamic neurons with intrinsic pacemaking properties (Steriade et al., 1993). Theta oscillations (4-12 Hz) are prominently observed in the HPC and are generated through the interaction of multiple cell types, including specific interneurons and pyramidal cells (Buzsáki, 2002). Gamma oscillations (>30 Hz) arise from the precise timing between pyramidal cells and fast-spiking interneurons in local circuits, particularly through GABA-mediated inhibition (Cardin et al., 2009; Tiesinga & Sejnowski, 2009). Beyond these fundamental oscillations, the brain also exhibits distinct oscillatory patterns that represent more complex neural dynamics. Sleep spindles (12-15 Hz bursts) are generated through interactions between thalamic and cortical neurons, requiring both oscillatory mechanisms and specific circuit properties (Steriade, 2006). Similarly, hippocampal ripples (150-250 Hz) emerge from the coordinated firing of pyramidal cells under the influence of specific interneuron populations, representing a pattern that depends on oscillatory mechanisms but includes additional organizing principles (Buzsáki, 2015). Sharp waves, often associated with ripples, are not oscillations themselves but rather represent brief

depolarizing events that can trigger oscillatory activity. These various rhythms and patterns allow the brain to organize its activity across different temporal and spatial scales, supporting functions from basic sensory processing to complex cognitive operations (Fries, 2015). The specific generation of each rhythm type depends on both the cellular properties of involved neurons and the circuit architecture in which they are embedded, demonstrating how the brain uses different oscillatory mechanisms to achieve distinct computational goals (X.-J. Wang, 2010).

2.2.2.2. Different coupling patterns

Brain oscillations interact through various coupling mechanisms to organize information processing and communication across different brain regions (Senkowski & Engel, 2024). One fundamental mechanism is phase synchronization between brain regions, which forms the basis of the Communication Through Coherence theory (Fries, 2005, 2015). According to this theory, neural communication is most effective when oscillatory activity in the sending and receiving regions is synchronized. When two regions oscillate coherently, the receiving region alternates between states of high and low excitability. Inputs arriving during periods of high excitability are more likely to trigger action potentials, effectively creating "communication windows". Importantly, this synchronization is not static but highly dynamic, with regions becoming synchronized only when communication is functionally required, such as during attention tasks. This flexible mechanism allows the brain to establish and dissolve communication channels based on cognitive demands (Figure).

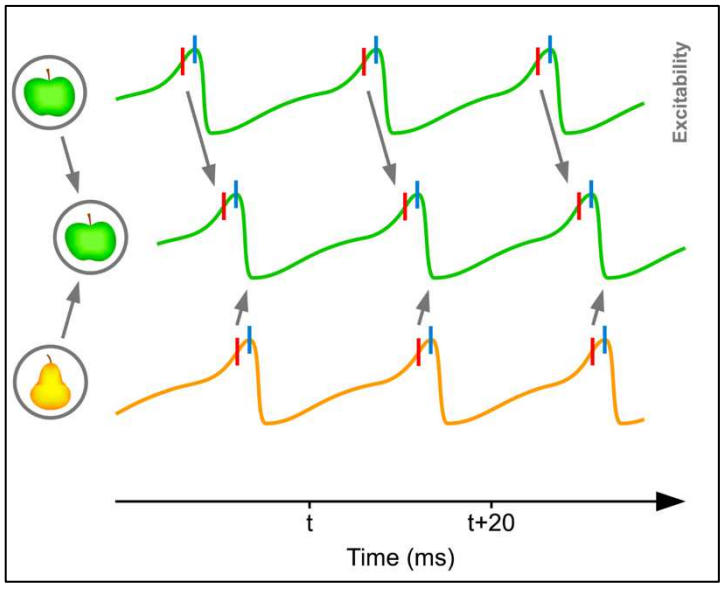

Figure 6. Communication Through Coherence

The upstream neurons coding for the apple spike at a moment of high excitability of the receiving neurons, allowing a transfer of the information.

From Fries 2015.

Another important form of oscillatory interaction is phase-amplitude coupling (PAC), where the phase of a slower oscillation modulates the amplitude of a faster oscillation (Tort et al., 2010). A well-studied example is theta-gamma coupling in the HPC, where the phase of theta oscillations modulates the amplitude of local gamma oscillations. This hierarchical organization allows for the precise temporal coordination of neural assemblies, with gamma-linked cell assemblies being organized within the broader temporal framework provided by theta oscillations (Lisman & Buzsaki, 2008). This coupling pattern play important role in memory and will be further discussed in chapter 2.3. Beyond PAC, other forms of cross-frequency coupling exist, such as phase-phase coupling or amplitude-amplitude coupling. For instance, during sleep, the coupling between delta waves and sleep spindles plays a crucial role in memory consolidation (Steriade, 2006).

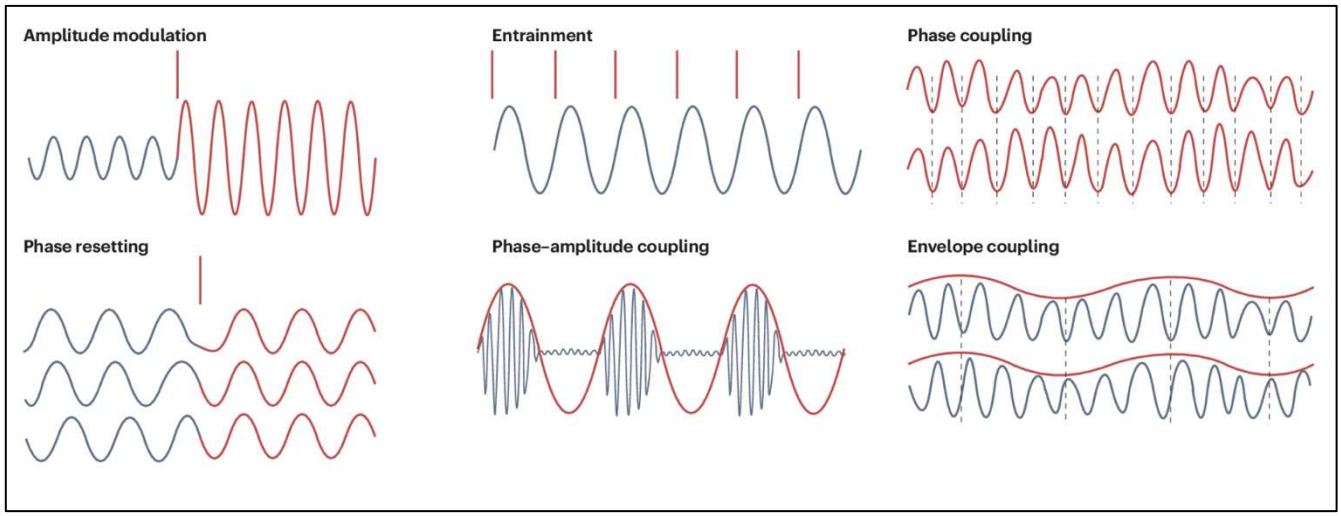

Figure 7. Different coupling patterns between different oscillations or between oscillations and stimuli

From Senkowski & Engel 2024

From a complex systems perspective, it's crucial to understand that these coupling patterns are not fixed but highly dynamic. Neural circuits generate oscillations that can vary in frequency and amplitude in response to background activity and incoming signals (Brunel & Hansel, 2006; Brunel & Wang, 2003). Despite their apparent irregularity, these dynamic patterns can still effectively route information through self-organizing mechanisms (Palmigiano et al., 2017). A single structural network can thus display multiple oscillatory patterns, creating different functional networks through

various coupling patterns of oscillatory activity (Battaglia et al., 2012; Kirst et al., 2016), illustrating the concept of *functional multiplicity*.

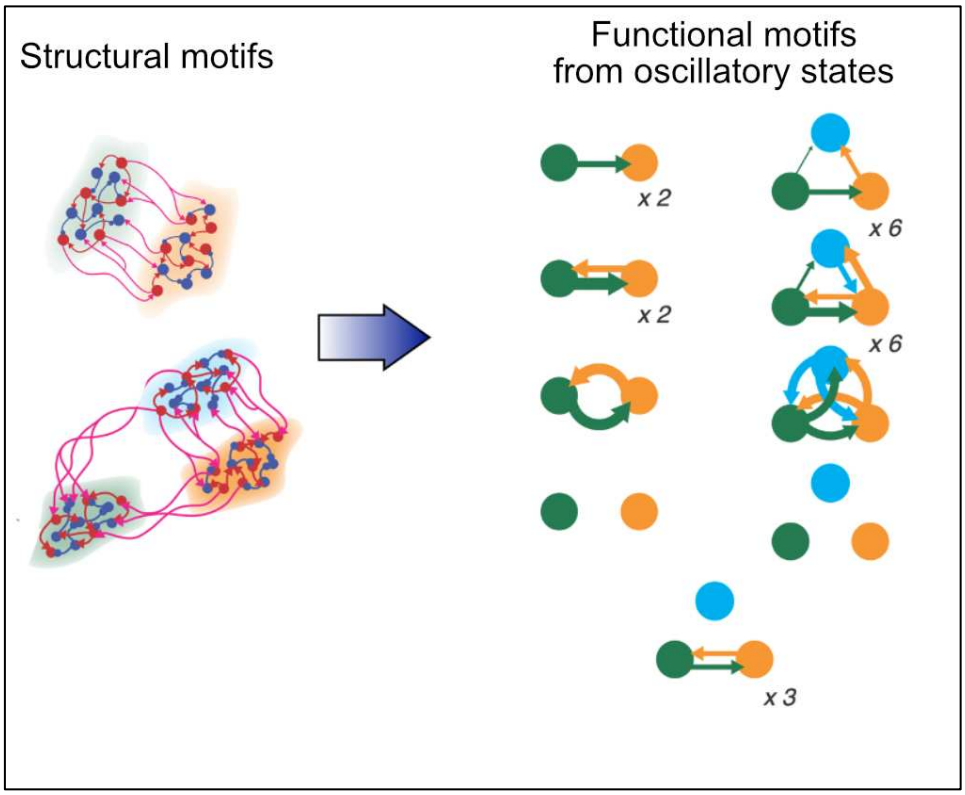

Figure 8. Functional multiplicity

Two structural networks can give rise to a multiplicity of functional motifs depending on their oscillatory states, a representation of functional multiplicity. Adapted from Battaglia et al., 2012.

This inherent flexibility in oscillatory coupling allows the brain to rapidly reconfigure its functional networks in response to changing cognitive demands, supporting various processes from attention and perception to learning and memory.

2.2.3. Brain networks dynamics

At a wider scale, activation or silencing of different regions or specific inter-regional relation can be dynamic and create recurrent patterns dynamically alternating in time to organize computation or information processing. This brain states dynamics give insight on how the brain function normally and how dynamic can be perturbed in pathologies and can be assessed by different means.

2.2.3.1. Microstates

Theoretical perspectives suggest that conscious cognition may occur as discrete, stable intervals—often called “perceptual frames” or “pulses of consciousness”—each capturing a single conscious thought or perception (Efron, 1970; James, 1890). Multichannel EEG first revealed these states, showing dynamic shifts in scalp potential with high temporal resolution. These EEG microstates are stable scalp topographies that alternate dynamically, providing a “building block” structure for conscious processing (Lehmann et al., 1987). Microstate maps generally reflect consistent spatial patterns across individuals, often associated with core networks like the Default Mode Network (DMN; Pascual-Marqui et al. 2014).

For the case of this manuscript something more interesting that the topographies per se is their dynamical alternations sequence. Interestingly, microstates sequences showed to follow a scale free dynamic in healthy humans at rest which might be the basis for the rapid reorganization and adaptation of the functional networks of the brain (Van De Ville et al., 2010). Further, disrupting the natural sequence of microstates does not affect this scale-free property, while modifying their duration does, highlighting the significance of dynamic timing (Van De Ville et al., 2010). Thus, EEG microstate dynamics offer a valuable view into the organization of brain activity, and disruptions in these dynamics have been observed in conditions like schizophrenia (for a comprehensive review, see Michel and Koenig 2018). However, due to the limited spatial resolution of EEG, microstates do not clearly delineate functional networks.

2.2.3.2. Dynamic functional connectivity and metaconnectivity

Beyond static measures, the brain’s functional connectivity dynamically shifts over time, influenced by cognitive demands. This dynamic functional connectivity (dFC) approach captures these transitions by computing connectivity within short time windows and correlating the resulting connectivity matrices. This method reveals transient network configurations that shift over time. Interestingly, the alternations between states appear to be between order and randomness, somehow approaching from a critical regime, which will enable the brain to switch rapidly between different functional states based on the cognitive demand, enabling the formation and dissolution of specific functional networks (Cabral et al., 2017). The speed of variations between the functional patterns can be impacted in pathological conditions showing a

decrease with age and can be reduced under conditions like sleep deprivation, both indicating a slowing of the brain dynamic (Battaglia et al., 2020; Lombardo et al., 2020). While dFC examines how connections between brain regions vary over time, metaconnectivity takes this analysis one step further by examining the relationships between these connections themselves. This higher-order analysis reveals networks of coordinated connectivity changes, called metahubs. A metahub represents a set of connections that tend to strengthen or weaken together over time. This organization adds another layer to our understanding of brain network dynamics, showing how the brain coordinates not just activity between regions, but entire patterns of connectivity.
The speed at which these metahub patterns change has been linked to cognitive performance, suggesting that the coordinated reconfiguration of multiple connections is important for efficient brain function (Battaglia et al., 2020). In pathological conditions, alterations in metaconnectivity patterns may reflect disrupted coordination of brain networks even before obvious changes in simpler connectivity measures are apparent. Notably, a pathological mark of metaconnectivity can be “frustration” (Vannimenus & Toulouse, 1977) where both positive and negative meta connections are occurring at the same time, thus leading to competition among the network, causing a slowing sown of the dynamic (Mézard & Parisi, 1988), a process notably observed in AD (Arbabyazd et al., 2023).

2.2.4. Nonlinear system dynamics

Brain activity emerges from complex interactions between neurons, regions and networks that cannot be totally understood through simple linear relationships. While linear systems follow the principle of superposition, where the response to combined inputs equals the sum of responses to individual inputs, brain dynamics are fundamentally nonlinear - the whole is different from the sum of its parts. This nonlinearity allows the brain to generate rich dynamics necessary for cognition, but also makes brain activity more challenging to analyze and predict.
In order to evaluate nonlinear brain dynamics, we need first to consider the time series of brain activity recorded in the phase state. The phase space is a mathematical space where all possible states of a dynamical system are represented. For brain dynamics, each point in this space might represent a particular configuration of neural activity

across multiple channels or brain regions. The system's evolution over time traces out a trajectory in this phase space.

2.2.4.1. Stability and Dimensionality

One of the main characteristics to assess the dynamics of a system resides in its stability and dimensionality. These measures allow characterization of the dynamical shape of the system and if it organizes around stable or unstable dynamical states called phase attractors. The Lyapunov spectrum represents a way to characterize dynamics system stability by capturing the rates of expansion or contraction along different directions in phase space (Wolf et al., 1985). Each Lyapunov exponent of the spectrum quantify the divergence, thus instability (if it is positive) or the convergence, thus stability (if negatitve) of nearby trajectory in the phase space.

The Lyapunov spectrum is intimately linked to the dimensionality of the system's attractor, known as Lyapunov or Kaplan-Yorke dimension. This measure estimates the number of degrees of freedom governing the systems dynamics. These measures allow to characterize the system, only negative exponent in the Lyapunov spectrum coupled with a low attractor dimension will describe a simple system where from anywhere in the phase space the system will be attracted over one stable attractor. On the other side, a positive exponent in the Lyapunov spectrum coupled with a high dimension attractor will describe a chaotic system which will be highly sensitive to the initial conditions. Indeed, when there is both negative and positive exponent in the Lyapunov spectrum, depending on the initial condition the dynamics can converge to an attractor or the trajectories in the phase space can diverge. Some prototypical attractors can also be characterized as zeros and negative exponent in the Lyapunov spectrum, describing a stable oscillatory attractor. In the brain, EEG dynamics appears to not show a specific nonlinear shape, but this system still showed changes of conformation depending on brain states with less complex dynamic shifting to lower dimension and lower maximum Lyapunov exponent during deep sleep (Stam, 2005). Thus, nonlinear characteristics of the system in the phase space can serve to measure global brain dynamics in healthy condition but also how it is impacted by pathologies, as done for epilepsy (Babloyantz & Destexhe, 1986).

2.2.4.2. Instantaneous stability and dimensions

Despite allowing first characterization of the dynamic system, previously mentioned Lyapunov measures present major caveats: they require full knowledge of the system's governing equations, extended time series data, and are not time resolved. However, while performing cognitive tasks, one could expect that the dynamic system can switch between stable and unstable conformations to allow complex dynamic patterns favoring information processing.

Recent advances in dynamical systems analysis have introduced metrics derived from extreme value theory that overcome these limitations. Two key metrics are inverse persistence (θ) and instantaneous dimension. Inverse persistence, mathematically linked to the extremal index in extreme value theory, quantifies how frequently a system transitions between states. A lower θ value indicates higher stability (the system stays in states longer), while higher values suggest more frequent state transitions. This metric thus reflecting fluidity of the system. The instantaneous dimension characterizes the density of neighboring states around a given configuration, reflecting local predictability and complexity.

These metrics are particularly valuable because they can be computed from empirical time series data alone, without requiring knowledge of the underlying system equations. While initially developed for studying atmospheric flows and extreme weather events (Faranda et al., 2017), these approaches are well-suited for analyzing brain dynamics. Just as atmospheric flows are characterized by chaotic dynamics and recurring large-scale patterns, brain activity shows similar complexity with transitions between different functional states.

When considering the brain as a dynamical system, early disease stages might manifest as changes in these instantaneous properties rather than global shifts in system behavior. Evaluating instantaneous system properties like persistence (or its inverse, fluidity) and dimension could thus represent a promising approach to understand brain functioning in healthy and pathological conditions. In this thesis manuscript, you will further see how we used instantaneous brain dynamics fluidity to assess early AD pathology, offering insights into system stability that may be difficult to access via traditional Lyapunov analysis as classical algorithms (Grassberger & Procaccia, 1983) require way more data to properly converge.

2.2.4.3. Energy landscapes

Attractors can be characterized as previously through stability measurement. However, they can also be seen as energy sink. Indeed, the system dynamics can be represented as a ball rolling on a plane comporting sink and hills, if the ball go up a hill, it will rapidly fall from this hill, on the contrary if it falls into a sink, it will most probably stay inside it and will require a lot of energy to get out of it. In this context, sinks will represent the most probable dynamical states, thus being low energy states and being attractors. On the contrary, hills represent less probable high energy unstable states. These energy landscapes can be determined using statistical approach as Maximum Entropy models which aims to find the distribution displaying the highest entropy that satisfy the observed constrain, the energy here is referred to the information-theory definition of energy instead of the metabolic one and will mainly represent the probability of appearances of states. These energy landscapes have been applied to brain functional and structural networks data and used to characterize resting states brain networks (Watanabe et al., 2014), showed to be appropriate to describe module dynamics in the human brain connectome (Ashourvan et al., 2017), and showed to be link to structural connectivity (S. Gu et al., 2018). Combining energy landscapes and previously discussed instantaneous fluidity and dimension could thus be a promising approach to properly characterize system dynamics. Would reduced fluidity result from the creation of a new energy sink or the deepening of an existing one? Examining these energy patterns would then allow to identify the networks implicated in these specific energy and fluidity patterns.

2.2.4.4. Latent neural manifolds

When it could be difficult to interpret data in the phase space, one can try to approach the representation of these phase space by using nonlinear embeddings of the multidimensional data to represent it in a lower dimensional space. Classical nonlinear embeddings would be the t-Stochastic Neighbor Embedding (t-sne, Maaten and Hinton 2008) or Isomap which were recently widely used in neurosciences (Mitchell-Heggs et al., 2023). Thus, when the multidimensionnal activity is mapped into a low-dimensional “latent” space, the projection of dynamic trajectories tend to sample a so-called “neural manifold” (Mitchell-Heggs et al., 2023), possibly reflecting the non-linearly deformed projection of strange attractors of the dynamics existing in the original full-dimensional

phase space. These manifolds reveal patterns in brain activity without predefined assumptions about regional or cellular interactions, offering an unbiased perspective on neural organization, as for the phase space nonlinear analyses. Remarkably, manifold shapes often vary with cognitive task demands, positioning the brain in different parts of the manifold depending on the task phase and cognitive or motor requirements (Gallego et al., 2017). Manifold structures commonly include “attractors” which are more or less dynamically stable states of the system around which the dynamical system will organize to gain stability (Dudkowski et al., 2016). In the study of neural manifolds, those attractors will mostly shape the manifold in some stereotypical stable shapes. These attractors can vary with cognitive demands, moving from simple, one-dimensional forms (e.g., ring attractors) to complex, multi-dimensional forms as the brain shifts between states (Chaudhuri et al., 2019). Organized trajectories in low-dimensional space thus provide insight into the intricate dynamics underpinning cognitive processes, revealing how the brain leverages stability and flexibility to respond to changing conditions. However, nonlinear embeddings can’t represent the whole complexity of the phase space and while they represent a good tool to reveal patterns and identify clusters in high-dimensional data they don’t maintain necessarily the dynamic relationship between states. Additionally, depending on the chosen embedding, different multi-dimensional relationships will be prioritized. For instance, t-SNE preserves local structure but may distort global relationships, whereas Isomap aims to preserve geodesic distances along the manifold.

2.2.4.5. The arrow of time

Recently, new nonlinear approaches have emerged for measuring information processing in brain systems over time, particularly through EEG and BOLD signals, using principles rooted in thermodynamics. The second law of thermodynamics states that closed systems naturally evolve toward increased entropy, introducing an inherent direction in the sequence of events, known as the “thermodynamic arrow of time” (Eddington, 1928; Schrödinger, 1929). This arrow of time reflects an asymmetry between reversible and irreversible processes, distinguishing systems in reversible equilibrium from those in irreversible nonequilibrium states (Seif et al., 2021).

In the context of brain dynamics, recent studies suggest that large-scale, self-organizing processes in the brain operate away from thermodynamic equilibrium,

enabling a state of dynamic multistability. This nonequilibrium regime allows the brain to sustain diverse and adaptable states, contributing to healthy neural function (Deco et al., 2017; Demirtaş et al., 2019; Fingelkurts & Fingelkurts, 2004; Luppi et al., 2019; Sanz Perl et al., 2021). A key finding in this field is the positive correlation between the complexity of brain dynamics and the degree of temporal irreversibility, supporting the idea that complex, healthy brain activity relies on nonequilibrium dynamics (Deco et al., 2022).

This temporal asymmetry provides a unique "signature" that mirrors the intricacy of the brain's functional organization. Importantly, studies have linked this temporal irreversibility to the level of consciousness (De La Fuente et al., 2023; Sanz Perl et al., 2021), differentiation of brain states (Camassa et al., 2024), cognitive performance (Deco et al., 2021; Ibanez, 2022; Lynn et al., 2021), and variations seen in neuropsychiatric conditions (Zanin et al., 2020). These insights underscore the role of nonequilibrium dynamics not only in maintaining cognitive and functional health but also in defining the brain's adaptability and responsiveness.

2.2.5. Across the scales: the brain criticality

In nature, plenty of different dynamical system exists over different scales. However, whereas it is bird flawks, fireflies' population, or the brain, these systems are believed to display a specific type of collective behavior in which nature produce complexity, the criticality (Bak, 2013; Langton, 1990; Sarfati et al., 2021; Vanni et al., 2011).

In the brain, criticality firstly emerge from a dynamic characteristic of neuronal firing, the propagation of activity from one neuron to others, a phenomenon known as a neuronal avalanche (Beggs & Plenz, 2003). An avalanche occurs when an initially active neuron triggers the firing of one or more other neurons through their connections, creating a "chain reaction" (O'Byrne & Jerbi, 2022). The size of an avalanche (i.e., the number of neurons involved) and its duration (i.e., the time between the initiation and resolution of the avalanche) define the dynamical regime of the system, often modeled after the Ising model (O'Byrne & Jerbi, 2022).

In a subcritical regime, the system is disordered, with weak coupling between neurons. This results in small, short-lived avalanches, limiting the spread of neuronal firing. In contrast, a supercritical regime is highly ordered, with strong coupling that leads to large, prolonged avalanches, where the firing of a few neurons can activate the entire

network. At the critical point, the system strikes a balance between these two extremes—each neuronal spike gives rise to, on average, one additional spike. This balance prevents avalanches from either dying out too quickly or spreading uncontrollably across the entire network. Avalanches at the critical point exhibit scale invariance, meaning their patterns look similar across different scales, and their size and duration follow a power-law distribution (Beggs & Plenz, 2003).

This scale free parameters observed at criticality coupled to the fact that neuronal firing is believed to modulate higher scale brain activity, allowed to observe critical avalanche at different brain scales as in LFP where avalanche were based on negative deflections of the LFP in monkey cortical recordings (Petermann et al., 2009), in EEG where avalanches were based on high amplitude events in the EEG (de Arcangelis et al., 2006) and in fMRI signals (Tagliazucchi et al., 2012).

It is believed that brain activity hovers slightly below criticality, in a near-critical regime, and some cortical regions have been shown to function near a critical regime in vivo (Ma et al., 2019). This balance depends on a proper equilibrium between excitation and inhibition, where excessive inhibition drives the system toward a subcritical state, and excessive excitation pushes it toward supercriticality (Poil et al., 2012). Having the brain functioning in vivo at a critical state would thus be beneficial as it has been shown to be the best regime for computation as it maximizes the dynamic range (i.e. the range of different input signals a cortical circuit can process), the fidelity of information transmission and the information capacity (Shew & Plenz, 2013).

More than critical avalanching, the brain criticality dynamical regime also implied the brain to function at the edge of chaos, at the phase transition point between an ordered and a chaotic system. This concepts link with phase space stability previously discussed as it mainly relies on the phase space pattern of the system. The edge of chaos would help the system to perform optimally by maximizing the network's information storage and information transfer properties (Boedecker et al., 2012) and maximizing the signal to noise ratio of network inputs (Toyoizumi & Abbott, 2011). The chaos is difficult to assess in brain data notably through computation of Lyapunov spectrum as the intial state of the system is unknow. However, measure as Lempel-Ziv complexity, a measure used to assess the complexity and the richness of time series depending on how much the information of this time serie can be compressed, were used to assess the chaos in the system as it was proposed to being maximized at the edge of chaos (Toker et al., 2022). This edge of chaos regime has been observed in

awake human and monkeys and reduced in anesthetized states (Toker et al., 2022). It is to note that edge of chaos and brain criticality are not mutually exclusive as balance between excitation and inhibition, primordial parameter for avalanche criticality, does not appear to be a prerequisite to transition dynamics between stability and chaos (Haldeman & Beggs, 2005). However, excitatory only edge of chaos networks does not seem to display the rich repertoire of nonlinear transformations and diverse integration timescales that make the excitatory-inhibitory version of the edge of chaos so appealing (Dahmen et al., 2019; Morales et al., 2022; Wainrib & Touboul, 2013).
Thus, the brain criticality framework can complement the observation done in the phase space of the dynamical system by giving insight on the optimal functioning regime of the brain to store, transfer and process information, regardless of the scale of the system observed, from neuronal firing to whole brain activity.

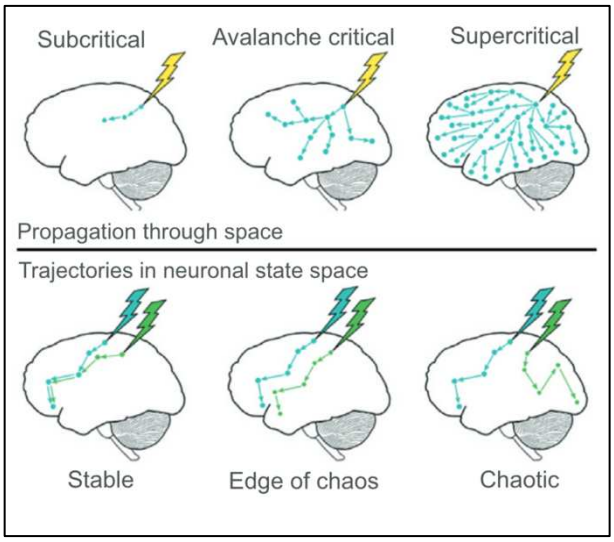

Figure 9. Critical regime of the brain

Avalanche criticality (Top) and Edge of Chaos (Bottom) regimes in the brain. Adapted form O'Byrne & Jerbi 2022

2.3. Brain Dynamics and Memory

Since brain dynamics play a crucial role in information processing, it thus appears essential for the proper establishment of memory processes, which are a key element of this manuscript. This section will explore the involvement of brain dynamics in various well-studied memory processes.

2.3.1. Recognition memory

Recognition memory represents an example of how brain dynamics support cognitive function through multiple complementary mechanisms. It is proposed that recognition memory relies on attractor dynamics within neural networks. When memories are initially formed, specific assemblies of neurons fire together, strengthening their synaptic connections through Hebbian plasticity. These strengthened connections create stable attractors in the network's state space, each corresponding to a distinct memory trace. When a familiar stimulus is encountered, sensory inputs guide neural activity toward these pre-established attractors. This dynamic process not only enables direct recognition but also supports pattern completion (i.e. the ability to reconstruct complete memories from partial or degraded cues), as even incomplete inputs can drive the system toward the appropriate attractor basin (Daelli & Treves, 2010).

However, recognition memory is not solely based on attractor dynamics for detecting familiarity. It also critically depends on the brain's ability to detect novelty through distinct dynamical processes. In a NOR task, the HPC exhibits increased theta oscillatory power when exploring the new object, potentially signaling the detection of new information. This novelty response involves coordinated dynamics between the HPC and PFC, primarily through theta-frequency synchronization mediated by direct projections from the HPC to the PFC, thereby establishing a functional circuit for novelty processing. The importance of this dynamic interaction is underscored by findings that disrupting HPC-PFC theta coupling impairs performance in novel object recognition tasks (C. Wang et al., 2021).

These complementary dynamic processes - attractor-based familiarity detection and oscillation-mediated novelty detection - work together to enable flexible and reliable recognition memory.

2.3.2. Spatial Memory

Spatial memory is believed to mainly rely on the constant comparison in HPC CA1 between current sensory inputs, or the encoding of the information, arriving from the EC and stored memories in CA3, or the retrieval of past information (Hasselmo et al., 2002).

To decipher the origin of inputs and thus compare encoding and retrieval processes, Hasselmo proposed in 2002 that these two information channels would be temporally

segregated by occurring at different phases of the theta oscillation in CA1. According to this model, encoding-related inputs from the EC arrive at the trough of the theta oscillation when CA3 inputs are weak, while retrieval-related processes occur at the peak of theta when CA3 inputs are strong and entorhinal inputs are weak. This temporal segregation hypothesis has been further developed by subsequent studies, suggesting that the encoding and retrieval information streams are additionally channeled through distinct gamma frequency bands (Colgin et al. 2009; Schomburg et al. 2014; Lopes-dos-Santos et al. 2018; for review, see Aguilera et al. 2022). However, a recent study examining individual gamma bursts, rather than averaged gamma activity, revealed that the hippocampal dynamics underlying the separation between encoding and retrieval are more complex than initially proposed, exhibiting a high diversity of possible theta-gamma coupling patterns in the HPC. While this diversity may initially appear as noise, it carries meaningful information about the animal's location within a maze (Douchamps et al., 2024). This dynamic organization of inputs ultimately shapes the firing patterns of place cell sequences in CA1. Place cell activity is precisely coordinated by these underlying oscillations, with theta cycles providing a temporal framework for organizing place cell sequences through successive gamma cycles (Lisman & Buzsaki, 2008). This precise temporal organization of place cell firing significantly contributes to spatial memory processes.

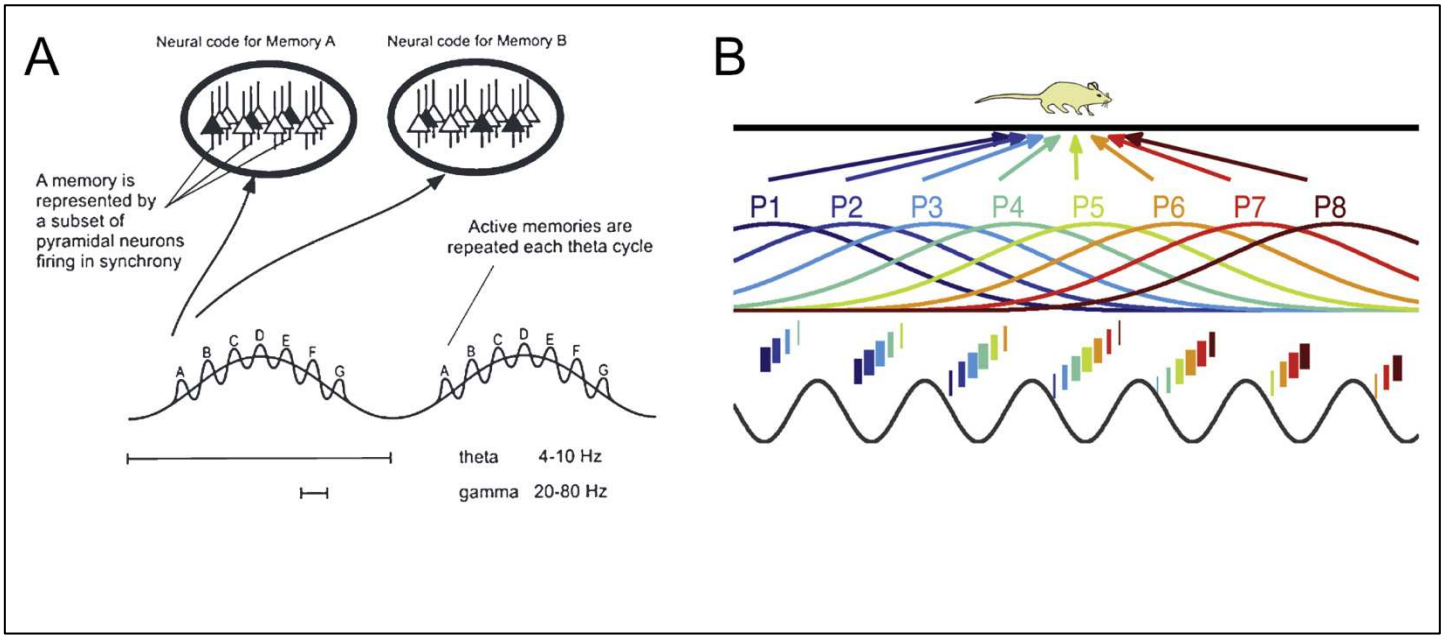

Figure 10. Theta-Gamma modulation of cell assemblies

(A) Modulation of cell assemblies firing by Theta and Gamma rhythms. (B) Theta phase modulation of place cell sequences showing phase precession. Adapted from Lismann & Buzsaki 2008 and Buzsaki 2010

2.3.3. Memory Consolidation

When new memories are formed, they initially exist as fragile traces that require consolidation to achieve long-term stability, enabling future recall or updating. This consolidation process relies on a coordinated dialogue between the HPC and the neocortex, primarily occurring during sleep, particularly in slow-wave sleep (SWS), following learning. In this low-ACh state, the brain is better equipped to process internal information without interference from external inputs, a concept known as the 'two-stage' model (Buzsáki, 1989; Girardeau & Zugaro, 2011; Hasselmo, 1999).

Memory consolidation depends on specific brain oscillations that synchronize activity across regions. In the HPC, high-frequency events known as sharp wave-ripples (SPW-Rs) represent the synchronized activation of large groups of neurons, occurring at a frequency that supports synaptic modifications or spike-dependent plasticity (Girardeau & Zugaro, 2011). During SPW-Rs, hippocampal neurons replay activity sequences from prior experiences in a temporally compressed format (A. K. Lee & Wilson, 2002; M. A. Wilson & McNaughton, 1994). This temporal compression allows neuronal firing to align with timeframes that facilitate synaptic plasticity, potentially strengthening memory traces.

Simultaneously, during SWS, the neocortex alternates between periods of high and low population activity, referred as UP and DOWN states. These alternations are translated in the LFP by specific patterns, in particular DOWN states are associated with LFP deflection known as Delta waves. Although often used interchangeably, delta oscillations and delta waves are distinct concepts; delta oscillations refer to brain activity within the 1-4 Hz frequency range, while delta waves are slow events specifically related to DOWN states. In other words, while delta waves can occur within delta oscillations, delta oscillations do not equate to delta waves. These delta waves in the cortex are followed by spindles, oscillatory patterns that range between 10 and 15 Hz and arise from thalamocortical interactions. These cortical rhythms are precisely coordinated with hippocampal sharp wave-ripples (SPW-Rs), which tend to occur as cortical neurons transition to UP states and align with the troughs of spindles (Maingret et al., 2016; Sirota et al., 2003). This timing is believed to facilitate effective communication between the HPC and neocortex during memory consolidation.

While SW-Rs are necessary for memory consolidation as suppressing hippocampal ripples during post-learning sleep impairs spatial memory consolidation (Girardeau et

al., 2009), the dynamic timing of these hippocampal and cortical patterns seems to play a fundamental role. Specifically, the artificial enhancement of hippocampal SW-Rs and cortical Delta wave coupling during post-learning SWS increased memory consolidation (Maingret et al., 2016). These findings underscore the importance of precise timing in hippocampal-cortical interactions for successful consolidation.

SWS is not the only sleep stage contributing to consolidation, as theta oscillations during REM sleep have also been linked with memory consolidation. Disruptions in theta oscillations during post-learning REM sleep impair memory retention, further underscoring the multi-stage nature of memory consolidation (Boyce et al., 2016).

At a more global scale, the communication between HPC and cortex might not engage the entire cortex simultaneously. During sleep, slow wave activity does not occur uniformly across the cortex. Instead, different cortical regions can transiently enter slow wave states independently, a phenomenon known as local sleep (Vyazovskiy et al., 2011). These local sleep patterns appear to play an important role in memory consolidation, as they may allow different cortical regions to sequentially process hippocampal inputs. The spatial distribution of these local sleep patterns is not random but appears to target cortical areas that were more active during prior learning experiences (Huber et al., 2004; Tononi & Cirelli, 2014).

In summary, memory consolidation relies on dynamic processes that span both local and global brain scales, involving region-specific oscillatory synchronization and broader spatial patterns of cortical activity during sleep.

2.3.4. Working memory

Not every memory or event can be consolidated during sleep, as some information needs to be stored only temporarily for rapid recall. For this purpose, working memory is employed, defined as a system for maintaining and manipulating information over short periods (Baddeley, 1986). A key brain region implicated in working memory is the PFC, as it is active during working memory tasks (Funahashi, 2006; Leung et al., 2002; Ungerleider et al., 1998; Zarahn et al., 2000) and its lesions affect working memory performance (Goldman-Rakic, 2011; Milner, 1963). Importantly, the buffering of information within the PFC is largely facilitated by dynamic processes.

One key dynamic process involves the transfer of the memory trace to the PFC, facilitated by long-range functional interactions between the HPC and the PFC.

Notably, this transfer relies on a previously mentioned dynamic pattern: theta-gamma phase-amplitude coupling (PAC). During working memory tasks, a coupling emerges between the amplitude of gamma oscillations in the PFC and the phase of hippocampal theta oscillations. This coupling intensifies with longer memory retention periods, particularly when task delays are introduced or when tasks increase in complexity (Tamura et al., 2017). It is believed that this theta-gamma PAC organizes PFC firing activity in relation to hippocampal dynamics.

Interestingly, the PFC exhibits attractor networks with recurrent excitatory connections among pyramidal neurons, allowing these networks to maintain stable patterns of neuronal activity even after the stimulus is removed, thereby enabling short-term memory maintenance (Deco & Rolls, 2003). However, this 'memory maintenance' is based on a dynamic representation instead of a stable one, as decoders trained to decode the identity of visual stimuli when visible based on PFC neural activity were unable to decode the memory of this stimulus even after a short 250 ms delay (Stokes et al., 2013). Finally, on a larger scale, working memory appears to rely on critical regime functioning within the brain. Individuals exhibiting whole-brain avalanche activity closer to criticality demonstrate more complex functional connectivity and improved performance in working memory tasks (Xu et al., 2022, p. 202).

2.4. Brain Dynamics in Pathological conditions

2.4.1. Epilepsy

Epilepsy provides a striking example of how disrupted brain dynamics can lead to pathological states. During seizures, the excitatory/inhibitory balance of neural activity is disturbed, resulting in hyperexcitation and hypersynchronization, where large populations of neurons fire together in an excessive and coordinated manner, leading to an epileptic seizure. However, this process is not trivial, as seizures can be divided into three distinct phases: onset, propagation, and termination, each exhibiting unique network alterations (for review, see Kramer and Cash 2012). Interestingly, variations in brain dynamics can be observed during different stages of a seizure, which may explain some of the associated symptoms. During the seizure, the dFC speed is significantly reduced, with no changes in functional network configuration, placing the brain in a "frozen" state. As the seizure recovers, dFC speed increases, but the

dynamics remain unorganized, resembling more of a “gas” state. During this period, patients may experience a specific language impairment known as aphasia, which is characterized by a loss of the ability to express language. Subsequently, the dFC gradually regains organized dynamics, allowing the return to a healthy “liquid” state, which is associated with the recovery of language abilities (Pedreschi et al., 2024). This underscores that dynamic activity alone is insufficient for proper cognitive processes; instead, organized dynamics are crucial. The impact of epilepsy is not limited to seizure activity. Indeed, outside of seizures, epileptic patients can exhibit small electrical events known as interictal spikes, which predominantly occur during sleep. Furthermore, epilepsy appears to perturb information processing complexity in a permanent manner, potentially contributing to cognitive impairments in epileptic patients (Clawson et al., 2023). Interestingly, epileptic activity is also commonly reported in AD, with comorbidities ranging from 2.1% to more than 50% (F. Yang et al., 2022).

2.4.2. Alzheimer’s disease

AD is characterized by significant alterations in brain dynamics, with one of the first observable network changes being neuronal hyperactivity. This hyperactivity is first noted in clusters of hyperactive neurons located near amyloid plaques (Busche et al., 2008). Interestingly, signs of hyperactivity may emerge earlier in the disease and are often associated with symptoms commonly seen in epilepsy, a major comorbidity among AD patients, particularly those with genetically linked early-onset forms (Horváth et al., 2018; Lam et al., 2020; Vossel et al., 2016). In AD, hyperexcitability is frequently indicated by the presence of interictal spikes during sleep in mouse models, which serve as markers of pathological hypersynchrony within neural networks (Bezzina et al., 2015; Palop et al., 2007; Szabo et al., 2023; Verret et al., 2012). This hyperactivity is thought to stem from dysfunction in inhibitory interneurons expressing parvalbumin, which directly influence the activity of pyramidal neurons that become hyperactive in AD. These interneurons are crucial for generating gamma rhythms, which have been shown to be diminished in both AD mouse models and patients (Casula et al., 2022; Hamm et al., 2017; Iaccarino et al., 2016; Verret et al., 2012). Notably, restoring the normal functioning of PV interneurons in an animal model of AD

has been shown to enhance gamma activity, reduce hyperactivity, and improve cognitive function (Verret et al., 2012). These alterations in gamma activity will be a key focus in Chapter III of this introduction.

However, reductions in gamma oscillations are not the sole oscillatory alterations observed in AD. The PAC between theta and gamma oscillations, critical for memory processes discussed in the previous chapter, is disrupted in the HPC before the accumulation of Aβ (Goutagny et al., 2013).

This finding indicates broader shifts in the functional dynamics of oscillatory networks in AD, characterized by what is referred to as a "slowing of the EEG" (Dauwels et al., 2011). Specifically, while the power of higher frequency rhythms such as gamma and beta is diminished, there is an increase in the power of slower rhythms like delta and theta, resulting in this overall slowing effect (Baker et al., 2008; Claus et al., 1998; Czigler et al., 2008; Moretti et al., 2009; van der Hiele et al., 2007).

At a larger scale, a general slowing of dynamics is also observed in AD. EEG microstate analysis has shown that the sequences are less dynamic, characterized by longer durations of individual microstates (Lian et al., 2021; Tait et al., 2020). As previously mentioned, alterations in the duration of microstates can affect the scale-free dynamics of these sequences (Van De Ville et al., 2010). In fact, AD patients exhibit not only reduced dynamic state transitions but also fewer complex microstate sequences, as evidenced by a decrease in Lempel-Ziv complexity, suggesting a shift away from the system's edge of chaos (Tait et al., 2020). Analysis of dynamic large-scale brain networks through dFC reveals that AD is associated with disordered spatiotemporal fluctuations that are characteristic of healthy dFC (Arbabyazd et al., 2023; Canal-Garcia et al., 2024; Y. Gu et al., 2020; Núñez et al., 2021; Schumacher et al., 2019). Notably, during resting states, AD patients demonstrate reduced network flexibility and increased integration among regions in different resting state networks, indicating a loss of dynamic capability (Canal-Garcia et al., 2024). Furthermore, brain dynamics in AD patients was found to become trapped in hypersynchronized states, leading to alterations in meta-connectivity and a general "frustration" within the system, which contributes to a slowdown in dynamics (Arbabyazd et al., 2023). These observations align with the previously discussed loss of system complexity (Tait et al., 2020). Additionally, studies using fMRI and EEG have shown that AD is associated with reduced irreversibility in neural signals, correlating with cognitive decline and atrophy (Cruzat et al., 2023).

In summary, AD is marked by dynamic alterations at multiple scales, all converging towards a diminished repertoire of dynamic regimes and a loss of complexity. These changes negatively impact the healthy functioning of brain networks, undermining the capacity to generate efficient cognitive processes.

2.5. Take home message

After going through several key aspects of brain dynamics here is some important points to summarize this first chapter:

- **Brain activity not only rely on structural network but importantly on dynamics functional networks**
- **Brain dynamics manifest at every scale of brain networks, from cellular to system levels, and are displayed across these scales.**
- **The brain functions as a global nonlinear system, operating within an optimal critical regime between order and chaos**
- **Brain dynamics is necessary for cognitive processes such as memory**
- **Brain dynamics is altered in various ways in AD.**

Brain dynamics, therefore, form a foundation for brain functioning and for supporting cognitive processes. In pathological conditions, changes in brain dynamics may emerge before structural or histological markers. Given the noninvasive methods for assessing brain dynamics, such as EEG and fMRI, studying these dynamics could offer promising avenues for earlier diagnosis and a better understanding of diseases like AD. Finally, interventions targeting abnormal brain dynamics might be a viable therapeutic strategy, especially considering that sensory stimuli can directly influence these dynamics.

3. Sensory stimulations to cure AD: the GENUS

Recently, a new noninvasive therapy consisting in multi-sensorial stimulation at a 40 Hz frequency called Gamma ENtrainment Using Sensory stimulus (GENUS) (Singer et al., 2018) is getting more and more attention after providing surprisingly interesting results in AD and other neuropathology.

3.1. GENUS and AD

GENUS was firstly developed against AD pathology and is still now mainly studied in the AD pathology context.

3.1.1. Why we started flickering light in AD

An important question arises: how did we come to use 40Hz light or sound flicker as a potential treatment for AD? While it may seem unconventional at first, this approach is grounded in findings that gamma oscillations are disrupted in AD mouse models. If you recall our discussion in the previous chapter, we highlighted how, in AD, gamma oscillation disruptions are linked to altered function of PV-expressing fast-spiking interneurons. In 2012, Verret and collaborators demonstrated that the hAPP J20 mouse model exhibits alterations in PV interneurons, notably a reduced expression of NaV1.1 channels. These voltage-gated sodium channels, critical for generating action potentials in PV interneurons, support their inhibitory action and help regulate the excitatory-inhibitory balance in cortical networks. In the hAPP J20 model, NaV1.1 downregulation was associated with diminished gamma oscillations (20–80 Hz range) and impaired memory. Remarkably, increasing NaV1.1 levels specifically within PV interneurons in these hAPP J20 mice restored gamma activity and reduced memory deficits (Verret et al., 2012). Furthermore, it was found that the 5XFAD mouse model displays reduced hippocampal slow gamma (30–50 Hz) activity during SW-R events, which is associated with elevated levels of Aβ without significant plaque accumulation or evidence of cognitive impairment (Iaccarino et al., 2016). Together, these results indicate that alterations in gamma oscillations may serve as a proxy for cortical and hippocampal network disruptions in AD. As such, restoring gamma activity might positively impact the pathology.

To test this hypothesis, Iacarrino and colleagues built on findings that optogenetically driving PV interneurons at 40Hz increases cortical gamma power (Cardin et al., 2009). They therefore stimulated CA1 PV cells at 40 Hz to modulate hippocampal gamma oscillations. One hour of this stimulation indeed increased 40Hz LFP power in CA1, but more intriguingly, it also reduced levels of both $A\beta_{40}$ and $A\beta_{42}$ peptides in this region. This effect appeared to result from decreased production of Aβ, as reductions in APP cleavage byproducts, such as C-terminal fragments (CTFs), were also observed after one hour of stimulation. These results suggest that driving hippocampal PV cells at 40Hz (and thereby increasing gamma oscillations) reduces amyloid pathology.

As promising as this approach may be, optogenetic stimulation of specific neural types is not easily transferable to Human patients. However, many studies have shown that visual stimulation can drive oscillations in the gamma range (Fries et al., 2007; Gray et al., 1989). They therefore wondered whether visual 40Hz stimulation could similarly drive gamma oscillations and exhibit the same beneficial effects. One hour of 40Hz visual flicker successfully induced 40Hz oscillations in the visual cortex and reduced levels of both soluble and insoluble $A\beta_{40}$ and $A\beta_{42}$ in this brain area. Strikingly, the effect was specific to 40 Hz flicker as neither constant light nor 20 Hz, 80 Hz, or random flicker significantly reduced A*β* levels compared to dark and light controls. Finally, a seven-day chronic protocol of one hour daily visual stimulation reduced amyloid plaque load in the visual cortex of six-month-old 5XFAD mice (Iaccarino et al., 2016).

Since the publication of this seminal paper, the 40Hz external stimulations have been termed Gamma ENtrainment Using Sensory stimuli (GENUS) and have become the subject of intense research.

3.1.2. GENUS beneficial effects in AD

While GENUS began as a visual stimulation protocol, it has been expanded to test multiple sensory modalities, including vibrotactile stimulation (Suk et al., 2023). However, it quickly evolved to combine visual and auditory stimuli, which showed superior results (Martorell et al., 2019). Among the most compelling evidence for GENUS efficacy is its consistent improvement of cognitive performance across multiple AD mouse models and age groups. Studies have demonstrated the restoration of spatial memory (Adaikkan et al., 2019; S. Liu et al., 2023; Martorell et al., 2019) and

object recognition memory (Martorell et al., 2019; Murdock et al., 2024). However, the mechanisms underlying these beneficial effects remain incompletely understood, with several hypotheses proposed to explain the therapeutic actions of GENUS.

3.1.2.1. Gamma oscillations restoration hypothesis

Non-invasive GENUS stimulation has been shown to entrain 40Hz oscillations and modulate neuronal firing across multiple brain regions, including the auditory, visual, somatosensory, and prefrontal cortices, as well as the HPC (Adaikkan et al., 2019). As mentioned earlier, gamma oscillations are consistently decreased in animal models of AD and in human patients. Given the purported role of gamma oscillations in organizing cell assemblies and facilitating network interactions (Buzsaki, 2006), the induction of gamma activity through GENUS may contribute to improvements in memory function. Accordingly, recent evidence shows that GENUS can strengthen gamma coordination between hippocampal CA3 and CA1 regions, potentially contributing to improved spatial memory performance (Paulson et al., 2024).

3.1.2.2. The focus on amyloid hypothesis

Given the initial observations of GENUS effects on Aβ peptide and amyloid plaques (Iaccarino et al., 2016) and the prominence of the amyloid hypothesis in AD research (Selkoe & Hardy, 2016), early mechanistic studies focused on amyloidopathy as a primary explanation for GENUS's cognitive benefits. Non-invasive GENUS stimulation reduced neurodegeneration (Adaikkan et al., 2019) and decreased concentrations of both soluble and insoluble $A\beta_{40}$ and $A\beta_{42}$, along with reduced amyloid plaque load across several regions (S. Liu et al., 2023; Martorell et al., 2019; Shen et al., 2022). While initial evidence suggested that reduced Aβ levels might stem from decreased production—specifically, through reduced amyloidogenic APP processing by β-secretase and enhanced non-amyloidogenic α-secretase pathways (Iaccarino et al., 2016; Shen et al., 2022)—subsequent research has emphasized enhanced Aβ clearance mechanisms through multiple pathways. First, it modifies microglial activity through several mechanisms: altering microglial morphology (Iaccarino et al., 2016; Martorell et al., 2019), reducing neuroinflammation (Adaikkan et al., 2019), and promoting microglial clustering around amyloid plaques, which increases Aβ uptake (Iaccarino et al., 2016; Martorell et al., 2019). Second, GENUS enhances brain vascular function by promoting arterial pulsatility and vascular flow, particularly through

astrocytic modulation (Martorell et al., 2019; Murdock et al., 2024). Finally, it facilitates Aβ clearance via the glymphatic system through regulation of Aquaporin 4 channels (Murdock et al., 2024).

According to this amyloid-centric framework, GENUS would improve cognitive function primarily by enhancing brain Aβ clearance through both microglial and glymphatic pathways. This reduction in pathological Aβ levels would then lead to improved neuronal function and reduced AD pathology. However, as discussed later, recent studies have challenged aspects of this mechanism, indicating the need to explore additional explanatory frameworks.

3.1.2.3. Neuroprotection, Neurogenesis and synapse plasticity

Beyond its effects on amyloid pathology, GENUS demonstrates multiple beneficial effects that could contribute to improved AD outcomes. Chronic GENUS exposure reduces neurodegeneration and provides direct neuroprotective benefits by upregulating cytoprotective proteins and reducing DNA damage (Adaikkan et al., 2019). This neuroprotective effect is particularly significant given that AD is primarily a neurodegenerative disease.

The protective effects of GENUS extend beyond neurons to include white matter integrity. In AD, myelin sheaths produced by oligodendrocytes undergo significant alterations, impairing axonal signal transmission (Nasrabady et al., 2018; Y. Wu et al., 2017). Recent studies demonstrate that GENUS can reduce demyelination, prevent oligodendrocyte loss, and stimulate oligodendrogenesis in models of demyelination, suggesting a potential mechanism for maintaining functional neural connectivity (Rodrigues-Amorim et al., 2024).

In addition to its protective effects, GENUS may also promote the generation of new neurons. While adult neurogenesis is typically limited to specific brain regions like the hippocampal dentate gyrus or the olfactory bulb and produces relatively few neurons (Gage, 2019), recent studies indicate that GENUS can enhance this process. This neurogenic effect appears to depend on parvalbumin-expressing interneurons and correlates with improved cognitive function (Islam et al., 2024; Yan et al., 2024).

3.1.3. Too good to be true?

Recent studies have raised important questions about several fundamental aspects of GENUS and its purported mechanisms of action. A primary point of debate concerns

the nature of the induced oscillatory activity. While most GENUS studies report "increased gamma power" during stimulation, careful analysis reveals that this increase primarily manifests as an acute peak in the power spectrum at 40Hz, directly driven by the stimulation frequency. This has led to the argument that GENUS may not actually entrain native gamma oscillations or physiological gamma oscillators, but rather drives brain regions at 40Hz, suggesting a distinct process that initially proposed with different mechanistic implications (Duecker et al., 2021; Soula et al., 2023).

A second significant debate centers on the spatial extent of GENUS effects. While initial studies reported 40Hz entrainment spreading to distant regions including the HPC and PFC (Adaikkan et al., 2019; Martorell et al., 2019), recent investigations suggest more limited spatial propagation. Some studies report that visual 40Hz entrainment barely extends beyond the visual cortex and is notably absent in the HPC (Schneider et al., 2023; Soula et al., 2023). Interestingly, the strongest entrainment appears in the Lateral Geniculate Nucleus excitatory cells, while visual cortex activation preferentially targets parvalbumin-expressing fast-spiking interneurons (Schneider et al., 2023).

The third major point of contention concerns GENUS's effects on amyloid pathology. Recent studies have failed to replicate the reported reductions in amyloid plaque load following GENUS stimulation (Soula et al., 2023; Y. L. Yang & Lai, 2023). However, it is important to note that some of these studies employed only acute stimulation protocols, highlighting the potential importance of chronic stimulation for achieving therapeutic effects.

Notably, despite these challenges to specific mechanistic aspects of GENUS, none of these studies have directly assessed what may be the most crucial effect: the restoration of memory performance. Thus, while these debates necessitate a reevaluation of the mechanisms underlying GENUS effects, they do not invalidate the therapeutic potential of the approach. Rather, they suggest the need for new hypotheses regarding its mode of action that extend beyond simple 40Hz entrainment and amyloid-centric explanations.

3.1.4. Results in human patients

The promising results and noninvasive nature of GENUS have facilitated its translation to human clinical applications. Initial studies have explored various stimulation delivery

methods, including LED panels combined with sound systems (Chan et al., 2022) and LED-incorporated glasses paired with sound helmets (Q. He et al., 2021). These early investigations have established that GENUS light and sound stimulation is both safe and well-tolerated, with no severe side effects reported (Chan et al., 2022; Q. He et al., 2021). Importantly, the stimulation does not induce epileptiform activity even in epileptic patients (Chan et al., 2022).

At the neurophysiological level, scalp EEG recording and deep electrodes recording have shown that acute GENUS light and sound stimulation successfully entrains multiple cortical and subcortical structures, including the HPC (Chan et al., 2022). More extended treatment protocols have revealed substantial therapeutic benefits. A three-month daily GENUS protocol led to multiple positive outcomes in patients with mild AD: reduced brain atrophy, preserved functional connectivity, improved sleep markers, and enhanced performance on associative memory tasks (Chan et al., 2022). In patients with MCI, eight weeks of GENUS protocol increased functional connectivity within the Default Mode Network, although CSF Aβ and Tau levels remained unchanged (Q. He et al., 2021).

These encouraging results suggest that GENUS, with its noninvasive nature and straightforward clinical implementation, could become a widely accessible early intervention. It could represent a helpful tool for slowing disease progression in patients with SCD or MCI, while potentially reducing symptoms in those with established AD.

3.2. Broader GENUS applications

The diverse mechanisms of action demonstrated by GENUS in AD suggest potential therapeutic applications beyond this single pathology. Many of GENUS's observed effects, from enhanced neurogenesis to improved vascular function, could benefit various neurological conditions. For instance, the neurogenic effects of GENUS were linked to improve memory performance in Down syndrome models (Islam et al., 2024), a condition with established links to AD pathology as discussed earlier.

GENUS's effects on brain vasculature have led to test its applications in cerebrovascular disorders, especially stroke. Initial studies demonstrated that ipsilesional 40Hz optogenetic stimulation of interneurons immediately following stroke improved blood flow, reduced lesion volume, and enhanced behavioral outcomes during the first post-stroke week (Balbi et al., 2021). Subsequently, 40Hz light

stimulation applied within two hours post-ischemia was found to protect CA1 neurons and improve cognitive function (Zheng et al., 2020). These findings suggest GENUS could serve as a readily implementable clinical intervention in the crucial hours following stroke to minimize brain damage.

The finding that exposing epileptic patients to 40Hz flickering light doesn't trigger epileptic activity might appear unexpected (Chan et al., 2022). However, considering GENUS's ability to enhance inhibitory interneuron activity and restore functional brain activity, its potential benefits for epilepsy become more apparent. Indeed, a recent study in pharmacoresistant epileptic patients implanted with deep electrodes showed that 40Hz multisensory GENUS not only modulates activity in sensory regions but also in more integrated areas such as the Medial Temporal Lobe and PFC. More importantly, it reduced interictal epileptiform discharges, thus reducing the severity of the epileptic phenotype (Blanpain et al., 2024).

Notably, GENUS's ability to influence brain dynamics extends even to healthy individuals, as evidenced by increased complexity of EEG microstate sequences following visual stimulation (Y. Zhang et al., 2021). This observation, while looking promising in AD context as microstates sequence complexity is reduced in AD patients (Tait et al., 2020), suggests that GENUS can modulate fundamental aspects of brain function regardless of pathological status.

Given its broad range of effects, ease of clinical implementation, and apparent safety profile, multisensory GENUS represents a promising therapeutic approach for various neurological conditions. Its ability to influence multiple aspects of brain function while remaining non-invasive makes it particularly attractive for clinical applications.

3.3. Take Home message

After going through different aspects and application of multisensory GENUS, here is some important point to summarize this chapter:

- **40 Hz Multisensory GENUS restores memory performance and ameliorates the pathological phenotype in AD mouse models through processes that remain unclear.**

- **Principal hypotheses underlying GENUS beneficial effects in AD rely on 40 Hz entrainment of brain regions and enhanced Aβ clearance**

- **While recent studies have questioned these hypotheses, they do not call into question the restoration of memory performance observed with GENUS.**

- **Multisensory GENUS show beneficial effects in human patient with early AD**

- **Multisensory GENUS exhibits a wide range of beneficial effects that reduce pathological phenotypes across various conditions.**

While the beneficial effects of multisensory GENUS on AD pathology are well-established, the mechanisms driving these effects remain poorly understood. Ongoing debates regarding the roles of 40Hz entrainment and Aβ clearance highlight the need for new hypotheses about GENUS mechanisms. Considering the broad impacts of multisensory GENUS across various pathologies, including its influence on brain dynamics, and recognizing that alterations in brain dynamics may precede amyloid pathology in AD, new hypotheses are warranted. These could explore how GENUS's effects on brain dynamics contribute to its benefits in AD, independent of previously debated mechanisms.

Thesis Objectives

AD is a neurodegenerative disorder and the leading cause of dementia worldwide. Despite over a century of research, the mechanisms behind its onset and progression remain poorly understood. Currently, AD is diagnosed late, often using invasive clinical procedures such as PET scans or lumbar punctures to detect biological hallmarks like Aβ, hyperphosphorylated Tau, amyloid plaques, and NFTs only after cognitive symptoms have emerged. This delayed diagnosis poses significant limitations as AD likely begins years—or even decades—before symptoms appear. Recently, clinical patterns such as SCD, where patients report cognitive issues despite showing no objective impairments, have been recognized as potential early indicators. Yet, invasive diagnostic methods are not feasible at these stages, creating a gap in early AD detection.

In recent decades, advances in brain imaging and activity monitoring have provided new insights into brain dynamics. While the brain has structural networks based on anatomical connections between regions, effective cognitive processing relies on complex, dynamic alternations of functional networks that extend beyond these anatomical backbones. Alterations in brain dynamics are increasingly linked to cognitive impairments and observed in neurodegenerative processes like AD. Importantly, brain dynamics changes can appear before the typical biological hallmarks of AD. In humans, non-invasive techniques like EEG and fMRI make it possible to assess brain dynamics, suggesting a promising clinical approach for early AD diagnosis.

Besides late diagnosis, AD still lacks effective treatment. Many clinical trials have been inconclusive, often due to minimal results or severe side effects. Recently, a non-invasive protocol based on 40Hz sensory stimulation (GENUS) has shown promising effects in AD models and patients. However, the mechanisms driving these benefits, currently focused on the amyloid hypothesis, remain misunderstood and under debate.

This thesis therefore investigates key questions regarding early AD detection and intervention. Can early alterations in brain dynamics serve as reliable indicators of AD onset, well before the emergence of traditional biomarkers like amyloid plaques and NFTs? Could non-invasive interventions, such as chronic visual GENUS stimulation, restore brain function and memory performance in preclinical AD? To explore these questions, we characterize brain dynamics in young App^{NL-F}/MAPT mouse models of preclinical AD as they perform memory tasks, capturing early-stage dynamics before

amyloid plaque and NFT onset. Using high-density EEG - a technique translatable to clinical applications - we assess brain dynamics and memory performances before and after two weeks of vGENUS stimulation.

In the results section, Part 1 employs global nonlinear analysis to uncover broad patterns of dynamic alteration and their behavioral correlates, while Part 2 delves into specific oscillatory dynamics.

General Methods

This chapter outlines the methodological approaches employed throughout this thesis work. While specific methods and analyses for individual experiments are detailed in their respective experimental contributions sections, here we present the fundamental techniques common to all studies.

1. Animals and ethics

Homozygous Double Knock-in APP^NL-F/MAPT (dKI) and Wild-Type (WT) mice were obtained through breeding in our facility as detailed in previous work (Borcuk et al., 2022). Animals were individually housed under a 12h light/dark cycle with food and water available ad libitum. To achieve population representativeness without specifically studying sex effects, both male and female mice were included in balanced proportions across experimental groups.
All experimental protocols agreed with the European Committee Council directive (2010/63/UE) and were approved by the French Ministry of Research (APAFIS#28839-2021010509459441).

2. High density EEG electrodes

2.1. Surgical procedures

Surgeries were performed in 3 months old C57BL6 mice either WT or dKI, male and female. Mice were weighted before surgery and the surgery wasn't performed if the animal weighted less than 20g.

2.1.1. Anesthesia and skull preparation

Animals were anesthetized using isoflurane (IsoFlo, Zoetis), with induction at 4% in an induction box for 2-3 minutes, followed by maintenance at 1.5% through a respiratory mask in the stereotaxic frame. After shaving the head with an electric trimmer, the incision site was cleaned sequentially with Betadine Scrub 4% and 70% ethanol.
Prior to incision, subcutaneous bupivacaine (2mg/kg) and lidocaine (Lurocaine, Vetoquinol, 2mg/kg) diluted in NaCl was administered at the incision site. Post-surgery analgesia was provided through a subcutaneous injection of Metacam (1mg/kg) diluted in water. After sagittal incision of the scalp, the exposed skull was thoroughly cleaned

using ethanol and NaCl. This critical cleaning step will allow better recordings from electrodes which will be placed on the skull.

2.1.2. Placement and consolidation of the electrode

Before placing the electrode, two holes were made in the skull using a dentist drill. A pre-welded screw serving as the ground electrode was secured over the right cerebellum, while a second screw was placed rostral to the intended electrode position to serve as a support anchor. The probe configuration was then selected by cutting the reference cable and keeping the reference wire jumper in order to use the internal reference of the probe (positioned above the left cerebellum). After welding the ground cable to the cerebellum screw, the probe was carefully positioned on the skull by aligning the cross landmark in the middle of the grid with the skull bregma. Once correctly positioned, saline solution was applied to both the probe and skull to create initial adhesion. The grid was gently dried with paper and allowed to air dry. When the skull and probe were thoroughly dry and the probe was securely attached, UV glue was applied to the external parts of the grid and around the screws. After establishing this UV glue border, the probe was covered with dental glue (SuperBond) and dental cement (Paladur).

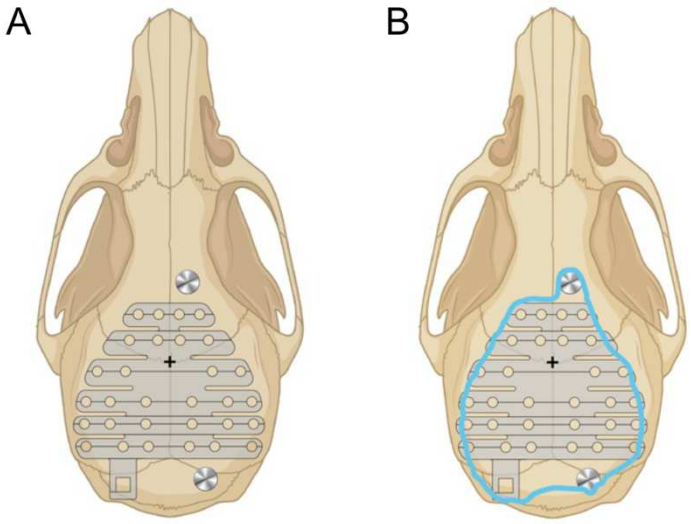

Figure 11. EEG grid surgery

EEG grid placement on the skull aligned on the Bregma with the ground and support screw (A) consolidated with UV glue border (B)

2.1.3. Recovery

Animals were monitored under a heating lamp until full recovery from anesthesia before returning to the animal facility. A minimum 2-week recovery period was observed before experimental procedures.

2.2. Head-stage habituation

The 32-channel INTAN pre-amplifier connection system required gradual habituation due to its weight ranging between 1 and 1.5 grams and a gradual habituation to the cabling system. Animals underwent several hours of home cage recording across multiple days within a week to acclimate to the preamplifier and cabling system.

3. Assessing memory in dKI mice

Various behavioral tasks are used in research to assess memory in rodents. In this thesis, we focus on two specific tasks: the NOR task and the OiP task. Both tasks require rodents to explore objects, and their memory performance depends on a single key principle: rodents are naturally curious and drawn to novelty. When an object's configuration changes, they are likely to spend more time exploring the changed object, indicating they remember the previous configuration.

3.1. Set Up and Habituation

3.1.1. Apparatus

Behavioral experiments were conducted in a 55 x 55 cm open field featuring black walls and a white ground with a grid pattern. A single visual cue was fixed on one wall. Objects used for memory tasks were specifically selected to differ in shape, texture, and color. These object combinations had been previously validated in earlier studies from the laboratory (Borcuk et al., 2022; Hamm et al., 2017).

3.1.2. Habituation

To minimize handling stress during experimental procedures, animals were never handled directly but transported using dedicated containers. For implanted animals, a transport box without ceiling was used to accommodate the recording cables, while

non-implanted control animals were transported using a plastic tube. For tube habituation, the plastic tube was continuously present in the home cage for a week before beginning experiments to allow animals to become familiar with it. Transport box habituation consisted of one hour of daily exposure for a week. Prior to the first memory task, all animals underwent a three-day habituation sequence to the experimental setup. The first day consisted of a 10-minute exploration of the empty open field to habituate the animal to the experimental apparatus. On the second day, animals performed a 10-minute exploration session with a single object placed in the middle of the arena to habituate the animal to object exploration. Finally, to habituate animals to object exploration after a 24-hour delay, a third 10-minute exploration session was conducted with a different single object.

3.2. Novel Object Recognition Task

3.2.1. Background

The Novel Object Recognition (NOR) task is a widely used method to assess recognition memory in several rodent models. It offers several key advantages, particularly as it relies on innate behavior and requires no reward conditioning (Grayson et al., 2015). A critical parameter in this task is the ITI. In our protocol, we use a 24-hour ITI to examine long-term recognition memory, which relies on memory consolidation processes. The neural circuits implicated in NOR task performance primarily include the HPC, PFC, RSC, and PRC (de Landeta et al., 2020; Preston & Eichenbaum, 2013; Warburton & Brown, 2015).

3.2.2. Protocol

The task began with a 10-minute sampling phase, during which animals explored two identical objects in the arena. After returning to the animal facility for 24 hours, mice underwent a test phase in which one of the objects was replaced with a novel item. The open field was cleaned with 35% ethanol between animals. To control for potential place preference, we always replaced the object that received less exploration during the sampling phase.

3.3. Object in Place Task

3.3.1. Context

The OiP task evaluates associative memory by testing an animal's ability to detect when a familiar object appears in a location previously occupied by another familiar object (Dix & Aggleton, 1999). This assessment of object-place association particularly engages the LEC and PFC (Chao et al., 2016; D. I. G. Wilson et al., 2013, p. 2).

3.3.2. Protocol

During the 10-minute sampling phase, animals explored two different objects in the open field. After a 5-minute interval in their home cage, they completed a 10-minute test phase where one object was replaced by a copy of the other. The arena was cleaned with 35% ethanol between phases and between animals. As in the NOR task, we replaced the object that received less exploration during sampling.

3.4. Assessment of memory performance

Object exploration was assessed manually by observing mouse behavior. Exploration was defined as being near and oriented toward the object, sniffing it, or interacting with it without climbing on it. Exploration times were recorded at both 5 and 10 minutes, with the 10-minute values used for all behavioral analyses. Animals displaying total exploration times below 2 seconds during sampling were excluded from the study.
Memory performance was quantified through a memory index computed from test phase exploration times as follow:

$$MI = \frac{New\ Object\ Exploration\ Time\ -\ Familiar\ Object\ Exploration\ Time}{New\ Object\ Exploration\ Time\ +\ Familiar\ Object\ Exploration\ Time}$$

A positive memory index indicates that an animal explored the new object more than the familiar one, demonstrating good memory performance, while a memory index of zero indicates equal exploration time between the two objects.

4. Visual GENUS protocol

Although combining light and sound stimulation has shown beneficial effects (Martorell et al., 2019, see introductory part), only visual stimulation was used in this thesis work, as that protocol was more fully developed at the project's start in 2020 and was simpler to implement.

4.1. Light stimulation set up

The stimulation apparatus was constructed using the soldered version protocol from Singer et al. (2018). The setup was housed in a dedicated room, with a 1200-lumen LED strip (4000K; Ledkia) mounted on a shelf against a white wall. The LED strip was connected to a custom-soldered circuit, controlled by an Arduino, and powered by a 12V AC adaptor. Standard cages were modified for stimulation by painting three walls with black matte paint, leaving one transparent wall facing the LED strip.

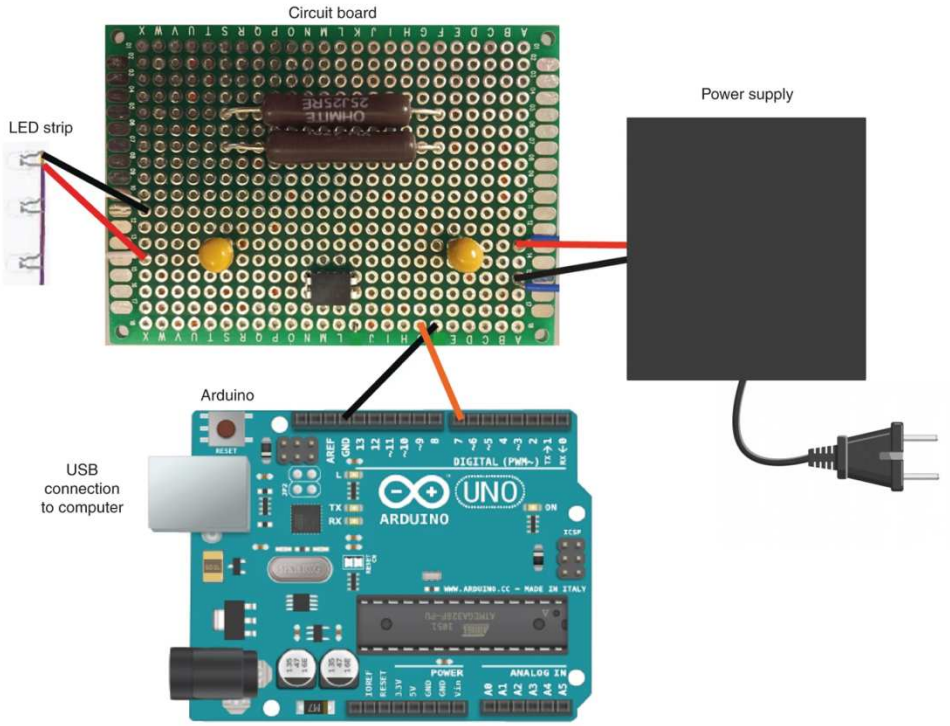

Figure 12. GENUS light flickering hardware setup.

The LED strip is connected to a custom circuit board, powered by a 12V power supply and connected to an Arduino controlling flickering frequencies. Adapted from Singer et al., 2018

4.2. Protocol

The stimulation protocol consisted of 15 daily sessions of one-hour stimulation. Each day began with a one-hour habituation period in the home cage within the stimulation room. Animals were then transferred to stimulation cages containing no bedding, food, or water. These cages were positioned with their transparent wall facing the LED strip and white wall. Room lights were turned off and LED stimulation was initiated, delivering either 40Hz flicker or continuous light. After the one-hour stimulation period, room lights were restored and LED stimulation stopped. Animals returned to their home cages for a one-hour post-stimulation period before either returning to the animal facility or proceeding to behavioral testing. Stimulation cages were cleaned with 70% ethanol between sessions. Continuous light was selected as the control condition rather than random flicker.

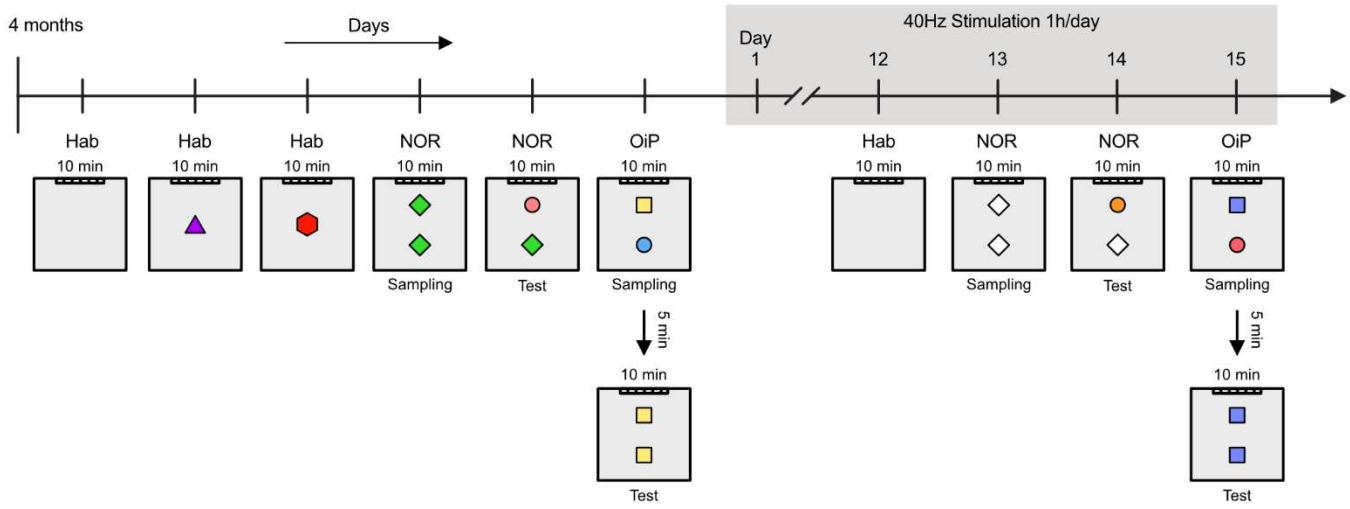

Figure 13. Behavior and vGENUS protocol schedule.

Different object pairs were used between before and after GENUS to avoid familiarity.

Results

Part 1: Nonlinear characterization of global brain dynamics alterations in young dKI mice model of preclinical AD and the effects of a chronic vGENUS protocol

Results from this part were formatted in an article submitted to a journal and simultaneously submitted as a preprint in BiorXiv under the following DOI: https://doi.org/10.1101/2024.10.21.619392

In the following article, figures are indexed with 2 numbers in their legends, the first number is the index of the thesis manuscript and the second is the index fin in the text of the article.

Complementary unpublished results will be provided at the end of the article

Main results article

40 Hz light stimulation restores early brain dynamics alterations and associative memory in Alzheimer's disease model mice

Matthieu Aguilera[1], Chantal Mathis[1], Karin Herbeaux[1], Amine Isik[1], Davide Faranda[2], Demian Battaglia[1,*] & Romain Goutagny[1,*]

[1] Université de Strasbourg, CNRS, Laboratoire de Neurosciences Cognitives et Adaptatives (LNCA), UMR 7364, F–67000 Strasbourg, France.

[2] Université Paris Saclay, CEA – CNRS – UVSQ, Laboratoire des Sciences du Climat et de l'Environnement (LSCE), F-91191 Gif-sur-Yvette, France

* Demian Battaglia – Romain Goutagny.

Email: dbattaglia@unistra.fr – goutagny@unistra.fr

Author Contributions: M.A. and R.G. performed the experiments and analyzed the data. C.M. provided the animals and gave inputs for behavioral experiments. K.H. performed immunochemistry experiments. A.I. managed the animal breeding and genotyping. D.F. provided code for dynamic fluidity analyses. R.G. and D.B. conceived the experimental and analytical design; M.A., R.G. and D.B. wrote the article.

Competing Interest Statement: The authors declare no competing interests.

Classification: Biological sciences, Neurosciences

Keywords: Alzheimer's disease, EEG, Dynamics, Gamma stimulation, GENUS

Abstract

Early biomarkers are crucial for timely intervention in Alzheimer's disease (AD). We investigated brain dynamics alterations in young App^{NL-F}/MAPT double knock-in (dKI) mice, a model of early AD, before amyloid plaque onset. Using high-density EEG recordings and novel metrics from fields outside neuroscience, we assessed brain dynamics fluidity—a measure of the brain's ability to transition between activity states. We revealed that dKI mice exhibit early, awake state-specific reductions in brain dynamics fluidity associated with cognitive deficits in complex memory tasks. To investigate potential interventions targeting these altered brain dynamics, we applied visual gamma entrainment using sensory stimuli (vGENUS). Daily vGENUS sessions over two weeks restored brain dynamics fluidity and rescued memory deficits in dKI mice. Importantly, these effects build up during the stimulation protocol and persist after stimulation ended, suggesting long-term modulation of brain function. Our findings identify altered brain dynamics as an early marker of AD-related changes and demonstrate vGENUS as a promising non-pharmacological intervention. This study provides new insights into early AD pathophysiology and suggests novel approaches for early diagnosis and treatment.

Introduction

Alzheimer's disease (AD) is a devastating neurodegenerative disorder and the leading cause of dementia worldwide, defined by the conjunction of progressive memory loss and cognitive decline with specific neuropathological changes. Despite its high and likely underestimated prevalence (1), effective treatments and early diagnostic tools remain elusive. Pathological hallmarks of AD include extracellular amyloid plaques formed by aggregated Amyloid-beta (Aβ) peptide, and intracellular neurofibrillary tangles of hyperphosphorylated Tau proteins. For decades, the amyloid hypothesis has dominated AD research, positing that Aβ accumulation and amyloid plaques induce network dysfunctions responsible for cognitive deficits (2)

The diagnosis of AD requires the presence of both cognitive impairment and evidence of amyloid pathology which is detected either through cerebrospinal fluid (CSF) analysis via lumbar puncture to measure reduced soluble Aβ levels (3), or through

neuroimaging techniques such as positron emission tomography (PET) to visualize insoluble Aβ deposits (4). However, mounting evidence challenges the timing and specificity of these diagnostic criteria: memory deficits often precede detectable amyloid plaque formation (5–8) and can occur independently of Aβ (9). Conversely, amyloid plaques are sometimes present in non-pathological or asymptomatic elderly individuals (10–12). While the amyloid pathway undeniably plays a role in AD (2), these findings underscore the need for alternative early biomarkers that capture other critical aspects of the disease progression.

One promising early indicator of AD, alongside memory deficits, is alterations in brain network activity, which can manifest before amyloid plaque onset (9). Advanced neuroimaging techniques such as functional Magnetic Resonance Imaging (fMRI) and Electroencephalography (EEG) enable the study of global brain dynamics, focusing on entire brain networks rather than region-specific changes. These tools have revealed that global brain dynamics follow scale-free patterns (13), slow down during aging (14), and are altered in AD (15–17). Thus, changes in global brain dynamics could serve as an early biomarker of AD, opening new windows for early diagnosis and intervention strategies.

The lack of effective treatments remains another major challenge in AD. While numerous drugs targeting Aβ reduction have been developed based on the amyloid hypothesis, many have failed to reverse AD symptoms and were discontinued due to side effects (18, 19). In this context, a novel non-invasive therapy based on 40 Hz gamma stimulation using sensory stimuli (GENUS (20)) has shown promising memory benefits in both AD mouse models (21, 22) and patients with mild probable AD (23) (for review, see (24)). Various mechanisms have been proposed to explain these effects, including reduced neurodegeneration and improved memory through lowered amyloid plaque load, primarily via microglial activation and glial responses (21, 22), or enhanced brain clearance (25).

However, recent studies have challenged these ideas, questioning the significance of gamma entrainment via sensory stimulations. Some report limited propagation beyond the visual cortex and lack of engagement in key regions such as hippocampal CA1 (26), while others debate whether true gamma oscillations are even being entrained (27). The impact of these stimulations on amyloid plaque loads also remains controversial (27, 28). Despite these ongoing debates, discussions about GENUS have largely remained focused on its effects related to the amyloid hypothesis.

We propose an alternative hypothesis: GENUS may restore memory by modulating global brain network dynamics, which are altered early in AD, rather than through 40 Hz-specific effects. This novel perspective is supported by recent evidence demonstrating GENUS can affect brain dynamics beyond AD pathology (29, 30), suggesting broader impacts on brain function.

To test this hypothesis, we conducted high-density EEG (hdEEG) recordings in a preclinical AD mouse model (AppNL-F/MAPT double knock-in mice (31); dKI, n=8, both sexes) and control littermates (n=8, both sexes) during memory task performance. Our previous work (32) demonstrated that at 4 months, dKI mice maintain normal performance in simple tasks (e.g., short-term Novel Object Recognition or Object Location) but exhibit specific and subtle deficits in more complex associative memory tasks such as Object-Place association. In this study, we evaluated memory performance and brain dynamics during the Object-Place association and long-term Novel Object Recognition tasks before and after 2 weeks of daily 1-hour visual GENUS (vGENUS) exposure.

Results

Young dKI mice display memory deficits in complex tasks before amyloid plaque onset.

We first evaluate the extent of amyloid pathology in 4-month-old dKI mice. To this aim, we performed 6E10 immunohistochemistry on brain sections from 4 WT and 4 dKI mice (Fig. 1A, B; 2 males and 2 females per group). Across 262 brain slices from dKI mice, we detected only one plaque, in stark contrast to 12-month-old dKI positive controls (1 male, 1 female) where we observed more than 10 plaques per slice. These results confirm that 4-month-old dKI mice do not yet exhibit significant amyloid plaque deposition.

We next assessed the memory performance of dKI mice at this pre-plaque stage. The Novel Object Recognition (NOR) task with a 24-hour delay, a standard test for evaluating recognition memory (33), revealed no significant deficits in young dKI mice (Fig. 1C, Fig. S1). This indicates that long-term recognition memory remains intact at this stage, unlike in mouse models with established amyloid pathology (34). However, when we employed a more complex memory task taxing short-term associative

memory, the Object in Place (OiP) task, we detected subtle but significant early memory deficits in dKI mice (Fig. 1D, Fig. S1).

These findings, consistent with our previous work (32), demonstrate that 4-month-old dKI mice exhibit measurable memory impairments in complex tasks prior to the development of significant amyloid plaque pathology. This provides a critical window to study early brain network alterations associated with AD and to test potential early interventions before substantial pathology develops.

Global brain dynamics of dKI mice are altered before amyloid plaque onset.

To investigate whether these early memory deficits were associated with alterations in global brain dynamics, we first focused our analysis on the OiP task, where we observed cognitive impairments. We recorded high-density EEG during the performance of the task and characterized global brain dynamics using an unbiased approach. This method treated multivariate EEG time-series as trajectories in a high-dimensional space of brain activity topographies (30 dimensions, corresponding to the number of hdEEG channels). Using t-SNE (35), a nonlinear, distance-preserving embedding method, we visualized these configurations as points in a two-dimensional space. For each point, we computed local dynamics fluidity (36), a metric related to the time the system takes to leave a neighborhood of the visited point in the space of dynamic configurations (Methods). This quantity, grounded in concepts from the statistical theory of extreme events (37) and previously used in the analysis of climatic time-series (36), offers important advantages on more classic metrics (38) of dynamic stability as it can be properly estimated from a considerably lower amount of data. While the overall shape of the sampled manifold was similar across genotypes, the average distribution of dynamics fluidity across the manifold was significantly lower in dKI mice (Fig. 2C Top; $KS = 0.2283 \pm 0.0277$, $p < 0.001$). This reduction was associated with dKI mice exploring dynamic configurations not observed in WT mice, potentially corresponding to states with abnormally low fluidity (Fig. 2B, Top, where configurations unique to dKI mice appear as black points in the WT scatter plot).

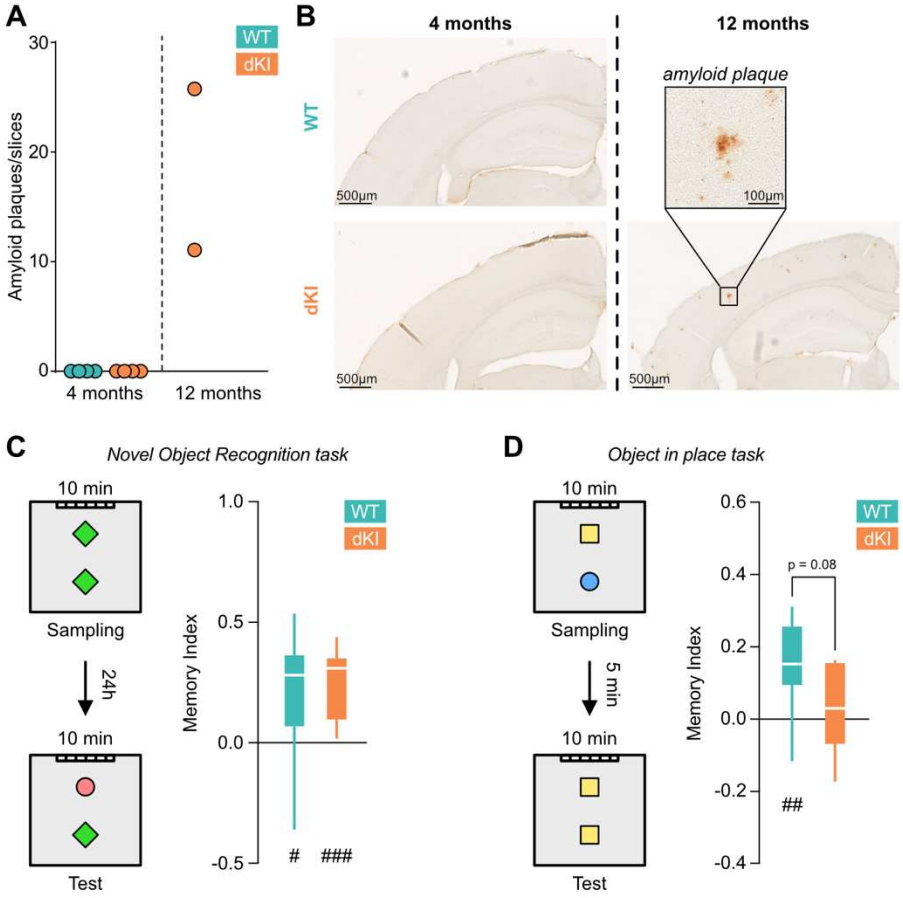

Figure 14 / 1. Young dKI mice display memory deficits in complex task before amyloid plaques onset.

(A) Number of amyloid plaques per brain slices at 4 months (left) for WT (n = 4, blue) and dKI (n = 4, orange). We detect only 1 plaque in 262 brain slices from 4 dKI mice. As a positive control, plaques were counted for 12 months old (right) dKI (n = 2, orange). Plaques were counted over numerous frontal brain slices of several brain region plans. The total amount of plaques counted was divided by the total amount of slices for each animal. **(B)** Amyloid plaques immuno-staining of dorsal hippocampus at 4 months (left) for a WT (top) and a dKI (bottom) mouse and at 12 months (right) for a dKI mouse. Amyloid plaques were present in dKI mice at 12 months (top right for magnification) but not at 4 months. **(C)** Novel Object Recognition (NOR) task protocol (left), and memory index for WT (n = 8, blue) and dKI (n = 8, orange) mice (right). Both WT and dKI shows memory performances higher than chance levels (one-sided t-test against chance, #: $p < 0.05$, ##: $p < 0.01$, ###: $p < 0.001$). Box ranges from 25 to 75 percentile and whiskers for minimum to maximum values, median is represented by white line. **(D)** Object-in-Place (OiP) task protocol (left), and memory index for WT (n = 8, blue) and dKI (n = 8, orange) mice (right). dKI mices shows memory performances not higher than chance levels (one-sided t-test against chance, #: $p < 0.05$, ##: $p < 0.01$, ###: $p < 0.001$) and almost significantly lower than WT (two sample two sided t-test, $p = 0.08$). Box ranges from 25 to 75 percentile and whiskers for minimum to maximum values, median is represented by white line.

These findings suggest that by 4 months of age, dKI mice experience events where brain dynamics transiently exhibit reduced fluidity.

To determine whether these alterations in brain dynamics were specific to tasks showing cognitive deficits, we also analyzed dynamics fluidity during the NOR task performance. Notably, dynamics fluidity was also significantly lower in dKI (Fig. 2C, Bottom; KS = 0.1626 ± 0.0279, p = 0.026), despite the absence of observable memory deficits in this task. We found no significant differences in dynamics fluidity between the two tasks for either WT (KS = 0.0558 ± 0.026, p = 1) or dKI mice (KS = 0.1296 ± 0.0263, p = 0.1468). This suggests that reduced dynamics fluidity is a general feature of dKI mice, independent of task-specific demands, and may serve as a sensitive early indicator of AD-related brain changes.

To corroborate these findings, we conducted EEG microstate analyses (39). Microstates represent a small number of stereotypical hdEEG topographies, extracted via unsupervised clustering. Continuous recordings were then converted into sequences of symbolic labels indicating the microstate closest to the current topography (Fig. 2A, Bottom). From these sequences, we calculated a fluidity-equivalent measure by quantifying the inverse probability of remaining in the same microstate from time t to t+1 (Methods). This measure was computed for several microstates (from 3 to 8) and then averaged to generate a single value. Microstates fluidity was significantly reduced in dKI mice in both OiP and NOR tasks compared to WT (Fig. 2D, Two-way ANOVA, $F(1,28) = 6.656$, $p = 0.015$) and showed a strong correlation with the previously computed dynamics fluidity (Fig. 2D, $R^2 = 0.4539$, $p < 0.001$).

Additionally, we assessed the complexity of microstate sequences using a minimum description length approach, which has previously been shown to be affected in AD (17). Consistent with the microstates fluidity results, microstate sequence complexity was significantly reduced in dKI mice during both OiP and NOR tasks compared to WT mice (Fig. 2E, Two-way ANOVA, $F(1,28) = 7.522$, $p = 0.011$) and also correlated strongly with dynamics fluidity (Fig. 2E $R^2 = 0.4371$, $p < 0.001$). These results were robust, remaining independent of the average number of microstates extracted (, Fig. S2), microstates self-repetitions (Fig. S2), and were confirmed using an alternative EEG microstates extraction method (Fig. S3).

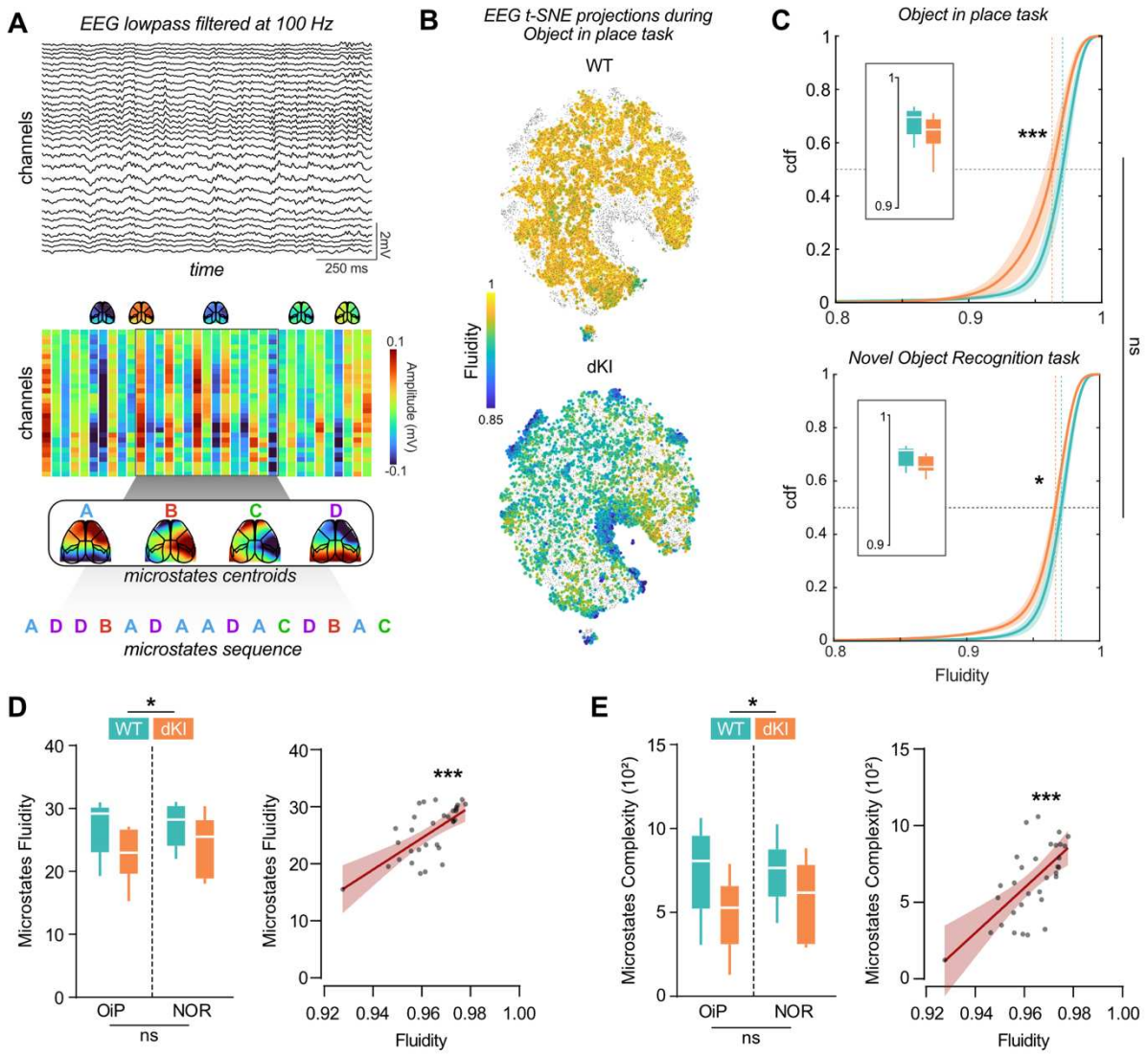

Figure 15 / 2. Global brain dynamics of dKI mice is altered before amyloid plaques onset.
(A) Top, example of 30-channel hdEEG recorded during behavior. Middle, hdEEG is then coarsegrained with 40 ms window generating 30-channel amplitude vectors over time. Bottom, k-means clustering of these vectors identifies microstate centroids and sequences. **(B)** t-SNE projection of these previous vectors from a representative WT and dKI mouse during OiP task, color-coded by EEG dynamics fluidity. Grey dots represent the full distribution of both genotypes. **(C)** A shift between the cumulative distribution functions (cdf) of the EEG dynamics fluidity distributions for WT (blue) and dKI (orange) mice during OiP (top) and NOR (bottom) task (n = 8 per group) indicated reduced dynamics fluidity in dKI mice in OiP (KS = 0.2283 ± 0.0277, $p < 0.001$, here and for all other KS statistics in the following measured from a bootstrap comparison between association and null hypothesis, see Methods), and NOR (KS = 0.1626 ± 0.0279, $p = 0.026$). Data are presented as mean ± s.e.m. Dotted lines show distribution medians. Box displays individuals mean dynamics fluidity distributions. **(D)** Microstates fluidity during OiP and NOR task for WT and dKI mice (left, n = 8 per group). Two-way ANOVA indicate only a Genotype effect ($F(1, 28) = 6.656$, $p = 0.015$) indicating a reduced microstates fluidity in dKI mice for the 2 tasks. Box ranges from 25 to 75 percentile and whiskers for minimum to maximum values, median is represented by white line. Microstates fluidity correlates with mean dynamics fluidity (right, $R^2 = 0.4539$, $p < 0.001$). **(E)** Microstates sequence complexity during OiP and NOR task for WT and dKI mice (left, n = 8 per group). Two-way ANOVA indicate only a Genotype effect ($F(1, 28) = 7.522$, $p = 0.011$) indicating a reduced microstates sequence complexity in dKI mice for the 2 tasks. Box ranges from 25 to 75 percentile and whiskers for minimum to maximum values, median is represented by white line. Microstates fluidity correlates with mean dynamics fluidity (right, $R^2 = 0.4371$, $p < 0.001$).

Global brain dynamics of dKI mice are unaltered during sleep.

Given that global brain dynamics were altered in both OiP and NOR tasks, yet dKI mice showed memory deficits only in the OiP task, we sought to understand this discrepancy. We hypothesized that the difference might be attributed to either the complexity of the task (NOR being simpler than OiP) or the difference in delay between tasks. The 24h delay in the NOR task allows for sleep during the intertrial interval, potentially enabling offline memory consolidation. To address whether brain dynamics are altered during sleep, we analyzed dynamics fluidity during rapid eyes movements (REM) and slow-wave sleep (SWS) in the hours following learning in the 24h NOR task (Fig. 3A), as these states are critical for memory consolidation (40, 41).

Intriguingly, we found that both SWS (KS = 0.0876 ± 0.0273, p = 0.3122) and REM (KS = 0.0653 ± 0.0232, p = 0.617) exhibited similar dynamics fluidity between dKI and WT mice (Fig. 3B). This preserved dynamics fluidity during sleep, in contrast to the altered dynamics during wakefulness, may explain the differential impact on behavior observed between the two memory tasks. Specifically, while the OiP task relies on online associative processes that may be disrupted by transient reductions in dynamics fluidity, the 24h NOR task may benefit from offline memory consolidation during sleep. The intact dynamics during sleep might therefore help compensate for errors introduced by altered dynamics during wakefulness.

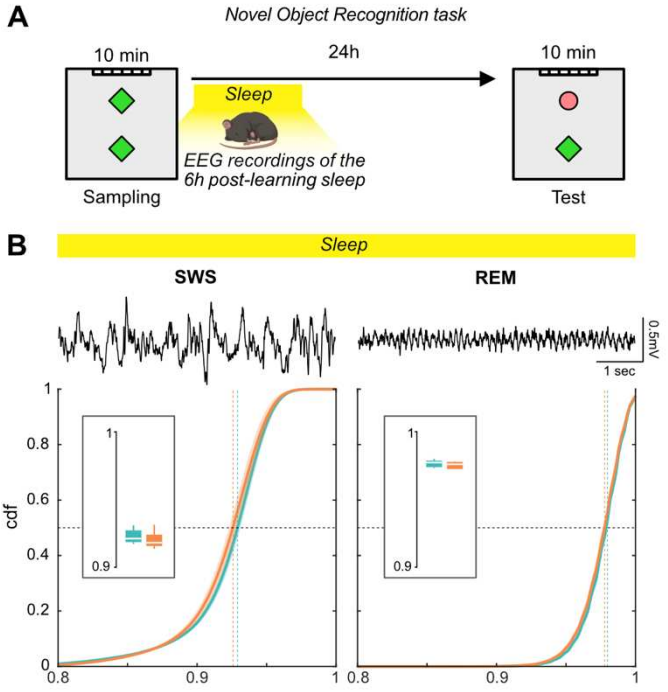

Figure 16 / 3. Global brain dynamics of dKI mice is unaltered during sleep.
(A) EEG was recorded during the first 6 hours post-learning of the NOR task. **(B)** Top, example EEG signals during slow-wave sleep (SWS, left) and REM sleep (right). Bottom, no significant differences in EEG dynamics fluidity between WT and dKI mice during SWS or REM. Data are presented as mean ± s.e.m. Dotted lines show distribution medians. Box displays individuals mean dynamics fluidity distributions.

vGENUS differentially entrains cortical regions at 40Hz and increases brain dynamics in dKI mice.

Given the reduced dynamics fluidity observed in dKI mice, we next investigated whether vGENUS could potentially modulate these altered brain dynamics. We conducted 2 weeks of daily 1-hour vGENUS sessions and analyzed hdEEG for 10 minutes during stimulation on both the first and last (15th) day of the protocol to assess the immediate and long-term effects of the intervention.

First, we examined the effects of vGENUS on cortical activity. EEG channels were grouped per cortical region based on Allen institute mouse brain parcellation to facilitate interpretation (Fig. 4A). A 40Hz peak in the power spectrum was observed across regions for both genotypes, with a higher proportion of the power spectrum in occipital (i.e. visual) regions (Fig. 4B, C). However, the relative 40Hz power during stimulation differed between genotypes and between Day 1 and Day 15 of the stimulation protocol (Fig. 4D, Three way repeated ANOVA, $F(1,84) = 4.619$, $p = 0.034$).

Specifically, relative 40Hz power during stimulation was lower in dKI mice at Day 1 ($t(84) = 3.265$, $p = 0.009$) but not significantly different from WT levels at Day 15 ($t(84) = 1.975$, $p = 0.309$). These findings suggest that the cortical response to 40Hz visual stimulation is initially reduced in young dKI mice but changes over the course of the 15-day vGENUS protocol.

Given the ongoing debate on the significance of 40Hz stimulation, we next assessed whether vGENUS impacted global brain dynamics beyond its effects on 40Hz power. To this end, we computed dynamics fluidity during the stimulation periods on both Day 1 and Day 15. On Day 1, dKI mice exhibited significantly lower dynamics fluidity compared to WT mice (Fig. 4E, $KS = 0.2548 \pm 0.0284$, $p < 0.001$). However, after 15 days of stimulation, dynamics fluidity in dKI mice increased ($KS = 0.1587 \pm 0.0275$, $p = 0.03$), reaching levels comparable to WT mice ($KS = 0.1459 \pm 0.0266$, $p = 0.066$).

These results suggest that while vGENUS has an immediate differential effect on 40Hz power in dKI mice, its impact on global brain dynamics becomes evident only after prolonged stimulation. This highlights the importance of chronic stimulation in promoting vGENUS effects on overall brain function and suggests that the mechanisms underlying these effects may involve processes beyond simple entrainment of cortical oscillations.

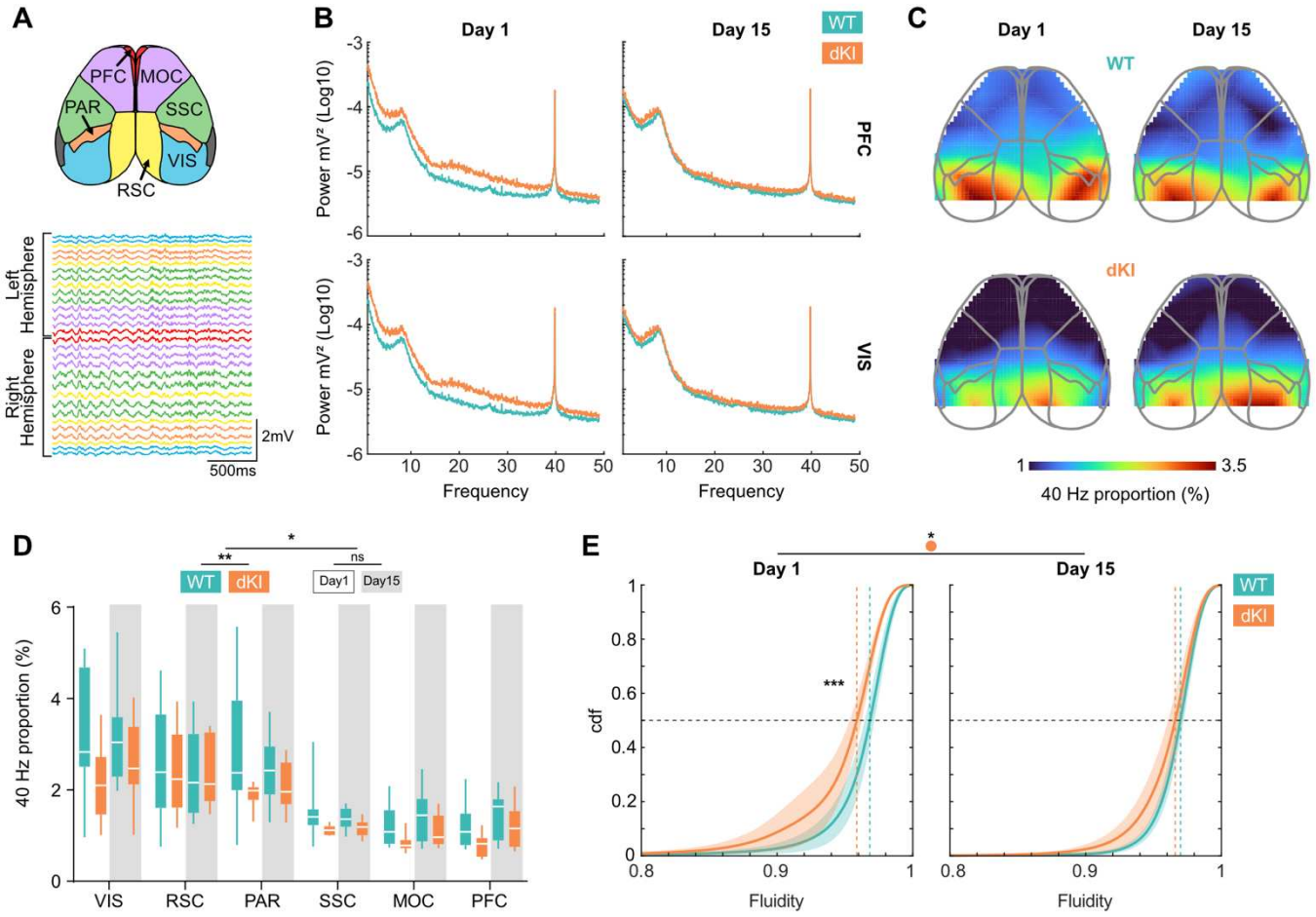

Figure 17 / 4. vGENUS differentially entrain cortical regions at 40Hz and increase brain dynamic in dKI mice.

(A) Cortical parcelation map (Top) of the 30 channels hdEEG (Bottom) based on Allen Atlas, allowing the parcelation of the data into these following cortical regions: Visual Cortex (VIS, blue); Retrosplenial Cortex (RSC, yellow); Parietal Cortex (PAR, orange); Somato Sensory Cortex (SSC, green); Motor cortex (MOC, purple); Prefrontal Cortex (PFC, red). The power of these channels are averaged over regions for next analyses. **(B)** Power spectrum of PFC (Top) and VIS (Bottom) during first (left) and last (right) day of 40Hz vGENUS stimulation for one WT (blue) and one dKI (orange) mouse. A peak at 40Hz can be observed in both mice, both regions and both first and final day meaning a cortical entrainment by the vGENUS stimulation. **(C)** Cortical map of 40Hz proportion of the power spectrum (40Hz Power / all Power Spectrum) during first (left) and last (right) day of stimulation for one WT (Top) and one dKI (Bottom) mouse. As expected visual areas are the more entrained by 40Hz, this entrainment appears lower in the dKI mouse. **(D)** To quantify observations of previous maps, we measured the average 40Hz proportion of the power spectrum across different cortical regions during the first (no background) and last (grey background) day of stimulation for WT (n=8, blue) and dKI (n=8, orange) mice. Two-way ANOVA on repeated measures revealed a significant interaction between the day of stimulation and genotype ($F_{(1,84)}$ = 4.619, p=0.034). Post hoc tests showed that the 40Hz proportion was lower in dKI mice on Day 1 ($t_{(84)}$ = 3.265, p = 0.009), and no difference between genotypes on Day 15 ($t_{(84)}$ = 1.975, p =0.309). Box ranges from 25 to 75 percentile and whiskers for minimum to maximum values, median is represented by white line. **(E)** EEG Fluidity distribution during first (Left) and last (Right) day of vGENUS stimulation for WT (blue, n=8) and dKI (orange, n= 8) mice showed a lower EEG fluidity at Day 1 for dKI mice (KS = 0.2548 ± 0.0284; p < 0.001) which normalized to WT levels at Day 15 (KS = 0.1459 ± 0.0266; p = 0.066) after a specific increased fluidity in dKI mice (KS = 0.1587 ± 0.0275; p = 0.03). Data are presented as mean ± s.e.m. Dotted lines show distribution medians.

Increased brain dynamics in dKI mice persist after end of stimulation and restore memory performance.

Since memory deficits in young dKI mice were likely linked to altered brain dynamics, we examined whether vGENUS-mediated restoration of brain dynamics would also improve memory performance. At the end of the 2 weeks of vGENUS, NOR and OiP tasks were performed in the same order as before vGENUS (Fig. 5A). vGENUS did not affect performance in the NOR task, as dKI mice showed no memory impairments both before and after vGENUS (Fig. 5B, Left, Fig. S4). However, there was no longer a significant difference in dynamics fluidity between genotypes (Fig. 5B, Right, KS = 0.0798 ± 0.0235, p = 0.6405) due to a significant increase in dynamics fluidity in dKI mice after vGENUS (KS = 0.2137 ± 0.0293, p = 0.0042).

Thus, the vGENUS-induced increase in brain dynamics appears to persist even after stimulation sessions, suggesting a stable shift toward more physiological brain dynamics that could benefit cognitive performance. Indeed, after two weeks of vGENUS, dKI mice no longer showed deficits in the OiP task (Fig. 5C, Left, Fig. S4). Similarly to the NOR task, brain dynamics fluidity during the OiP task showed no significant difference between genotypes after vGENUS (Fig. 5C, Right, KS = 0.1298 ± 0.0270, p = 0.0999) due to a specific increase in dKI mice (KS = 0.237 ± 0.0283, p < 0.001).

Discretized microstates analysis supported these findings, showing no significant difference between genotypes in either microstates fluidity (Fig. 5E, Fig. S5) or microstates sequence complexity (Fig. 5F, Fig. S5) after two weeks of vGENUS.

Our results demonstrate that vGENUS restores memory performance in the OiP task by significantly increasing dynamics fluidity, even after the end of the stimulation, specifically in dKI mice. Indeed, vGENUS appears to specifically target the previously identified states of low dynamics fluidity in dKI mice. This effect can be visualized in Fig. 5D, where configurations present in dKI mice before vGENUS but absent after treatment are shown as red points. By eliminating these low fluidity states, vGENUS effectively "thaws" brain dynamics, returning them to a more fluid state similar to that observed in WT mice. Importantly, these effects of vGENUS on brain dynamics fluidity appear to be specific to pathological states. Sleep dynamics, which were unaffected in dKI mice before treatment, showed no differences in fluidity after vGENUS (Fig. S6),

suggesting that vGENUS selectively targets abnormal awake brain states without disrupting normal sleep dynamics.

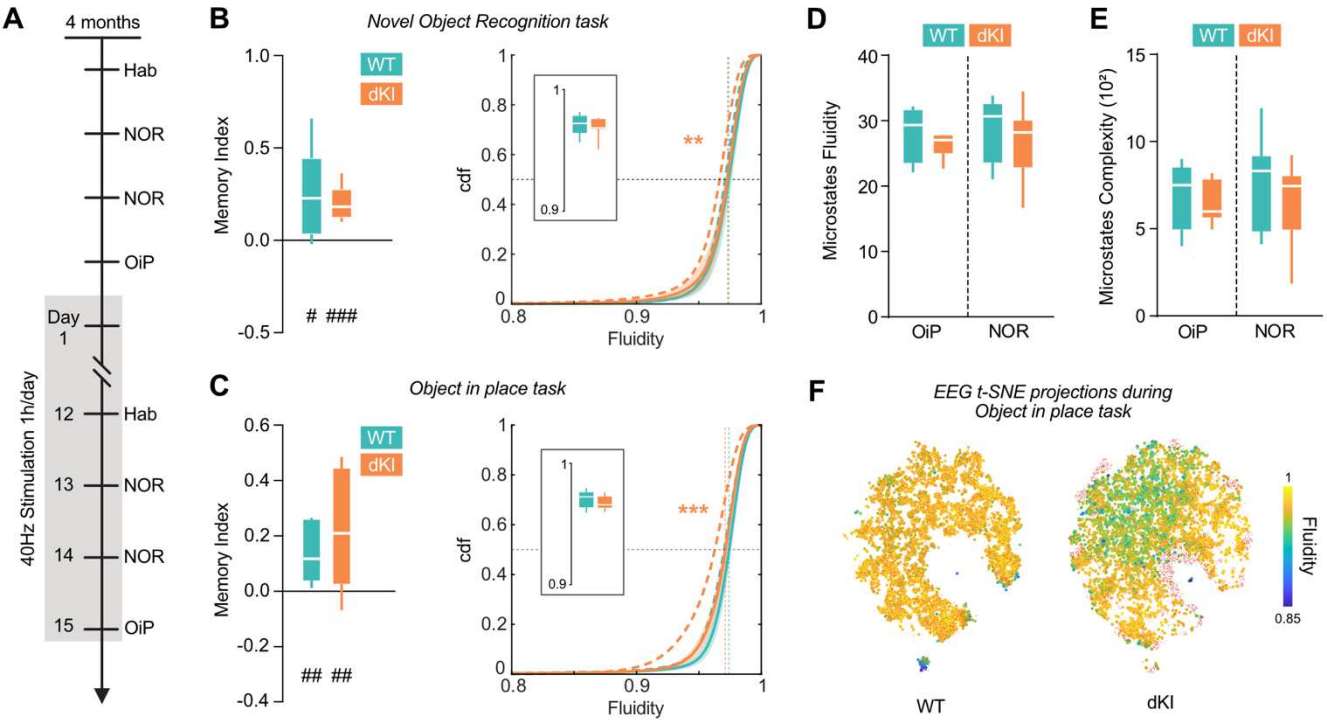

Figure 18 / 5. Increased brain dynamics in dKI mice remain after end of stimulation and restore memory performances in dKI mice.
(A) 15 days vGENUS protocol schedule. **(B)** Post-GENUS NOR memory index for WT (n = 8, blue) and dKI (n = 8, orange) mice (left). Both WT and dKI shows memory performances higher than chance levels (one-sided t-test against chance, #: $p < 0.05$, ##: $p < 0.01$, ###: $p < 0.001$). Box ranges from 25 to 75 percentile and whiskers for minimum to maximum values, median is represented by white line. Brain dynamics fluidity show no more genotype differences (right, KS = 0.0798 ± 0.0235, p = 0.6405) due to a significant increase in dynamics fluidity in dKI mice after vGENUS (KS = 0.2137 ± 0.0293, p = 0.0042). Data are presented as mean ± s.e.m. Dotted lines show distribution medians. Box displays individuals mean dynamics fluidity distributions. **(C)** Post-GENUS OiP memory index for WT (n = 8, blue) and dKI (n = 8, orange) mice (left). Both WT and dKI shows memory performances higher than chance levels (one-sided t-test against chance, #: $p < 0.05$, ##: $p < 0.01$, ###: $p < 0.001$). Box ranges from 25 to 75 percentile and whiskers for minimum to maximum values, median is represented by white line. Brain dynamics fluidity show no more genotype differences (right, KS = 0.1298 ± 0.0270, p = 0.0999) due to a specific increase in dKI mice (KS = 0.237 ± 0.0283, $p < 0.001$) after vGENUS. Data are presented as mean ± s.e.m. Dotted lines show distribution medians. Box displays individuals mean dynamics fluidity distributions. **(D)** Microstates fluidity during OiP and NOR task for WT and dKI mice post vGENUS (n = 8 per group). Box ranges from 25 to 75 percentile and whiskers for minimum to maximum values, median is represented by white line. **(E)** Microstates sequence complexity during OiP and NOR task for WT and dKI mice post vGENUS (n = 8 per group). Box ranges from 25 to 75 percentile and whiskers for minimum to maximum values, median is represented by white line. **(F)** t-SNE projection of hdEEG multidimensional vectors from a representative WT and dKI mouse during OiP task after vGENUS, color-coded by EEG dynamics fluidity. Red dots represent the full genotype distribution pre and post vGENUS combined, highlighting genotype-specific patterns.

Discussion

Using high-density EEG recordings during specific memory task performances in a preclinical AD mouse model and assessing global brain dynamics through novel metrics originally employed in fields outside of neuroscience (36), we have demonstrated that dKI mice exhibit early, awake state-specific alterations in brain dynamics associated with cognitive deficits in complex memory tasks. Crucially, these alterations occur prior to amyloid plaque onset, challenging the traditional amyloid-centric view of early AD pathology. Furthermore, we showed that two weeks of vGENUS increased brain dynamics between the first and the final day of the protocol. This increase in brain dynamics fluidity persisted after the end of stimulations, during performances of memory tasks where previously observed deficits were rescued.

Our findings suggest that alterations in awake-state brain dynamics could be an early hallmark of AD, occurring prior to amyloid plaque formation. The similarity between the hdEEG recordings in this study and those typically performed in humans suggests that brain dynamics fluidity could emerge as a promising diagnostic marker. This is supported by previous findings showing that microstates sequence complexity is reduced in AD patients and can help predict progression from Mild Cognitive Impairment (MCI) to AD (17). In addition, slowing down and increasing blocking frustration in resting state fMRI dynamic Functional Connectivity had already been reported in AD (15) or cognitive challenge models of early mnesic impairments (42). Given the non-invasive nature and accessibility of EEG, assessing brain dynamics fluidity could enable earlier detection of AD, potentially during MCI and Subjective Cognitive Decline (SCD) stages, where patients report cognitive issues but show no deficits in standard neuropsychological tests. An easily implementable diagnostic tool for early-stage AD could significantly improve the timing and effectiveness of treatment interventions. The potential clinical translation of this approach warrants further investigation, including longitudinal studies in human populations to validate the predictive power of brain dynamics fluidity in AD progression.

Consistent with previous reports (21, 22), we found that 2 weeks of vGENUS rescued AD-related memory deficits in dKI mice. However, as recent studies have highlighted (27, 28), since 4-month-old dKI mice lack amyloid plaques, it is improbable that vGENUS targets amyloid pathology directly, or at least not exclusively or primarily. Instead, our data suggest that vGENUS restores healthy brain dynamics fluidity, an

effect that persists even after stimulation ends. This finding points to a broader impact of vGENUS on brain dynamics beyond 40Hz entrainment, which has been debated in recent literature (26, 27). Notably, the restoration of global brain dynamics was not immediate but required a chronic 2-week protocol, indicating that long-term processes rather than immediate brain entrainment likely drive these changes.

One potential explanation for the observed effects could be metabolic reorganization of brain networks. Indeed, vGENUS has been shown to entrain vascular reactions in the brain, notably increasing blood vessel diameter (22, 25) and has already demonstrated beneficial effects in mouse models of stroke (43). Given that cerebral hypoperfusion has been linked to AD development (44) and cerebrovascular dysfunctions are associated with cognitive impairments (45), vGENUS-induced increases in brain blood flow could improve brain metabolism and, in turn, brain dynamics.

Another possibility is that vGENUS modulates specific neuromodulatory systems, particularly given that the reduction in brain dynamics fluidity observed in dKI mice is awake-state specific. vGENUS showed no effect on brain dynamics during sleep, suggesting that the mechanism may involve specific wake-related neuromodulators such as the noradrenergic system, which is both an early target in AD pathology (46) and known to affect large-scale brain dynamics (47). Future research will be needed to clarify the precise mechanisms by which vGENUS exerts its effects. However, our results, along with previous findings, converge to suggest that vGENUS beneficial effects on global brain dynamics are not specific to AD, as it has also shown benefits in epileptic patients (30). This suggests that vGENUS may represent a promising non-invasive treatment option for a variety of neurological disorders by targeting and modulating large-scale brain dynamics. Specifically, it could trigger endogeneous mechanisms for compensating early circuit dysfunction via a “reprogramming” of the working point of dynamic operation of brain networks (48, 49).

While our study provides novel insights into early AD pathophysiology and potential interventions, it is important to keep in mind that the use of a mouse model, while allowing for precise control and manipulation, may not fully recapitulate human AD pathology. Additionally, the long-term effects of vGENUS beyond the two-week period studied here remain to be explored.

In conclusion, our study reveals altered brain dynamics as an early marker of AD-related changes, detectable before significant amyloid plaque formation and

correlating with subtle cognitive deficits. We demonstrate that vGENUS can restore these altered dynamics and ameliorate associated memory impairments. These findings not only provide new insights into early AD pathophysiology but also suggest novel approaches for early diagnosis and intervention in AD and potentially other neurological disorders characterized by disrupted brain dynamics.

Materials and Methods

Animals and surgery

Subjects. Double Knock-in App^{NL-F}/MAPT (dKI) and Wild-Type (WT) mice were obtained as described in (32). For EEG-behavior experiments, 8 WT and 8 dKI mice were housed in individual cages post-surgery. For behavior only experiments, 35 WT and 37 dKI 4 months-old mice were housed in individual cages. All animals were under a 12h light/dark cycle with food and water present *ad libitum*. Both sexes were balanced in population to get closer to real population representation without studying sex effect. All experimental protocols agreed with the European Committee Council directive (2010/63/UE) and were approved by the French Ministry of Research (APAFIS#28839-2021010509459441).

Surgery. Surgeries were performed at 3 months old. Animals were anesthetized with isoflurane (IsoFlo, Zoetis) during the entire surgery (4% for induction then maintained at 1.5%). Local anesthesia was performed on incision site by Bupivacaïne and Lidocaïne (Lurocaine, Vetoquinol) injection prior to incision. Post-surgery analgesia was provided via sub cutaneous Metacam injection. EEG surface grid (H32 mouse EEG grid, Neuronexus, Ann Arbor, USA) were placed on the skull aligning the skull bregma with the grid landmark. The grid is fixed to the skull by applying Saline solution and letting it dry. One screw was inserted above the right cerebellum to serve as ground, and another one, placed rostral to the grid was used as fixation support for the implant. The implant was secured for long term use using dental glue (Super-bond, Sun Medical) and dental cement (Paladur).

Mice perfusion and immunochemistry

Mice were deeply anesthetized with an intraperitoneal injection of ketamine (200 mg/kg) and xylazine (30 mg/kg) and then transcardially perfused with 0.1% heparin in 0.1 M phosphate-buffered saline (PBS), followed by 4% paraformaldehyde (PFA) in 0.1 M phosphate buffer (PB; pH 7.4, 4 °C). Brains were post-fixed in PFA for 24 hours, cryoprotected in 20% sucrose in PB for 48 hours, and subsequently stored at -80 °C. Coronal sections (40 µm) were obtained using a cryostat, covering the region from Bregma +2.58 to Bregma -5.88. Labeling was performed on one section every 160 µm, yielding approximately 62 sections per animal. Sections were processed at room temperature with agitation at 260 rpm as follows: three washes with PBS, followed by a 15-minute incubation in 70% formic acid, another three PBS washes, a 30-minute incubation in methanol with 0.3% H_2O_2, a 15-minute wash in ultrapure water, and two additional PBS washes. Sections were blocked for one hour in 5% normal horse serum (NHS) diluted in PBS containing 0.5% Triton X-100, followed by an 18-hour incubation at 4°C with mouse anti-6E10 antibody (1:1000 in 2% NHS, BioLegend #803001). After three PBS washes, sections were incubated for two hours with a biotinylated horse anti-mouse antibody (1:500 in PBS containing 0.5% Triton X-100, Vector Laboratories, #BA-2001-.5), followed by three PBS washes. Sections were then incubated for 30 minutes in an avidin-biotin solution (Vector Laboratories), washed twice in PBS, and finally in PB-Tris. Detection was performed using a 15-minute incubation in 3,3-diaminobenzidine (Vector Laboratories). Sections were mounted onto gelatin-coated slides, air-dried for 24 hours, dehydrated through a graded series of alcohol baths (70%, 90%, 95%, 100%, 100%), cleared with Clearify (American MasterTech Scientific), and fixed on microscopic slides with Diamount (Diapath S.P.A). Slides were then dried for 48 hours in the dark. Whole-section images were acquired at 20x magnification using a Hamamatsu NanoZoomer S60 digital slide scanner (Hamamatsu Photonics K.K., Japan). Amyloid plaques were counted using the cell counter tool in ndpView2 software (Hamamatsu Photonics K.K., Japan). Plaques were identified based on their shape and the density of 6E10 labeling relative to the background. Specificity of labeling was confirmed by including a negative control in which the primary antibody (6E10) was omitted. As a positive control, sections from two 12-month-old dKI mice were processed and analyzed using the same protocol.

Behavior

Apparatus. Behavioral tasks are conducted in a 55cm x 55cm open field with black wall and a white ground with a grid pattern.

Habituation. Two weeks after surgery, animals were habituated to the experimental apparatus. Transportation box was progressively presented over a week for the transport habituation. A recording cable was plugged several hours per day for 2 days to the head-mounted pre-amplifier so the mice could get used to its presence and weight. During the three days prior the behavioral task, an Open Field habituation consisting in ten minutes exploration of an empty Open Field and two object habituations consisting in two 10-minute sessions with a single object in the open field were performed.

Novel Object Recognition Task. At 4 months old and after vGENUS protocol, after the previously described habituation, mice perform a Novel Object Recognition (NOR) task. The mouse explores the open field where two similar objects are placed during a 10-minute sampling phase, and 24h after, realizing a 10-minute test phase consisting in an exploration of the open field where one of the previous objects is replaced by a new one. Objects exploration time is measured during the sampling and the test phase. To avoid place preference the object replaced is the one that was the less explored during the sampling phase.

Object in Place Task. At 4 months old and after vGENUS protocol, after the previously described NOR task, mice perform an Object in Place task. The mouse explores the open field where two different objects are placed during a 10-minute sampling phase, then wait a 5 minute inter trial interval in the home cage, before a second 10-minute test phase consisting in an exploration of the open field where one of the previous object is replaced by the copy of the other. Here neither the environment nor the object is new during the test phase but only the association between the specific object and its place in the environment. Objects exploration time is measured during the sampling and the test phase. To avoid place preference the object replaced is the one that was the less explored during the sampling phase.

Memory performances. To assess memory performances a Memory Index (MI) is computed from object exploration times during test as follow:

$$MI = \frac{New\ Object\ Exploration\ Time\ -\ Familiar\ Object\ Exploration\ Time}{New\ Object\ Exploration\ Time\ +\ Familiar\ Object\ Exploration\ Time}$$

Sleep recordings. After the sampling phase of the NOR, mice are recorded in their home cage for a minimum of 6 hour during light phase to record first post learning sleep episodes.

Visual Gamma Entrainment Stimulation (vGENUS) protocol

Visual GENUS protocol and setup was performed as described in (20). The day after the performance of the OiP task start a 15-day protocol. Each day, mice are placed in their home cages in the stimulation room with light on for a 1-hour stalling. Mice are then individually placed in stimulation cages, consisting in regular cages with 3 black painted walls to let transparent only the wall facing the stimulation light, without litter, food and water access. For one hour, the light of the room is turned off and only a 12V LED strip with a 4000/4500K light temperature and a 1200lm/m (Ledkia) controlled by an Arduino is either flickering at 40 Hz or displaying continuous light. After the stimulation, mice are back in the home cage for a 1-hour stalling in the stimulation room with the light on and the LED strip off before returning to the animal facility or doing behavioral task.

Electrophysiological recordings and analysis

Recording and preprocessing. The electrophysiological activity was recorded with an Intan recording controller (RHD Recording Controller, Intan Technologies, USA). The signals were amplified 200x, recorded whole-band (0.1Hz-15 kHz) and digitized at 1kHz. Qualitative rejection of faulty channels was conducted, any animals presenting more than five faulty channels were excluded from the study. EEG signals were then lowpass filtered at 100Hz and artefact related activity were removed via Independent Component Analysis (ICA). The signals were then coarse-grained with a 40ms time windows to fit the frame rate of the behavior video recording.

Spectral analysis. Spectrograms were computed on non coarsegrained signals of 10 min recordings during vGENUS stimulation using Matlab Chronux toolbox *mtspecgram* function. Power spectrums were obtained by averaging the spectrogram over time. Relative 40Hz power was obtain by dividing the 40Hz power by the total power spectrum. 40Hz relative power was then averaged over cortical regions (Prefrontal

Cortex:PFC; Motor Cortex: MOC; Somato-sensory Cortex: SSC; Parietal Cortex: PAR; Retrosplenial Cortex: RSC; Visual Cortex: VIS) based on Allen Institute mouse cortical parcelation.

Microstates extraction with k-mean clustering. Microstates were extracted independently for each animal and each trial to favorize individual characterization. To extract microstates sequences in an unsupervised way, k-mean clustering using native Matlab function with correlation distance were performed on the coarse-grained EEG time series for a wide ranges of cluster extraction (3 to 8).

Microstates extraction with Global Field Power peaks. To extract EEG microstates through a procedure closer to the human EEG literature (39), Global Field Power was computed as the variance of the coarse-grained EEG of all channels at each time points. Peak of GFP were determined using a minimum peak prominence of 0.5. EEG at GFP peaks was then clustered using k-mean clustering with native Matlab function with correlation distance and centroid were extracted. Microstates sequences were constructed by applying at each time point of the coarse-grained EEG the centroid showing the highest Pearson correlation.

Microstates Fluidity. To study switching across microstates, transition probability matrices were computed as the probability to switch from a microstate visited at time *t* to a different microstate at times *t*+1. Diagonal entries in this transition matrix correspond to the probability of remaining in the currently visited microstate without switching, which is proportional to the average dwell-time within the considered microstate. The average of diagonal transition matrix entities was thus a measure of microstates stability, and we defined its inverse as Microstates Fluidity. Such a quantity decreases if dwell-times increase and time to the next microstate switching is increased.

Microstates Sequence Complexity. Microstates sequence complexity is computed following (50), through a minimum description length approach. Following Kolmogorov and Chaitin (51), the shortest the symbolic sequence can be described in a suitable lossless-compressed format, the less complex it is. Each microstates sequence is considered as a sequence of symbolic labels corresponding to the microstate visited at each time. Let suppose that *A*, *B*, *C…* are the labels of different microstates. Their set forms the dictionary Δ. An original description of the sequence can be given by listing all the individual positions in the sequence where a given label is used, e.g. $A\ a_1\ a_2\ a_3\ \ldots B\ b_1\ b_2\ b_3\ \ldots C\ c_1\ c_2\ c_{3\ldots}$ where a_i, b_i, c_i …are positions where the labels *A, B,*

C… respectively appear in the sequence. The length of the original description is thus given by

$$L_{orig} = |\Delta| + N_{words}$$

where $|\Delta|$ is the size of the dictionary and N_{words} is the number of labels in the symbolic stream. If there are repetitions of consecutive symbols associated to permanence within a same microstate for a certain epoch of longer duration than a single time-step, a potentially compressed description of the same sequence can be obtained using a different encoding, *A* l_1 s_1 l_2 s_2…*B* l_1 s_1 l_2 s_2…*C* l_1 s_1 l_2 $s_{2...}$ where the numbers l_i and s_i occurring alternatingly after a symbolic label, e.g. *A,* correspond, respectively to the length l_i of the *i*-th block of consecutive symbols *A* and to the shift of positions to find within the sequence the next (*i+1)*-th block of symbols *A.* If the number of blocks of symbols is much smaller than the number of individual symbols in the sequence, then the length L_{comp} of this second description will be shorter than L_{orig}. The complexity of the state transitions was quantified as the ratio of the compressed length to the original length Specifically, we also applied a base 100 exponential transformation so that the obtained values follow a normal distribution and statistical testing is simplified:

$$DL_{Complexity} = 100^{\frac{L_{comp}}{L_{orig}}}$$

Brain dynamics Fluidity. What we call here Dynamics fluidity corresponds to a quantity which has been called inverse persistence in the literature about the analysis of dynamical systems and, specifically, climatic time-series (36). This quantity is evaluated based on empirical multivariate and continuous-valued time-series, here the 30-dimensional coarse-grained multi-channel EEG. The mathematical theory of this quantity is sophisticated, and we invite the reader to refer to the original publications for full detail (37, 52, 53). We can however provide some intuition. We consider the values $u_{t,i}$ of the EEG activity of different channels *i* at time *t* as describing a trajectory u_t in a high dimensional space. We can then consider a system configuration u_0 visited by the system at a certain time and ask how much time is needed for the system's trajectory leaving a neighborhood of the current configuration, i.e. flowing away to far configurations that do not resemble u_0. The fluidity of the dynamics in proximity of the configuration *u* will be inversely reflecting the persistence time. The more persistent the configuration *u*, the longer the previous and subsequent states of the system will

resemble u, and the lower will be the dynamics fluidity. To estimate fluidity from time-series observations, a connection between dynamical systems theory and extreme-value statistics can be exploited. To quantify the deviation of the trajectory u_t from the reference point u_0, we introduce a distance measure dist(u_t,u_0), using the Euclidean distance. We are interested in detecting clustering behavior, i.e., "sticky" behavior where the trajectory u_t spends more time than usual around the reference point u_0. To highlight the short distance values in these clustering situations, we use the log-distance and define the function $g(t;u_0)=-\log(\text{dist}(u_t,u_0))$. This function is large when the trajectory u_t is in close proximity to u_0. Consequently, the probability of persistence or returns around u_0 corresponds to the probability of observing extreme values of $g(t;u_0)$.

Requiring that a point on the orbit falls within a ball of radius e^{-s} around u_0 is equivalent to asking that the corresponding value of the series $g(t)$ exceeds the threshold s. Assuming independence of exceedances $g(t)$, we obtain:

$$P\left[\left(X - s(q)\right) > y \mid X \geq s(q)\right] \cong \exp\left[-\left(\frac{y}{\sigma(\boldsymbol{u}_0)}\right)\right]$$

where $s(q)$ is a high threshold associated with a quantile q of the series X≡g(t) The resulting distribution is an exponential member of the Generalized Pareto Distribution (GPD) family. The parameter σ, the scale parameter of the distribution, depends on the point $u0$ in phase space and, for finite time series, on t. If we define $M_n = \max(X_0,X_1,\ldots,X_{n-1})$, we can then write:

$$P[M_n < y] \cong \exp\left[-\theta n \exp\left(-\frac{y}{\sigma}\right)\right]$$

where M_n is the maximum of the series over n time-steps.The details of this computation are given in (54). A metric of persistence can then be obtained as the inverse of the extremal index θ, dimensionalized by the time step of the data used, whereas σ can be linked to the dimensionality of the data.

The parameters θ, μ and σ can be fitted practically on data using a suitable maximum likelihood estimator, by adopting a large threshold η. MATLAB code is provided in the Supporting Material for their evaluation, based on the Süveges estimator (55). In our study we set η to be equal to the 98% quantile of the distribution of $g(t; u_0)$. The quantity that we call here dynamics fluidity corresponds to the fitted parameter θ. The larger will be θ, the less persistent (and thus the more fluid) will be the dynamics. The case

of θ = 0 corresponds notably to u_0 being a fixed point, so that the probability of remaining in its proximity after having reached it is 1. The case of θ = 1 corresponds to the probability of the return time being a Poisson distribution and thus to the absence of trajectory points clustering. Furthermore, the parameter σ provides information on the local dimension of the attractor manifold surrounding u_0 (see again (36)) but we do not exploit this information in this study.

The estimated parameters, including dynamics fluidity θ depend on the local point $\boldsymbol{u}_0$ chosen as reference. Thus, fluidity analysis of a multivariate time-series of EEG will yield a time-series of values of fluidity, each estimated using as reference a different instantaneous observation of EEG multi-channel topography.

Statistical analysis

All statistics were performed using either built-in Matlab (r2024a) functions, Toolboxes, custom script or Jamovi 2.5. For all statistical test the significance threshold α was fixed at 0.05.

Behavior. Memory Index was analyzed using either unpaired t-test between both genotypes for each task before and after vGENUS for implanted animals displayed in Fig.1 & 5, 2-way ANOVA (factor: Genotype, Task) were used on the larger non implanted cohort before vGENUS and repeated 2-way ANOVA (non-repeated factor: Genotype; repeated factor: vGENUS) were used on the larger non implanted cohort after vGENUS. Post hoc tests were used when necessary, using a Bonferroni correction for multiple comparison. Before and after GENUS, memory index was compared for each Genotypes against chance levels using one sided t-test testing $H_1 > 0$ or memory index “above” chance levels. Exploration Time was analyzed using a 3-way ANOVA (factor: Genotype, Task and Phase (Sampling/Test) before vGENUS and 3-way repeated ANOVA (non-repeated factor: Genotype and Phase (Sampling/Test); repeated factor: GENUS (before/after)) after vGENUS. Post hoc tests were used when necessary, using a Bonferroni correction for multiple comparison.

EEG Microstates. Microstates Fluidity and Complexity were analyzed using 4-way ANOVA (factor: Genotype, Phase, Clusters, Task; Fig. S2). Post hoc tests were used when necessary, using a Bonferroni correction for multiple comparison. As the factor Phase (Sampling/Test) & Clusters showed no significant interaction with other factors, to reduce dimensions analyses were further conducted on concatenated EEG between

Sampling and Phase, and Microstates fluidity and complexity averaged over the number of microstates extracted with a 2-way ANOVA (factor: Genotype, Task; Fig. 2). Beside similar 2-way ANOVA (Fig. 5), post vGENUS results were also analyzed with a repeated 4-way ANOVA (factor: Genotype, Task, Clusters, vGENUS, Fig. 5).

Dynamics Fluidity. EEG fluidity was computed on EEG time-series concatenated between Sampling and Test. Average distributions were then compared two by two using bootstrapped Kolmogorov-Smirnoff (KS) statistics to probe whether the two distributions had significantly shifted mean and range respectively to a null hypothesis of no shift.

Using a Montecarlo procedure (pre-implemented in Matlab via the randsample function with a controlled random number stream), we redrawn 5000 random samples according to each of the distributions of fluidity to compare (modeled as histograms with a resolution of 200 uniform-width bins, with different histograms for different genotypes and conditions before of after vGENUS). We performed then random subsampling of these large Montecarlo samples, generating reduced bootstrap with replacements replicas each including 500 resampled observations, under two alternative hypotheses. In a H1 hypothesis of association between fluidity and genotype and condition, subsampling was performed separately over each of the Montecarlo sample specific to the different cases. In a H0 hypothesis of lack of association, we merged the Montecarlo samples for the two genotypes and generated two random subsamples from this common merged sample. We then computed KS statistics between the two subsamples, quantifying over bootstrap replicas the distribution of KS statistics between fluidity distributions for different genotypes, under both the H1 and H0 hypotheses. In the Results, we communicate the mean and standard deviation of KS statistics across iterations in the association hypothesis. Statistical significance of the difference between genotypes was assessed by comparing the H1-distribution of KS divergence values with the chance-level distribution under the H0 hypotheses, estimating a *p*-value based on the fraction of overlap between the two distributions, and correctd for multiple comparison with a Bonferroni correction. Note that this procedure is more conservative than the classical testing based on KS statistics non-parametric comparison.

Continuous dynamics-Microstates fluidity correlation. For each animal OiP and NOR preGENUS, mean dynamics fluidity was computed as the average of the EEG dynamics fluidity previously computed, mean microstates fluidity and complexity were

computed by averaging microstates fluidity or complexity obtained with 3 to 8 clusters to obtain a single value. Pearson correlations were then computed between mean dynamics fluidity and mean microstates fluidity or mean dynamics fluidity and mean microstates complexity taking all animals during OiP and NOR.

Acknowledgments

This work was supported by CNRS, Université de Strasbourg and grants from Agence Nationale de la Recherche: ANR HippoComp (ANR-21-CE37-0011) to RG and DB, and Fondation pour la Recherche Médicale (FRM): FRM- ALZ201912009643 to CM. The authors wish to thank Pr. Jesse Jackson and Dr. Yaroslav Sych for critical reading of the manuscript, Viktor Jirsa for inspiring discussions, the PIV (Plateforme d'Imagerie in Vitro, INCI, Strasbourg), Coline Portet and Flora Thellier, PhD students from the lab, for offering their technical help for the experiments.

References

1. A. Gustavsson, *et al.*, Global estimates on the number of persons across the Alzheimer's disease continuum. *Alzheimers Dement.* 19, 658–670 (2023).
2. D. J. Selkoe, J. Hardy, The amyloid hypothesis of Alzheimer's disease at 25 years. *EMBO Mol. Med.* 8, 595–608 (2016).
3. D. Josefson, Lumbar punctures could be used to diagnose Alzheimer's disease. *BMJ* 326, 950 (2003).
4. C. Marcus, E. Mena, R. M. Subramaniam, Brain PET in the Diagnosis of Alzheimer's Disease. *Clin. Nucl. Med.* 39, e413–e426 (2014).
5. J. S. Jacobsen, *et al.*, Early-onset behavioral and synaptic deficits in a mouse model of Alzheimer's disease. *Proc. Natl. Acad. Sci.* 103, 5161–5166 (2006).
6. C. Balducci, *et al.*, Cognitive deficits associated with alteration of synaptic metaplasticity precede plaque deposition in AβPP23 transgenic mice. *J. Alzheimers Dis. JAD* 21, 1367–1381 (2010).

7. A. Y. Hsia, *et al.*, Plaque-independent disruption of neural circuits in Alzheimer's disease mouse models. *Proc. Natl. Acad. Sci.* 96, 3228–3233 (1999).
8. D. Van Dam, *et al.*, Age-dependent cognitive decline in the APP23 model precedes amyloid deposition. *Eur. J. Neurosci.* 17, 388–396 (2003).
9. V. Hamm, *et al.*, Differential contribution of APP metabolites to early cognitive deficits in a TgCRND8 mouse model of Alzheimer's disease. *Sci. Adv.* 3, e1601068 (2017).
10. C. C. Rowe, *et al.*, Amyloid imaging results from the Australian Imaging, Biomarkers and Lifestyle (AIBL) study of aging. *Neurobiol. Aging* 31, 1275–1283 (2010).
11. S. E. Monsell, *et al.*, Comparison of symptomatic and asymptomatic persons with Alzheimer disease neuropathology. *Neurology* 80, 2121–2129 (2013).
12. D. Iacono, *et al.*, Mild Cognitive Impairment and Asymptomatic Alzheimer Disease Subjects: Equivalent A-Amyloid and Tau Loads With Divergent Cognitive Outcomes. *J Neuropathol Exp Neurol* 73 (2014).
13. D. Van De Ville, J. Britz, C. M. Michel, EEG microstate sequences in healthy humans at rest reveal scale-free dynamics. *Proc. Natl. Acad. Sci.* 107, 18179–18184 (2010).
14. D. Battaglia, *et al.*, Dynamic Functional Connectivity between order and randomness and its evolution across the human adult lifespan. *NeuroImage* 222, 117156 (2020).
15. L. Arbabyazd, *et al.*, State-switching and high-order spatiotemporal organization of dynamic functional connectivity are disrupted by Alzheimer's disease. *Netw. Neurosci.* 7, 1420–1451 (2023).
16. H. Lian, Y. Li, Y. Li, Altered EEG microstate dynamics in mild cognitive impairment and Alzheimer's disease. *Clin. Neurophysiol.* 132, 2861–2869 (2021).
17. L. Tait, *et al.*, EEG microstate complexity for aiding early diagnosis of Alzheimer's disease. *Sci. Rep.* 10, 17627 (2020).
18. R. S. Doody, *et al.*, Phase 3 Trials of Solanezumab for Mild-to-Moderate Alzheimer's Disease. *N. Engl. J. Med.* 370, 311–321 (2014).
19. J. L. Cummings, T. Morstorf, K. Zhong, Alzheimer's disease drug-development pipeline: few candidates, frequent failures. *Alzheimers Res. Ther.* 6, 37 (2014).
20. A. C. Singer, *et al.*, Noninvasive 40-Hz light flicker to recruit microglia and reduce amyloid beta load. *Nat. Protoc.* 13, 1850–1868 (2018).

21. C. Adaikkan, *et al.*, Gamma Entrainment Binds Higher-Order Brain Regions and Offers Neuroprotection. *Neuron* 102, 929-943.e8 (2019).
22. A. J. Martorell, *et al.*, Multi-sensory Gamma Stimulation Ameliorates Alzheimer's-Associated Pathology and Improves Cognition. *Cell* 177, 256-271.e22 (2019).
23. D. Chan, *et al.*, Gamma frequency sensory stimulation in mild probable Alzheimer's dementia patients: Results of feasibility and pilot studies. *PLOS ONE* 17, e0278412 (2022).
24. V. Manippa, *et al.*, An update on the use of gamma (multi)sensory stimulation for Alzheimer's disease treatment. *Front. Aging Neurosci.* 14, 1095081 (2022).
25. M. H. Murdock, *et al.*, Multisensory gamma stimulation promotes glymphatic clearance of amyloid. *Nature* (2024). https://doi.org/10.1038/s41586-024-07132-6.
26. M. Schneider, A. Tzanou, C. Uran, M. Vinck, Cell-type-specific propagation of visual flicker. *Cell Rep.* 42, 112492 (2023).
27. M. Soula, *et al.*, Forty-hertz light stimulation does not entrain native gamma oscillations in Alzheimer's disease model mice. *Nat. Neurosci.* 26, 570–578 (2023).
28. Y. L. Yang, T. W. Lai, Chronic Visual Stimulation with LED Light Flickering at 24, 40, or 80 Hz Failed to Reduce Amyloid β Load in the 5XFAD Alzheimer's Disease Mouse Model. *eneuro* 10, ENEURO.0189-23.2023 (2023).
29. Y. Zhang, *et al.*, 40 Hz Light Flicker Alters Human Brain Electroencephalography Microstates and Complexity Implicated in Brain Diseases. *Front. Neurosci.* 15, 777183 (2021).
30. L. T. Blanpain, *et al.*, Multisensory flicker modulates widespread brain networks and reduces interictal epileptiform discharges. *Nat. Commun.* 15, 3156 (2024).
31. T. Saito, *et al.*, Humanization of the entire murine Mapt gene provides a murine model of pathological human tau propagation. *J. Biol. Chem.* 294, 12754–12765 (2019).
32. C. Borcuk, *et al.*, Early memory deficits and extensive brain network disorganization in the App/MAPT double knock-in mouse model of familial Alzheimer's disease. *Aging Brain* 2, 100042 (2022).
33. B. Grayson, *et al.*, Assessment of disease-related cognitive impairments using the novel object recognition (NOR) task in rodents. *Behav. Brain Res.* 285, 176–193 (2015).

34. G. Taglialatela, D. Hogan, W.-R. Zhang, K. T. Dineley, Intermediate- and long-term recognition memory deficits in Tg2576 mice are reversed with acute calcineurin inhibition. *Behav. Brain Res.* 200, 95–99 (2009).

35. L. van der Maaten, G. Hinton, Visualizing Data using t-SNE. *J. Mach. Learn. Res.* 9, 2579–2605 (2008).

36. D. Faranda, G. Messori, P. Yiou, Dynamical proxies of North Atlantic predictability and extremes. *Sci. Rep.* 7, 41278 (2017).

37. V. Lucarini, D. Faranda, J. Wouters, Universal behaviour of extreme value statistics for selected observables of dynamical systems. *J. Stat. Phys.* 147, 63–73 (2012).

38. P. Grassberger, I. Procaccia, Measuring the strangeness of strange attractors. *Phys. Nonlinear Phenom.* 9, 189–208 (1983).

39. C. M. Michel, T. Koenig, EEG microstates as a tool for studying the temporal dynamics of whole-brain neuronal networks: A review. *NeuroImage* 180, 577–593 (2018).

40. R. Boyce, S. D. Glasgow, S. Williams, A. Adamantidis, Causal evidence for the role of REM sleep theta rhythm in contextual memory consolidation. *Science* 352, 812–816 (2016).

41. Y. Lu, *et al.*, A Critical Time-Window for the Selective Induction of Hippocampal Memory Consolidation by a Brief Episode of Slow-Wave Sleep. *Neurosci. Bull.* 34, 1091–1099 (2018).

42. D. Lombardo, *et al.*, Modular slowing of resting-state dynamic functional connectivity as a marker of cognitive dysfunction induced by sleep deprivation. *NeuroImage* 222, 117155 (2020).

43. L. Zheng, *et al.*, Rhythmic light flicker rescues hippocampal low gamma and protects ischemic neurons by enhancing presynaptic plasticity. *Nat. Commun.* 11, 3012 (2020).

44. R. N. Kalaria, R. Akinyemi, M. Ihara, Does vascular pathology contribute to Alzheimer changes? *J. Neurol. Sci.* 322, 141–147 (2012).

45. A. Y. Fouda, S. C. Fagan, A. Ergul, Brain Vasculature and Cognition. *Arterioscler. Thromb. Vasc. Biol.* 39, 593–602 (2019).

46. R. A. Bekdash, The Cholinergic System, the Adrenergic System and the Neuropathology of Alzheimer's Disease. *Int J Mol Sci* (2021).

47. J. M. Shine, *et al.*, Computational models link cellular mechanisms of neuromodulation to large-scale neural dynamics. *Nat. Neurosci.* 24, 765–776 (2021).
48. S. Petkoski, P. Ritter, V. K. Jirsa, White-matter degradation and dynamical compensation support age-related functional alterations in human brain. *Cereb. Cortex* 33, 6241–6256 (2023).
49. S. B. Stulz, S. Castro, G. Dumont, B. Gutkin, D. Battaglia, Compensating functional connectivity changes due to structural connectivity damage via modifications of local dynamics. [Preprint] (2024). Available at: https://www.biorxiv.org/content/10.1101/2024.05.31.596792v1 [Accessed 19 October 2024].
50. W. Clawson, *et al.*, Computing hubs in the hippocampus and cortex. *Sci. Adv.* (2019).
51. G. J. Chaitin, Algorithmic Information Theory (Cambridge Tracts in Theoretical Computer Science). (1987).
52. A. C. M. Freitas, J. M. Freitas, M. Todd, Hitting time statistics and extreme value theory. *Probab. Theory Relat. Fields* 147, 675–710 (2010).
53. N. R. Moloney, D. Faranda, Y. Sato, An overview of the extremal index. *Chaos Interdiscip. J. Nonlinear Sci.* 29 (2019).
54. D. Faranda, *et al.*, A statistical physics and dynamical systems perspective on geophysical extreme events. *arXiv.org* (2023). Available at: https://arxiv.org/abs/2309.15393v2 [Accessed 9 October 2024].
55. M. Süveges, Likelihood estimation of the extremal index. *Extremes* 10, 41–55 (2007).

Supplementary Figures

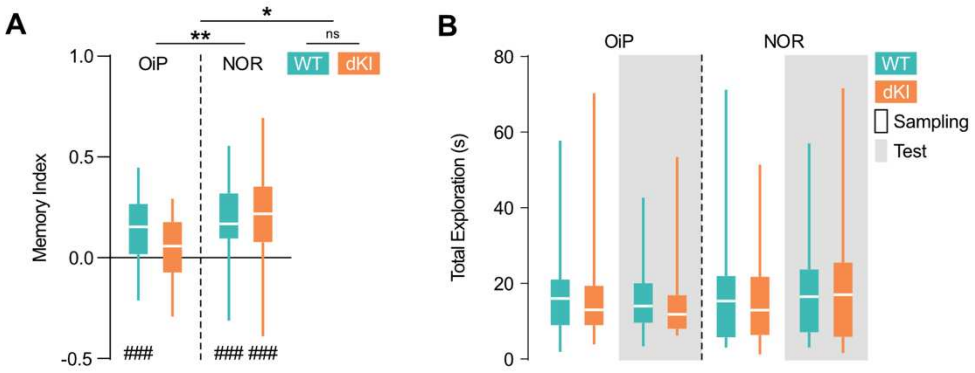

Figure 19 / S1. dKI mice memory deficits in complex task are unrelated to exploration time. Box ranges from 25 to 75 percentile and whiskers for minimum to maximum values, median is represented by white line. (A) Memory Index for WT (blue, n = 35) and dKI (orange, n = 37) mices performing Object in Place (OiP) and Novel Object Recognition (NOR) Tasks. Two way ANOVA (factor: Task, Genotype) reveal a significant interaction between Genotype and Task ($F(1,140) = 5.17$, $p = 0.024$) and only dKI mice performing OiP showed performances not higher than chance level (one sided t-test against chance, # : $p < 0.05$, ### : $p < 0.001$). (B) Total exploration time of the two objects for WT and dKI mice during Sampling (no background) and Test (grey background) of OiP and NOR task. Three way ANOVA (factor: Genotype, Task, Phase) shows no significant effects, thus indicating no difference in exploration between genotypes in both tasks.

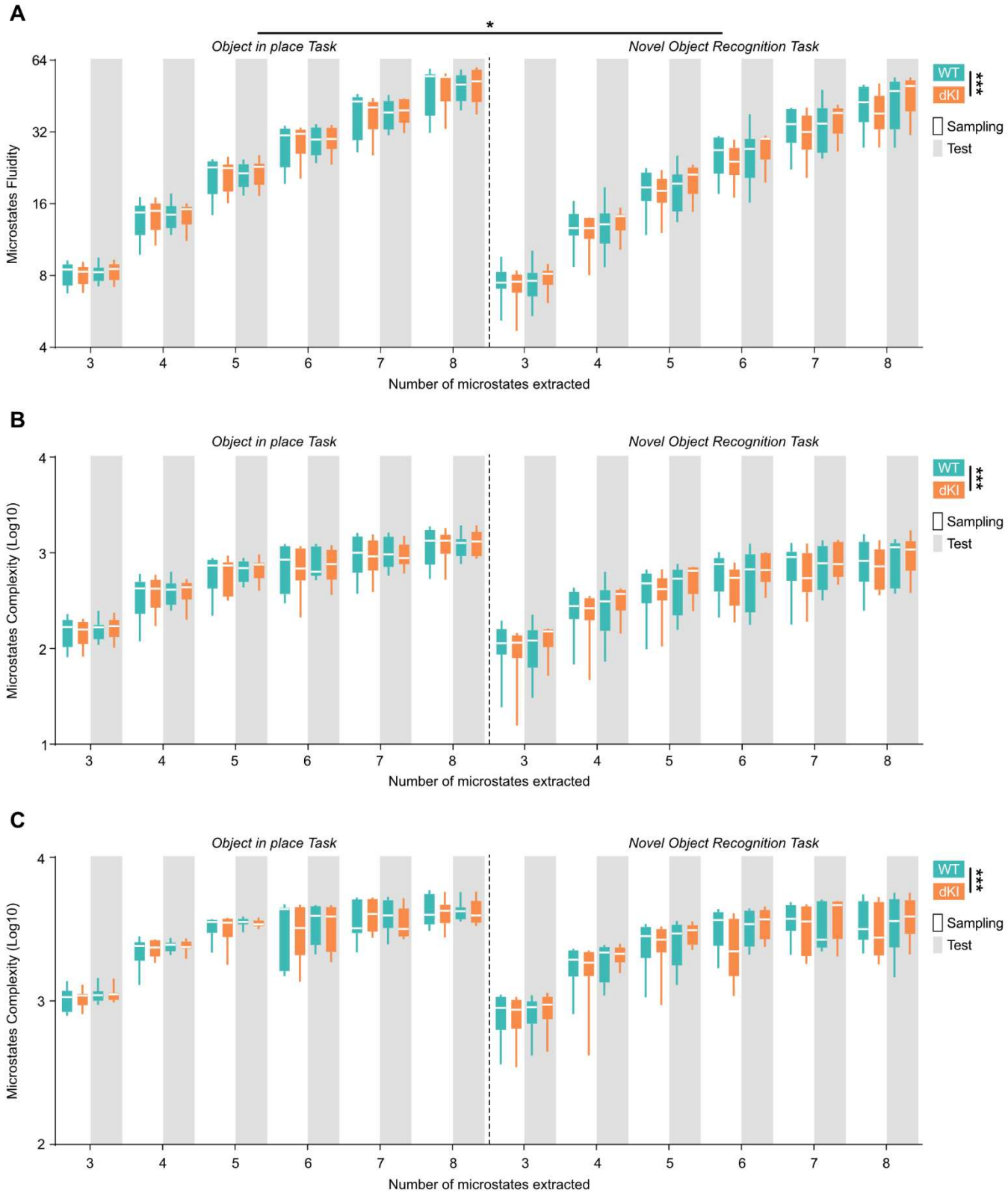
A
*
Object in place Task
Novel Object Recognition Task
Microstates Fluidity
64
32
16
8
4
3
4
5
6
7
8
Number of microstates extracted
WT
dKI
***
Sampling
Test
B
Object in place Task
Novel Object Recognition Task
Microstates Complexity (Log10)
4
3
2
1
Number of microstates extracted
C
Object in place Task
Novel Object Recognition Task
Microstates Complexity (Log10)
4
3
2
Number of microstates extracted

Figure 20 / S2. Microstates dynamics and complexity alteration are independent from the number of microstates extracted and not only explained by microstates repetition.
Box ranges from 25 to 75 percentile and whiskers for minimum to maximum values, median is represented by white line. (A) Microstate fluidity during sampling (no background) and test (grey background) phase of OiP and NOR tasks for WT (blue) and dKI (orange) mice (n=8 per group) across 3 to 8 microstates extracted. Four-way ANOVA (factor: Genotype, Task, Phase, Clusters; *: $p<0.05$ **: $p<0.01$ ***: $p<0.001$) showed significant Genotype effect ($F(1,336) = 41.884$; $p < 0.001$) indicating a lower fluidity in dKI mice. This effect showed no interactions with Task or Phase. (B) Microstate sequence complexity during sampling (no background) and test (grey background) phase of OiP and NOR tasks for WT (blue) and dKI (orange) mice (n=8 per group) across 3 to 8 microstates extracted. Four-way ANOVA (factor: Genotype, Task, Phase, Clusters; *: $p<0.05$ **: $p<0.01$ ***: $p<0.001$) showed significant Genotype effect ($F(1,336) = 40.185$; $p < 0.001$) indicating a lower complexity in dKI mice. This effect showed no interactions with Task or Phase. (C) Repetition free microstate sequence complexity during sampling (no background) and test (grey background) phase of OiP and NOR tasks for WT (blue) and dKI (orange) mice (n=8 per group) across 3 to 8 microstates extracted. Four-way ANOVA (factor: Genotype, Task, Phase, Clusters; *: $p<0.05$ **: $p<0.01$ ***: $p<0.001$) showed significant Genotype effect ($F(1,336) = 22.701$; $p < 0.001$) indicating a lower complexity in dKI mice. This effect showed no interactions with Task or Phase.

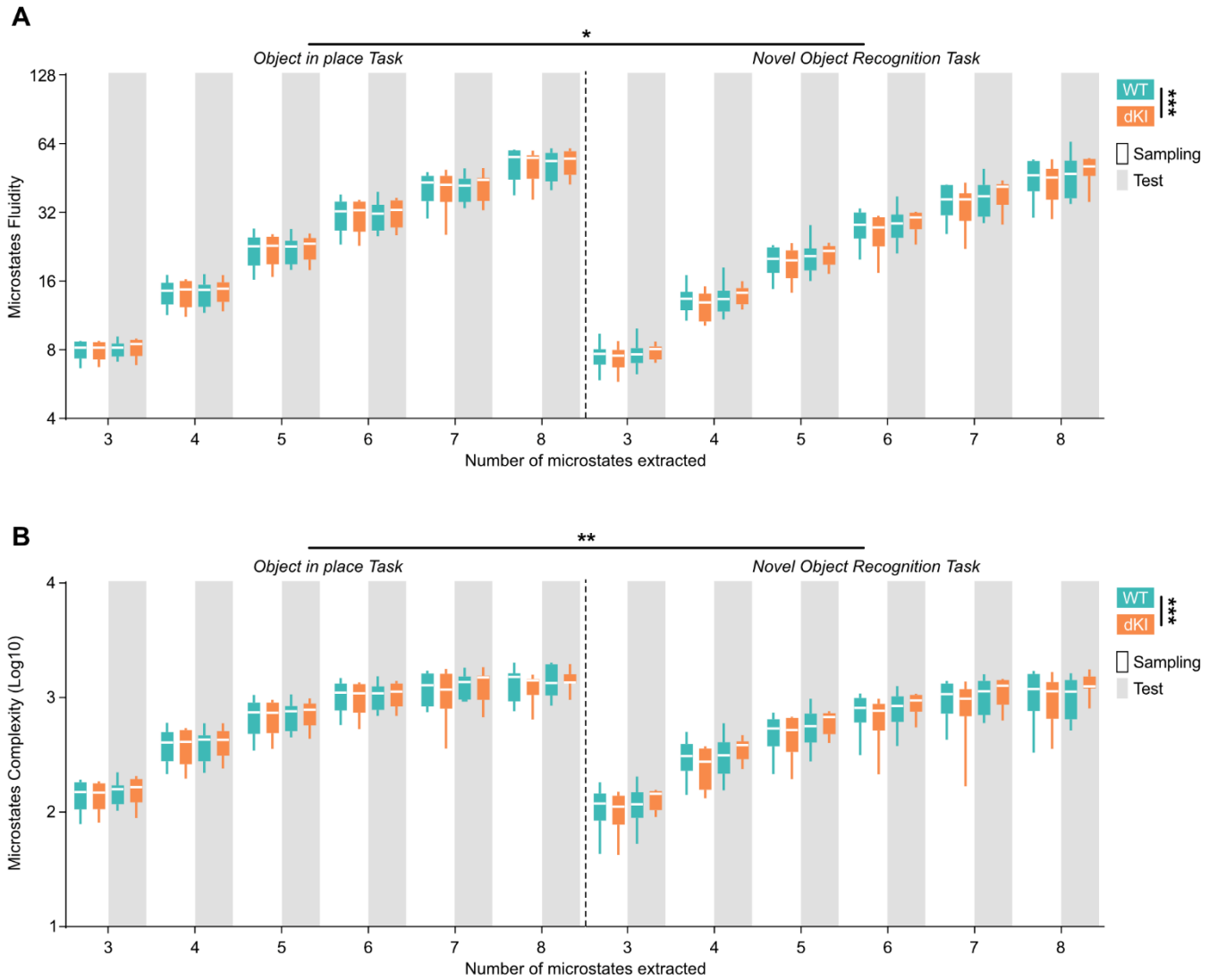

Figure 21 / S3. Microstates sequence dynamics and complexity are altered in dKI mice and rescued by vGENUS when using Global Field Power microstates extraction method.

Box ranges from 25 to 75 percentile and whiskers for minimum to maximum values, median is represented by white line. (A) Microstate fluidity during sampling (no background) and test (grey background) phase of OiP and NOR tasks for WT (blue) and dKI (orange) mice (n=8 per group) across 3 to 8 microstates extracted. Four-way ANOVA (factor: Genotype, Task, Phase, Clusters; *: $p<0.05$ **: $p<0.01$ ***: $p<0.001$) showed significant Genotype effect ($F(1,336) = 33.948$; $p < 0.001$) indicating a lower fluidity in dKI mice. This effect showed no interactions with Task or Phase. (B) Microstate sequence complexity during sampling (no background) and test (grey background) phase of OiP and NOR tasks for WT (blue) and dKI (orange) mice (n=8 per group) across 3 to 8 microstates extracted. Four-way ANOVA (factor: Genotype, Task, Phase, Clusters; *: $p<0.05$ **: $p<0.01$ ***: $p<0.001$) showed significant Genotype effect ($F(1,336) = 39.279$; $p < 0.001$) indicating a lower complexity in dKI mice. This effect showed no interactions with Task or Phase.

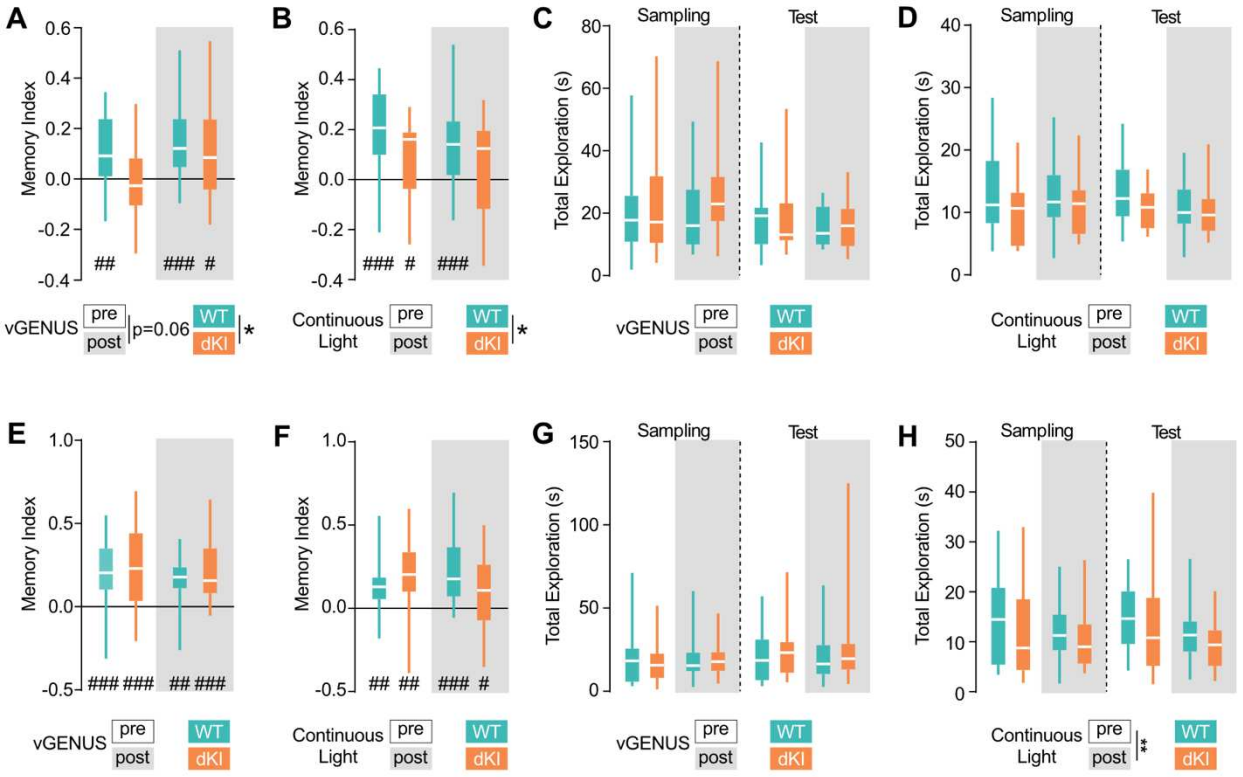
A
Memory Index
0.6
0.4
0.2
0.0
-0.2
-0.4
#
vGENUS
pre
post
p=0.06
WT
dKI
*
B
Memory Index
###
Continuous Light
pre
post
WT
dKI
*
C
Sampling
Test
Total Exploration (s)
80
60
40
20
0
vGENUS
pre
post
WT
dKI
D
Sampling
Test
Total Exploration (s)
40
30
20
10
0
Continuous Light
pre
post
WT
dKI
E
Memory Index
1.0
0.5
0.0
-0.5
###
vGENUS
pre
post
WT
dKI
F
Memory Index
#
Continuous Light
pre
post
WT
dKI
G
Sampling
Test
Total Exploration (s)
150
100
50
0
vGENUS
pre
post
WT
dKI
H
Sampling
Test
Total Exploration (s)
50
40
30
20
10
0
Continuous Light
pre
post
**
WT
dKI

Figure 22 / S4. vGENUS restoration of memory performances is dependant on 40Hz frequency.
Box ranges from 25 to 75 percentile and whiskers for minimum to maximum values, median is represented by white line. **(A)** Memory index for the OiP task in WT (n=17, blue) and dKI (n=19, orange) non EEG-recorded mice pre- (no background) and post- (grey background) vGENUS. Two-way ANOVA on repeated measures showed a genotype effect ($F(1,34) = 4.46$, $p = 0.042$) but no stimulation effect ($F(1,34) = 3.736$, $p = 0.062$). In dKI mice, memory performance did not exceed chance levels pre-vGENUS but improved significantly post-vGENUS (one-sided t-test against chance, #: $p < 0.05$, ##: $p < 0.01$, ###: $p < 0.001$). **(B)** Memory index for the OiP task in WT (n=18, blue) and dKI (n=18, orange) non EEG-recorded mice pre- (no background) and post- (grey background) 2 weeks of daily continuous light stimulation. Two-way ANOVA on repeated measures showed a genotype effect ($F(1,34) = 5.38$, $p = 0.026$) but no stimulation effect ($F(1,34) = 0.4463$, $p = 0.509$). dKI mice showed a memory index not higher from chance chance post-Continuous light (one-sided t-test against chance, #: $p < 0.05$, ##: $p < 0.01$, ###: $p < 0.001$). **(C)** Total exploration time during OiP task in WT (n=17, blue) and dKI (n=19, orange) non EEG-recorded mice pre- (no background) and post- (grey background) vGENUS. Three-way ANOVA on repeated measures showed no genotype ($F(1,68) = 1.208$, $p = 0.276$), vGENUS ($F(1,68) = 0.411$, $p = 0.524$), or phase effects ($F(1,68) = 2.953$, $p = 0.09$). **(D)** Total exploration time during OiP task in WT (n=18, blue) and dKI (n=18, orange) non EEG-recorded mice pre- (no background) and post- (grey background) 2 weeks of daily continuous light stimulation. Three-way ANOVA on repeated measures showed no genotype ($F(1,68) = 2.901$, $p = 0.093$), stimulation ($F(1,68) = 1.324$, $p = 0.254$), or phase effect ($F(1,68) = 0.714$, $p = 0.401$). **(E)** Memory index for the NOR task in WT (n=17, blue) and dKI (n=19, orange) non EEG-recorded mice pre- (no background) and post- (grey background) vGENUS. Two-way ANOVA on repeated measures showed no genotype ($F(1,34) = 0.698$, $p = 0.409$) nor vGENUS effect ($F(1,34) = 0.117$, $p = 0.734$). Both WT and dKI mice memory performances were higher than chance levels pre and post-vGENUS (one-sided t-test against chance, #: $p < 0.05$, ##: $p < 0.01$, ###: $p < 0.001$). **(F)** Memory index for the NOR task in WT (n=18, blue) and dKI (n=18, orange) non EEG-recorded mice pre- (no background) and post- (grey background) 2 weeks of daily continuous light stimulation. Two-way ANOVA on repeated measures showed no genotype ($F(1,34) = 0.449$, $p = 0.507$) nor stimulation effect ($F(1,34) = 0.218$, $p = 0.643$). Both WT and dKI mice memory performances were higher than chance levels pre and post-Continuous light (one-sided t-test against chance, #: $p < 0.05$, ##: $p < 0.01$, ###: $p < 0.001$). **(G)** Total exploration time during NOR task in WT (n=17, blue) and dKI (n=19, orange) non EEG-recorded mice pre- (no background) and post- (grey background) vGENUS. Three-way ANOVA on repeated measures showed no genotype ($F(1,68) = 0.648$, $p = 0.424$), vGENUS ($F(1,68) = 0.544$, $p = 0.463$), or phase effects ($F(1,68) = 1.403$, $p = 0.240$). **(H)** Total exploration time during NOR task in WT (n=18, blue) and dKI (n=18, orange) non EEG-recorded mice pre- (no background) and post- (grey background) 2 weeks of daily continuous light stimulation. Three-way ANOVA on repeated measures showed no genotype ($F(1,68) = 1.367$, $p = 0.246$) or phase effect ($F(1,68) = 9.78x10\text{-}4$, $p = 0.975$) but a stimulation effect ($F(1,68) = 11.08$, $p = 0.001$) indicating a reduced exploration after 2 weeks of continuous light exposure in both genotypes.

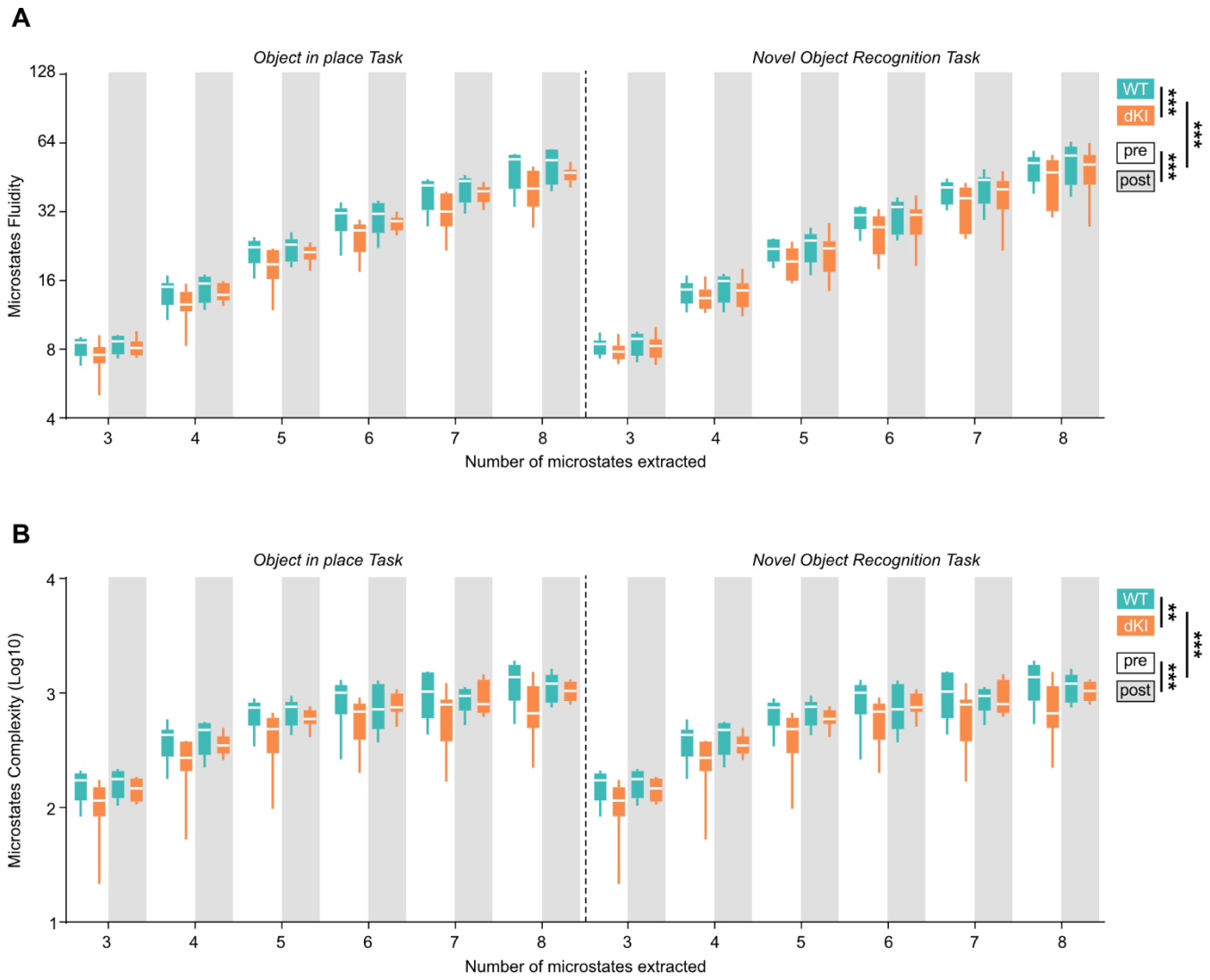

Figure 23 / S5 Microstates dynamics and complexity restoration by vGENUS are independent from the number of microstates extracted.

Box ranges from 25 to 75 percentile and whiskers for minimum to maximum values, median is represented by white line. **(A)** Microstate fluidity during OiP and NOR tasks for WT (blue) and dKI (orange) mice pre (no background) and post (grey background) vGENUS (n=8 per group) across 3 to 8 microstates extracted. Four-way repeated ANOVA (non –repeated factors: Genotype, Task, Clusters; repeated factor: vGENUS; *: p<0.05 **: p<0.01 ***: p<0.001) showed significant interaction between Genotype and vGENUS ($F(1,168) = 12.265$; $p < 0.001$). Post hoc test showed that vGENUS increased fluidity in WT ($t(168) = -3.09$; $p = 0.014$) and in dKI mice ($t(168) = -8.05$; $p < 0.001$) bringing a fluidity lower than WT ($t(168) = 5.23$; $p < 0.001$) to a fluidity almost similar to WT level ($t(168) = 2.69$, $p = 0.048$). **(B)** Microstate sequence complexity during OiP and NOR tasks for WT (blue) and dKI (orange) mice pre (no background) and post (grey background) vGENUS (n=8 per group) across 3 to 8 microstates extracted. Four-way repeated ANOVA (non –repeated factors: Genotype, Task, Clusters; repeated factor: vGENUS; *: p<0.05 **: p<0.01 ***: p<0.001) showed significant interaction between Genotype and vGENUS ($F(1,168) = 15.865$; $p < 0.001$). Post hoc test showed that vGENUS increased fluidity in WT ($t(168) = -5.144$; $p < 0.001$) and in dKI mice ($t(168) = -4.869$; $p < 0.001$) bringing a complexity lower than WT ($t(168) = 5.443$; $p < 0.001$) to a complexity non different to WT level ($t(168) = 2.153$, $p = 0.196$).

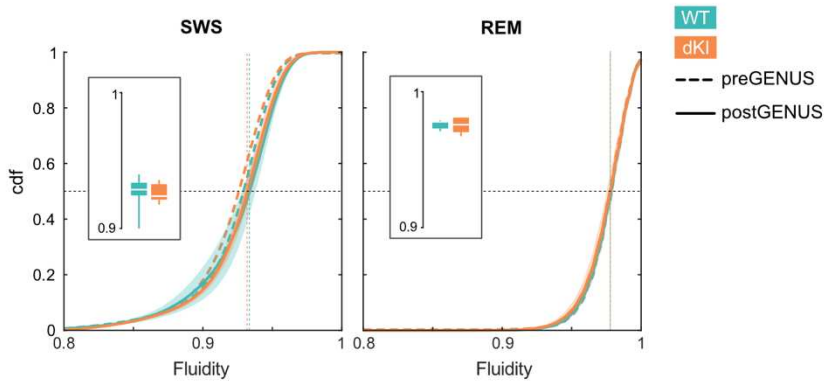

Figure 24 / S6. vGENUS induces no change in sleep brain fluidity.
Brain dynamics fluidity cumulative density distribution for WT and dKI mice show no differences in both REM and SWS after vGENUS (plain curve). No significant differences were observed for each genotype with dynamics fluidity before vGENUS (dotted curve). Data are presented as mean ± s.e.m. Dotted lines show distribution medians. Box displays individuals mean dynamics fluidity distributions.

Complementary Results 1: Spontaneous behavior dynamics

Scientific Background

Brain activity ultimately drives behavior, raising the question of whether the reduced brain dynamics fluidity observed in dKI mice also manifests as behavioral alterations beyond memory impairments. One might expect that periods of reduced brain dynamics fluidity may correspond to specific behavioral signatures, such as "stuck" or repetitive patterns, potentially affecting cognitive performance.

Recent advances in machine learning-based pose estimation now enable precise tracking of animal movements during behavioral tasks. These methods generate high-dimensional time series data representing the coordinates of multiple body parts across time. Much like brain activity, these postural dynamics can be analyzed as trajectories in a high-dimensional state space, making them amenable to the same nonlinear analytical tools previously applied to brain activity recordings.

Given our findings of altered brain dynamics fluidity in dKI mice, we sought to examine whether similar dynamical alterations could be detected in their postural dynamics. We applied the same fluidity analysis to the time series of pose-estimated skeleton coordinates, focusing specifically on postural configurations (i.e., the relative positions of body parts independent of the animal's location in space). This approach allows us to investigate potential early pathological patterns in movement that could be associated with the observed changes in brain dynamics fluidity.

Methods

Video Recording.

Behavioral tasks are recorded with a camera placed over the open field and filming it from a top view at a constant 25 frame per second rate.

Video Tracking.

Video tracking of the animal is performed *a posteriori* using DeepLabCut (Mathis et al., 2018). The animal is tracked at eight distinct points forming its skeletal structure: the nose, both ears, the neck, the midpoint of the body, the tail base, the middle of the tail,

and the tail end. X and Y coordinates for each point are extracted for every frame of the video.

Preprocessing of DeepLabCut data.

Since the apparatus can shift slightly between videos, normalizing the coordinates obtained from DeepLabCut is crucial for comparing different recordings. For each video, the coordinates of the four corners of the Open Field are manually identified. Using these, we calculate the vector *OA_OC*, which represents the offset between the origin of the Open Field reference frame and the camera's original referential, along with the angle θ (i.e., the angle between the top wall of the Open Field and the upper border of the camera's field of view). The *OA_OC* vector allows for centering the X and Y coordinates of each body parts ζ within the new camera referential as follows:

$$\begin{bmatrix} X_{\zeta OpenField} \\ Y_{\zeta OpenField} \end{bmatrix} = \begin{bmatrix} X_{\zeta Camera} \\ Y_{\zeta Camera} \end{bmatrix} + OA\_OC$$

Then θ angle allows the computation of the rotation matrix as follows:

$$RM = \begin{bmatrix} cos\theta & -sin\theta \\ sin\theta & cos\theta \end{bmatrix}$$

The Rotation matrix is then used to rotate the coordinates to align with the Open Field referential as follows:

$$\begin{bmatrix} X_{\zeta realigned} \\ Y_{\zeta realigned} \end{bmatrix} = RM \times \begin{bmatrix} X_{\zeta OpenField} \\ Y_{\zeta OpenField} \end{bmatrix}$$

Thus, body parts coordinates are now represented in a referential where the bottom wall of the Open Field aligns with the X-axis and the left wall with the Y-axis. The final step consists in normalizing the distances so the length of each Open Field wall spans from 0 to 1. To do so, each X coordinate of the body parts is divided by the norm of the vector representing the bottom wall and each Y coordinate is divided by the norm of the vector representing the left wall.

Barycenter extraction.

For several measure where precise body parts are unnecessary and only the animal's overall position is required, we use a reference point called the Barycenter. The Barycenter is obtained by averaging the coordinates of the neck and body for each frame.

Posture extraction. For each point ζ of the skeleton, the X and Y coordinates are normalized by the barycenter coordinates effectively centering them on the Barycenter as follows:

$$\begin{bmatrix} X_{\zeta centered} \\ Y_{\zeta centered} \end{bmatrix} = \begin{bmatrix} X_{\zeta} - X_{Barycenter} \\ Y_{\zeta} - Y_{Barycenter} \end{bmatrix}$$

Next, a rotation correction is applied to eliminate the effect of the animal's orientation in space, ensuring a consistent desired orientation. The angle φ is defined as the rotation angle between the Barycenter and the realigned "neck" position. Each skeletal point ζ is then realigned using the following transformation:

$$Coordinates_{\zeta realigned} = \left(X_{\zeta centered} + iY_{\zeta centered}\right)e^{i\left(\frac{\pi}{2}-\varphi\right)}$$

$$X_{\zeta realigned} = \Re\left(Coordinates_{\zeta realigned}\right)$$

$$Y_{\zeta realigned} = \Im\left(Coordinates_{\zeta realigned}\right)$$

Posture dynamics Fluidity.

Posture fluidity is computed as EEG dynamics fluidity based on a matrix presenting X and Y postures coordinates of 6 skeleton points (nose, both ears, neck, body and stem of the tail, Fig).

Mutual information

To assess potential relation between EEG dynamics fluidity and posture fluidity we computed mutual information between the two variables.

First, both EEG and postural fluidity were discretized into deciles using quantile binning. The sequences were then bootstrapped 100 times by either shuffling EEG and postural fluidity keeping the temporal association between the two or independently shuffling the two time series to generate a null model. For each bootstrap iteration, Mutual Information between the two time series was computed as follow:

$$MI(i,j) = \sum_{i,j} P(i,j) log_2 \frac{P(i,j)}{P(i)P(j)}$$

where i and j represent the decile states (1-10) of EEG and postural fluidity respectively, P(i,j) is the joint probability distribution, and P(i) and P(j) are the marginal probability distributions.

The MI was then normalized by the largest entropy between the two time series:

$$H = \max\left(-\sum_i P(i)log_2P(i)\ ;\ -\sum_j P(j)log_2P(j)\right)$$

The mean MI/H of bootstrap distribution was kept for each subject and experimental condition. The mean MI/H of independent bootstrap null model was used to compare test the first bootstrap data against chance levels.

Statistical analysis

Posture fluidity was computed on posture time-series concatenated between Sampling and Test. Average distributions were then compared two by two using bootstrapped Kolmogorov-Smirnoff (KS) statistics as described earlier for EEG dynamics fluidity distribution.

For each task, stage and genotype, Relative mutual information was compared via two sample Wilcoxon rank sum test to the null model of relative mutual info for the same task, stage and genotype to test significance against chance.

Difference of relative mutual information across conditions was assessed either by two-way ANOVA (Factor: Genotype, Task) or three-way repeated ANOVA (repeated factor: GENUS, non-repeated factors: Genotype, Task).

When necessary, p-value were corrected for multiple testing via Bonferroni correction.

Results

Posture dynamics fluidity is unaltered in dKI mice and weakly related to EEG dynamics fluidity

After extracting the coordinates of various body parts during task performance, these coordinates were normalized relative to the animal's position in space, resulting in time series of posture coordinates (Fig. 25A). Postural dynamics fluidity was then assessed using these posture time series, following the same methodology used for EEG dynamics fluidity. We found no differences in the distribution of postural dynamics fluidity between WT and dKI mice, either during the OiP task (Fig. 25B Left; KS = 0.071 ± 0.023, p = 0.609) or during the NOR task (Fig. 25B Right; KS = 0.0614 ± 0.0193, p = 0.775).

To investigate whether postural dynamics fluidity was associated with the previously studied EEG dynamics fluidity, we computed the relative mutual information (MI)

between the two variables for each animal in each task (Fig. 25C). Both WT and dKI mice showed relative MI values significantly different from chance in both tasks (two-sample Wilcoxon test against the null model, $p < 0.001$ for all conditions). However, there were no significant differences in relative MI between tasks (Two-way ANOVA: $F(1,28) = 0.137$, $p = 0.714$) or between genotypes, although a non-significant trend toward a decrease in dKI mice was noted (Two-way ANOVA: $F(1,28) = 4.05$, $p = 0.054$). Nevertheless, it is important to highlight that, despite these trends, the relative MI values ranged only from 0.1% to 0.35% of the maximal explained entropy, indicating that, overall, there is no substantial relationship between postural and EEG dynamics.

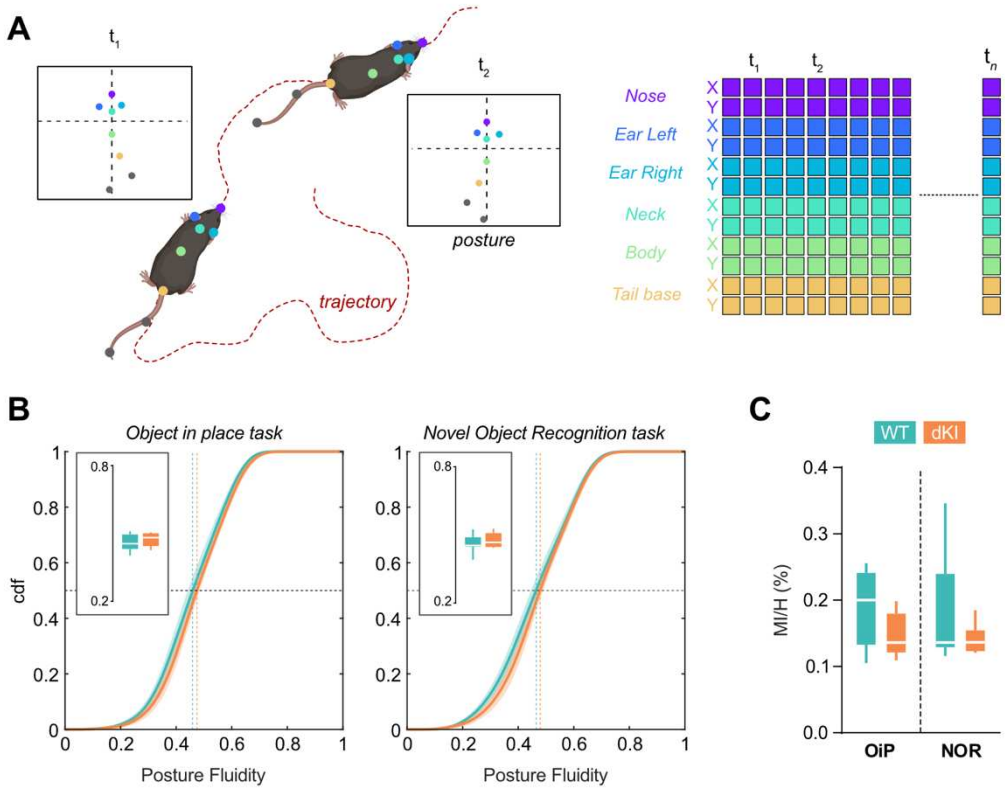

Figure 25. Posture dynamics fluidity is unaltered in dKI mice and weakly related to EEG dynamics fluidity.
(A) Skeleton coordinates of the animal are normalized to obtain posture coordinates which represent then a multidemnsional time series of the different posture coordinates. **(B)** No significant differences in posture dynamics fluidity between WT and dKI mice during OiP or NOR tasks. Data are presented as mean ± s.e.m. Dotted lines show distribution medians. Box displays individuals mean dynamics fluidity distributions. **(C)** Relative MI computed as MI/H. No differences were observed between Genotype or task, all condition were significantly different from chance levels. Box ranges from 25 to 75 percentile and whiskers for minimum to maximum values, median is represented by white line.

Two weeks of daily vGENUS didn't impact posture fluidity neither its relationship to EEG dynamics fluidity

Given that the two-week daily one-hour vGENUS protocol restores EEG dynamics fluidity in dKI mice, we examined its potential impact on postural dynamics fluidity and its relationship to EEG dynamics fluidity. We found no differences in the distribution of posture dynamics fluidity before (dotted curve) and after (solid curve) the vGENUS protocol for either genotype, during the NOR task (Fig. 26A *Left*, KS_{WT} = 0.1238 ± 0.0287, p_{WT} = 0.208; KS_{dKI} = 0.1229 ± 0.0271, p_{dKI} = 0.2164) or the OiP task (Fig. 26A *Right*, KS_{WT} = 0.1207 ± 0.0285, p_{WT} = 0.258; KS_{dKI} = 0.1052 ± 0.0243, p_{dKI} = 0.3784). Additionally, no differences between genotypes were observed after vGENUS during the NOR task (KS = 0.0628 ± 0.0166, p = 1) or the OiP task (KS = 0.0729 ± 0.019, p = 1). Relative MI remained significantly different from chance levels (Fig. 26B, two-sample Wilcoxon test against the null model, p < 0.001 for all conditions); however, vGENUS did not significantly impact relative MI (Three-way repeated ANOVA, F(1, 28) = 0.2672, p = 0.609). Thus, vGENUS showed no effects on postural dynamics fluidity or its relationship to EEG dynamics fluidity.

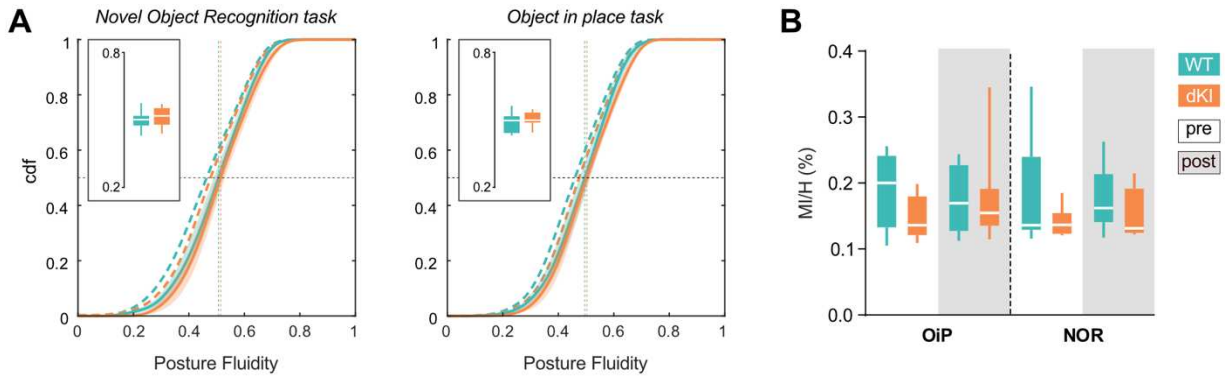

Figure 26. Two weeks of daily vGENUS didn't impact posture fluidity neither its relationship to EEG dynamics fluidity.
(A) Posture dynamics fluidity cumulative density distribution for WT and dKI mice show no differences in both NOR and OiP after vGENUS (plain curve). No significant differences were observed for each genotype with posture dynamics fluidity before vGENUS (dotted curve). Data are presented as mean ± s.e.m. Dotted lines show distribution medians. Box displays individuals mean dynamics fluidity distributions. **(B)** Relative MI computed as MI/H. No differences were observed between pre (white backgroung) or post (grey background) vGENUS, genotype or task, all condition were significantly different from chance levels. Box ranges from 25 to 75 percentile and whiskers for minimum to maximum values, median is represented by white line.

Discussion

Using nonlinear instantaneous fluidity analysis applied to pose-estimated postural coordinates, we found that dKI mice, despite exhibiting associative memory impairments and reduced brain dynamics fluidity, maintain normal postural dynamics fluidity. These findings align with a recent study employing similar pose-estimation software, followed by egocentric alignment of body parts, clustering of motifs into behavioral communities, and advanced kinematic and network analyses, which showed no alterations in spontaneous behavior in 6-month-old App^{NL-G-F} knock-in mice but robust alterations in 13 months old App^{NL-G-F} mice with an increased randomness of behavioral sequence (Miller et al., 2024).

To examine potential relationships between neural and behavioral dynamics, we computed the relative mutual information (MI) between EEG and postural fluidity. While both WT and dKI mice demonstrated above-chance relative MI, the values remained below 0.4% of maximum entropy, indicating that EEG and postural dynamics fluidity are largely independent.

These findings underscore the early nature of EEG dynamics alterations in our AD model, showing that changes in brain dynamics precede detectable alterations in fine motor behavior. The weak coupling between EEG and postural dynamics supports our interpretation that the reduced brain dynamics fluidity in dKI mice represents a pathological state specifically affecting wake brain function, rather than being a secondary consequence or cause of behavioral abnormalities. Thus, while dKI mice display normal fine-tuned behavior in both the OiP and NOR tasks, their reduced brain dynamics fluidity appears to specifically impair memory processing, particularly in tasks where memory consolidation is likely not occurring.

Following chronic vGENUS treatment, we observed no significant changes in either postural dynamics fluidity or its relationship with EEG dynamics fluidity. This selective effect on brain dynamics, without modification in behavioral patterns, suggests that vGENUS restores memory performance by specifically targeting pathological brain dynamics rather than inducing compensatory behavioral strategies.

Thus, the wake-specific alterations in global brain dynamics observed in dKI mice, associated with memory deficits and restored by vGENUS, prompt us to investigate whether specific functional networks, particularly oscillatory ones, might explain these effects.

Complementary Results 2: Time lasting of vGENUS cognitive effects

Scientific background

Most of the behavioral benefits of the GENUS protocol, as observed in our study, manifest immediately following intervention (Adaikkan et al., 2019; Islam et al., 2024; Martorell et al., 2019). However, to the best of our knowledge, no studies have explored the long-term stability of GENUS effects. For clinical application, it is critical to determine whether a single, two-week GENUS protocol is sufficient or if ongoing maintenance sessions are necessary to preserve these benefits.

We previously validated early memory deficits and the effects of vGENUS in a large, non-implanted cohort (n=17 WT and 19 dKi; see Fig. 19 / S1; 22 / S4). To examine the persistence of vGENUS effects, we reassessed memory performance in the OiP task one month after protocol completion in this large cohort.

Results & Discussion

WT and dKI mice showed OiP memory performance significantly higher than chance levels both post-GENUS and 1-month post-GENUS (Fig. 27, one sample t-test against chance levels, # : $p < 0.05$, ## : $p < 0.01$, ### : $p < 0.001$). Two ways ANOVA on repeated mesures showed no effects of genotype ($F(1,33) = 0.194$, $p = 0.663$) nor time between pre-GENUS and one month post-GENUS ($F(1,33) = 0.124$, $p = 0.727$).

Thus, dKI mice which showed memory deficits in OiP task, rescued by two weeks of vGENUS, still display good memory performances one month after the end of the GENUS protocol, implying a maintenance of beneficial effects on memory for at least one month.

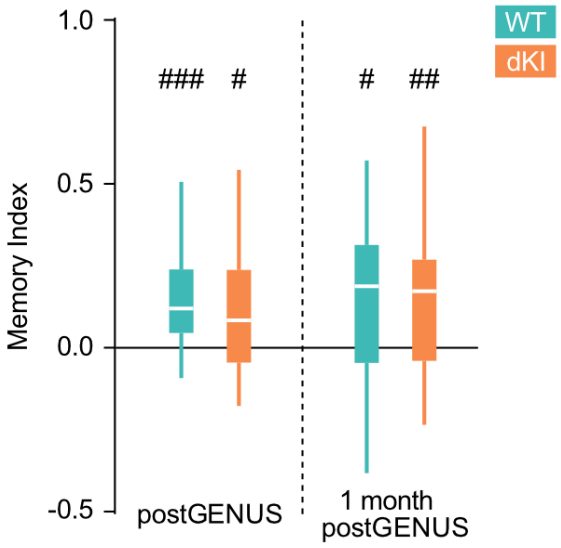

Figure 27. Maintenance of vGENUS beneficial memory effects.

Box ranges from 25 to 75 percentile and whiskers for minimum to maximum values, median is represented by white line. Memory index for the OiP task in WT (n=17, blue) and dKI (n=19, orange) non EEG-recorded mice pre- and post-vGENUS. Two-way ANOVA on repeated measures showed no genotype effect ($F(1,33 = 0.194$, $p = 0.663$) and no time delay effect ($F(1,33) = 0.124$, $p = 0.727$). WT and dKI mice display memory performances higher than chance levels both pre- and post-GENUS (one-sided t-test against chance, #: $p < 0.05$, ##: $p < 0.01$, ###: $p < 0.001$).

Part 2: Spectral mapping of wake-specific brain dynamics alteration and vGENUS-mediated recovery in dKI mouse model of preclinical AD

Scientific Background

The findings from our previous chapter revealed that dKI mice exhibit early memory deficits associated with reduced brain dynamics fluidity specifically during wakefulness. However, the broadband and global nature of these alterations makes it challenging to identify the specific neural networks or dynamical mechanisms underlying these wake-specific changes. As discussed in the introduction, oscillatory activity and its resulting functional networks, created through various coupling patterns, play fundamental roles in brain dynamics and cognitive processes.

In actively behaving rodents, theta and gamma oscillations emerge as the predominant rhythms, with their coupling patterns (such as coherence and theta-gamma PAC) being crucial for proper information processing and memory function (Fries, 2015; Tort et al., 2010). These oscillatory regimes and their coupling patterns are known to be disrupted in AD. Notable alterations include reduced gamma power (Hamm et al., 2017; Iaccarino et al., 2016; Verret et al., 2012), altered theta coherence (Ahnaou et al., 2017), and diminished theta-gamma PAC (Goutagny et al., 2013; X. Zhang et al., 2016) - some of which manifest even before Aβ deposition. The reduction in gamma power has been identified as a particularly significant alteration, as its restoration has been shown to improve memory performance in AD mouse models (Verret et al., 2012). These finding forms one of the key hypotheses behind the beneficial effects of vGENUS.

Our previous results demonstrated that two weeks of daily one-hour vGENUS sessions restore memory performance in dKI mice by rescuing impaired wake-specific global brain dynamics. This raises an important question: are these improvements mediated through gamma rhythm restoration, as previously hypothesized, despite the observation that GENUS has not been shown to produce sustained increases in gamma oscillations after the cessation of stimulation?

To address this question, we analyzed the oscillatory activity in EEG recordings from dKI mice during NOR and OiP tasks - conditions where global brain dynamics showed impairment - both before and after two weeks of vGENUS protocol. Specifically, we characterized theta and gamma oscillatory power, coherence, and phase-amplitude coupling networks to better understand the mechanistic basis of these therapeutic effects.

Methods

Data acquisition and preprocessing

Present analyses were performed on the same dataset described in Part 1 of the results, following identical behavioral tasks and EEG recording protocols. The only modification to the preprocessing pipeline was the retention of the original 1000Hz sampling rate, rather than using 40ms coarse-graining, to enable proper characterization of oscillatory activity.

Oscillatory Relative Power

Relative power was assessed using multi-taper spectrograms computed for each channel and animal using the *mtspecgram* function from the Chronux toolbox (http://chronux.org). Parameters included a 20s time window with 10s overlap. Power spectra were obtained by averaging spectrograms across the time dimension. Relative power was computed for both theta (5-12 Hz) and gamma (30-80 Hz) bands as the ratio of power within each specific frequency range to total power across all frequencies. To minimize potential artifacts, power spectrum values between 49-51 Hz were excluded from gamma calculations to avoid contamination from residual 50 Hz line noise.

Coherence

Pairwise coherence between EEG channels was computed using multi-taper time-frequency coherence (*cohgramc* function, Chronux toolbox). The resulting time-frequency coherence magnitudes were averaged across time to generate coherence spectra. Mean coherence values were then calculated for both theta and gamma frequency ranges.

Theta Gamma PAC

Theta-gamma PAC was assessed by first separating the broadband EEG signals using zero-phase lag filters into theta (5-12 Hz) and gamma (30-80 Hz) bands. Theta phase was obtained from the angle of the Hilbert transform of the theta-filtered signal, while gamma amplitude was derived from the magnitude of the Hilbert transform of the gamma-filtered signal. The Modulation Index (ModInd) was then calculated following methods described in (Tort et al., 2008, 2010).

Statistical Analysis

To reduce testing conditions, values were averaged between sampling and test phases for each animal. For channel-wise comparisons, relative power was compared between genotypes using Wilcoxon rank tests for each channel, while coherence and PAC were compared between genotypes for each channel pair. These comparisons were performed separately for each task, both before and after GENUS protocol. Pre- versus post-GENUS comparisons were performed separately for each genotype and task using the same statistical approach. For global measure comparisons, values were concatenated across all channels (power) or channel pairs (coherence and PAC) for each genotype and experimental stage. Distributions were compared using the same methodology as in Part 1, with multiple comparisons corrected using Bonferroni correction.

Results

dKI mice show no alterations of Theta relative power

We first investigated theta rhythms due to their prominence during active wake and their critical role in cognitive processes. Analysis of both NOR (Fig. 28A) and OiP tasks (Fig. 28B) revealed that dKI mice maintained normal theta relative power both globally and locally, before and after vGENUS protocol ($p > 0.15$ for all comparisons). The vGENUS protocol had minimal impact across conditions, with only dKI mice showing a slight increase in global theta relative power during the NOR task (KS = 0.1787 ± 0.0263, $p = 0.01$). These results indicate that theta oscillatory relative power remains largely intact in dKI mice, with only minor modulation by vGENUS protocol.

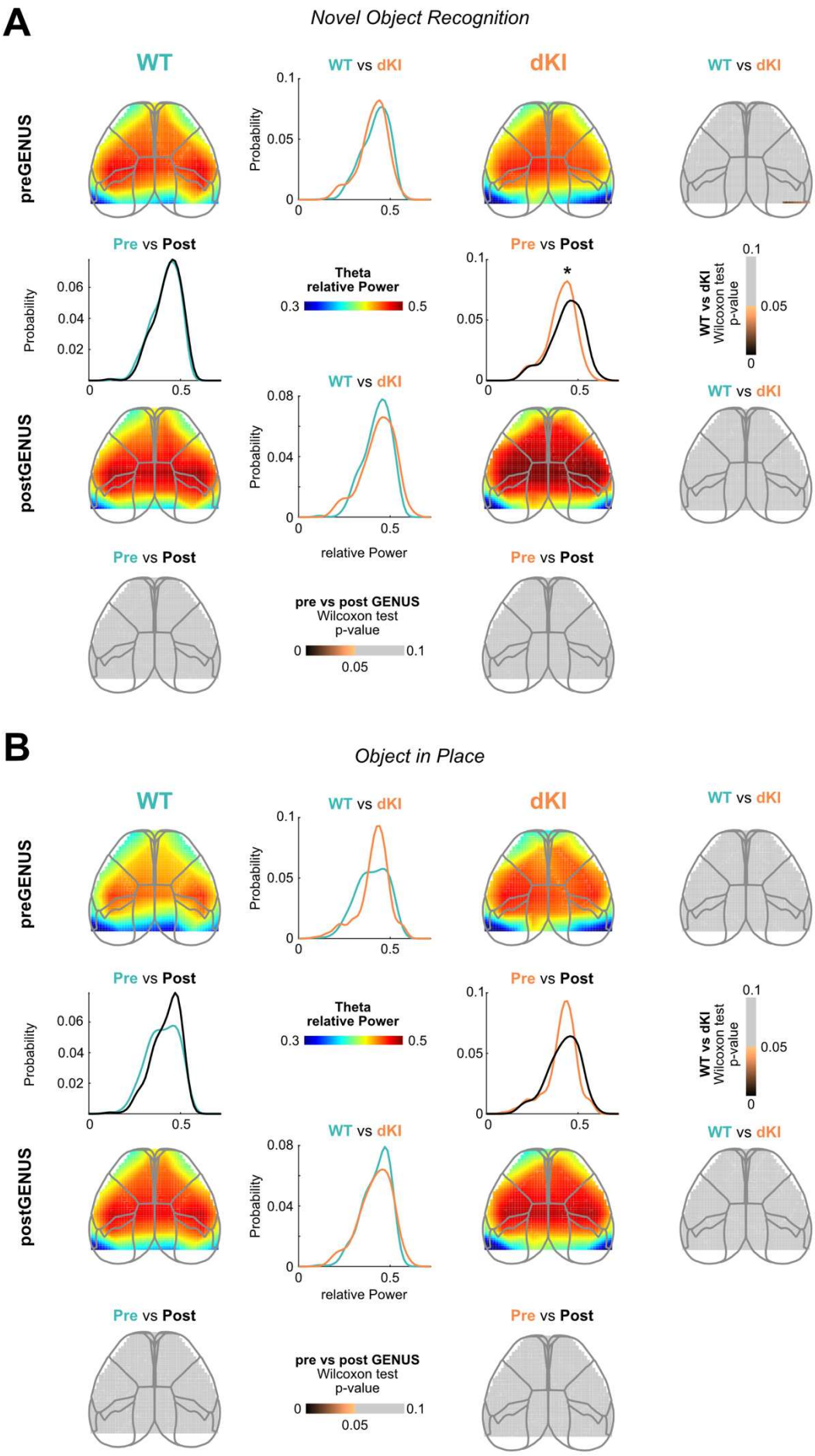
A
Novel Object Recognition
WT
dKI
WT vs dKI
preGENUS
postGENUS
Pre vs Post
Probability
relative Power
Theta
relative Power
0.3
0.5
*
WT vs dKI
Wilcoxon test
p-value
pre vs post GENUS
Wilcoxon test
p-value
0
0.05
0.1
B
Object in Place

Figure 28. Theta Relative power.
For both NOR (A) and OiP (B). *Top row from Left to Right*. preGENUS cortical map of relative power for WT mice, distribution of relative power for WT (blue) and dKI (orange) mice, preGENUS cortical map of relative power for dKI mice, cortical map of Wilcoxon p-value between WT and dKI preGENUS. *Second row.* Relative power distribution pre- (colored line) and post-GENUS (black line) for each genotype. *Third row from Left to Right*. postGENUS cortical map of relative power for WT mice, distribution of relative power for WT (blue) and dKI (orange) mice, postGENUS cortical map of relative power for dKI mice, cortical map of Wilcoxon p-value between WT and dKI postGENUS. *Bottom row.* Cortical map of Wilcoxon p-value between pre- and post-GENUS for each genotype.

Theta coherence is not altered in dKI mice and not impacted by vGENUS

Following our assessment of theta relative power, we examined potential alterations in theta-based functional networks through pairwise coherence analysis. Global coherence measures in both NOR (Fig. 29A) and OiP tasks (Fig. 29B) showed no significant differences between dKI and WT mice, either before or after vGENUS protocol ($p < 0.7$ for all comparisons). Local analysis revealed only one notable difference: reduced coherence between a visual cortex channel and regions in the SSC, MOC, and PFC in dKI mice across both tasks. The two-week vGENUS protocol did not affect theta coherence at either global or local levels in any condition ($p = 1$ for all comparisons). These findings demonstrate that theta coherence networks remain fundamentally intact in dKI mice and are unaffected by vGENUS protocol.

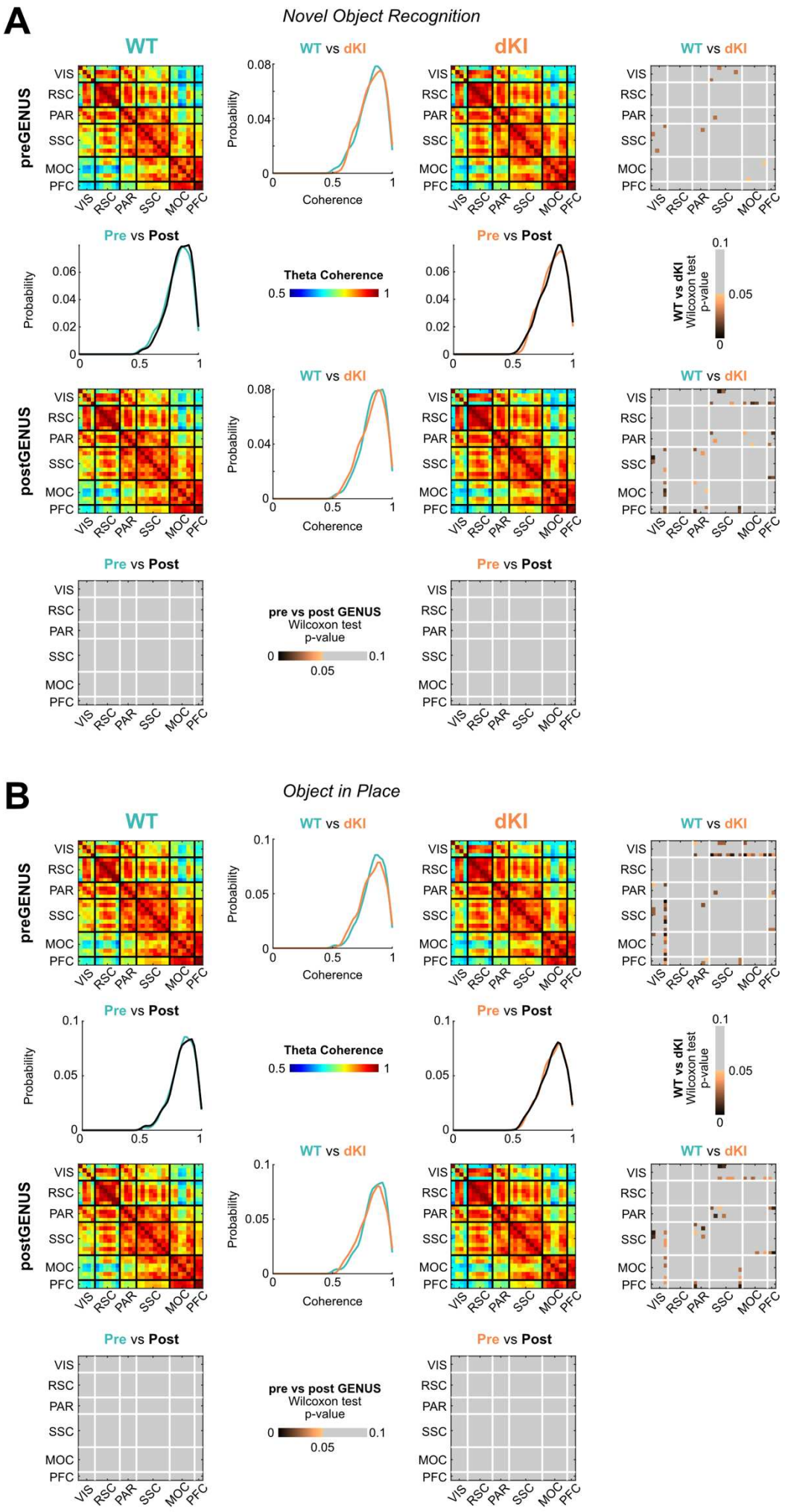
A
Novel Object Recognition
WT
dKI
WT vs dKI
preGENUS
postGENUS
VIS
RSC
PAR
SSC
MOC
PFC
Probability
Coherence
Pre vs Post
Theta Coherence
0.5
1
WT vs dKI
Wilcoxon test
p-value
0.1
0.05
0
pre vs post GENUS
Wilcoxon test
p-value
B
Object in Place

Figure 29. Theta Coherence.
For both NOR (A) and OiP (B). *Top row from Left to Right*. preGENUS Theta pairwise coherence matrices for WT mice, distribution of relative coherence for WT (blue) and dKI (orange) mice, preGENUS Theta pairwise coherence matrices for dKI mice, cortical map of Wilcoxon p-value between WT and dKI preGENUS. *Second row.* Relative coherence distribution pre- (colored line) and post-GENUS (black line) for each genotype. *Third row from Left to Right*. postGENUS Theta pairwise coherence matrices for WT mice, distribution of relative coherence for WT (blue) and dKI (orange) mice, postGENUS Theta pairwise coherence matrices for dKI mice, cortical map of Wilcoxon p-value between WT and dKI postGENUS. *Bottom row.* Matrices of Wilcoxon p-value between pre- and post-GENUS for each genotype. Parcellation of matrices in brain regions is based on Allen brain atlas; VIS : Visual Cortex, RSC : Retrosplenial Cortex, PAR : Parietal Cortex, SSC: Somatosensory Cortex, MOC: Motor Cortex, PFC: Prefrontal Cortex.

Gamma relative power is reduced in dKI mice and not rescued by vGENUS

During the NOR task, dKI mice exhibited significantly reduced global gamma relative power compared to WT controls (Fig. 30A), both before (KS = 0.3197 ± 0.0275, $p < 0.001$) and after vGENUS protocol (KS = 0.2306 ± 0.0276, $p < 0.001$). This reduction was initially most pronounced in the retrosplenial cortex and right visual and motor cortices, later becoming more widespread following vGENUS. Interestingly, the protocol showed no significant effect on gamma power during NOR in either genotype (WT: KS = 0.0617 ± 0.0162, $p = 1$; dKI: KS = 0.122 ± 0.0252, $p = 0.1$). During the OiP task, initial gamma relative power was comparable between genotypes (Fig. 30B, KS = 0.06 ± 0.02, $p = 1$), reflecting a task-specific reduction in WT gamma relative power (KS = 0.206 ± 0.021, $p < 0.001$) that was absent in dKI mice (KS = 0.135 ± 0.027, $p = 0.086$). Following vGENUS, WT mice showed increased gamma relative power (KS = 0.267 ± 0.029, $p < 0.001$), while dKI mice remained unchanged (KS = 0.095 ± 0.022, $p = 0.322$), resulting in a significant power differential (KS = 0.273 ± 0.026, $p < 0.001$). These results confirm a persistent gamma relative power deficit in dKI mice that remains unresponsive to vGENUS protocol.

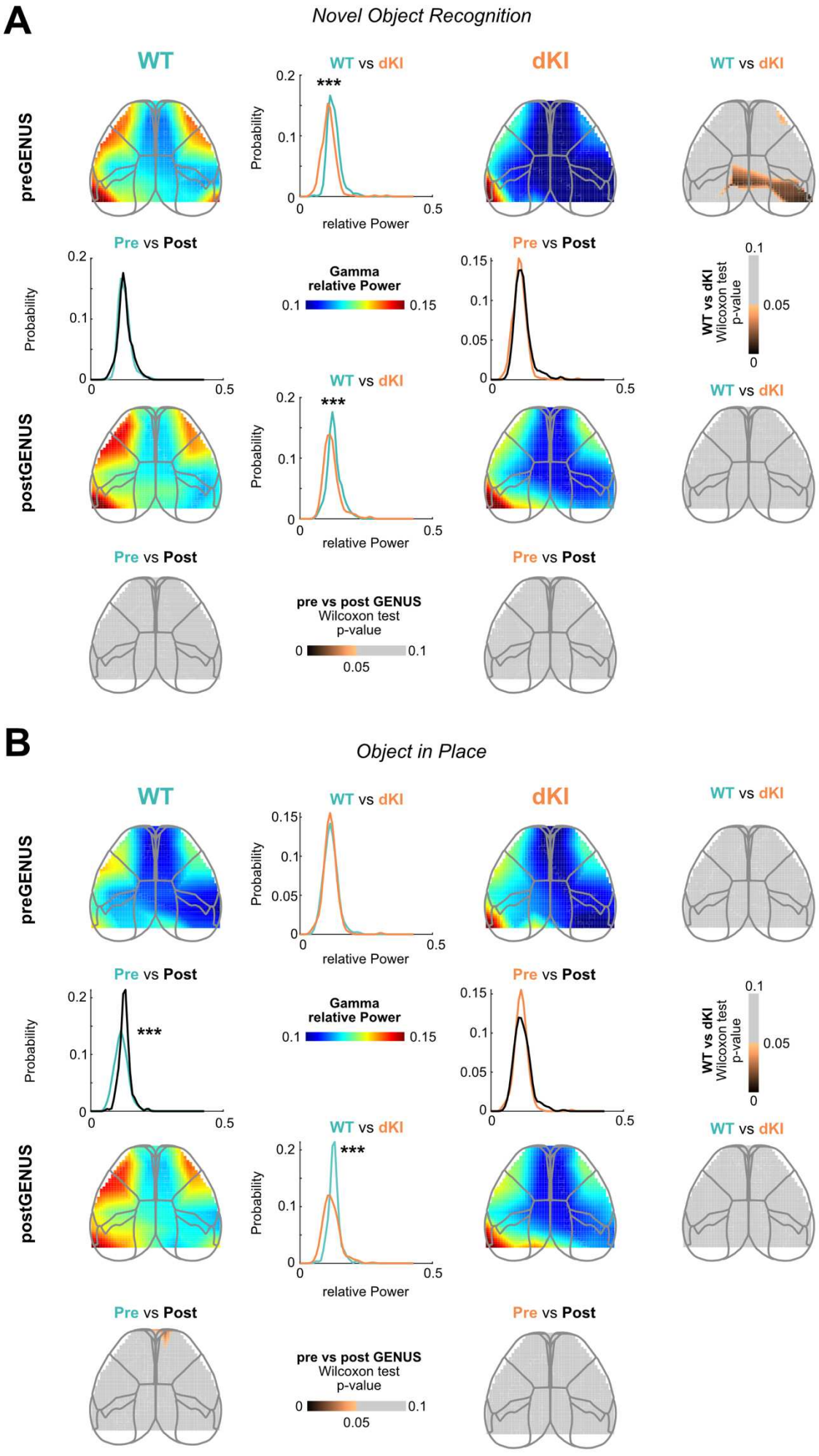
A
Novel Object Recognition
WT
dKI
WT vs dKI
preGENUS
postGENUS
Pre vs Post
Probability
relative Power
***
Gamma
relative Power
0.1
0.15
WT vs dKI
Wilcoxon test
p-value
0.05
pre vs post GENUS
B
Object in Place

Figure 30. Gamma Relative Power
For both NOR (A) and OiP (B). *Top row from Left to Right*. preGENUS cortical map of relative power for WT mice, distribution of relative power for WT (blue) and dKI (orange) mice, preGENUS cortical map of relative power for dKI mice, cortical map of Wilcoxon p-value between WT and dKI preGENUS. *Second row.* Relative power distribution pre- (colored line) and post-GENUS (black line) for each genotype. *Third row from Left to Right*. postGENUS cortical map of relative power for WT mice, distribution of relative power for WT (blue) and dKI (orange) mice, postGENUS cortical map of relative power for dKI mice, cortical map of Wilcoxon p-value between WT and dKI postGENUS. *Bottom row.* Cortical map of Wilcoxon p-value between pre- and post-GENUS for each genotype.

Gamma coherence is globally unaltered in dKI mice and not impacted by vGENUS

Despite reduced gamma relative power, gamma coherence networks showed remarkable preservation in dKI mice. Global coherence measures revealed no significant differences between genotypes across both tasks, before and after vGENUS protocol (Fig. 31A, B; $p = 1$ for all comparisons). The vGENUS protocol similarly showed no effect on gamma coherence in any condition. Local analysis identified only minor alterations, primarily a weak but significant decrease in parietal-prefrontal coherence in dKI mice pre-GENUS, which normalized post-GENUS without direct intervention effects. These findings indicate that gamma coherence networks remain largely intact in dKI mice despite reduced relative power, with neither pathology nor vGENUS protocol significantly impacting network organization.

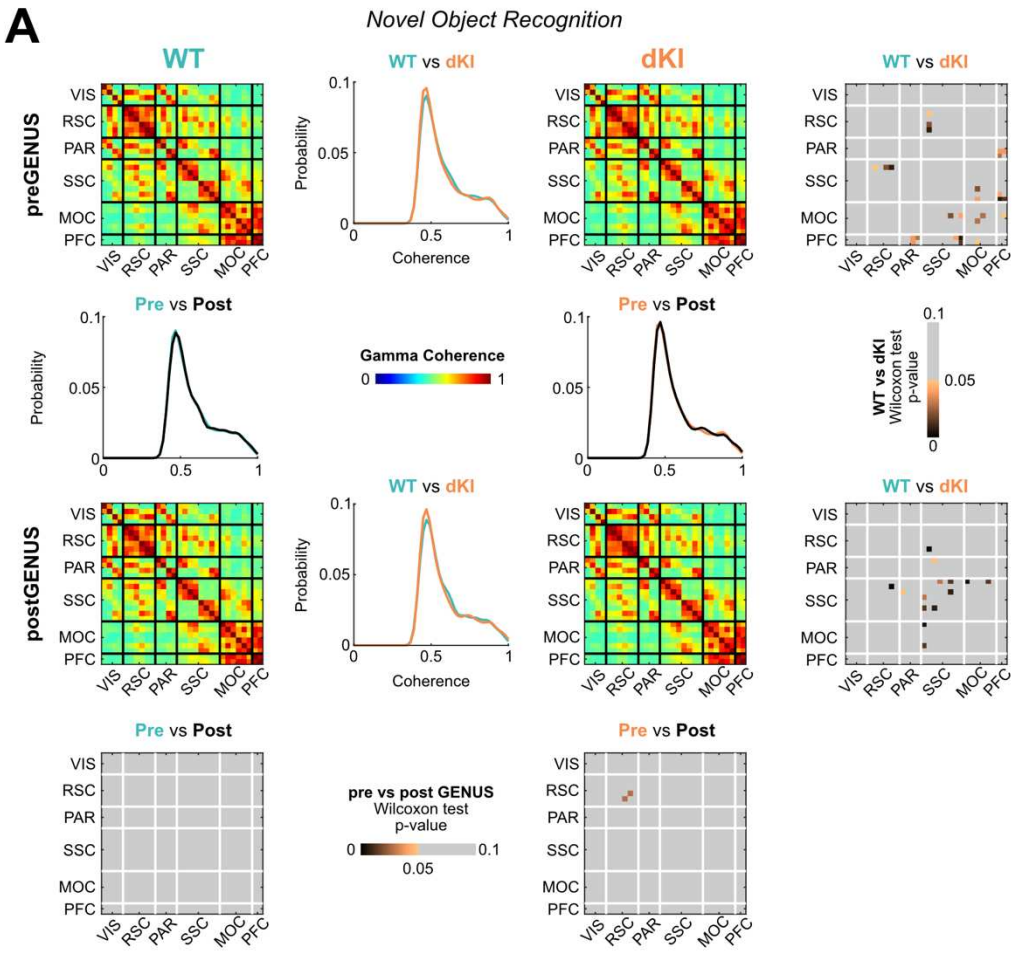
A
Novel Object Recognition
WT
dKI
WT vs dKI
preGENUS
postGENUS
Pre vs Post
Probability
Coherence
Gamma Coherence
pre vs post GENUS
Wilcoxon test
p-value
WT vs dKI
Wilcoxon test
p-value
VIS
RSC
PAR
SSC
MOC
PFC

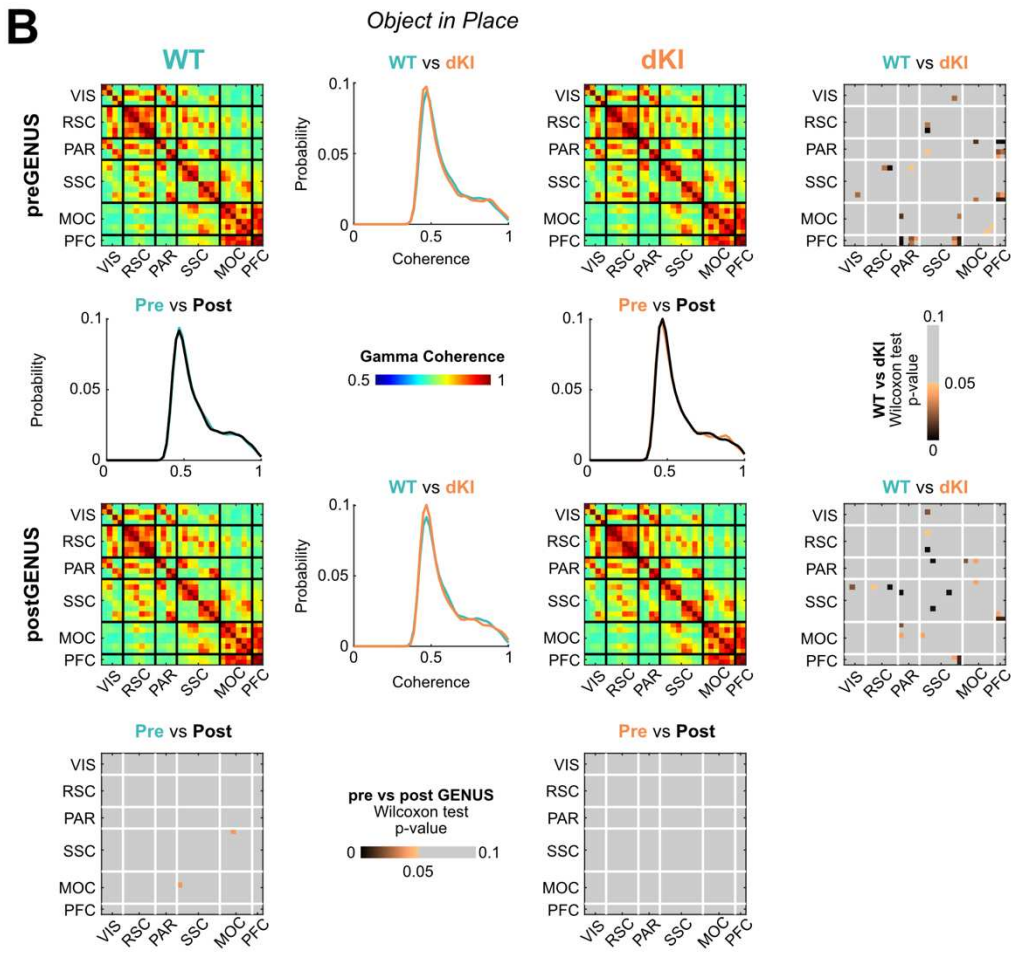
B
Object in Place
WT
dKI
WT vs dKI
preGENUS
postGENUS
Pre vs Post
Probability
Coherence
Gamma Coherence
pre vs post GENUS
Wilcoxon test
p-value
WT vs dKI
Wilcoxon test
p-value
VIS
RSC
PAR
SSC
MOC
PFC

Figure 31. Gamma Coherence
For both NOR (A) and OiP (B). *Top row from Left to Right*. preGENUS Gamma pairwise coherence matrices for WT mice, distribution of relative coherence for WT (blue) and dKI (orange) mice, preGENUS Gamma pairwise coherence matrices for dKI mice, cortical map of Wilcoxon p-value between WT and dKI preGENUS. *Second row.* Relative coherence distribution pre- (colored line) and post-GENUS (black line) for each genotype. *Third row from Left to Right*. postGENUS Gamma pairwise coherence matrices for WT mice, distribution of relative coherence for WT (blue) and dKI (orange) mice, postGENUS Gamma pairwise coherence matrices for dKI mice, cortical map of Wilcoxon p-value between WT and dKI postGENUS. *Bottom row.* Matrices of Wilcoxon p-value between pre- and post-GENUS for each genotype. Parcellation of matrices in brain regions is based on Allen brain atlas; VIS : Visual Cortex, RSC : Retrosplenial Cortex, PAR : Parietal Cortex, SSC: Somatosensory Cortex, MOC: Motor Cortex, PFC: Prefrontal Cortex.

Theta Gamma PAC in dKI mice pre- and post-GENUS

Given the selective reduction in gamma relative power alongside preserved theta oscillations, we examined potential alterations in theta-gamma cross-frequency coupling. Global theta-gamma PAC remained intact in dKI mice across both tasks and protocol conditions (Fig. 32A, B; $p < 0.18$ for all comparisons), with vGENUS showing no significant impact on global coupling measures ($p < 0.5$ for all comparisons). Local analysis revealed specific reductions in dKI mice between gamma amplitude in somatosensory and parietal channels and theta phase across most channels. Notably, vGENUS selectively enhanced frontal coupling during the OiP task, particularly between distributed theta phase and frontal gamma amplitude in motor and prefrontal regions. These results suggest that while global theta-gamma coupling remains intact in dKI mice, vGENUS can induce specific local enhancements in cross-frequency coupling during complex cognitive tasks.

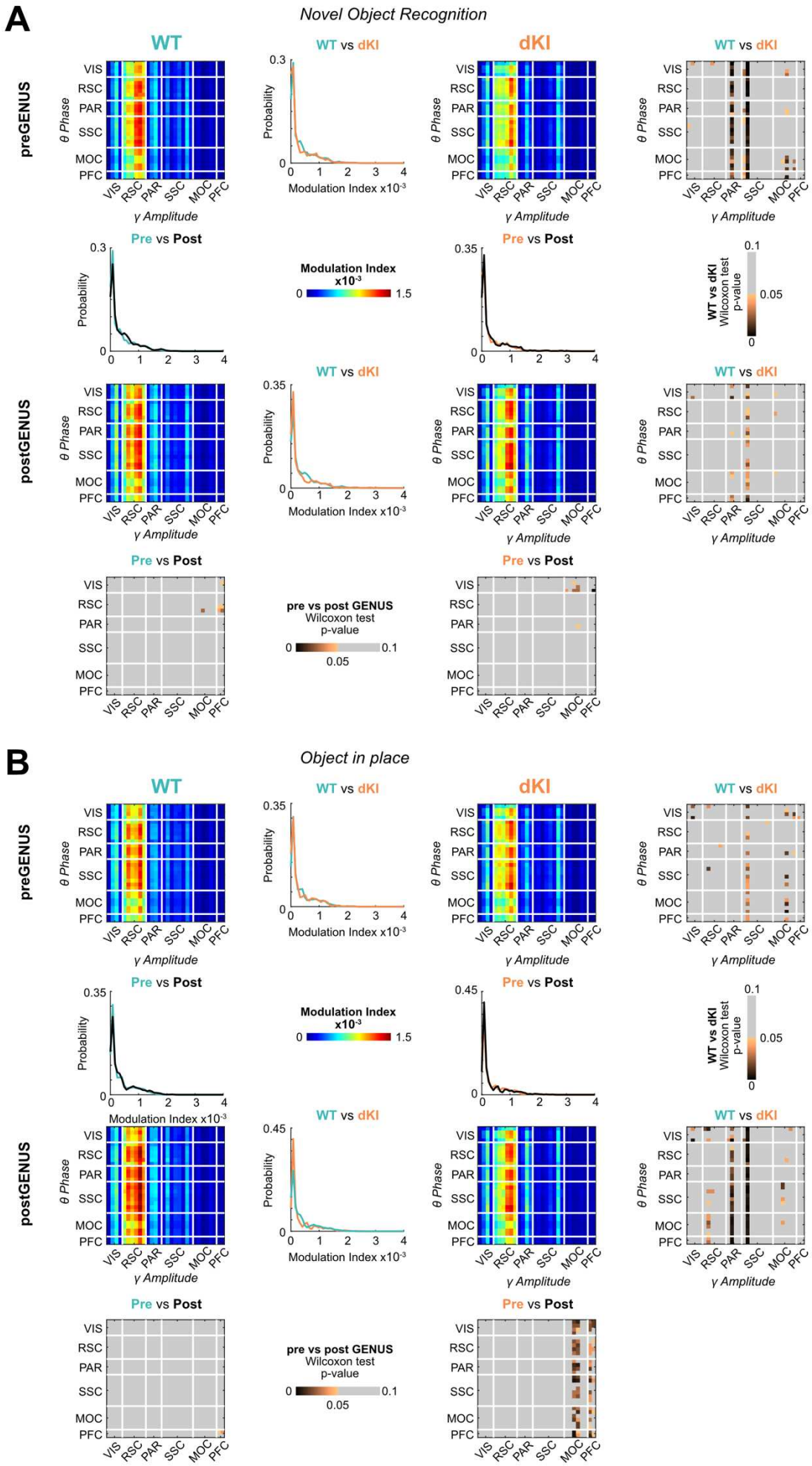
A
Novel Object Recognition
WT
dKI
WT vs dKI
preGENUS
postGENUS
θ Phase
γ Amplitude
VIS
RSC
PAR
SSC
MOC
PFC
Probability
Modulation Index x10-3
Pre vs Post
Modulation Index x10-3
0
1.5
WT vs dKI Wilcoxon test p-value
0.1
0.05
pre vs post GENUS Wilcoxon test p-value
B
Object in place

Figure 32. Theta-Gamma PAC
For both NOR (A) and OiP (B). *Top row from Left to Right*. preGENUS pairwise Theta-Gamma PAC Modulation Index (MI) matrices for WT mice with the y axis representing the region for theta phase and x axis the region for gamma amplitude, distribution of ModInd for WT (blue) and dKI (orange) mice, preGENUS pairwise Theta-Gamma PAC ModInd matrices for dKI mice, cortical map of Wilcoxon p-value between WT and dKI preGENUS. *Second row.* ModInd distribution pre- (colored line) and post-GENUS (black line) for each genotype. *Third row from Left to Right*. postGENUS pairwise Theta-Gamma PAC ModInd matrices for WT mice, distribution of relative coherence for WT (blue) and dKI (orange) mice, postGENUS pairwise Theta-Gamma PAC ModInd matrices for dKI mice, cortical map of Wilcoxon p-value between WT and dKI postGENUS. *Bottom row.* Matrices of Wilcoxon p-value between pre- and post-GENUS for each genotype. Parcellation of matrices in brain regions is based on Allen brain atlas; VIS : Visual Cortex, RSC : Retrosplenial Cortex, PAR : Parietal Cortex, SSC: Somatosensory Cortex, MOC: Motor Cortex, PFC: Prefrontal Cortex.

Discussion

Our high-density EEG analysis of dKI mice performing NOR and OiP tasks reveals a selective deficit in cortical gamma power, while other oscillatory features remain intact. Specifically, theta oscillations were preserved in both power and coherence networks, and despite the observed reduction in gamma power, gamma coherence networks were unaffected. Theta-gamma PAC also remained largely unaltered, though vGENUS treatment induced specific enhancements in dKI frontal theta-gamma PAC during OiP tasks.

This reduction in gamma power aligns with previous reports of gamma deficits in AD mouse models (Iaccarino et al., 2016; Verret et al., 2012), with gamma alterations often emerging at early stages of the disease (Hamm et al., 2017). These findings laid the groundwork for developing GENUS as a therapeutic approach, based on the hypothesis that restoring gamma rhythms might help ameliorate memory deficits, as shown in earlier studies (Verret et al., 2012).

Interestingly, while two weeks of vGENUS successfully restored memory performance and normalized global brain dynamics (see Part 1 of Results), it did not rescue gamma power deficits in dKI mice. This suggests that early AD memory impairments might not be solely attributable to reduced cortical gamma power. Thus, the beneficial effects of vGENUS likely involve more complex mechanisms beyond merely enhancing gamma oscillations.

One potential mechanism could be the modulation of complex oscillatory patterns such as theta-gamma PAC. Although dKI mice showed no baseline alterations in PAC, vGENUS selectively enhanced frontal gamma amplitude modulation by theta phase during the OiP task specifically in dKI mice. Given the PFC's key role in associative memory, mediated by its connections with the LEC, and in short-term working memory, by its connections with the HPC, this increase in frontal theta-gamma coupling may contribute to improved task performance. However, the modest magnitude of these changes suggests that enhanced PAC alone is unlikely to fully account for the cognitive benefits of vGENUS.

Several technical considerations are important when interpreting these findings. The spatial resolution of our recordings was limited by surface electrodes without source localization, leading to potential volume conduction effects, particularly in theta oscillations. This could be observed by gamma amplitude of specific regions being mostly modulated by theta phase of the majority of channels. Additionally, since our analysis focused on cortical activity, any relevant oscillatory alterations or vGENUS effects in subcortical networks could have been missed.

In summary, at an early AD stage, prior to amyloid plaque formation and during the onset of subtle memory deficits, dKI mice exhibit a selective reduction in cortical gamma power without broader oscillatory disruptions. The ability of vGENUS to restore cognitive function without normalizing gamma power suggests that its effects and the alterations in dKI mice involve more complex, higher-order network dynamics. These results underscore the need for further investigation into brain network dynamics to fully understand the mechanisms underlying both AD pathology and vGENUS therapy, notably looking at dynamic functional networks, which was limited in this study by the poor spatial localization of the signal.

General Discussion

Discussion

Main findings

In this thesis work, we first recorded hdEEG of a preclinical AD mouse model, the dKI App^{NL-F}/MAPT mouse model, during the performance of memory tasks, to assess early global brain dynamics. We then tested the effects on memory and brain dynamics of a new non-invasive protocol that showed beneficial effects on AD, the vGENUS, consisting of daily one hour of noninvasive light stimulation at 40Hz for 2 weeks.

Early spontaneous exploration associative memory deficits before classical goal directed learning deficits

Consistent with previous findings (Borcuk et al., 2022), our 4-month-old dKI mice displayed selective memory impairments, showing deficits in the associative OiP task while maintaining normal performance in the long-term NOR task. This pattern of impairment is particularly interesting as it suggests that early alterations in AD may not primarily arise from entorhinal-hippocampal dysfunction, as traditionally believed. Instead, the selective deficit in the OiP task points to early involvement of other circuits, particularly the LEC and PFC, which are crucial for performing two-object OiP task (Chao et al., 2016).
Using object recognition paradigms to assess memory, rather than traditional tasks like the Morris Water Maze (MWM) or maze-based paradigms, may offer a more effective approach to identifying early AD-related memory impairments. Object recognition tasks rely on animals' natural and spontaneous exploratory behavior, providing a more ethologically valid assessment than goal directed learning tasks which could also present a higher stress component in the case of the MWM where being forced to swim represent a stress factor in mice (Grayson et al., 2015). This approach allows us to examine innate memory function, potentially revealing subtle cognitive changes that might be masked in more artificial testing environments.

Early global brain dynamics alterations

Using a novel nonlinear characterization of the global brain dynamics inspired by methodologies from other fields, such as extreme climatology, we showed that brain dynamics fluidity was altered in dKI mice, before amyloid plaques deposition.

Specifically, global brain dynamics exhibited reduced fluidity, with periods becoming “stuck” in low fluidity states. This global brain dynamics fluidity presents the advantage to study time resolve brain dynamics without *a priori* on brain regions by looking at the whole cortex EEG. In animal studies of brain dynamics alteration, activity is often assessed between specific regions or network presumed to be involved. However, as we previously saw, proper brain processing relies on dynamics variation across multiple functional networks. Although our techniques may be less adapted to identify specific networks involved in dynamic alteration, it is potentially more sensitive to these alterations by considering broader systems. These results were further confirmed using a more established method, EEG microstates, where we showed that dynamic transitions between microstates were altered in dKI mice, with microstate sequences exhibiting reduced fluidity and complexity. Interestingly, these effects were present during both behavioral tasks: the OiP task, where memory impairments were observed, and the NOR task, where no memory impairments were noted.

Global brain dynamics alterations precede spontaneous pathological behavior

Despite showing brain dynamics alteration in both tasks, dKI mice did not displayed changes in spontaneous behavior dynamics. Spontaneous behavior studies represent a recent advance in neurosciences following the development of reliable machine learning pose estimation tools, such as Deeplabcut, to precisely extract animal skeleton body coordinates during locomotion. In the preclinical stages of AD, years before dementia onset, many patients develop behavioral or neuropsychiatric changes including agitation irritability or decreased motivation, and these behavioral changes could represent symptoms of pre-clinical AD (G. M. McKhann et al., 2011; M. E. Peters et al., 2013; Rosenberg et al., 2013). In AD mice models, locomotor hyperactivity has also been observed in several models and sometimes in the early stages of the disease development (Jul et al., 2016; Walker et al., 2011; T. Wang et al., 2022). The absence of spontaneous behavioral alterations in our study may therefore highlight the early nature of the brain dynamics alterations we observed. Using the same machine learning pose estimation approach, coupled with clustering of spontaneous behavioral patterns and sequences analysis, a recent study reported age-dependent behavioral alteration in App^{NL-G-F} single KI mice starting after 6 months of age (Miller et al., 2024). As this model exhibits more severe AD pathology than ours, the lack of spontaneous behavioral deficits at 4 months in our model appears logical.

Global brain dynamics alterations precede sleep and oscillatory alterations

Although EEG brain dynamics fluidity alterations were present during both behavioral tasks and were unrelated to spontaneous behavior, they were absent during sleep, including both REM and SWS. Sleep disruptions are well-documented in AD patients and represent one of the earliest alterations in AD mouse models, often occurring prior to amyloid plaque or neurofibrillary tangle accumulation and sometimes preceding cognitive decline (Jyoti et al., 2010; F. Zhang et al., 2019). The absence of brain dynamics alterations during both SWS and REM sleep in our paradigms suggests that these awake, task-dependent changes may serve as very early markers of pathology, with sleep-related dynamics remaining unaffected at this initial stage. Also, given the importance of sleep for memory consolidation (see Introduction) this absence of sleep-related activity alterations may explain the lack of deficits in the long-term memory task, which could benefit from unaffected sleep-dependent consolidation. However, a common feature of early sleep alterations in AD is disrupted sleep architecture (F. Zhang et al., 2019) which we did not assess in this study.

The presence of brain dynamics alterations during both behavioral tasks, but their absence during sleep, led us to characterize these changes as wake-specific. Looking more precisely at oscillatory activity during these pathological wake states, and more precisely at theta and gamma oscillations, we showed that oscillatory activity, oscillatory coherence and theta-gamma PAC remains mainly unaltered in dKI mice. The only exception was a consistent reduction in cortical gamma power, a pathological trait previously described in several AD mouse models (Hamm et al., 2017; Iaccarino et al., 2016; Verret et al., 2012).

GENUS rescued cognitive deficits and global brain dynamics

WT and dKI mice then underwent a 2 weeks vGENUS protocol consisting of 1 hour of daily 40Hz visual stimulation. During stimulation, a 40Hz peak was observed in the power spectrum of all cortical areas, with the strongest entrainment occurring in the visual cortex, as previously described (Adaikkan et al., 2019; Martorell et al., 2019). On the first day of stimulation, no differences were observed in brain dynamics fluidity. However, by the final day of the protocol, brain dynamics fluidity was rescued in dKI mice. More interestingly, after two weeks of vGENUS, memory performances in the OiP tasks and brain dynamics fluidity during both NOR and OiP tasks were rescued in

dKI mice. These results thus show a maintenance in time of the effects of the stimulation as they are observed at least one hour after the end of the stimulation. This sustained effect is even more notable regarding memory performance recovery, as improvements remained evident even one month post-protocol. Demonstrating long-term effects—especially when the protocol is applied in the early stages of the disease—suggests potential clinical advantages, such as implementing shorter chronic protocols (e.g., two weeks), which may be less burdensome for patients compared to extended treatments.

Looking at oscillatory, activity, vGENUS didn't impact either theta or gamma oscillatory activity. Strikingly, it didn't increase cortical gamma power as it was previously hypothesized to be one of the mechanisms explaining GENUS beneficials effect.

Global brain dynamics being more sensitive than local oscillatory alterations?

The absence of changes in gamma power after the vGENUS protocol despite the restoration of brain dynamics fluidity and cognitive performance, suggests that the reduced gamma power previously observed in dKI mice may not directly contribute to the phenotype. Instead, the reduced brain dynamics fluidity may be a more critical factor. This implies that brain dynamics fluidity is not necessarily linked to oscillatory patterns and could occur before the emergence of specific pathological oscillations typically associated with the early stages of the disease (Hamm et al., 2015).

A slight oscillatory change observed after GENUS was a small increase in theta power during the NOR task in dKI mice, which could indicate that GENUS, while stimulating in the gamma frequency range, might also impact other oscillatory patterns.

Finally, vGENUS protocol had no effects on brain dynamics during sleep and on behavioral posture dynamics. While these results provide a new characterization of brain dynamics alterations in early AD stages and the beneficial effects of GENUS, questions remain regarding the underlying mechanisms, which we will try to discuss in the following sections.

The slowing of EEG or more a shift of systems dynamic to pathological regimes

Traditional EEG slowing against reduced dynamics fluidity

In AD research, EEG alterations have traditionally been characterized by what is known as the "slowing of the EEG" - a phenomenon marked by increased power in lower frequency oscillations (theta and delta) and decreased power in higher frequencies like beta and gamma (Baker et al., 2008; Benz et al., 2014; Czigler et al., 2008). However, this description relies on time-averaged signal spectral analysis, raising the question: does this spectral shift, refer as "slowing", truly reflect a moment-to-moment slowing in brain dynamics?

Our time-resolved analysis provides new insights into this question. We demonstrated that brain dynamics do indeed show a genuine slowing down, manifesting as reduced fluidity and complexity in dynamic transitions. Importantly, in our dKI mice, this dynamic slowing appeared without the classical increase in theta power, although we did observe a decreased gamma power. However, the fact that vGENUS restored normal dynamics and cognitive function without normalizing gamma power suggests that reduced gamma activity may not be the primary driver of this dynamical slowing and early cognitive deficits.

The observation of slowed EEG dynamics before the classical spectral shifts holds particular clinical significance. Since spectral shifts to lower frequency are typically observed in MCI patients (Baker et al., 2008; Dauwels et al., 2011), our findings suggest that dynamic alterations might serve as even earlier diagnostic markers. This could be especially valuable for identifying pathological changes during asymptomatic stages preceding MCI, such as in SCD.

Dynamic slowing and hyperexcitability

Another widely described pathological alterations in AD brain dynamics, as mentioned in the introduction, is brain hyperexcitability Specifically, the reduction of gamma rhythms in AD has been linked to decreased PV interneuron inhibitory activity, which increases excitatory activity and can trigger epileptic signs, such as interictal spikes (Bezzina et al., 2015; Palop et al., 2007; Szabo et al., 2023; Verret et al., 2012). Despite appearing counterintuitive, the reduction in brain dynamics fluidity that we observed

could be explained by hyperactivity within the system. In dKI mice cortical hyperactivity might lead to transient hypersynchrony, which reduces the variability of the system's functional states, thus decreasing its overall dynamics, much like what is observed in epilepsy (Pedreschi et al., 2024).

Global system moves away from optimal space

Conceptualizing brain dynamics within a phase space, this diminished fluidity suggests that global brain dynamics more readily converge to a stable attractor, limiting the system's flexibility. This increased tendency toward stable attractors may signal a shift in the system's functional regime. Optimal brain function is theorized to operate at the edge of chaos to enhance information processing, signal-to-noise ratio (Boedecker et al., 2012), and task adaptability (Toyoizumi & Abbott, 2011). For dKI mice, shifting away from this edge-of-chaos state may impair information processing and lower signal-to-noise ratio, potentially affecting performance in complex memory tasks that require detecting new associations between familiar objects and locations in familiar environments.

This shift is further supported by our EEG microstates analysis. Previous work by Van de Ville (2010) highlighted that healthy microstate dynamics exhibit scale-free organization, and alterations in the duration rather than the label of microstates disrupt this balance. In dKI mice, increased microstate duration and reduced fluidity (inverse dwell time) indicate a similar disruption. Additionally, maximum Lempel-Ziv complexity of brain activity is thought to reflect edge-of-chaos operation, with drops in this measure signaling a shift toward either ordered or chaotic extremes (Toker et al., 2022). Although we did not use Lempel-Ziv complexity, our analogous measure for microstates sequence complexity showed reduced complexity in dKI mice, suggesting a move away from edge of chaos state.

Energy landscape perspectives

An open question remains: how does the system shift to this slower, pathological regime? Viewing this through the system's energy landscape, the reduction in fluidity may correspond to an increased likelihood of settling into low-energy, stable attractors. This could result from either the formation of pathological energy sinks or a deepening of existing ones. Low-dimensional t-SNE visualization reveals that low-fluidity states in dKI mice exist outside the typical range of WT brain activity, suggesting the emergence

of pathological energy sinks that constrain dynamics and reduce fluidity, potentially alongside a global increase in attractor depth.

A potential role of noradrenergic modulation

Given that these dynamics alterations in dKI mice are specific to wakefulness, one plausible explanation could involve deficits in neuromodulation, particularly NA. Alterations in the cholinergic system, which is known to be disrupted in AD (Bekdash, 2021), would likely affect activity during both REM sleep and wakefulness, as the cholinergic system is involved in REM sleep regulation (Tononi & Pompeiano, 1995). NA plays a key role in wakefulness (Berridge et al., 2012), and the LC, a primary source of NA, is among the earliest brain regions affected in AD (Braak et al., 2011). NA might influence system dynamics by facilitating state transitions within the energy landscape, potentially by flattening it (Munn et al., 2023). This suggests that lower NA levels in dKI mice may lead to deeper energy sinks, thereby limiting state transitions and altering overall brain dynamics.

Impact of vGENUS

The two-week vGENUS protocol restored both fluidity and microstates sequence complexity in dKI mice, potentially shifting brain dynamics back toward an edge-of-chaos regime. This change also improved memory performance, indicating that the restoration of a functional dynamical state supports cognitive benefits. Notably, WT mice did not show this increase, suggesting that their brain dynamics may already operate near the edge of chaos, maximizing information transfer and processing. This raises further questions: does this increased dynamics fluidity stem from the removal of pathological attractors or a general flattening of the energy landscape?
Examining pre- and post-GENUS brain activity via t-SNE, we observed that points with pathological dynamics pre-GENUS were outside the post-GENUS activity landscape, hinting at the elimination of pathological attractors. This increase in brain dynamics was gradual, becoming apparent only after the 15-day protocol, suggesting potential involvement of metabotropic effects rather than immediate changes. One hypothesis is that chronic 40Hz stimulation engages specific networks or promotes high-order network interactions, leading to incremental restoration of NA levels, flattening the energy landscape, and facilitating state transitions. Another possibility is that vGENUS

enhances blood flow (Martorell et al., 2019; Murdock et al., 2024), improving oxygen supply and supporting dynamics that bring brain activity closer to the edge of chaos.

40Hz always the perfect frequency?

The GENUS protocol originally identified 40Hz stimulation as the most effective frequency compared to other frequencies such as 20Hz and 80Hz, which showed no beneficial effects (Martorell et al., 2019). However, recent studies suggest that frequencies around 35Hz may actually entrain brain gamma oscillations more effectively than 40Hz (K. Lee et al., 2021; Y. Park et al., 2022). Furthermore, a recent investigation using flickering stimulation in deeply implanted epileptic patients found that the flicker response varied according to intrinsic circuit properties, suggesting that the optimal frequency may differ between individuals (Blanpain et al., 2024). These findings indicate that while 40Hz stimulation has demonstrated overall benefits, it might not be the ideal frequency for every individual. A patient-specific tuning of GENUS frequency could potentially enhance the treatment's effectiveness.

Understanding nonlinear brain dynamics, including their alteration in AD and response to vGENUS, is essential for developing computational models of brain activity that identify key system parameters distinguishing healthy, AD, and GENUS conditions. By pinpointing which model parameters vary between these states, the GENUS protocol could be optimized according to each patient's initial brain state. Consequently, assessing brain dynamics could serve both as a diagnostic tool and a means to identify the precise stimulation frequency required to shift a patient's specific pathological state toward a more functional regime. This approach supports a personalized medicine strategy, leveraging noninvasive techniques to deliver targeted, patient-specific interventions.

Potential suspects for brain alterations in dKI mice

Which networks involved?

An essential question raised by this study is which neural networks alterations underlie memory impairments and reduced brain dynamics fluidity observed in dKI mice. Addressing this requires revisiting the observed memory impairments. dKI mice displayed deficits in an associative memory task, the OiP task, with a 5-minute ITI, but

showed no impairment in the NOR task, which has a longer 24-hour ITI. This discrepancy suggests a potential disruption in associative memory, possibly involving the RSC and the LEC- PFC connections (Chao et al., 2022, p. 202). Strong evidence supports this hypothesis, showing hyperactivity in the LEC and reduced involvement of the RSC and PFC in dKI mice during memory retention (Borcuk et al., 2022).
However, the wake-specific nature of the altered brain dynamics points to a broader network influence beyond associative memory alone. The shorter ITI of the OiP task compared to the NOR task may imply a reliance on short-term memory, with dKI mice badly performing in a task with a short ITI but correctly performing when the ITI allow a sleep dependent memory consolidation, as dynamics fluidity showed to be unaltered in sleep. However, dKI mice successfully performed the NOR task with a 5-minute ITI in a previous study (Borcuk et al., 2022). This discrepancy could be attributed to the greater novelty component of the NOR task, which may mitigate short-term memory deficits. It is also worth noting that working memory-specific tasks have not been thoroughly assessed in dKI mice. The overlap between associative and short-term memory likely involves the PFC, which serves as a buffer for information. Optogenetic stimulation of the PFC during the OiP task's 5-minute ITI has been shown to improve performance (Benn et al., 2016). Thus, alterations in PFC dynamics may provide a key explanation for early cognitive deficits. Further, in dKI mice, compromised PFC function could also account for the increase in theta-gamma PAC observed in the PFC after GENUS treatment, which coincides with restored memory performance during the OiP task.

Noradrenegic hypothesis

Given the wake-specific nature of these alterations, a plausible explanation could involve neuromodulatory deficits, particularly in NA, as previously evoked. The LC, which is the primary source of NA in the brain, sends widespread noradrenergic projections to regions including the PFC. The LC is also among the first regions affected by tauopathy in AD (Braak et al., 2011), its noradrenergic axon density is reduced in KI mouse model of AD (Sakakibara et al., 2021) and LC neuron loss has been associated with working memory deficits (Coradazzi et al., 2016). NA levels typically increase in the PFC during working memory tasks (Rossetti & Carboni, 2005), and reductions in NA levels impair PFC activity. Thus, NA deficits in dKI mice could contribute to the memory impairments observed in the OiP task. Meanwhile, the well-

known physiological decrease in NA levels during SWS and REM sleep likely prevents any alteration in brain dynamics during these stages, thereby supporting proper sleep-dependent memory consolidation.

The Claustrum as a potential suspect

An alternative hypothesis involves the Claustrum (CLA), a small subcortical structure that exhibits hyperactivity in dKI mice during OiP task performance (Borcuk et al., 2022). Under normal conditions, the CLA is primarily active during synchronized states like SWS, where it may play a role in memory consolidation (Do et al., 2024; Marriott et al., 2024). CLA receive noradrenergic inputs rom LC (Q. Wang et al., 2023). A reduction in NA could blur the “wake” state marker, allowing the CLA to become active during wakefulness. With its extensive bidirectional connections to a wide range of cortical regions including the PFC and RSC (J. B. Smith et al., 2020; Q. Wang et al., 2017; Zingg et al., 2018), abnormal CLA hyperactivity could propagate irregular activity across the cortex. This effect might be especially pronounced in the PFC, given the strong CLA-PFC projections and the hypothesized reduced noradrenergic regulation in PFC, potentially disrupting information buffering necessary for short-term working and associative memory, as required in the OiP task.

Moreover, the CLA’s hyperactivity could contribute to a global reduction in brain dynamics fluidity, possibly through increased hyper-synchronization across cortical regions, which would dampen overall brain dynamics. Given that CLA activity during wakefulness is also heavily dependent on ACh levels, the reduction in NA would not be sufficient for the CLA to exhibit the same activity pattern seen during SWS. A CLA activation pattern intermediate between healthy wakefulness and SWS could explain the global brain dynamics alterations without inducing oscillatory changes. During sleep, the CLA would resume its normal activity pattern, supporting proper memory consolidation and preserving unaltered brain dynamics fluidity during SWS (and REM).

GENUS as an enrichment?

The GENUS protocol was initially developed as an intervention for AD aiming to reduce amyloid plaques and Aβ load through clearance mechanisms or by restoring altered gamma oscillations (Adaikkan et al., 2019; Martorell et al., 2019; Murdock et al., 2024). In our study, we demonstrated that vGENUS could restore memory performance and

enhance brain dynamics fluidity in dKI mice even before amyloid plaque accumulation, and without increasing the already-reduced gamma power. Although the positive impact of GENUS on memory has become widely accepted, the underlying mechanisms may not directly tie to the amyloid hypothesis or the restoration of gamma rhythms. The need for chronic exposure to observe these benefits suggests that more prolonged, complex processes are involved.

Beyond promoting brain clearance, GENUS has been shown to increase cerebral blood flow, potentially boosting metabolic intake and thus supporting enhanced brain activity (Martorell et al., 2019; Murdock et al., 2024). Additionally, other beneficial factors such as neuroprotective effects, reduced demyelination, and enhanced neurogenesis could play a significant role in the overall effects of GENUS (Adaikkan et al., 2019; Islam et al., 2024; Rodrigues-Amorim et al., 2024; Yan et al., 2024). In fact, many of these effects have also been observed with environmental enrichment protocols—housing conditions that combine social interaction, cognitive, sensory, and motor stimulation in animal models. Environmental enrichment has been shown to improve memory performance, delay cognitive decline in AD mouse models, reduce AD pathology (Berardi et al., 2007; Griñán-Ferré et al., 2018), provide neuroprotective effects (Young et al., 1999), enhance brain clearance (Herring et al., 2008), and stimulate hippocampal neurogenesis (Nilsson et al., 1999).

Thus, GENUS could function as a form of enrichment, promoting cognitive reserve similarly to environmental enrichment (Petrosini et al., 2009). This potential, along with promising effects observed in other conditions such as epilepsy (Blanpain et al., 2024) and Down syndrome (Islam et al., 2024), highlights the applicability of GENUS as a non-invasive and easily implemented protocol for broader therapeutic use.

Amyloid hypothesis and the problem of the model

As stated in the introduction of this manuscript, AD pathological characterization still mainly relies on the amyloid hypothesis stating that cognitive impairments and progression of AD pathology is mainly explained by the accumulation of pathological Aβ oligomers and finally amyloid plaques (Selkoe & Hardy, 2016). However, giving the failure of treatment based on reducing Aβ load (J. L. Cummings et al., 2014; Doody et al., 2013, 2014; Strooper, 2014), the difficulty to detect Aβ early in clinical settings, and the possible presence of Aβ in healthy elderly, there is a critical need to identify

alternative biomarkers for AD that are not solely tied to the amyloid hypothesis. In our study, we find global brain dynamics alteration before amyloid plaques deposition. However, this finding cannot be entirely dissociated from the amyloid hypothesis for several reasons. First, previous research has shown a slight increase in Aβ levels in the medial temporal lobe (MTL) of 4-month-old dKI mice (Borcuk et al., 2022). Second, the model used in this thesis is based on familiar forms of AD, which inherently promote the amyloidogenic pathway. Finally, although the dKI model is less aggressive and more physiological compared to some Tg models, with only two mutations in APP and a non-mutated human MAPT gene, it still involves amyloid accumulation. However, our goal was not to search for amyloid markers in an amyloid brain. Instead, we identified a global alteration in brain dynamics, which correlates with early, subtle memory impairments. Given the non-invasive nature of our tool, it could potentially detect these early alterations years before amyloid accumulation becomes detectable with classical methods Moreover, while a slight increase in Aβ levels has been observed in the MTL and, more specifically, in the EC of 4-month-old dKI mice, our observed brain dynamics alterations involve the entire cortex. This suggests that the underlying mechanisms may extend beyond localized Aβ accumulation in the MTL. Additionally, considering the previously discussed involvement of the noradrenergic pathway, these dynamics alterations may be more closely tied to pathological tau hyperphosphorylation and aggregation in the LC (Braak et al., 2011), rather than solely to Aβ deposition.
Nevertheless, giving the familial AD mutations in dKI mice, we still can't really extrapolate the observation to the whole AD spectrum as 98% of AD patient present the spontaneous forms of the disease which rely on other factors. To address this limitation, several approaches could be considered. One option would be to use spontaneous animal models of AD as previously seen in the Introduction. However, the uncommon profile of these animal models makes them hard to use in most of the labs. An alternative approach would be, be to study aged animals, as age is the primary risk factor for AD, and older animals often exhibit age-related memory deficits (Ingram, 1988).

Difference between sex need to be considered

For this thesis work, male and female were pooled into the same groups and sex effects were not assessed due to the small sample size. However, it is increasingly

recognized that there are sex differences in AD, with females being more affected by the disease, likely due to menopause and the associated drop in estrogen levels (Laws et al., 2018; Mosconi et al., 2021). This sex difference is also observed in AD mouse models (J.-T. Yang et al., 2018). Therefore, future studies should incorporate both sexes and ensure an adequately powered sample size to assess sex-specific effects.

Perspective

Energy landscape

One of the first perspective of this project would be to study energy landscapes of dKI mice brain activity. This would help determine whether the reduced brain dynamics fluidity in dKI mice correspond to pathological states or the deepening of pre-existing energy sinks, and how GENUS modifies this energy landscape to restore brain dynamics fluidity. These energy landscapes will be analyzed using Maximum Entropy models on existing EEG recordings, in collaboration with Dr. Jyotika Bahuguna from our lab.

NA levels

We hypothesize that alterations of global brain dynamics fluidity are caused by reduced NA levels, which might be restored by vGENUS. It thus appears logical to assess NA levels and activity in dKI mice before and after GENUS protocol. This will be done using $GRAB_{NE}$ sensor and fiber photometry, allowing to study the temporal variations of NA levels by fluorescent variation recorded in the brain through an optic fiber. This work will be done in collaboration with Dr. Yaroslav Sych, expert in fiberphotometry.

Dynamic functional networks

The limited spatial resolution of EEG prevented us to assess dynamic functional networks. However, evaluating dFC in dKI mice would help identify functional networks that are dynamically altered and contribute to the global slowing of brain dynamics. Moreover, this analysis could provide insight into whether the slowing of brain dynamics in dKI mice is linked to altered meta-connectivity and the onset of "frustration" in meta-connectivity networks, as previously described in AD patients

(Arbabyazd et al., 2023), and shown to contribute to brain dynamics slowing (Mezard et al., 1988). While this type of analysis is not possible with our non-source localized EEG recordings, it could be conducted using fMRI data from dKI mice, collected by Dr. Laura Harsan's team in Strasbourg. Preliminary results, analysed by Dr. Samy Castro, former postdoc of our lab, suggest a slowing of dFC speed, which supports the idea of slowed brain dynamics in dKI mice.

Prefrontal and short-term memory

Given our hypothesis that pathological alterations in PFC dynamics may contribute to memory impairments in dKI mice, it seems logical to further investigate PFC activity during different brain states, before and after GENUS. To do so, we plan to record PFC LFP and spike activity using multi-shank linear probes, which will be implanted across the different layers of the PFC, in combination with LFP recordings from the HPC during the performance of a working memory task, such as the spontaneous alternation T-maze task. In this task, the animal must choose one of the two arms of the T-maze to obtain a reward, and after returning to the starting point, it must select the opposite arm to receive the reward. A delay between trials can be introduced, requiring the animal to buffer the information for a longer period. Notably, it has been shown that HPC theta-PFC gamma PAC increases with the ITI duration (Tamura et al., 2017). If the PFC activity is altered during wake in dKI, we expect reduced coupling with HPC during the task and impaired performance with longer delays. Further, if the PFC indeed buffer the information and send it back to the HPC to inform future choice, it would be interesting to apply the decoding methods developed in the team (Douchamps et al., 2024) to predict animal performance (i.e. the correct arm choice) based on oscillatory patterns and cell assemblies observed during the delay period. We hypothesize that decoding performance will be diminished in animals with altered PFC dynamics. This project is set to begin in the lab in 2025 with the arrival of a new student.

General Conclusion

In this thesis, we demonstrate that the dKI AppNL-F/MAPT mouse model of early AD pathology exhibits early memory deficits in a subtle associative memory task, alongside alterations in global brain dynamics. These alterations reveal that brain dynamics are slower or less fluid in dKI mice, with instances of pathological low-fluidity states emerging before the appearance of classic biological hallmarks of the disease. We identified these changes using scalp EEG recordings—a noninvasive and clinically accessible technique—highlighting the potential of EEG-based brain dynamics fluidity as a promising diagnostic tool for detecting AD at preclinical stages. This would be particularly valuable for cases of SCD, where current diagnostic options, such as PET scans or CSF Aβ measurements, are limited due to their invasiveness.

In our study, two weeks of daily, one-hour 40Hz light stimulation (vGENUS) successfully restored memory function in dKI mice and normalized brain dynamics to a healthy state. Notably, these benefits occurred before the onset of traditional AD biomarkers and without correcting altered cortical gamma oscillations, underscoring the broad neuroprotective effects of this noninvasive intervention during the disease's early stages—even before significant pathological development. Due to the noninvasiveness and ease of implementation of this protocol, it could be feasibly adopted in clinical settings, providing a safe, side-effect-free intervention for individuals with early signs of cognitive decline, potentially slowing disease progression.

Together, our findings propose a dual approach for AD: a noninvasive method for early detection coupled with a noninvasive intervention strategy that is effective even in early stages of the disease. This could contribute to reducing the future prevalence of AD dementia, alleviate projected increases in AD cases, and ultimately improve the quality of life for affected individuals and their families.

References

A

Aamodt, E. J., & Williams, R. C. (1984). Microtubule-associated proteins connect microtubules and neurofilaments in vitro. *Biochemistry*, *23*(25), 6023–6031. https://doi.org/10.1021/bi00320a019

Adaikkan, C., Middleton, S. J., Marco, A., Pao, P.-C., Mathys, H., Kim, D. N.-W., Gao, F., Young, J. Z., Suk, H.-J., Boyden, E. S., McHugh, T. J., & Tsai, L.-H. (2019). Gamma Entrainment Binds Higher-Order Brain Regions and Offers Neuroprotection. *Neuron*, *102*(5), 929-943.e8. https://doi.org/10.1016/j.neuron.2019.04.011

Aguilera, M., Douchamps, V., Battaglia, D., & Goutagny, R. (2022). How Many Gammas? Redefining Hippocampal Theta-Gamma Dynamic During Spatial Learning. *Frontiers in Behavioral Neuroscience*, *16*, 811278. https://doi.org/10.3389/fnbeh.2022.811278

Ahnaou, A., Moechars, D., Raeymaekers, L., Biermans, R., Manyakov, N. V., Bottelbergs, A., Wintmolders, C., Van Kolen, K., Van De Casteele, T., Kemp, J. A., & Drinkenburg, W. H. (2017). Emergence of early alterations in network oscillations and functional connectivity in a tau seeding mouse model of Alzheimer's disease pathology. *Scientific Reports*, *7*(1), 14189. https://doi.org/10.1038/s41598-017-13839-6

Alzheimer's disease international. (2015). *World Alzheimer Report 2015, The Global Impact of Dementia: An analysis of prevalence, incidence, cost and trends*.

Alzheimer's disease international. (2023). *World Alzheimer Report 2023, Reducing Dementia Risk: Never too early, never too late*.

Ameen-Ali, K. E., Simpson, J. E., Wharton, S. B., Heath, P. R., Sharp, P. S., Brezzo, G., & Berwick, J. (2019). The Time Course of Recognition Memory Impairment and Glial Pathology in the hAPP-J20 Mouse Model of Alzheimer's Disease. *Journal of Alzheimer's Disease*, *68*(2), 609–624. https://doi.org/10.3233/JAD-181238

Ametamey, S. M., Honer, M., & Schubiger, P. A. (2008). Molecular Imaging with PET. *Chemical Reviews*, *108*(5), 1501–1516. https://doi.org/10.1021/cr0782426

Arbabyazd, L., Petkoski, S., Breakspear, M., Solodkin, A., Battaglia, D., & Jirsa, V. (2023). State-switching and high-order spatiotemporal organization of dynamic functional connectivity are disrupted by Alzheimer's disease. *Network Neuroscience*, *7*(4), 1420–1451. https://doi.org/10.1162/netn_a_00332

Ardiles, Á. O., Tapia-Rojas, C. C., Mandal, M., Alexandre, F., Kirkwood, A., Inestrosa, N. C., & Palacios, A. G. (2012). Postsynaptic dysfunction is associated with spatial and object recognition memory loss in a natural model of Alzheimer's disease. *Proceedings of the National Academy of Sciences*, *109*(34), 13835–13840. https://doi.org/10.1073/pnas.1201209109

Armstrong, R. A., Cairns, N. J., & Lantos, P. L. (1997). Laminar distribution of cortical Lewy bodies and neurofibrillary tangles in dementia with Lewy bodies. *Neuroscience Research Communications*, *21*(2), 145–152. https://doi.org/10.1002/(SICI)1520-6769(199709/10)21:2<145::AID-NRC218>3.0.CO;2-L

Arriagada, P. V., Marzloff, K., & Hyman, B. T. (1992). Distribution of Alzheimer-type pathologic changes in nondemented elderly individuals matches the pattern in Alzheimer's disease. *Neurology*, *42*(9), 1681–1681. https://doi.org/10.1212/WNL.42.9.1681

Ashourvan, A., Gu, S., Mattar, M. G., Vettel, J. M., & Bassett, D. S. (2017). The energy landscape underpinning module dynamics in the human brain connectome. *NeuroImage*, *157*, 364–380. https://doi.org/10.1016/j.neuroimage.2017.05.067

Assini, F. L., Duzzioni, M., & Takahashi, R. N. (2009). Object location memory in mice: Pharmacological validation and further evidence of hippocampal CA1 participation. *Behavioural Brain Research*, *204*(1), 206–211. https://doi.org/10.1016/j.bbr.2009.06.005

Atri, A. (2019). Current and Future Treatments in Alzheimer's Disease. *Seminars in Neurology*, *39*(2), 227–240. https://doi.org/10.1055/s-0039-1678581

B

Babloyantz, A., & Destexhe, A. (1986). Low-dimensional chaos in an instance of epilepsy. *Proceedings of the National Academy of Sciences*, *83*(10), 3513–3517. https://doi.org/10.1073/pnas.83.10.3513

Baddeley, A. D. (1986). *Working Memory*. Clarendon Press. https://books.google.fr/books?id=ZKWbdv__vRMC

Bak, P. (2013). *How nature works: The science of self-organized criticality* (Springer Science&Business Media.).

Baker, M., Akrofi, K., Schiffer, R., & Boyle, M. W. O. (2008). EEG Patterns in Mild Cognitive Impairment (MCI) Patients. *The Open Neuroimaging Journal*, *2*(1). https://doi.org/10.2174/1874440000802010052

Balbi, M., Xiao, D., Vega, M. J., Hu, H., Vanni, M. P., Bernier, L.-P., LeDue, J., MacVicar, B., & Murphy, T. H. (2021). Gamma frequency activation of inhibitory neurons in the acute phase after stroke attenuates vascular and behavioral dysfunction. *Cell Reports*, *34*(5). https://doi.org/10.1016/j.celrep.2021.108696

Ballinger, E. C., Ananth, M., Talmage, D. A., & Role, L. W. (2016). Basal Forebrain Cholinergic Circuits and Signaling in Cognition and Cognitive Decline. *Neuron*, *91*(6), 1199–1218. https://doi.org/10.1016/j.neuron.2016.09.006

Barbagallo, A. P. M., Wang, Z., Zheng, H., & D'Adamio, L. (2011). A Single Tyrosine Residue in the Amyloid Precursor Protein Intracellular Domain Is Essential for Developmental Function. *The Journal of Biological Chemistry*, *286*(11), 8717–8721. https://doi.org/10.1074/jbc.C111.219873

Barker, G. R. I., Bird, F., Alexander, V., & Warburton, E. C. (2007). Recognition Memory for Objects, Place, and Temporal Order: A Disconnection Analysis of the Role of the Medial Prefrontal Cortex and Perirhinal Cortex. *Journal of Neuroscience*, *27*(11), 2948–2957. https://doi.org/10.1523/JNEUROSCI.5289-06.2007

Barnes, D. E., Byers, A. L., Gardner, R. C., Seal, K. H., Boscardin, W. J., & Yaffe, K. (2018). Association of Mild Traumatic Brain Injury With and Without Loss of Consciousness With Dementia in US Military Veterans. *JAMA Neurology*, *75*(9), 1055–1061. https://doi.org/10.1001/jamaneurol.2018.0815

Barttfeld, P., Uhrig, L., Sitt, J. D., Sigman, M., Jarraya, B., & Dehaene, S. (2015). Signature of consciousness in the dynamics of resting-state brain activity. *Proceedings of the National Academy of Sciences*, *112*(3), 887–892. https://doi.org/10.1073/pnas.1418031112

Barulli, D., & Stern, Y. (2013). Efficiency, capacity, compensation, maintenance, plasticity: Emerging concepts in cognitive reserve. *Trends in Cognitive Sciences*, *17*(10), 502–509. https://doi.org/10.1016/j.tics.2013.08.012

Basser, P. J., Mattiello, J., & LeBihan, D. (1994). MR diffusion tensor spectroscopy and imaging. *Biophysical Journal*, *66*(1), 259–267. https://doi.org/10.1016/S0006-3495(94)80775-1

Battaglia, D. (2014). Function Follows Dynamics: State-Dependency of Directed Functional Influences. In M. Wibral, R. Vicente, & J. T. Lizier (Eds.), *Directed Information Measures in Neuroscience* (pp. 111–135). Springer. https://doi.org/10.1007/978-3-642-54474-3_5

Battaglia, D., Boudou, T., Hansen, E. C. A., Lombardo, D., Chettouf, S., Daffertshofer, A., McIntosh, A. R., Zimmermann, J., Ritter, P., & Jirsa, V. (2020). Dynamic Functional Connectivity between order and randomness and its evolution across the human adult lifespan. *NeuroImage*, *222*, 117156. https://doi.org/10.1016/j.neuroimage.2020.117156

Battaglia, D., Witt, A., Wolf, F., & Geisel, T. (2012). Dynamic Effective Connectivity of Inter-Areal Brain Circuits. *PLOS Computational Biology*, *8*(3), e1002438. https://doi.org/10.1371/journal.pcbi.1002438

Batty, G. D., Frank, P., Kujala, U., Sarna, S., Valencia-Hernández, C., & Kaprio, J. (2022). *Dementia and Alzheimer's Disease in Former Contact Sports Participants:*

Population-Based Cohort Study, Systematic Review, and Meta-Analysis (SSRN Scholarly Paper 4229877). https://doi.org/10.2139/ssrn.4229877

Bayat, A.-H., Azimi, H., Hassani Moghaddam, M., Ebrahimi, V., Fathi, M., Vakili, K., Mahmoudiasl, G.-R., Forouzesh, M., Boroujeni, M. E., Nariman, Z., Abbaszadeh, H.-A., Aryan, A., Aliaghaei, A., & Abdollahifar, M.-A. (2022). COVID-19 causes neuronal degeneration and reduces neurogenesis in human hippocampus. *Apoptosis*, *27*(11), 852–868. https://doi.org/10.1007/s10495-022-01754-9

Beggs, J. M., & Plenz, D. (2003). Neuronal Avalanches in Neocortical Circuits. *Journal of Neuroscience*, *23*(35), 11167–11177. https://doi.org/10.1523/JNEUROSCI.23-35-11167.2003

Bekdash, R. A. (2021). The Cholinergic System, the Adrenergic System and the Neuropathology of Alzheimer's Disease. *Int. J. Mol. Sci.*

Bekris, L. M., Yu, C.-E., Bird, T. D., & Tsuang, D. W. (2010). Genetics of Alzheimer Disease. *Journal of Geriatric Psychiatry and Neurology*, *23*(4), 213–227. https://doi.org/10.1177/0891988710383571

Benilova, I., Karran, E., & De Strooper, B. (2012). The toxic Aβ oligomer and Alzheimer's disease: An emperor in need of clothes. *Nature Neuroscience*, *15*(3), 349–357. https://doi.org/10.1038/nn.3028

Benn, A., Barker, G. R. I., Stuart, S. A., Roloff, E. V. L., Teschemacher, A. G., Warburton, E. C., & Robinson, E. S. J. (2016). Optogenetic Stimulation of Prefrontal Glutamatergic Neurons Enhances Recognition Memory. *The Journal of Neuroscience*, *36*(18), 4930–4939. https://doi.org/10.1523/JNEUROSCI.2933-15.2016

Benz, N., Hatz, F., Bousleiman, H., Ehrensperger, M. M., Gschwandtner, U., Hardmeier, M., Ruegg, S., Schindler, C., Zimmermann, R., Monsch, A. U., & Fuhr, P. (2014). Slowing of EEG Background Activity in Parkinson's and Alzheimer's Disease with Early Cognitive Dysfunction. *Frontiers in Aging Neuroscience*, *6*. https://doi.org/10.3389/fnagi.2014.00314

Berardi, N., Braschi, C., Capsoni, S., Cattaneo, A., & Maffei, L. (2007). Environmental Enrichment Delays the Onset of Memory Deficits and Reduces Neuropathological

Hallmarks in a Mouse Model of Alzheimer-Like Neurodegeneration. *Journal of Alzheimer's Disease*, *11*(3), 359–370. https://doi.org/10.3233/JAD-2007-11312

Berridge, C. W., Schmeichel, B. E., & España, R. A. (2012). Noradrenergic modulation of wakefulness/arousal. *Sleep Medicine Reviews*, *16*(2), 187–197. https://doi.org/10.1016/j.smrv.2011.12.003

Bezzina, C., Verret, L., Juan, C., Remaud, J., Halley, H., Rampon, C., & Dahan, L. (2015). Early Onset of Hypersynchronous Network Activity and Expression of a Marker of Chronic Seizures in the Tg2576 Mouse Model of Alzheimer's Disease. *PLOS ONE*, *10*(3), e0119910. https://doi.org/10.1371/journal.pone.0119910

Bhardwaj, T., Gadhave, K., Kapuganti, S. K., Kumar, P., Brotzakis, Z. F., Saumya, K. U., Nayak, N., Kumar, A., Joshi, R., Mukherjee, B., Bhardwaj, A., Thakur, K. G., Garg, N., Vendruscolo, M., & Giri, R. (2023). Amyloidogenic proteins in the SARS-CoV and SARS-CoV-2 proteomes. *Nature Communications*, *14*(1), 945. https://doi.org/10.1038/s41467-023-36234-4

Billings, L. M., Oddo, S., Green, K. N., McGaugh, J. L., & LaFerla, F. M. (2005). Intraneuronal Aβ Causes the Onset of Early Alzheimer's Disease-Related Cognitive Deficits in Transgenic Mice. *Neuron*, *45*(5), 675–688. https://doi.org/10.1016/j.neuron.2005.01.040

Blanpain, L. T., Cole, E. R., Chen, E., Park, J. K., Walelign, M. Y., Gross, R. E., Cabaniss, B. T., Willie, J. T., & Singer, A. C. (2024). Multisensory flicker modulates widespread brain networks and reduces interictal epileptiform discharges. *Nature Communications*, *15*(1), 3156. https://doi.org/10.1038/s41467-024-47263-y

Boedecker, J., Obst, O., Lizier, J. T., Mayer, N. M., & Asada, M. (2012). Information processing in echo state networks at the edge of chaos. *Theory in Biosciences*, *131*(3), 205–213. https://doi.org/10.1007/s12064-011-0146-8

Bonardi, C., Pardon, M.-C., & Armstrong, P. (2021). Time or place? Dissociation between object-in-place and relative recency in young APPswe/PS1dE9 mice. *Behavioral Neuroscience*, *135*(1), 39–50. https://doi.org/10.1037/bne0000431

Borcuk, C., Héraud, C., Herbeaux, K., Diringer, M., Panzer, É., Scuto, J., Hashimoto, S., Saido, T. C., Saito, T., Goutagny, R., Battaglia, D., & Mathis, C. (2022). Early memory deficits and extensive brain network disorganization in the App/MAPT double knock-in mouse model of familial Alzheimer's disease. *Aging Brain*, *2*, 100042. https://doi.org/10.1016/j.nbas.2022.100042

Boyce, R., Glasgow, S. D., Williams, S., & Adamantidis, A. (2016). Causal evidence for the role of REM sleep theta rhythm in contextual memory consolidation. *Science*, *352*(6287), 812–816. https://doi.org/10.1126/science.aad5252

Braak, H., & Braak, E. (1991). Neuropathological stageing of Alzheimer-related changes. *Acta Neuropathologica*, *82*(4), 239–259. https://doi.org/10.1007/BF00308809

Braak, H., Thal, D. R., Ghebremedhin, E., & Del Tredici, K. (2011). Stages of the Pathologic Process in Alzheimer Disease: Age Categories From 1 to 100 Years. *Journal of Neuropathology & Experimental Neurology*, *70*(11), 960–969. https://doi.org/10.1097/NEN.0b013e318232a379

Brothers, H. M., Gosztyla, M. L., & Robinson, S. R. (2018). The Physiological Roles of Amyloid-β Peptide Hint at New Ways to Treat Alzheimer's Disease. *Frontiers in Aging Neuroscience*, *10*. https://doi.org/10.3389/fnagi.2018.00118

Brunel, N., & Hansel, D. (2006). How Noise Affects the Synchronization Properties of Recurrent Networks of Inhibitory Neurons. *Neural Computation*, *18*(5), 1066–1110. https://doi.org/10.1162/neco.2006.18.5.1066

Brunel, N., & Wang, X.-J. (2003). What Determines the Frequency of Fast Network Oscillations With Irregular Neural Discharges? I. Synaptic Dynamics and Excitation-Inhibition Balance. *Journal of Neurophysiology*, *90*(1), 415–430. https://doi.org/10.1152/jn.01095.2002

Brunnström, H., Friberg, N., Lindberg, E., & Englund, E. (2011). Differential degeneration of the locus coeruleus in dementia subtypes. *Clinical Neuropathology*, *30*(3), 104–110. https://doi.org/10.5414/npp30104

Busche, M. A., Eichhoff, G., Adelsberger, H., Abramowski, D., Wiederhold, K.-H., Haass, C., Staufenbiel, M., Konnerth, A., & Garaschuk, O. (2008). Clusters of Hyperactive Neurons Near Amyloid Plaques in a Mouse Model of Alzheimer's Disease. *Science*, *321*(5896), 1686–1689. https://doi.org/10.1126/science.1162844

Buzsáki, G. (1989). Two-stage model of memory trace formation: A role for "noisy" brain states. *Neuroscience*, *31*(3), 551–570. https://doi.org/10.1016/0306-4522(89)90423-5

Buzsáki, G. (2002). Theta Oscillations in the Hippocampus. *Neuron*, *33*(3), 325–340. https://doi.org/10.1016/S0896-6273(02)00586-X

Buzsaki, G. (2006). *Rhythms of the Brain*. Oxford university press.

Buzsáki, G. (2010). Neural Syntax: Cell Assemblies, Synapsembles, and Readers. *Neuron*, *68*(3), 362–385. https://doi.org/10.1016/j.neuron.2010.09.023

Buzsáki, G. (2015). Hippocampal sharp wave-ripple: A cognitive biomarker for episodic memory and planning. *Hippocampus*, *25*(10), 1073–1188. https://doi.org/10.1002/hipo.22488

Buzsáki, G., Anastassiou, C. A., & Koch, C. (2012). The origin of extracellular fields and currents—EEG, ECoG, LFP and spikes. *Nature Reviews Neuroscience*, *13*(6), 407–420. https://doi.org/10.1038/nrn3241

Buzsáki, G., & Draguhn, A. (2004). Neuronal Oscillations in Cortical Networks. *Science*, *304*(5679), 1926–1929. https://doi.org/10.1126/science.1099745

C

Cabral, J., Kringelbach, M. L., & Deco, G. (2017). Functional connectivity dynamically evolves on multiple time-scales over a static structural connectome: Models and mechanisms. *NeuroImage*, *160*, 84–96. https://doi.org/10.1016/j.neuroimage.2017.03.045

Caillé, I., Allinquant, B., Dupont, E., Bouillot, C., Langer, A., Müller, U., & Prochiantz, A. (2004). Soluble form of amyloid precursor protein regulates proliferation of progenitors in the adult subventricular zone. *Development*, *131*(9), 2173–2181. https://doi.org/10.1242/dev.01103

Camassa, A., Torao-Angosto, M., Manasanch, A., Kringelbach, M. L., Deco, G., & Sanchez-Vives, M. V. (2024). The temporal asymmetry of cortical dynamics as a signature of brain states. *Scientific Reports*, *14*(1), 24271. https://doi.org/10.1038/s41598-024-74649-1

Campbell, N. L., Unverzagt, F., LaMantia, M. A., Khan, B. A., & Boustani, M. A. (2013). Risk Factors for the Progression of Mild Cognitive Impairment to Dementia. *Clinics in Geriatric Medicine*, *29*(4), 873–893. https://doi.org/10.1016/j.cger.2013.07.009

Canal-Garcia, A., Veréb, D., Mijalkov, M., Westman, E., Volpe, G., Pereira, J. B., & For the Alzheimer's Disease Neuroimaging Initiative. (2024). Dynamic multilayer functional connectivity detects preclinical and clinical Alzheimer's disease. *Cerebral Cortex*, *34*(2), bhad542. https://doi.org/10.1093/cercor/bhad542

Cardin, J. A., Carlén, M., Meletis, K., Knoblich, U., Zhang, F., Deisseroth, K., Tsai, L.-H., & Moore, C. I. (2009). Driving fast-spiking cells induces gamma rhythm and controls sensory responses. *Nature*, *459*(7247), 663–667. https://doi.org/10.1038/nature08002

Casula, E. P., Pellicciari, M. C., Bonnì, S., Borghi, I., Maiella, M., Assogna, M., Minei, M., Motta, C., D'Acunto, A., Porrazzini, F., Pezzopane, V., Mencarelli, L., Roncaioli, A., Rocchi, L., Spampinato, D. A., Caltagirone, C., Santarnecchi, E., Martorana, A., & Koch, G. (2022). Decreased Frontal Gamma Activity in Alzheimer Disease Patients. *Annals of Neurology*, *92*(3), 464–475. https://doi.org/10.1002/ana.26444

Chan, D., Suk, H.-J., Jackson, B. L., Milman, N. P., Stark, D., Klerman, E. B., Kitchener, E., Fernandez Avalos, V. S., De Weck, G., Banerjee, A., Beach, S. D., Blanchard, J., Stearns, C., Boes, A. D., Uitermarkt, B., Gander, P., Howard, M., Sternberg, E. J., Nieto-Castanon, A., … Tsai, L.-H. (2022). Gamma frequency sensory stimulation in mild probable Alzheimer's dementia patients: Results of feasibility and pilot studies. *PLOS ONE*, *17*(12), e0278412. https://doi.org/10.1371/journal.pone.0278412

Chao, O. Y., Huston, J. P., Li, J.-S., Wang, A.-L., & de Souza Silva, M. A. (2016). The medial prefrontal cortex—Lateral entorhinal cortex circuit is essential for episodic-like memory and associative object-recognition. *Hippocampus*, *26*(5), 633–645. https://doi.org/10.1002/hipo.22547

Chao, O. Y., Nikolaus, S., Yang, Y.-M., & Huston, J. P. (2022). Neuronal circuitry for recognition memory of object and place in rodent models. *Neuroscience & Biobehavioral Reviews*, *141*, 104855. https://doi.org/10.1016/j.neubiorev.2022.104855

Chasseigneaux, S., & Allinquant, B. (2012). Functions of Aβ, sAPPα and sAPPβ: Similarities and differences. *Journal of Neurochemistry*, *120*(s1), 99–108. https://doi.org/10.1111/j.1471-4159.2011.07584.x

Chaudhuri, R., Gerçek, B., Pandey, B., Peyrache, A., & Fiete, I. (2019). The intrinsic attractor manifold and population dynamics of a canonical cognitive circuit across waking and sleep. *Nature Neuroscience*, *22*(9), 1512–1520. https://doi.org/10.1038/s41593-019-0460-x

Chen, J., Kanai, Y., Cowan, N. J., & Hirokawa, N. (1992). Projection domains of MAP2 and tau determine spacings between microtubules in dendrites and axons. *Nature*, *360*(6405), 674–677. https://doi.org/10.1038/360674a0

Chen, Z.-Y., & Zhang, Y. (2022). Animal models of Alzheimer's disease: Applications, evaluation, and perspectives. *Zoological Research*, *43*(6), 1026–1040. https://doi.org/10.24272/j.issn.2095-8137.2022.289

Cheng, C.-H., Hung, C.-C., Chao, Y.-P., Nouchi, R., & Wang, P.-N. (2023). Subjective cognitive decline exhibits alterations of resting-state phase-amplitude coupling in precuneus. *Clinical Neurophysiology*, *156*, 281–289. https://doi.org/10.1016/j.clinph.2023.08.015

Cheng, I. H., Scearce-Levie, K., Legleiter, J., Palop, J. J., Gerstein, H., Bien-Ly, N., Puolivaöli, J., Lesné, S., Ashe, K. H., Muchowski, P. J., & Mucke, L. (2007). Accelerating Amyloid-β Fibrillization Reduces Oligomer Levels and Functional Deficits in Alzheimer Disease Mouse Models. *Journal of Biological Chemistry*, *282*(33), 23818–23828. https://doi.org/10.1074/jbc.M701078200

Chiricosta, L., Gugliandolo, A., & Mazzon, E. (2021). SARS-CoV-2 Exacerbates Beta-Amyloid Neurotoxicity, Inflammation and Oxidative Stress in Alzheimer's Disease Patients. *International Journal of Molecular Sciences*, *22*(24), Article 24. https://doi.org/10.3390/ijms222413603

Chishti, M. A., Yang, D.-S., Janus, C., Phinney, A. L., Horne, P., Pearson, J., Strome, R., Zuker, N., Loukides, J., French, J., Turner, S., Lozza, G., Grilli, M., Kunicki, S., Morissette, C., Paquette, J., Gervais, F., Bergeron, C., Fraser, P. E., … Westaway, D. (2001). Early-onset Amyloid Deposition and Cognitive Deficits in Transgenic Mice Expressing a Double Mutant Form of Amyloid Precursor Protein 695. *Journal of Biological Chemistry*, *276*(24), 21562–21570. https://doi.org/10.1074/jbc.M100710200

Christ, W., Kapell, S., Sobkowiak, M. J., Mermelekas, G., Evertsson, B., Sork, H., Saher, O., Bazaz, S., Gustafsson, O., Cardenas, E. I., Villa, V., Ricciarelli, R., Sandberg, J. K., Bergquist, J., Sturchio, A., Svenningsson, P., Malm, T., Espay, A. J., Pernemalm, M., … Ezzat, K. (2024). *SARS-CoV-2 and HSV-1 Induce Amyloid Aggregation in Human CSF Resulting in Drastic Soluble Protein Depletion* (p. 2022.09.15.508120). bioRxiv. https://doi.org/10.1101/2022.09.15.508120

Chui, D. H., Dobo, E., Makifuchi, T., Akiyama, H., Kawakatsu, S., Petit, A., Checler, F., Araki, W., Takahashi, K., & Tabira, T. (2001). Apoptotic neurons in Alzheimer's disease frequently show intracellular Aβ42 labeling. *Journal of Alzheimer's Disease*, *3*(2), 231–239. https://doi.org/10.3233/JAD-2001-3208

Cinalli Jr., D. A., Cohen, S. J., Guthrie, K., & Stackman Jr., R. W. (2020). Object Recognition Memory: Distinct Yet Complementary Roles of the Mouse CA1 and Perirhinal Cortex. *Frontiers in Molecular Neuroscience*, *13*. https://doi.org/10.3389/fnmol.2020.527543

Citron, M., Oltersdorf, T., Haass, C., McConlogue, L., Hung, A. Y., Seubert, P., Vigo-Pelfrey, C., Lieberburg, I., & Selkoe, D. J. (1992). Mutation of the β-amyloid precursor protein in familial Alzheimer's disease increases β-protein production. *Nature*, *360*(6405), 672–674. https://doi.org/10.1038/360672a0

Citron, M., Westaway, D., Xia, W., Carlson, G., Diehl, T., Levesque, G., Johnson-wood, K., Lee, M., Seubert, P., Davis, A., Kholodenko, D., Motter, R., Sherrington, R., Perry,

B., Yao, H., Strome, R., Lieberburg, I., Rommens, J., Kim, S., … Selkoe, D. J. (1997). Mutant presenilins of Alzheimer's disease increase production of 42-residue amyloid β-protein in both transfected cells and transgenic mice. *Nature Medicine*, *3*(1), 67–72. https://doi.org/10.1038/nm0197-67

Clark, R. F., Hutton, M., Fuldner, M., Froelich, S., Karran, E., Talbot, C., Crook, R., Lendon, C., Prihar, G., He, C., Korenblat, K., Martinez, A., Wragg, M., Busfield, F., Behrens, M. I., Myers, A., Norton, J., Morris, J., Mehta, N., … Goate, A. (1995). The structure of the presenilin 1 (S182) gene and identification of six novel mutations in early onset AD families. *Nature Genetics*, *11*(2), 219–222. https://doi.org/10.1038/ng1095-219

Claus, J. J., Kwa, V. I., Teunisse, S., Walstra, G. J., van Gool, W. A., Koelman, J. H., Bour, L. J., & Ongerboer de Visser, B. W. (1998). Slowing on quantitative spectral EEG is a marker for rate of subsequent cognitive and functional decline in early Alzheimer disease. *Alzheimer Disease and Associated Disorders*, *12*(3), 167–174. https://doi.org/10.1097/00002093-199809000-00008

Clawson, W., Waked, B., Madec, T., Ghestem, A., Quilichini, P. P., Battaglia, D., & Bernard, C. (2023). Perturbed Information Processing Complexity in Experimental Epilepsy. *Journal of Neuroscience*, *43*(38), 6573–6587. https://doi.org/10.1523/JNEUROSCI.0383-23.2023

Cohen, S. J., Munchow, A. H., Rios, L. M., Zhang, G., Ásgeirsdóttir, H. N., & Stackman, R. W. (2013). The Rodent Hippocampus Is Essential for Nonspatial Object Memory. *Current Biology*, *23*(17), 1685–1690. https://doi.org/10.1016/j.cub.2013.07.002

Colgin, L. L., Denninger, T., Fyhn, M., Hafting, T., Bonnevie, T., Jensen, O., Moser, M.-B., & Moser, E. I. (2009). Frequency of gamma oscillations routes flow of information in the hippocampus. *Nature*, *462*(7271), 353–357. https://doi.org/10.1038/nature08573

Coradazzi, M., Gulino, R., Fieramosca, F., Falzacappa, L. V., Riggi, M., & Leanza, G. (2016). Selective noradrenaline depletion impairs working memory and hippocampal neurogenesis. *Neurobiology of Aging*, *48*, 93–102. https://doi.org/10.1016/j.neurobiolaging.2016.08.012

Corder, E. H., Saunders, A. M., Risch, N. J., Strittmatter, W. J., Schmechel, D. E., Gaskell, P. C., Rimmler, J. B., Locke, P. A., Conneally, P. M., Schmader, K. E., Small, G. W., Roses, A. D., Haines, J. L., & Pericak-Vance, M. A. (1994). Protective effect of apolipoprotein E type 2 allele for late onset Alzheimer disease. *Nature Genetics*, *7*(2), 180–184. https://doi.org/10.1038/ng0694-180

Cossart, R., Aronov, D., & Yuste, R. (2003). Attractor dynamics of network UP states in the neocortex. *Nature*, *423*(6937), 283–288. https://doi.org/10.1038/nature01614

Cowan, C. M., Bossing, T., Page, A., Shepherd, D., & Mudher, A. (2010). Soluble hyper-phosphorylated tau causes microtubule breakdown and functionally compromises normal tau in vivo. *Acta Neuropathologica*, *120*(5), 593–604. https://doi.org/10.1007/s00401-010-0716-8

Cowan, C. M., & Mudher, A. (2013). Are Tau Aggregates Toxic or Protective in Tauopathies? *Frontiers in Neurology*, *4*. https://doi.org/10.3389/fneur.2013.00114

Cruzat, J., Herzog, R., Prado, P., Sanz-Perl, Y., Gonzalez-Gomez, R., Moguilner, S., Kringelbach, M. L., Deco, G., Tagliazucchi, E., & Ibañez, A. (2023). Temporal Irreversibility of Large-Scale Brain Dynamics in Alzheimer's Disease. *The Journal of Neuroscience*, *43*(9), 1643–1656. https://doi.org/10.1523/JNEUROSCI.1312-22.2022

Cummings, B. J., Head, E., Afagh, A. J., Milgram, N. W., & Cotman, C. W. (1996). β-Amyloid Accumulation Correlates with Cognitive Dysfunction in the Aged Canine. *Neurobiology of Learning and Memory*, *66*(1), 11–23. https://doi.org/10.1006/nlme.1996.0039

Cummings, J. L., Morstorf, T., & Zhong, K. (2014). Alzheimer's disease drug-development pipeline: Few candidates, frequent failures. *Alzheimer's Research & Therapy*, *6*(4), 37. https://doi.org/10.1186/alzrt269

Czigler, B., Csikós, D., Hidasi, Z., Anna Gaál, Z., Csibri, É., Kiss, É., Salacz, P., & Molnár, M. (2008). Quantitative EEG in early Alzheimer's disease patients—Power spectrum and complexity features. *International Journal of Psychophysiology*, *68*(1), 75–80. https://doi.org/10.1016/j.ijpsycho.2007.11.002

D

Daelli, V., & Treves, A. (2010). Neural attractor dynamics in object recognition. *Experimental Brain Research*, *203*(2), 241–248. https://doi.org/10.1007/s00221-010-2243-1

Dahmen, D., Grün, S., Diesmann, M., & Helias, M. (2019). Second type of criticality in the brain uncovers rich multiple-neuron dynamics. *Proceedings of the National Academy of Sciences*, *116*(26), 13051–13060. https://doi.org/10.1073/pnas.1818972116

Dauwels, J., Srinivasan, K., Ramasubba Reddy, M., Musha, T., Vialatte, F.-B., Latchoumane, C., Jeong, J., & Cichocki, A. (2011). Slowing and Loss of Complexity in Alzheimer's EEG: Two Sides of the Same Coin? *International Journal of Alzheimer's Disease*, *2011*, 1–10. https://doi.org/10.4061/2011/539621

Dawson, G. R., Seabrook, G. R., Zheng, H., Smith, D. W., Graham, S., O'Dowd, G., Bowery, B. J., Boyce, S., Trumbauer, M. E., Chen, H. Y., Van Der Ploeg, L. H. T., & Sirinathsinghji, D. J. S. (1999). Age-related cognitive deficits, impaired long-term potentiation and reduction in synaptic marker density in mice lacking the β-amyloid precursor protein. *Neuroscience*, *90*(1), 1–13. https://doi.org/10.1016/S0306-4522(98)00410-2

De La Fuente, L. A., Zamberlan, F., Bocaccio, H., Kringelbach, M., Deco, G., Perl, Y. S., Pallavicini, C., & Tagliazucchi, E. (2023). Temporal irreversibility of neural dynamics as a signature of consciousness. *Cerebral Cortex*, *33*(5), 1856–1865. https://doi.org/10.1093/cercor/bhac177

De la Rosa, A., Olaso-Gonzalez, G., Arc-Chagnaud, C., Millan, F., Salvador-Pascual, A., García-Lucerga, C., Blasco-Lafarga, C., Garcia-Dominguez, E., Carretero, A., Correas, A. G., Viña, J., & Gomez-Cabrera, M. C. (2020). Physical exercise in the prevention and treatment of Alzheimer's disease. *Journal of Sport and Health Science*, *9*(5), 394–404. https://doi.org/10.1016/j.jshs.2020.01.004

de Landeta, A. B., Pereyra, M., Medina, J. H., & Katche, C. (2020). Anterior retrosplenial cortex is required for long-term object recognition memory. *Scientific Reports*, *10*(1), 4002. https://doi.org/10.1038/s41598-020-60937-z

de Arcangelis, L., Perrone-Capano, C., & Herrmann, H. J. (2006). Self-Organized Criticality Model for Brain Plasticity. *Physical Review Letters*, *96*(2), 028107. https://doi.org/10.1103/PhysRevLett.96.028107

Deco, G., Kringelbach, M. L., Jirsa, V. K., & Ritter, P. (2017). The dynamics of resting fluctuations in the brain: Metastability and its dynamical cortical core. *Scientific Reports*, *7*(1), 3095. https://doi.org/10.1038/s41598-017-03073-5

Deco, G., Perl, Y. S., Sitt, J. D., Tagliazucchi, E., & Kringelbach, M. L. (2021). *Deep learning the arrow of time in brain activity: Characterising brain-environment behavioural interactions in health and disease*. https://doi.org/10.1101/2021.07.02.450899

Deco, G., & Rolls, E. T. (2003). Attention and working memory: A dynamical model of neuronal activity in the prefrontal cortex. *European Journal of Neuroscience*, *18*(8), 2374–2390. https://doi.org/10.1046/j.1460-9568.2003.02956.x

Deco, G., Sanz Perl, Y., Bocaccio, H., Tagliazucchi, E., & Kringelbach, M. L. (2022). The INSIDEOUT framework provides precise signatures of the balance of intrinsic and extrinsic dynamics in brain states. *Communications Biology*, *5*(1), 1–13. https://doi.org/10.1038/s42003-022-03505-7

Deco, G., Tononi, G., Boly, M., & Kringelbach, M. L. (2015). Rethinking segregation and integration: Contributions of whole-brain modelling. *Nature Reviews Neuroscience*, *16*(7), 430–439. https://doi.org/10.1038/nrn3963

Demirtaş, M., Burt, J. B., Helmer, M., Ji, J. L., Adkinson, B. D., Glasser, M. F., Van Essen, D. C., Sotiropoulos, S. N., Anticevic, A., & Murray, J. D. (2019). Hierarchical Heterogeneity across Human Cortex Shapes Large-Scale Neural Dynamics. *Neuron*, *101*(6), 1181-1194.e13. https://doi.org/10.1016/j.neuron.2019.01.017

Dix, S. L., & Aggleton, J. P. (1999). Extending the spontaneous preference test of recognition: Evidence of object-location and object-context recognition. *Behavioural Brain Research*, *99*(2), 191–200. https://doi.org/10.1016/S0166-4328(98)00079-5

Do, A. D., Portet, C., Goutagny, R., & Jackson, J. (2024). The claustrum and synchronized brain states. *Trends in Neurosciences*, *0*(0). https://doi.org/10.1016/j.tins.2024.10.003

Doggui, S., Brouillette, J., Chabot, J.-G., Farso, M., & Quirion, R. (2010). Possible Involvement of Transthyretin in Hippocampal β-Amyloid Burden and Learning Behaviors in a Mouse Model of Alzheimer's Disease (TgCRND8). *Neurodegenerative Diseases*, *7*(1–3), 88–95. https://doi.org/10.1159/000285513

Donovan, N. J., Okereke, O. I., Vannini, P., Amariglio, R. E., Rentz, D. M., Marshall, G. A., Johnson, K. A., & Sperling, R. A. (2016). Association of Higher Cortical Amyloid Burden With Loneliness in Cognitively Normal Older Adults. *JAMA Psychiatry*, *73*(12), 1230–1237. https://doi.org/10.1001/jamapsychiatry.2016.2657

Doody, R. S., Raman, R., Farlow, M., Iwatsubo, T., Vellas, B., Joffe, S., Kieburtz, K., He, F., Sun, X., Thomas, R. G., Aisen, P. S., Siemers, E., Sethuraman, G., & Mohs, R. (2013). A Phase 3 Trial of Semagacestat for Treatment of Alzheimer's Disease. *New England Journal of Medicine*, *369*(4), 341–350. https://doi.org/10.1056/NEJMoa1210951

Doody, R. S., Thomas, R. G., Farlow, M., Iwatsubo, T., Vellas, B., Joffe, S., Kieburtz, K., Raman, R., Sun, X., Aisen, P. S., Siemers, E., Liu-Seifert, H., & Mohs, R. (2014). Phase 3 Trials of Solanezumab for Mild-to-Moderate Alzheimer's Disease. *New England Journal of Medicine*, *370*(4), 311–321. https://doi.org/10.1056/NEJMoa1312889

Douaud, G., Lee, S., Alfaro-Almagro, F., Arthofer, C., Wang, C., McCarthy, P., Lange, F., Andersson, J. L. R., Griffanti, L., Duff, E., Jbabdi, S., Taschler, B., Keating, P., Winkler, A. M., Collins, R., Matthews, P. M., Allen, N., Miller, K. L., Nichols, T. E., & Smith, S. M. (2022). SARS-CoV-2 is associated with changes in brain structure in UK Biobank. *Nature*, *604*(7907), 697–707. https://doi.org/10.1038/s41586-022-04569-5

Douchamps, V., Di Volo, M., Torcini, A., Battaglia, D., & Goutagny, R. (2024). Gamma oscillatory complexity conveys behavioral information in hippocampal networks. *Nature Communications*, *15*(1), 1849. https://doi.org/10.1038/s41467-024-46012-5

Dubois, B., Feldman, H. H., Jacova, C., Hampel, H., Molinuevo, J. L., Blennow, K., DeKosky, S. T., Gauthier, S., Selkoe, D., Bateman, R., Cappa, S., Crutch, S., Engelborghs, S., Frisoni, G. B., Fox, N. C., Galasko, D., Habert, M.-O., Jicha, G. A., Nordberg, A., … Cummings, J. L. (2014). Advancing research diagnostic criteria for Alzheimer's disease: The IWG-2 criteria. *The Lancet Neurology*, *13*(6), 614–629. https://doi.org/10.1016/S1474-4422(14)70090-0

Dudkowski, D., Jafari, S., Kapitaniak, T., Kuznetsov, N. V., Leonov, G. A., & Prasad, A. (2016). Hidden attractors in dynamical systems. *Physics Reports*, *637*, 1–50. https://doi.org/10.1016/j.physrep.2016.05.002

Duecker, K., Gutteling, T. P., Herrmann, C. S., & Jensen, O. (2021). No Evidence for Entrainment: Endogenous Gamma Oscillations and Rhythmic Flicker Responses Coexist in Visual Cortex. *Journal of Neuroscience*, *41*(31), 6684–6698. https://doi.org/10.1523/JNEUROSCI.3134-20.2021

Duff, K., Eckman, C., Zehr, C., Yu, X., Prada, C.-M., Perez-tur, J., Hutton, M., Buee, L., Harigaya, Y., Yager, D., Morgan, D., Gordon, M. N., Holcomb, L., Refolo, L., Zenk, B., Hardy, J., & Younkin, S. (1996). Increased amyloid-β42(43) in brains of mice expressing mutant presenilin 1. *Nature*, *383*(6602), 710–713. https://doi.org/10.1038/383710a0

Dulin, F., Léveillé, F., Ortega, J. B., Mornon, J.-P., Buisson, A., Callebaut, I., & Colloc'h, N. (2008). P3 peptide, a truncated form of Aβ devoid of synaptotoxic effect, does not assemble into soluble oligomers. *FEBS Letters*, *582*(13), 1865–1870. https://doi.org/10.1016/j.febslet.2008.05.002

Dumanchin, C., Camuzat, A., Campion, D., Verpillat, P., Hannequin, D., Dubois, B., Saugier-Veber, P., Martin, C., Penet, C., Charbonnier, F., Agid, Y., Frebourg, T., & Brice, A. (1998). Segregation of a Missense Mutation in the Microtubule-Associated Protein Tau Gene with Familial Frontotemporal Dementia and Parkinsonism. *Human Molecular Genetics*, *7*(11), 1825–1829. https://doi.org/10.1093/hmg/7.11.1825

Dunot, J., Moreno, S., Gandin, C., Pousinha, P. A., Amici, M., Dupuis, J., Anisimova, M., Winschel, A., Uriot, M., Petshow, S. J., Mensch, M., Bethus, I., Giudici, C., Hampel, H., Wefers, B., Wurst, W., Naumann, R., Ashby, M. C., Laube, B., … Marie, H. (2024). APP fragment controls both ionotropic and non-ionotropic signaling of NMDA receptors. *Neuron*, *112*(16), 2708-2720.e9. https://doi.org/10.1016/j.neuron.2024.05.027

E

Eckman, C. B., Mehta, N. D., Crook, R., Perez-tur, J., Prihar, G., Pfeiffer, E., Graff-Radford, N., Hinder, P., Yager, D., Zenk, B., Refolo, L. M., Mihail Prada, C., Younkin, S. G., Hutton, M., & Hardy, J. (1997). A New Pathogenic Mutation in the APP Gene (I716V) Increases the Relative Proportion of A 42(43). *Human Molecular Genetics*, *6*(12), 2087–2089. https://doi.org/10.1093/hmg/6.12.2087

Eddington, A. S. (1928). The deviation of stellar material from a perfect gas. *Monthly Notices of the Royal Astronomical Society*, *88*, 352. https://doi.org/10.1093/mnras/88.5.352

Efron, R. (1970). The minimum duration of a perception. *Neuropsychologia*, *8*(1), 57–63. https://doi.org/10.1016/0028-3932(70)90025-4

Eichenbaum, H. (2014). Time cells in the hippocampus: A new dimension for mapping memories. *Nature Reviews Neuroscience*, *15*(11), 732–744. https://doi.org/10.1038/nrn3827

Eidenmüller, J., Fath, T., Maas, T., Pool, M., Sontag, E., & Brandt, R. (2001). Phosphorylation-mimicking glutamate clusters in the proline-rich region are sufficient to simulate the functional deficiencies of hyperphosphorylated tau protein. *The Biochemical Journal*, *357*(Pt 3), 759–767. https://doi.org/10.1042/0264-6021:3570759

Ennaceur, A., & Delacour, J. (1988). A new one-trial test for neurobiological studies of memory in rats. 1: Behavioral data. *Behavioural Brain Research*, *31*(1), 47–59. https://doi.org/10.1016/0166-4328(88)90157-X

Evans, I. E. M., Llewellyn, D. J., Matthews, F. E., Woods, R. T., Brayne, C., Clare, L., & Team, on behalf of the C.-W. research. (2018). Social isolation, cognitive reserve, and cognition in healthy older people. *PLOS ONE*, *13*(8), e0201008. https://doi.org/10.1371/journal.pone.0201008

F

Faranda, D., Messori, G., & Yiou, P. (2017). Dynamical proxies of North Atlantic predictability and extremes. *Scientific Reports*, *7*(1), 41278.

Felice, F. G. D., Velasco, P. T., Lambert, M. P., Viola, K., Fernandez, S. J., Ferreira, S. T., & Klein, W. L. (2007). Aβ Oligomers Induce Neuronal Oxidative Stress through an N-Methyl-D-aspartate Receptor-dependent Mechanism That Is Blocked by the Alzheimer Drug Memantine *. *Journal of Biological Chemistry*, *282*(15), 11590–11601. https://doi.org/10.1074/jbc.M607483200

Ferman, T. J., Smith, G. E., Kantarci, K., Boeve, B. F., Pankratz, V. S., Dickson, D. W., Graff-Radford, N. R., Wszolek, Z., Van Gerpen, J., Uitti, R., Pedraza, O., Murray, M. E., Aakre, J., Parisi, J., Knopman, D. S., & Petersen, R. C. (2013). Nonamnestic mild cognitive impairment progresses to dementia with Lewy bodies. *Neurology*, *81*(23), 2032–2038. https://doi.org/10.1212/01.wnl.0000436942.55281.47

Fingelkurts, A. A., & Fingelkurts, A. A. (2004). MAKING COMPLEXITY SIMPLER: MULTIVARIABILITY AND METASTABILITY IN THE BRAIN. *International Journal of Neuroscience*, *114*(7), 843–862. https://doi.org/10.1080/00207450490450046

Folstein, M. F., Folstein, S. E., & McHugh, P. R. (1975). “Mini-mental state.” *Journal of Psychiatric Research*, *12*(3), 189–198. https://doi.org/10.1016/0022-3956(75)90026-6

Francis, B. M., Kim, J., Barakat, M. E., Fraenkl, S., Yücel, Y. H., Peng, S., Michalski, B., Fahnestock, M., McLaurin, J., & Mount, H. T. J. (2012). Object recognition memory and BDNF expression are reduced in young TgCRND8 mice. *Neurobiology of Aging*, *33*(3), 555–563. https://doi.org/10.1016/j.neurobiolaging.2010.04.003

Fries, P. (2005). A mechanism for cognitive dynamics: Neuronal communication through neuronal coherence. *Trends in Cognitive Sciences*, *9*(10), 474–480. https://doi.org/10.1016/j.tics.2005.08.011

Fries, P. (2015). Rhythms for Cognition: Communication through Coherence. *Neuron*, *88*(1), 220–235. https://doi.org/10.1016/j.neuron.2015.09.034

Fries, P., Nikolić, D., & Singer, W. (2007). The gamma cycle. *Trends in Neurosciences*, *30*(7), 309–316. https://doi.org/10.1016/j.tins.2007.05.005

Funahashi, S. (2006). Prefrontal cortex and working memory processes. *Neuroscience*, *139*(1), 251–261. https://doi.org/10.1016/j.neuroscience.2005.07.003

Furman, S., Green, K., & Lane, T. E. (2024). COVID-19 and the impact on Alzheimer's disease pathology. *Journal of Neurochemistry*, *168*(10), 3415–3429. https://doi.org/10.1111/jnc.15985

Furukawa, K., Sopher, B. L., Rydel, R. E., Begley, J. G., Pham, D. G., Martin, G. M., Fox, M., & Mattson, M. P. (1996). Increased Activity-Regulating and Neuroprotective Efficacy of α-Secretase-Derived Secreted Amyloid Precursor Protein Conferred by a C-Terminal Heparin-Binding Domain. *Journal of Neurochemistry*, *67*(5), 1882–1896. https://doi.org/10.1046/j.1471-4159.1996.67051882.x

Fuster-Matanzo, A., de Barreda, E. G., Dawson, H. N., Vitek, M. P., Avila, J., & Hernández, F. (2009). Function of tau protein in adult newborn neurons. *FEBS Letters*, *583*(18), 3063–3068. https://doi.org/10.1016/j.febslet.2009.08.017

G

Gage, F. H. (2019). Adult neurogenesis in mammals. *Science*, *364*(6443), 827–828. https://doi.org/10.1126/science.aav6885

Gallego, J. A., Perich, M. G., Miller, L. E., & Solla, S. A. (2017). Neural Manifolds for the Control of Movement. *Neuron*, *94*(5), 978–984. https://doi.org/10.1016/j.neuron.2017.05.025

Gannon, M., Che, P., Chen, Y., Jiao, K., Roberson, E. D., & Wang, Q. (2015). Noradrenergic dysfunction in Alzheimer's disease. *Frontiers in Neuroscience*, *9*. https://doi.org/10.3389/fnins.2015.00220

Gao, Y., & Pimplikar, S. W. (2001). The γ-secretase-cleaved C-terminal fragment of amyloid precursor protein mediates signaling to the nucleus. *Proceedings of the National Academy of Sciences*, *98*(26), 14979–14984. https://doi.org/10.1073/pnas.261463298

Gelinas, J. N., & Nguyen, P. V. (2007). Neuromodulation of Hippocampal Synaptic Plasticity, Learning, and Memory by Noradrenaline. *Central Nervous System Agents in Medicinal Chemistry*, *7*(1), 17–33. https://doi.org/10.2174/187152407780059196

German, D. C., Manaye, K. F., White III, C. L., Woodward, D. J., McIntire, D. D., Smith, W. K., Kalaria, R. N., & Mann, D. M. A. (1992). Disease-specific patterns of locus coeruleus cell loss. *Annals of Neurology*, *32*(5), 667–676. https://doi.org/10.1002/ana.410320510

Giorgi, F. S., Ryskalin, L., Ruffoli, R., Biagioni, F., Limanaqi, F., Ferrucci, M., Busceti, C. L., Bonuccelli, U., & Fornai, F. (2017). The Neuroanatomy of the Reticular Nucleus Locus Coeruleus in Alzheimer's Disease. *Frontiers in Neuroanatomy*, *11*. https://doi.org/10.3389/fnana.2017.00080

Girardeau, G., Benchenane, K., Wiener, S. I., Buzsáki, G., & Zugaro, M. B. (2009). Selective suppression of hippocampal ripples impairs spatial memory. *Nature Neuroscience*, *12*(10), 1222–1223. https://doi.org/10.1038/nn.2384

Girardeau, G., & Zugaro, M. (2011). Hippocampal ripples and memory consolidation. *Current Opinion in Neurobiology*, *21*(3), 452–459. https://doi.org/10.1016/j.conb.2011.02.005

Goate, A., Chartier-Harlin, M.-C., Mullan, M., Brown, J., Crawford, F., Fidani, L., Giuffra, L., Haynes, A., Irving, N., James, L., Mant, R., Newton, P., Rooke, K., Roques, P., Talbot, C., Pericak-Vance, M., Roses, A., Williamson, R., Rossor, M., … Hardy, J. (1991). Segregation of a missense mutation in the amyloid precursor protein gene with

familial Alzheimer's disease. *Nature*, *349*(6311), 704–706. https://doi.org/10.1038/349704a0

Goedert, M., Spillantini, M. G., Jakes, R., Rutherford, D., & Crowther, R. A. (1989). Multiple isoforms of human microtubule-associated protein tau: Sequences and localization in neurofibrillary tangles of Alzheimer's disease. *Neuron*, *3*(4), 519–526. https://doi.org/10.1016/0896-6273(89)90210-9

Goldman, J. G., Aggarwal, N. T., & Schroeder, C. D. (2015). Mild cognitive impairment: An update in Parkinson's disease and lessons learned from Alzheimer's disease. *Neurodegenerative Disease Management*, *5*(5), 425. https://doi.org/10.2217/nmt.15.34

Goldman, J. S., Hahn, S. E., Catania, J. W., Larusse-Eckert, S., Butson, M. Barber., Rumbaugh, M., Strecker, M. N., Roberts, J. S., Burke, W., Mayeux, R., & Bird, T. (2011). Genetic counseling and testing for Alzheimer disease: Joint practice guidelines of the American College of Medical Genetics and the National Society of Genetic Counselors. *Genetics in Medicine*, *13*(6), 597–605. https://doi.org/10.1097/GIM.0b013e31821d69b8

Goldman-Rakic, P. S. (2011). Circuitry of Primate Prefrontal Cortex and Regulation of Behavior by Representational Memory. In *Comprehensive Physiology* (pp. 373–417). John Wiley & Sons, Ltd. https://doi.org/10.1002/cphy.cp010509

Gómez-Isla, T., Hollister, R., West, H., Mui, S., Growdon, J. H., Petersen, R. C., Parisi, J. E., & Hyman, B. T. (1997). Neuronal loss correlates with but exceeds neurofibrillary tangles in Alzheimer's disease. *Annals of Neurology*, *41*(1), 17–24. https://doi.org/10.1002/ana.410410106

Goode, B. L., Denis, P. E., Panda, D., Radeke, M. J., Miller, H. P., Wilson, L., & Feinstein, S. C. (1997). Functional interactions between the proline-rich and repeat regions of tau enhance microtubule binding and assembly. *Molecular Biology of the Cell*, *8*(2), 353–365. https://doi.org/10.1091/mbc.8.2.353

Goutagny, R., Gu, N., Cavanagh, C., Jackson, J., Chabot, J.-G., Quirion, R., Krantic, S., & Williams, S. (2013). Alterations in hippocampal network oscillations and theta–

gamma coupling arise before Aβ overproduction in a mouse model of Alzheimer's disease. *European Journal of Neuroscience*, *37*(12), 1896–1902. https://doi.org/10.1111/ejn.12233

Grassberger, P., & Procaccia, I. (1983). Measuring the strangeness of strange attractors. *Physica D: Nonlinear Phenomena*, *9*(1), 189–208. https://doi.org/10.1016/0167-2789(83)90298-1

Gray, C. M., König, P., Engel, A. K., & Singer, W. (1989). Oscillatory responses in cat visual cortex exhibit inter-columnar synchronization which reflects global stimulus properties. *Nature*, *338*(6213), 334–337. https://doi.org/10.1038/338334a0

Grayson, B., Leger, M., Piercy, C., Adamson, L., Harte, M., & Neill, J. C. (2015). Assessment of disease-related cognitive impairments using the novel object recognition (NOR) task in rodents. *Behavioural Brain Research*, *285*, 176–193. https://doi.org/10.1016/j.bbr.2014.10.025

Griñán-Ferré, C., Izquierdo, V., Otero, E., Puigoriol-Illamola, D., Corpas, R., Sanfeliu, C., Ortuño-Sahagún, D., & Pallàs, M. (2018). Environmental Enrichment Improves Cognitive Deficits, AD Hallmarks and Epigenetic Alterations Presented in 5xFAD Mouse Model. *Frontiers in Cellular Neuroscience*, *12*. https://doi.org/10.3389/fncel.2018.00224

Grutzendler, J., & Morris, J. C. (2001). Cholinesterase Inhibitors for Alzheimer??s Disease: *Drugs*, *61*(1), 41–52. https://doi.org/10.2165/00003495-200161010-00005

Gu, S., Cieslak, M., Baird, B., Muldoon, S. F., Grafton, S. T., Pasqualetti, F., & Bassett, D. S. (2018). The Energy Landscape of Neurophysiological Activity Implicit in Brain Network Structure. *Scientific Reports*, *8*(1), 2507. https://doi.org/10.1038/s41598-018-20123-8

Gu, Y., Lin, Y., Huang, L., Ma, J., Zhang, J., Xiao, Y., Dai, Z., & Initiative, A. D. N. (2020). Abnormal dynamic functional connectivity in Alzheimer's disease. *CNS Neuroscience & Therapeutics*, *26*(9), 962–971. https://doi.org/10.1111/cns.13387

Guo, T., Noble, W., & Hanger, D. P. (2017). Roles of tau protein in health and disease. *Acta Neuropathologica*, *133*(5), 665–704. https://doi.org/10.1007/s00401-017-1707-9

Gureviciene, I., Gurevicius, K., Mugantseva, E., Kislin, M., Khiroug, L., & Tanila, H. (2017). Amyloid Plaques Show Binding Capacity of Exogenous Injected Amyloid-β. *Journal of Alzheimer's Disease*, *55*(1), 147–157. https://doi.org/10.3233/JAD-160453

Gustavsson, A., Norton, N., Fast, T., Frölich, L., Georges, J., Holzapfel, D., Kirabali, T., Krolak-Salmon, P., Rossini, P. M., Ferretti, M. T., Lanman, L., Chadha, A. S., & Van Der Flier, W. M. (2023). Global estimates on the number of persons across the Alzheimer's disease continuum. *Alzheimer's & Dementia*, *19*(2), 658–670. https://doi.org/10.1002/alz.12694

H

Hafting, T., Fyhn, M., Molden, S., Moser, M.-B., & Moser, E. I. (2005). Microstructure of a spatial map in the entorhinal cortex. *Nature*, *436*(7052), 801–806. https://doi.org/10.1038/nature03721

Hagmann, P., Kurant, M., Gigandet, X., Thiran, P., Wedeen, V. J., Meuli, R., & Thiran, J.-P. (2007). Mapping Human Whole-Brain Structural Networks with Diffusion MRI. *PLOS ONE*, *2*(7), e597. https://doi.org/10.1371/journal.pone.0000597

Haldeman, C., & Beggs, J. M. (2005). Critical Branching Captures Activity in Living Neural Networks and Maximizes the Number of Metastable States. *Physical Review Letters*, *94*(5), 058101. https://doi.org/10.1103/PhysRevLett.94.058101

Hamm, V., Héraud, C., Bott, J.-B., Herbeaux, K., Strittmatter, C., Mathis, C., & Goutagny, R. (2017). Differential contribution of APP metabolites to early cognitive deficits in a TgCRND8 mouse model of Alzheimer's disease. *Science Advances*, *3*(2), e1601068. https://doi.org/10.1126/sciadv.1601068

Hamm, V., Héraud, C., Cassel, J.-C., Mathis, C., & Goutagny, R. (2015). Precocious Alterations of Brain Oscillatory Activity in Alzheimer's Disease: A Window of Opportunity for Early Diagnosis and Treatment. *Frontiers in Cellular Neuroscience*, *9*. https://doi.org/10.3389/fncel.2015.00491

Hampel, H., Mesulam, M.-M., Cuello, A. C., Farlow, M. R., Giacobini, E., Grossberg, G. T., Khachaturian, A. S., Vergallo, A., Cavedo, E., Snyder, P. J., & Khachaturian, Z. S. (2018). The cholinergic system in the pathophysiology and treatment of Alzheimer's disease. *Brain*, *141*(7), 1917–1933. https://doi.org/10.1093/brain/awy132

Hansen, N., & Manahan-Vaughan, D. (2015). Hippocampal long-term potentiation that is elicited by perforant path stimulation or that occurs in conjunction with spatial learning is tightly controlled by beta-adrenoreceptors and the locus coeruleus. *Hippocampus*, *25*(11), 1285–1298. https://doi.org/10.1002/hipo.22436

Harris, K. D. (2005). Neural signatures of cell assembly organization. *Nature Reviews Neuroscience*, *6*(5), 399–407. https://doi.org/10.1038/nrn1669

Hasselmo, M. E. (1999). Neuromodulation: Acetylcholine and memory consolidation. *Trends in Cognitive Sciences*, *3*(9), 351–359. https://doi.org/10.1016/S1364-6613(99)01365-0

Hasselmo, M. E. (2006). The role of acetylcholine in learning and memory. *Current Opinion in Neurobiology*, *16*(6), 710–715. https://doi.org/10.1016/j.conb.2006.09.002

Hasselmo, M. E., Bodelón, C., & Wyble, B. P. (2002). A Proposed Function for Hippocampal Theta Rhythm: Separate Phases of Encoding and Retrieval Enhance Reversal of Prior Learning. *Neural Computation*, *14*(4), 793–817. https://doi.org/10.1162/089976602317318965

Hasselmo, M. E., & Sarter, M. (2011). Modes and Models of Forebrain Cholinergic Neuromodulation of Cognition. *Neuropsychopharmacology*, *36*(1), 52–73. https://doi.org/10.1038/npp.2010.104

He, H. J., Wang, X. S., Pan, R., Wang, D. L., Liu, M. N., & He, R. Q. (2009). The proline-rich domain of tau plays a role in interactions with actin. *BMC Cell Biology*, *10*(1), 81. https://doi.org/10.1186/1471-2121-10-81

He, Q., Colon-Motas, K. M., Pybus, A. F., Piendel, L., Seppa, J. K., Walker, M. L., Manzanares, C. M., Qiu, D., Miocinovic, S., Wood, L. B., Levey, A. I., Lah, J. J., & Singer, A. C. (2021). A feasibility trial of gamma sensory flicker for patients with

prodromal Alzheimer's disease. *Alzheimer's & Dementia: Translational Research & Clinical Interventions*, *7*(1), e12178. https://doi.org/10.1002/trc2.12178

Hebb, D. O. (1949). *The organization of behavior; a neuropsychological theory* (pp. xix, 335). Wiley.

Hébert, S. S., Serneels, L., Tolia, A., Craessaerts, K., Derks, C., Filippov, M. A., Müller, U., & De Strooper, B. (2006). Regulated intramembrane proteolysis of amyloid precursor protein and regulation of expression of putative target genes. *EMBO Reports*, *7*(7), 739–745. https://doi.org/10.1038/sj.embor.7400704

Hernández, F., Gómez de Barreda, E., Fuster-Matanzo, A., Lucas, J. J., & Avila, J. (2010). GSK3: A possible link between beta amyloid peptide and tau protein. *Experimental Neurology*, *223*(2), 322–325. https://doi.org/10.1016/j.expneurol.2009.09.011

Herring, A., Yasin, H., Ambrée, O., Sachser, N., Paulus, W., & Keyvani, K. (2008). Environmental Enrichment Counteracts Alzheimer's Neurovascular Dysfunction in TgCRND8 Mice. *Brain Pathology*, *18*(1), 32–39. https://doi.org/10.1111/j.1750-3639.2007.00094.x

Hodgkin, A. L., & Huxley, A. F. (1952). A quantitative description of membrane current and its application to conduction and excitation in nerve. *The Journal of Physiology*, *117*(4), 500–544. https://doi.org/10.1113/jphysiol.1952.sp004764

Hong, X.-P., Peng, C.-X., Wei, W., Tian, Q., Liu, Y.-H., Yao, X.-Q., Zhang, Y., Cao, F.-Y., Wang, Q., & Wang, J.-Z. (2010). Essential role of tau phosphorylation in adult hippocampal neurogenesis. *Hippocampus*, *20*(12), 1339–1349. https://doi.org/10.1002/hipo.20712

Honjo, K., Van Reekum, R., & Verhoeff, N. P. L. G. (2009). Alzheimer's disease and infection: Do infectious agents contribute to progression of Alzheimer's disease? *Alzheimer's & Dementia*, *5*(4), 348–360. https://doi.org/10.1016/j.jalz.2008.12.001

Horváth, A., Szűcs, A., Hidasi, Z., Csukly, G., Barcs, G., & Kamondi, A. (2018). Prevalence, Semiology, and Risk Factors of Epilepsy in Alzheimer's Disease: An

Ambulatory EEG Study. *Journal of Alzheimer's Disease*, *63*(3), 1045–1054. https://doi.org/10.3233/JAD-170925

Howlett, D. R., Richardson, J. C., Austin, A., Parsons, A. A., Bate, S. T., Davies, D. C., & Gonzalez, M. I. (2004). Cognitive correlates of Aβ deposition in male and female mice bearing amyloid precursor protein and presenilin-1 mutant transgenes. *Brain Research*, *1017*(1–2), 130–136. https://doi.org/10.1016/j.brainres.2004.05.029

Hsiao, K., Chapman, P., Nilsen, S., Eckman, C., Harigaya, Y., Younkin, S., Yang, F., & Cole, G. (1996). Correlative Memory Deficits, Aβ Elevation, and Amyloid Plaques in Transgenic Mice. *Science*, *274*(5284), 99–103. https://doi.org/10.1126/science.274.5284.99

Huang, S.-M., Mouri, A., Kokubo, H., Nakajima, R., Suemoto, T., Higuchi, M., Staufenbiel, M., Noda, Y., Yamaguchi, H., Nabeshima, T., Saido, T. C., & Iwata, N. (2006). Neprilysin-sensitive Synapse-associated Amyloid-β Peptide Oligomers Impair Neuronal Plasticity and Cognitive Function *. *Journal of Biological Chemistry*, *281*(26), 17941–17951. https://doi.org/10.1074/jbc.M601372200

Hubel, D. H., & Wiesel, T. N. (1962). Receptive fields, binocular interaction and functional architecture in the cat's visual cortex. *The Journal of Physiology*, *160*(1), 106–154. https://doi.org/10.1113/jphysiol.1962.sp006837

Huber, R., Felice Ghilardi, M., Massimini, M., & Tononi, G. (2004). Local sleep and learning. *Nature*, *430*(6995), 78–81. https://doi.org/10.1038/nature02663

I

Iaccarino, H. F., Singer, A. C., Martorell, A. J., Rudenko, A., Gao, F., Gillingham, T. Z., Mathys, H., Seo, J., Kritskiy, O., Abdurrob, F., Adaikkan, C., Canter, R. G., Rueda, R., Brown, E. N., Boyden, E. S., & Tsai, L.-H. (2016). Gamma frequency entrainment attenuates amyloid load and modifies microglia. *Nature*, *540*(7632), Article 7632. https://doi.org/10.1038/nature20587

Iacono, D., Resnick, S. M., An, Y., Pletnikova, O., Rudow, G., Crain, B., & Troncoso, J. C. (2014). Mild Cognitive Impairment and Asymptomatic Alzheimer Disease Subjects: Equivalent A-Amyloid and Tau Loads With Divergent Cognitive Outcomes. *J Neuropathol Exp Neurol*, *73*(4).

Ibanez, A. (2022). The mind's golden cage and cognition in the wild. *Trends in Cognitive Sciences*, *26*(12), 1031–1034. https://doi.org/10.1016/j.tics.2022.07.008

Inestrosa, N. C., Reyes, A. E., Chacón, M. A., Cerpa, W., Villalón, A., Montiel, J., Merabachvili, G., Aldunate, R., Bozinovic, F., & Aboitiz, F. (2005). Human-like rodent amyloid-β-peptide determines Alzheimer pathology in aged wild-type *Octodon degu*. *Neurobiology of Aging*, *26*(7), 1023–1028. https://doi.org/10.1016/j.neurobiolaging.2004.09.016

Ingram, D. K. (1988). Complex maze learning in rodents as a model of age-related memory impairment. *Neurobiology of Aging*, *9*, 475–485. https://doi.org/10.1016/S0197-4580(88)80101-5

Iqbal, K., Liu, F., Gong, C.-X., & Grundke-Iqbal, I. (2010). Tau in Alzheimer Disease and Related Tauopathies. *Current Alzheimer Research*, *7*(8), 656–664. https://doi.org/10.2174/156720510793611592

Islam, M. R., Jackson, B., Schatz, B., Murdock, M., Tan, N., Park, D. S., Amorim, D. R., Jiang, F., Pineda, S. S., Adaikkan, C., Fernandez, V., Geigenmuller, U., Kellis, M., Boyden, E. S., & Tsai, L.-H. (2024). *Multisensory gamma stimulation enhances adult neurogenesis and improves cognitive function in a mouse model of Down syndrome*. https://doi.org/10.1101/2024.10.03.616486

J

Jacob, P.-Y., Casali, G., Spieser, L., Page, H., Overington, D., & Jeffery, K. (2017). An independent, landmark-dominated head-direction signal in dysgranular retrosplenial cortex. *Nature Neuroscience*, *20*(2), 173–175. https://doi.org/10.1038/nn.4465

James, W. (1890). The principles of psychology. *Henry Holt*.

Jessen, F., Amariglio, R. E., van Boxtel, M., Breteler, M., Ceccaldi, M., Chételat, G., Dubois, B., Dufouil, C., Ellis, K. A., van der Flier, W. M., Glodzik, L., van Harten, A. C., de Leon, M. J., McHugh, P., Mielke, M. M., Molinuevo, J. L., Mosconi, L., Osorio, R. S., Perrotin, A., … Wagner, M. (2014). A conceptual framework for research on subjective cognitive decline in preclinical Alzheimer's disease. *Alzheimer's & Dementia*, *10*(6), 844–852. https://doi.org/10.1016/j.jalz.2014.01.001

Jessen, F., Wolfsgruber, S., Wiese, B., Bickel, H., Mösch, E., Kaduszkiewicz, H., Pentzek, M., Riedel-Heller, S. G., Luck, T., Fuchs, A., Weyerer, S., Werle, J., van den Bussche, H., Scherer, M., Maier, W., Wagner, M., & German Study on Aging, Cognition and Dementia in Primary Care Patients. (2014). AD dementia risk in late MCI, in early MCI, and in subjective memory impairment. *Alzheimer's & Dementia: The Journal of the Alzheimer's Association*, *10*(1), 76–83. https://doi.org/10.1016/j.jalz.2012.09.017

Jonsson, T., Atwal, J. K., Steinberg, S., Snaedal, J., Jonsson, P. V., Bjornsson, S., Stefansson, H., Sulem, P., Gudbjartsson, D., Maloney, J., Hoyte, K., Gustafson, A., Liu, Y., Lu, Y., Bhangale, T., Graham, R. R., Huttenlocher, J., Bjornsdottir, G., Andreassen, O. A., … Stefansson, K. (2012). A mutation in APP protects against Alzheimer's disease and age-related cognitive decline. *Nature*, *488*(7409), 96–99. https://doi.org/10.1038/nature11283

Jul, P., Volbracht, C., de Jong, I. E. M., Helboe, L., Elvang, A. B., & Pedersen, J. T. (2016). Hyperactivity with Agitative-Like Behavior in a Mouse Tauopathy Model. *Journal of Alzheimer's Disease*, *49*(3), 783–795. https://doi.org/10.3233/JAD-150292

Jyoti, A., Plano, A., Riedel, G., & Platt, B. (2010). EEG, Activity, and Sleep Architecture in a Transgenic AβPP swe/PSEN1 A246E Alzheimer's Disease Mouse. *Journal of Alzheimer's Disease*, *22*(3), 873–887. https://doi.org/10.3233/JAD-2010-100879

K

Kanno, T., Tsuchiya, A., & Nishizaki, T. (2014). Hyperphosphorylation of Tau at Ser396 occurs in the much earlier stage than appearance of learning and memory disorders in 5XFAD mice. *Behavioural Brain Research*, *274*, 302–306. https://doi.org/10.1016/j.bbr.2014.08.034

Kawahara, M., & Kuroda, Y. (2000). Molecular mechanism of neurodegeneration induced by Alzheimer's β-amyloid protein: Channel formation and disruption of calcium homeostasis. *Brain Research Bulletin*, *53*(4), 389–397. https://doi.org/10.1016/S0361-9230(00)00370-1

Kayed, R., & Lasagna-Reeves, C. A. (2013). Molecular Mechanisms of Amyloid Oligomers Toxicity. *Journal of Alzheimer's Disease*, *33*(s1), S67–S78. https://doi.org/10.3233/JAD-2012-129001

Kim, D.-H., Kim, H.-A., Han, Y. S., Jeon, W. K., & Han, J.-S. (2020). Recognition memory impairments and amyloid-beta deposition of the retrosplenial cortex at the early stage of 5XFAD mice. *Physiology & Behavior*, *222*, 112891. https://doi.org/10.1016/j.physbeh.2020.112891

Kim, W., & Hecht, M. H. (2005). Sequence Determinants of Enhanced Amyloidogenicity of Alzheimer Aβ42 Peptide Relative to Aβ40. *Journal of Biological Chemistry*, *280*(41), 35069–35076. https://doi.org/10.1074/jbc.M505763200

Kimura, T., Whitcomb, D. J., Jo, J., Regan, P., Piers, T., Heo, S., Brown, C., Hashikawa, T., Murayama, M., Seok, H., Sotiropoulos, I., Kim, E., Collingridge, G. L., Takashima, A., & Cho, K. (2014). Microtubule-associated protein tau is essential for long-term depression in the hippocampus. *Philosophical Transactions of the Royal Society B: Biological Sciences*, *369*(1633), 20130144. https://doi.org/10.1098/rstb.2013.0144

Kirst, C., Timme, M., & Battaglia, D. (2016). Dynamic information routing in complex networks. *Nature Communications*, *7*(1), 11061. https://doi.org/10.1038/ncomms11061

Kobayashi, K., & Yasoshima, Y. (2001). The central noradrenaline system and memory consolidation. *The Neuroscientist: A Review Journal Bringing Neurobiology, Neurology and Psychiatry*, *7*(5), 371–376. https://doi.org/10.1177/107385840100700506

Koepsell, T. D., & Monsell, S. E. (2012). Reversion from mild cognitive impairment to normal or near-normal cognition: Risk factors and prognosis. *Neurology*, *79*(15), 1591–1598. https://doi.org/10.1212/WNL.0b013e31826e26b7

Kramer, M. A., & Cash, S. S. (2012). Epilepsy as a Disorder of Cortical Network Organization. *The Neuroscientist*, *18*(4), 360–372. https://doi.org/10.1177/1073858411422754

Kuperstein, I., Broersen, K., Benilova, I., Rozenski, J., Jonckheere, W., Debulpaep, M., Vandersteen, A., Segers-Nolten, I., Van Der Werf, K., Subramaniam, V., Braeken, D., Callewaert, G., Bartic, C., D'Hooge, R., Martins, I. C., Rousseau, F., Schymkowitz, J., & De Strooper, B. (2010). Neurotoxicity of Alzheimer's disease Aβ peptides is induced by small changes in the Aβ42 to Aβ40 ratio. *The EMBO Journal*, *29*(19), 3408–3420. https://doi.org/10.1038/emboj.2010.211

Kuruvilla, M. V., Wilson, D. I. G., & Ainge, J. A. (2020). Lateral entorhinal cortex lesions impair both egocentric and allocentric object–place associations. *Brain and Neuroscience Advances*, *4*, 2398212820939463. https://doi.org/10.1177/2398212820939463

L

Lam, A. D., Sarkis, R. A., Pellerin, K. R., Jing, J., Dworetzky, B. A., Hoch, D. B., Jacobs, C. S., Lee, J. W., Weisholtz, D. S., Zepeda, R., Westover, M. B., Cole, A. J., & Cash, S. S. (2020). Association of epileptiform abnormalities and seizures in Alzheimer disease. *Neurology*, *95*(16). https://doi.org/10.1212/WNL.0000000000010612

Langton, C. G. (1990). Computation at the edge of chaos: Phase transitions and emergent computation. *Physica D: Nonlinear Phenomena*, *42*(1–3), 12–37. https://doi.org/10.1016/0167-2789(90)90064-V

Lauritzen, I., Pardossi-Piquard, R., Bauer, C., Brigham, E., Abraham, J.-D., Ranaldi, S., Fraser, P., St-George-Hyslop, P., Thuc, O. L., Espin, V., Chami, L., Dunys, J., & Checler, F. (2012). The β-Secretase-Derived C-Terminal Fragment of βAPP, C99, But Not Aβ, Is a Key Contributor to Early Intraneuronal Lesions in Triple-Transgenic Mouse Hippocampus. *Journal of Neuroscience*, *32*(46), 16243–16255. https://doi.org/10.1523/JNEUROSCI.2775-12.2012

Lauritzen, I., Pardossi-Piquard, R., Bourgeois, A., Pagnotta, S., Biferi, M.-G., Barkats, M., Lacor, P., Klein, W., Bauer, C., & Checler, F. (2016). Intraneuronal aggregation of the β-CTF fragment of APP (C99) induces Aβ-independent lysosomal-autophagic pathology. *Acta Neuropathologica*, *132*(2), 257–276. https://doi.org/10.1007/s00401-016-1577-6

Laws, K. R., Irvine, K., & Gale, T. M. (2018). Sex differences in Alzheimer's disease. *Current Opinion in Psychiatry*, *31*(2), 133. https://doi.org/10.1097/YCO.0000000000000401

Lazzari, C., & Rabottini, M. (2022). COVID-19, loneliness, social isolation and risk of dementia in older people: A systematic review and meta-analysis of the relevant literature. *International Journal of Psychiatry in Clinical Practice*, *26*(2), 196–207. https://doi.org/10.1080/13651501.2021.1959616

Lee, A. K., & Wilson, M. A. (2002). Memory of Sequential Experience in the Hippocampus during Slow Wave Sleep. *Neuron*, *36*(6), 1183–1194. https://doi.org/10.1016/S0896-6273(02)01096-6

Lee, K., Park, Y., Suh, S. W., Kim, S.-S., Kim, D.-W., Lee, J., Park, J., Yoo, S., & Kim, K. W. (2021). Optimal flickering light stimulation for entraining gamma waves in the human brain. *Scientific Reports*, *11*(1), 16206. https://doi.org/10.1038/s41598-021-95550-1

Lee, M. G., Hassani, O. K., Alonso, A., & Jones, B. E. (2005). Cholinergic Basal Forebrain Neurons Burst with Theta during Waking and Paradoxical Sleep. *Journal of Neuroscience*, *25*(17), 4365–4369. https://doi.org/10.1523/JNEUROSCI.0178-05.2005

Legendy, C. R. (1967). On the scheme by which the human brain stores information. *Mathematical Biosciences*, *1*(4), 555–597. https://doi.org/10.1016/0025-5564(67)90003-X

Lehmann, D., Ozaki, H., & Pal, I. (1987). *EEG alpha map series: Brain micro-states by space-oriented adaptive segmentation i*.

Lesné, S., Koh, M. T., Kotilinek, L., Kayed, R., Glabe, C. G., Yang, A., Gallagher, M., & Ashe, K. H. (2006). RETRACTED ARTICLE: A specific amyloid-β protein assembly in the brain impairs memory. *Nature*, *440*(7082), 352–357. https://doi.org/10.1038/nature04533

Leung, H.-C., Gore, J. C., & Goldman-Rakic, P. S. (2002). Sustained Mnemonic Response in the Human Middle Frontal Gyrus during On-Line Storage of Spatial Memoranda. *Journal of Cognitive Neuroscience*, *14*(4), 659–671. Journal of Cognitive Neuroscience. https://doi.org/10.1162/08989290260045882

Lian, H., Li, Y., & Li, Y. (2021). Altered EEG microstate dynamics in mild cognitive impairment and Alzheimer's disease. *Clinical Neurophysiology*, *132*(11), 2861–2869. https://doi.org/10.1016/j.clinph.2021.08.015

Lichtenthaler, S. F., Wang, R., Grimm, H., Uljon, S. N., Masters, C. L., & Beyreuther, K. (1999). Mechanism of the cleavage specificity of Alzheimer's disease γ-secretase identified by phenylalanine-scanning mutagenesis of the transmembrane domain of the amyloid precursor protein. *Proceedings of the National Academy of Sciences*, *96*(6), 3053–3058. https://doi.org/10.1073/pnas.96.6.3053

Lisman, J., & Buzsaki, G. (2008). A Neural Coding Scheme Formed by the Combined Function of Gamma and Theta Oscillations. *Schizophrenia Bulletin*, *34*(5), 974–980. https://doi.org/10.1093/schbul/sbn060

Liu, F., Liang, Z., & Gong, C. X. (2006). Hyperphosphorylation of tau and protein phosphatases in Alzheimer disease. *Panminerva Medica*, *48*(2), 97–108.

Liu, J.-P., Tang, Y., Zhou, S., Toh, B. H., McLean, C., & Li, H. (2010). Cholesterol involvement in the pathogenesis of neurodegenerative diseases. *Molecular and Cellular Neuroscience*, *43*(1), 33–42. https://doi.org/10.1016/j.mcn.2009.07.013

Liu, S., Zhang, S., Guo, M., Lei, Q., He, L., & Li, Z. (2023). Acoustic stimulation during sleep improves cognition and ameliorates Alzheimer's disease pathology in APP/PS1 mice. *Experimental Gerontology*, *182*, 112299. https://doi.org/10.1016/j.exger.2023.112299

Löffler, J., & Huber, G. (1992). β-Amyloid Precursor Protein Isoforms in Various Rat Brain Regions and During Brain Development. *Journal of Neurochemistry*, *59*(4), 1316–1324. https://doi.org/10.1111/j.1471-4159.1992.tb08443.x

Lombardo, D., Cassé-Perrot, C., Ranjeva, J.-P., Le Troter, A., Guye, M., Wirsich, J., Payoux, P., Bartrés-Faz, D., Bordet, R., Richardson, J. C., Felician, O., Jirsa, V., Blin, O., Didic, M., & Battaglia, D. (2020). Modular slowing of resting-state dynamic functional connectivity as a marker of cognitive dysfunction induced by sleep deprivation. *NeuroImage*, *222*, 117155. https://doi.org/10.1016/j.neuroimage.2020.117155

Lopes-dos-Santos, V., Ven, G. M. van de, Morley, A., Trouche, S., Campo-Urriza, N., & Dupret, D. (2018). Parsing Hippocampal Theta Oscillations by Nested Spectral Components during Spatial Exploration and Memory-Guided Behavior. *Neuron*, *100*(4), 940-952.e7. https://doi.org/10.1016/j.neuron.2018.09.031

López-Sanz, D., Bruña, R., Garcés, P., Martín-Buro, M. C., Walter, S., Delgado, M. L., Montenegro, M., López Higes, R., Marcos, A., & Maestú, F. (2017). Functional Connectivity Disruption in Subjective Cognitive Decline and Mild Cognitive Impairment: A Common Pattern of Alterations. *Frontiers in Aging Neuroscience*, *9*. https://doi.org/10.3389/fnagi.2017.00109

Lott, I. T., & Dierssen, M. (2010). Cognitive deficits and associated neurological complications in individuals with Down's syndrome. *The Lancet Neurology*, *9*(6), 623–633. https://doi.org/10.1016/S1474-4422(10)70112-5

Luo, M., Zhou, J., Sun, C., Chen, W., Fu, C., Si, C., Zhang, Y., Geng, Y., & Chen, Y. (2024). *APP β-CTF triggers cell-autonomous synaptic toxicity independent of Aβ* (p. 2024.07.11.603028). bioRxiv. https://doi.org/10.1101/2024.07.11.603028

Luppi, A. I., Craig, M. M., Pappas, I., Finoia, P., Williams, G. B., Allanson, J., Pickard, J. D., Owen, A. M., Naci, L., Menon, D. K., & Stamatakis, E. A. (2019). Consciousness-specific dynamic interactions of brain integration and functional diversity. *Nature Communications*, *10*(1), 4616. https://doi.org/10.1038/s41467-019-12658-9

Lynn, C. W., Cornblath, E. J., Papadopoulos, L., Bertolero, M. A., & Bassett, D. S. (2021). Broken detailed balance and entropy production in the human brain. *Proceedings of the National Academy of Sciences*, *118*(47), e2109889118. https://doi.org/10.1073/pnas.2109889118

M

Ma, Z., Turrigiano, G. G., Wessel, R., & Hengen, K. B. (2019). Cortical Circuit Dynamics Are Homeostatically Tuned to Criticality In Vivo. *Neuron*, *104*(4), 655-664.e4. https://doi.org/10.1016/j.neuron.2019.08.031

Maaten, L. van der, & Hinton, G. (2008). Visualizing Data using t-SNE. *Journal of Machine Learning Research*, *9*(86), 2579–2605.

Magnani, E., Fan, J., Gasparini, L., Golding, M., Williams, M., Schiavo, G., Goedert, M., Amos, L. A., & Spillantini, M. G. (2007). Interaction of tau protein with the dynactin complex. *The EMBO Journal*, *26*(21), 4546–4554. https://doi.org/10.1038/sj.emboj.7601878

Maingret, N., Girardeau, G., Todorova, R., Goutierre, M., & Zugaro, M. (2016). Hippocampo-cortical coupling mediates memory consolidation during sleep. *Nature Neuroscience*, *19*(7), 959–964. https://doi.org/10.1038/nn.4304

Mann, D. M. A., Iwatsubo, T., Cairns, N. J., Lantos, P. L., Nochlin, D., Sumi, S. M., Bird, T. D., Poorkaj, P., Hardy, J., Hutton, M., Prihar, G., Crook, R., Rossor, M. N., & Haltia, M. (1996). Amyloid β protein (Aβ) deposition in chromosome 14–linked Alzheimer's disease: Predominance of Aβ42(43). *Annals of Neurology*, *40*(2), 149–156. https://doi.org/10.1002/ana.410400205

Mao, D., Kandler, S., McNaughton, B. L., & Bonin, V. (2017). Sparse orthogonal population representation of spatial context in the retrosplenial cortex. *Nature Communications*, *8*(1), 243. https://doi.org/10.1038/s41467-017-00180-9

Markesbery, W. R. (2010). Neuropathologic Alterations in Mild Cognitive Impairment: A Review. *Journal of Alzheimer's Disease*, *19*(1), 221–228. https://doi.org/10.3233/JAD-2010-1220

Marriott, B. A., Do, A. D., Portet, C., Thellier, F., Goutagny, R., & Jackson, J. (2024). Brain-state-dependent constraints on claustrocortical communication and function. *Cell Reports*, *43*(1). https://doi.org/10.1016/j.celrep.2023.113620

Martorell, A. J., Paulson, A. L., Suk, H.-J., Abdurrob, F., Drummond, G. T., Guan, W., Young, J. Z., Kim, D. N.-W., Kritskiy, O., Barker, S. J., Mangena, V., Prince, S. M., Brown, E. N., Chung, K., Boyden, E. S., Singer, A. C., & Tsai, L.-H. (2019). Multi-sensory Gamma Stimulation Ameliorates Alzheimer's-Associated Pathology and Improves Cognition. *Cell*, *177*(2), 256-271.e22. https://doi.org/10.1016/j.cell.2019.02.014

Mathis, A., Mamidanna, P., Cury, K. M., Abe, T., Murthy, V. N., Mathis, M. W., & Bethge, M. (2018). DeepLabCut: Markerless pose estimation of user-defined body parts with deep learning. *Nature Neuroscience*, *21*(9), Article 9. https://doi.org/10.1038/s41593-018-0209-y

Matrone, C., Luvisetto, S., La Rosa, L. R., Tamayev, R., Pignataro, A., Canu, N., Yang, L., Barbagallo, A. P. M., Biundo, F., Lombino, F., Zheng, H., Ammassari-Teule, M., & D'Adamio, L. (2012). Tyr682 in the Aβ-precursor protein intracellular domain regulates synaptic connectivity, cholinergic function, and cognitive performance. *Aging Cell*, *11*(6), 1084–1093. https://doi.org/10.1111/acel.12009

Mattson, M. P. (1997). Cellular actions of beta-amyloid precursor protein and its soluble and fibrillogenic derivatives. *Physiological Reviews*, *77*(4), 1081–1132. https://doi.org/10.1152/physrev.1997.77.4.1081

Maurer, K., Volk, S., & Gerbaldo, H. (1997). Auguste D and Alzheimer's disease. *THE LANCET*, *349*.

McKhann, G., Drachman, D., Folstein, M., Katzman, R., Price, D., & Stadlan, E. M. (1984). Clinical diagnosis of Alzheimer's disease. *Neurology*, *34*(7), 939–939. https://doi.org/10.1212/WNL.34.7.939

McKhann, G. M., Knopman, D. S., Chertkow, H., Hyman, B. T., Jack Jr., C. R., Kawas, C. H., Klunk, W. E., Koroshetz, W. J., Manly, J. J., Mayeux, R., Mohs, R. C., Morris, J. C., Rossor, M. N., Scheltens, P., Carrillo, M. C., Thies, B., Weintraub, S., & Phelps, C. H. (2011). The diagnosis of dementia due to Alzheimer's disease: Recommendations from the National Institute on Aging-Alzheimer's Association workgroups on diagnostic guidelines for Alzheimer's disease. *Alzheimer's & Dementia*, *7*(3), 263–269. https://doi.org/10.1016/j.jalz.2011.03.005

Medeiros, R., Baglietto-Vargas, D., & LaFerla, F. M. (2011). The Role of Tau in Alzheimer's Disease and Related Disorders. *CNS Neuroscience & Therapeutics*, *17*(5), 514–524. https://doi.org/10.1111/j.1755-5949.2010.00177.x

Mézard, M., & Parisi, G. (1988). The Euclidean matching problem. *Journal de Physique*, *49*(12), 2019–2025. https://doi.org/10.1051/jphys:0198800490120201900

Mezard, M., Parisi, G., Virasoro, M. A., & Thouless, D. J. (1988). Spin Glass Theory and Beyond. *Physics Today*, *41*(12), 109–110. https://doi.org/10.1063/1.2811676

Michel, C. M., & Koenig, T. (2018). EEG microstates as a tool for studying the temporal dynamics of whole-brain neuronal networks: A review. *NeuroImage*, *180*, 577–593. https://doi.org/10.1016/j.neuroimage.2017.11.062

Miller, S. R., Luxem, K., Lauderdale, K., Nambiar, P., Honma, P. S., Ly, K. K., Bangera, S., Bullock, M., Shin, J., Kaliss, N., Qiu, Y., Cai, C., Shen, K., Mallen, K. D., Yan, Z., Mendiola, A. S., Saito, T., Saido, T. C., Pico, A. R., … Palop, J. J. (2024). Machine learning reveals prominent spontaneous behavioral changes and treatment efficacy in humanized and transgenic Alzheimer's disease models. *Cell Reports*, *43*(11). https://doi.org/10.1016/j.celrep.2024.114870

Milner, B. (1963). Effects of Different Brain Lesions on Card Sorting: The Role of the Frontal Lobes. *Archives of Neurology*, *9*(1), 90–100. https://doi.org/10.1001/archneur.1963.00460070100010

Mišić, B., Betzel, R. F., de Reus, M. A., van den Heuvel, M. P., Berman, M. G., McIntosh, A. R., & Sporns, O. (2016). Network-Level Structure-Function Relationships in Human Neocortex. *Cerebral Cortex*, *26*(7), 3285–3296. https://doi.org/10.1093/cercor/bhw089

Mitchell-Heggs, R., Prado, S., Gava, G. P., Go, M. A., & Schultz, S. R. (2023). Neural manifold analysis of brain circuit dynamics in health and disease. *Journal of Computational Neuroscience*, *51*(1), 1–21. https://doi.org/10.1007/s10827-022-00839-3

Moehlmann, T., Winkler, E., Xia, X., Edbauer, D., Murrell, J., Capell, A., Kaether, C., Zheng, H., Ghetti, B., Haass, C., & Steiner, H. (2002). Presenilin-1 mutations of leucine 166 equally affect the generation of the Notch and APP intracellular domains independent of their effect on Aβ42 production. *Proceedings of the National Academy of Sciences*, *99*(12), 8025–8030. https://doi.org/10.1073/pnas.112686799

Monsell, S. E., Mock, C., Roe, C. M., Ghoshal, N., Morris, J. C., Cairns, N. J., & Kukull, W. (2013). Comparison of symptomatic and asymptomatic persons with Alzheimer disease neuropathology. *Neurology*, *80*(23), 2121–2129. https://doi.org/10.1212/WNL.0b013e318295d7a1

Morales, G. B., Santo, S. D., & Munoz, M. A. (2022). *Quasi-universal scaling in mouse-brain neuronal activity stems from edge-of-instability critical dynamics* (arXiv:2111.12067). arXiv. https://doi.org/10.48550/arXiv.2111.12067

Moretti, D. V., Fracassi, C., Pievani, M., Geroldi, C., Binetti, G., Zanetti, O., Sosta, K., Rossini, P. M., & Frisoni, G. B. (2009). Increase of theta/gamma ratio is associated with memory impairment. *Clinical Neurophysiology*, *120*(2), 295–303. https://doi.org/10.1016/j.clinph.2008.11.012

Morley, J. E., Farr, S. A., Banks, W. A., Johnson, S. N., Yamada, K. A., & Xu, L. (2010). A physiological role for amyloid-beta protein:enhancement of learning and memory. *Journal of Alzheimer's Disease: JAD*, *19*(2), 441–449. https://doi.org/10.3233/JAD-2009-1230

Morris, J. C. (1993). The Clinical Dementia Rating (CDR). *Neurology*, *43*(11), 2412-2412-a. https://doi.org/10.1212/WNL.43.11.2412-a

Morris, R. G. M. (1981). Spatial localization does not require the presence of local cues. *Learning and Motivation*, *12*(2), 239–260. https://doi.org/10.1016/0023-9690(81)90020-5

Morris, R. G. M., Garrud, P., Rawlins, J. N. P., & O'Keefe, J. (1982). Place navigation impaired in rats with hippocampal lesions. *Nature*, *297*(5868), 681–683. https://doi.org/10.1038/297681a0

Morris, R. G. M., Schenk, F., Tweedie, F., & Jarrard, L. E. (1990). Ibotenate Lesions of Hippocampus and/or Subiculum: Dissociating Components of Allocentric Spatial Learning. *European Journal of Neuroscience*, *2*(12), 1016–1028. https://doi.org/10.1111/j.1460-9568.1990.tb00014.x

Mosconi, L., Berti, V., Dyke, J., Schelbaum, E., Jett, S., Loughlin, L., Jang, G., Rahman, A., Hristov, H., Pahlajani, S., Andrews, R., Matthews, D., Etingin, O., Ganzer, C., de Leon, M., Isaacson, R., & Brinton, R. D. (2021). Menopause impacts human brain structure, connectivity, energy metabolism, and amyloid-beta deposition. *Scientific Reports*, *11*(1), 10867. https://doi.org/10.1038/s41598-021-90084-y

Mucke, L., Masliah, E., Yu, G.-Q., Mallory, M., Rockenstein, E. M., Tatsuno, G., Hu, K., Kholodenko, D., Johnson-Wood, K., & McConlogue, L. (2000). High-Level Neuronal Expression of Aβ1–42 in Wild-Type Human Amyloid Protein Precursor Transgenic Mice: Synaptotoxicity without Plaque Formation. *Journal of Neuroscience*, *20*(11), 4050–4058. https://doi.org/10.1523/JNEUROSCI.20-11-04050.2000

Müller, R., Heinrich, M., Heck, S., Blohm, D., & Richter-Landsberg, C. (1997). Expression of microtubule-associated proteins MAP2 and tau in cultured rat brain oligodendrocytes. *Cell and Tissue Research*, *288*(2), 239–249. https://doi.org/10.1007/s004410050809

Mumby, D. G., Gaskin, S., Glenn, M. J., Schramek, T. E., & Lehmann, H. (2002). Hippocampal Damage and Exploratory Preferences in Rats: Memory for Objects,

Places, and Contexts. *Learning & Memory*, *9*(2), 49–57. https://doi.org/10.1101/lm.41302

Munn, B. R., Müller, E. J., & Shine, J. M. (2023). *Noradrenergic neuromodulation of nonlinear bursting neurons controls critical dynamics* (arXiv:2106.07865). arXiv. https://doi.org/10.48550/arXiv.2106.07865

Murdock, M. H., Yang, C.-Y., Sun, N., Pao, P.-C., Blanco-Duque, C., Kahn, M. C., Kim, T., Lavoie, N. S., Victor, M. B., Islam, M. R., Galiana, F., Leary, N., Wang, S., Bubnys, A., Ma, E., Akay, L. A., Sneve, M., Qian, Y., Lai, C., … Tsai, L.-H. (2024). Multisensory gamma stimulation promotes glymphatic clearance of amyloid. *Nature*. https://doi.org/10.1038/s41586-024-07132-6

Murrell, J., Farlow, M., Ghetti, B., & Benson, M. D. (1991). A mutation in the Amyloid Precursor Protein Associated with Hereditary Alzheimer's Disease. *Science*, *254*(5028), 97–99. https://doi.org/10.1126/science.1925564

N

Nakayama, K., Ohkawara, T., Hiratochi, M., Koh, C.-S., & Nagase, H. (2008). The intracellular domain of amyloid precursor protein induces neuron-specific apoptosis. *Neuroscience Letters*, *444*(2), 127–131. https://doi.org/10.1016/j.neulet.2008.08.034

Nasrabady, S. E., Rizvi, B., Goldman, J. E., & Brickman, A. M. (2018). White matter changes in Alzheimer's disease: A focus on myelin and oligodendrocytes. *Acta Neuropathologica Communications*, *6*(1), 22. https://doi.org/10.1186/s40478-018-0515-3

Nawaz, A. D., Haider, M. Z., & Akhtar, S. (2024). COVID-19 and Alzheimer's disease: Impact of lockdown and other restrictive measures during the COVID-19 pandemic. *Biomolecules and Biomedicine*, *24*(2), Article 2. https://doi.org/10.17305/bb.2023.9680

Negash, S., Xie, S., Davatzikos, C., Clark, C. M., Trojanowski, J. Q., Shaw, L. M., Wolk, D. A., & Arnold, S. E. (2013). Cognitive and functional resilience despite molecular

evidence of Alzheimer's disease pathology. *Alzheimer's & Dementia*, *9*(3), e89–e95. https://doi.org/10.1016/j.jalz.2012.01.009

Nilsson, M., Perfilieva, E., Johansson, U., Orwar, O., & Eriksson, P. S. (1999). Enriched environment increases neurogenesis in the adult rat dentate gyrus and improves spatial memory. *Journal of Neurobiology*, *39*(4), 569–578. https://doi.org/10.1002/(SICI)1097-4695(19990615)39:4<569::AID-NEU10>3.0.CO;2-F

Núñez, P., Poza, J., Gómez, C., Rodríguez-González, V., Hillebrand, A., Tewarie, P., Tola-Arribas, M. Á., Cano, M., & Hornero, R. (2021). Abnormal meta-state activation of dynamic brain networks across the Alzheimer spectrum. *NeuroImage*, *232*, 117898. https://doi.org/10.1016/j.neuroimage.2021.117898

O

Oakley, H., Cole, S. L., Logan, S., Maus, E., Shao, P., Craft, J., Guillozet-Bongaarts, A., Ohno, M., Disterhoft, J., Eldik, L. V., Berry, R., & Vassar, R. (2006). Intraneuronal β-Amyloid Aggregates, Neurodegeneration, and Neuron Loss in Transgenic Mice with Five Familial Alzheimer's Disease Mutations: Potential Factors in Amyloid Plaque Formation. *Journal of Neuroscience*, *26*(40), 10129–10140. https://doi.org/10.1523/JNEUROSCI.1202-06.2006

Obregon, D., Hou, H., Deng, J., Giunta, B., Tian, J., Darlington, D., Shahaduzzaman, M., Zhu, Y., Mori, T., Mattson, M. P., & Tan, J. (2012). Soluble amyloid precursor protein-α modulates β-secretase activity and amyloid-β generation. *Nature Communications*, *3*(1), 777. https://doi.org/10.1038/ncomms1781

O'Byrne, J., & Jerbi, K. (2022). How critical is brain criticality? *Trends in Neurosciences*, *45*(11), 820–837. https://doi.org/10.1016/j.tins.2022.08.007

Oddo, S., Caccamo, A., Shepherd, J. D., Murphy, M. P., Golde, T. E., Kayed, R., Metherate, R., Mattson, M. P., Akbari, Y., & LaFerla, F. M. (2003). Triple-Transgenic Model of Alzheimer's Disease with Plaques and Tangles: Intracellular Aβ and Synaptic

Dysfunction. *Neuron*, *39*(3), 409–421. https://doi.org/10.1016/S0896-6273(03)00434-3

Ohsawa, I., Takamura, C., Morimoto, T., Ishiguro, M., & Kohsaka, S. (1999). Amino-terminal region of secreted form of amyloid precursor protein stimulates proliferation of neural stem cells. *European Journal of Neuroscience*, *11*(6), 1907–1913. https://doi.org/10.1046/j.1460-9568.1999.00601.x

O'Keefe, J., & Dostrovsky, J. (1971). The hippocampus as a spatial map. Preliminary evidence from unit activity in the freely-moving rat. *Brain Research*, *34*(1), 171–175. https://doi.org/10.1016/0006-8993(71)90358-1

Ouimet, C. C., Baerwald, K. D., Gandy, S. E., & Greengard, P. (1994). Immunocytochemical localization of amyloid precursor protein in rat brain. *Journal of Comparative Neurology*, *348*(2), 244–260. https://doi.org/10.1002/cne.903480207

P

Palm, G. (1982). From Neural Dynamics to Cell Assemblies. In G. Palm (Ed.), *Neural Assemblies* (Vol. 7, pp. 104–116). Springer Berlin Heidelberg. https://doi.org/10.1007/978-3-642-81792-2_12

Palm, G. (1987). Computing with Neural Networks. *Science*, *235*(4793), 1227–1228. https://doi.org/10.1126/science.235.4793.1227-b

Palmigiano, A., Geisel, T., Wolf, F., & Battaglia, D. (2017). Flexible information routing by transient synchrony. *Nature Neuroscience*, *20*(7), 1014–1022. https://doi.org/10.1038/nn.4569

Palmqvist, S., Schöll, M., Strandberg, O., Mattsson, N., Stomrud, E., Zetterberg, H., Blennow, K., Landau, S., Jagust, W., & Hansson, O. (2017). Earliest accumulation of β-amyloid occurs within the default-mode network and concurrently affects brain connectivity. *Nature Communications*, *8*(1), 1214. https://doi.org/10.1038/s41467-017-01150-x

Palop, J. J., Chin, J., Roberson, E. D., Wang, J., Thwin, M. T., Bien-Ly, N., Yoo, J., Ho, K. O., Yu, G.-Q., Kreitzer, A., Finkbeiner, S., Noebels, J. L., & Mucke, L. (2007). Aberrant Excitatory Neuronal Activity and Compensatory Remodeling of Inhibitory Hippocampal Circuits in Mouse Models of Alzheimer's Disease. *Neuron*, *55*(5), 697–711. https://doi.org/10.1016/j.neuron.2007.07.025

Papasozomenos, S. Ch., & Binder, L. I. (1987). Phosphorylation determines two distinct species of tau in the central nervous system. *Cell Motility*, *8*(3), 210–226. https://doi.org/10.1002/cm.970080303

Park, H.-J., & Friston, K. (2013). Structural and Functional Brain Networks: From Connections to Cognition. *Science*, *342*(6158), 1238411. https://doi.org/10.1126/science.1238411

Park, Y., Lee, K., Park, J., Bae, J. B., Kim, S.-S., Kim, D.-W., Woo, S. J., Yoo, S., & Kim, K. W. (2022). Optimal flickering light stimulation for entraining gamma rhythms in older adults. *Scientific Reports*, *12*(1), 15550. https://doi.org/10.1038/s41598-022-19464-2

Pascual-Marqui, R. D., Lehmann, D., Faber, P., Milz, P., Kochi, K., Yoshimura, M., Nishida, K., Isotani, T., & Kinoshita, T. (2014). *The resting microstate networks (RMN): Cortical distributions, dynamics, and frequency specific information flow* (arXiv:1411.1949). arXiv. https://doi.org/10.48550/arXiv.1411.1949

Paulson, A. L., Zhang, L., Prichard, A. M., & Singer, A. C. (2024). *40 Hz sensory stimulation enhances CA3-CA1 coordination and prospective coding during navigation in a mouse model of Alzheimer's disease* (p. 2024.10.23.619408). bioRxiv. https://doi.org/10.1101/2024.10.23.619408

Pauwels, K., Williams, T. L., Morris, K. L., Jonckheere, W., Vandersteen, A., Kelly, G., Schymkowitz, J., Rousseau, F., Pastore, A., Serpell, L. C., & Broersen, K. (2012). Structural Basis for Increased Toxicity of Pathological Aβ42:Aβ40 Ratios in Alzheimer Disease *. *Journal of Biological Chemistry*, *287*(8), 5650–5660. https://doi.org/10.1074/jbc.M111.264473

Pedreschi, N., Trebuchon, A., Barrat, A., & Battaglia, D. (2024). *States of functional connectivity flow and their multiplex dynamics in human epilepsy and postictal aphasia* (p. 2024.05.10.593507). bioRxiv. https://doi.org/10.1101/2024.05.10.593507

Peña-Casanova, J., Sánchez-Benavides, G., de Sola, S., Manero-Borrás, R. M., & Casals-Coll, M. (2012). Neuropsychology of Alzheimer's Disease. *Archives of Medical Research*, *43*(8), 686–693. https://doi.org/10.1016/j.arcmed.2012.08.015

Perez, D. M. (2020). A1-Adrenergic Receptors in Neurotransmission, Synaptic Plasticity, and Cognition. *Frontiers in Pharmacology*, *11*. https://doi.org/10.3389/fphar.2020.581098

Perez-Cruz, C., & Rodriguez-Callejas, J. de D. (2023). The common marmoset as a model of neurodegeneration. *Trends in Neurosciences*, *46*(5), 394–409. https://doi.org/10.1016/j.tins.2023.02.002

Petermann, T., Thiagarajan, T. C., Lebedev, M. A., Nicolelis, M. A. L., Chialvo, D. R., & Plenz, D. (2009). Spontaneous cortical activity in awake monkeys composed of neuronal avalanches. *Proceedings of the National Academy of Sciences*, *106*(37), 15921–15926. https://doi.org/10.1073/pnas.0904089106

Peters, J. M., Hummel, T., Kratzsch, T., Lötsch, J., Skarke, C., & Frölich, L. (2003). Olfactory Function in Mild Cognitive Impairment and Alzheimer's Disease: An Investigation Using Psychophysical and Electrophysiological Techniques. *American Journal of Psychiatry*, *160*(11), 1995–2002. https://doi.org/10.1176/appi.ajp.160.11.1995

Peters, M. E., Rosenberg, P. B., Steinberg, M., Norton, M. C., Welsh-Bohmer, K. A., Hayden, K. M., Breitner, J., Tschanz, J. T., & Lyketsos, C. G. (2013). Neuropsychiatric Symptoms as Risk Factors for Progression From CIND to Dementia: The Cache County Study. *The American Journal of Geriatric Psychiatry*, *21*(11), 1116–1124. https://doi.org/10.1016/j.jagp.2013.01.049

Petersen, R. C., Doody, R., Kurz, A., Mohs, R. C., Morris, J. C., Rabins, P. V., Ritchie, K., Rossor, M., Thal, L., & Winblad, B. (2001). Current Concepts in Mild Cognitive

Impairment. *Archives of Neurology*, *58*(12), 1985–1992. https://doi.org/10.1001/archneur.58.12.1985

Peters-Libeu, C., Campagna, J., Mitsumori, M., Poksay, K. S., Spilman, P., Sabogal, A., Bredesen, D. E., & John, V. (2015). sAβPP α is a Potent Endogenous Inhibitor of BACE1. *Journal of Alzheimer's Disease*, *47*(3), 545–555. https://doi.org/10.3233/JAD-150282

Petrosini, L., De Bartolo, P., Foti, F., Gelfo, F., Cutuli, D., Leggio, M. G., & Mandolesi, L. (2009). On whether the environmental enrichment may provide cognitive and brain reserves. *Brain Research Reviews*, *61*(2), 221–239. https://doi.org/10.1016/j.brainresrev.2009.07.002

Picciotto, M. R., Higley, M. J., & Mineur, Y. S. (2012). Acetylcholine as a Neuromodulator: Cholinergic Signaling Shapes Nervous System Function and Behavior. *Neuron*, *76*(1), 116–129. https://doi.org/10.1016/j.neuron.2012.08.036

Piller, C. (2022). *Potential fabrication in research images threatens key theory of Alzheimer's disease* [Dataset]. https://doi.org/10.1126/science.ade0209

Plassman, B. L., Havlik, R. J., Steffens, D. C., Helms, M. J., Newman, T. N., Drosdick, D., Phillips, C., Gau, B. A., Welsh–Bohmer, K. A., Burke, J. R., Guralnik, J. M., & Breitner, J. C. S. (2000). Documented head injury in early adulthood and risk of Alzheimer's disease and other dementias. *Neurology*, *55*(8), 1158–1166. https://doi.org/10.1212/WNL.55.8.1158

Poil, S.-S., Hardstone, R., Mansvelder, H. D., & Linkenkaer-Hansen, K. (2012). Critical-State Dynamics of Avalanches and Oscillations Jointly Emerge from Balanced Excitation/Inhibition in Neuronal Networks. *Journal of Neuroscience*, *32*(29), 9817–9823. https://doi.org/10.1523/JNEUROSCI.5990-11.2012

Preston, A. R., & Eichenbaum, H. (2013). Interplay of Hippocampus and Prefrontal Cortex in Memory. *Current Biology*, *23*(17), R764–R773. https://doi.org/10.1016/j.cub.2013.05.041

R

Radde, R., Bolmont, T., Kaeser, S. A., Coomaraswamy, J., Lindau, D., Stoltze, L., Calhoun, M. E., Jäggi, F., Wolburg, H., Gengler, S., Haass, C., Ghetti, B., Czech, C., Hölscher, C., Mathews, P. M., & Jucker, M. (2006). Aβ42-driven cerebral amyloidosis in transgenic mice reveals early and robust pathology. *EMBO Reports*, *7*(9), 940–946. https://doi.org/10.1038/sj.embor.7400784

Rajput, A. H., Uitti, R. J., Sudhakar, S., & Rozdilsky, B. (1989). Parkinsonism and neurofibrillary tangle pathology in pigmented nuclei. *Annals of Neurology*, *25*(6), 602–606. https://doi.org/10.1002/ana.410250612

Ramani, A., Müller, L., Ostermann, P. N., Gabriel, E., Abida-Islam, P., Müller-Schiffmann, A., Mariappan, A., Goureau, O., Gruell, H., Walker, A., Andrée, M., Hauka, S., Houwaart, T., Dilthey, A., Wohlgemuth, K., Omran, H., Klein, F., Wieczorek, D., Adams, O., … Gopalakrishnan, J. (2020). SARS-CoV-2 targets neurons of 3D human brain organoids. *The EMBO Journal*, *39*(20), e106230. https://doi.org/10.15252/embj.2020106230

Ramaroson, H., Helmer, C., Barberger-Gateau, P., Letenneur, L., Dartigues, J.-F., & PAQUID. (2003). [Prevalence of dementia and Alzheimer's disease among subjects aged 75 years or over: Updated results of the PAQUID cohort]. *Revue Neurologique*, *159*(4), 405—411.

Reisberg, B., Shulman, M. B., Torossian, C., Leng, L., & Zhu, W. (2010). Outcome over seven years of healthy adults with and without subjective cognitive impairment. *Alzheimer's & Dementia*, *6*(1), 11–24. https://doi.org/10.1016/j.jalz.2009.10.002

Reitz, C., Brayne, C., & Mayeux, R. (2011). Epidemiology of Alzheimer disease. *Nature Reviews Neurology*, *7*(3), 137–152. https://doi.org/10.1038/nrneurol.2011.2

Rodrigues-Amorim, D., Bozzelli, P. L., Kim, T., Liu, L., Gibson, O., Yang, C.-Y., Murdock, M. H., Galiana-Melendez, F., Schatz, B., Davison, A., Islam, M. R., Shin Park, D., Raju, R. M., Abdurrob, F., Nelson, A. J., Min Ren, J., Yang, V., Stokes, M. P., & Tsai, L.-H. (2024). Multisensory gamma stimulation mitigates the effects of demyelination

induced by cuprizone in male mice. *Nature Communications*, *15*(1), 6744. https://doi.org/10.1038/s41467-024-51003-7

Rönnlund, M., Sundström, A., Adolfsson, R., & Nilsson, L.-G. (2015). Subjective memory impairment in older adults predicts future dementia independent of baseline memory performance: Evidence from the Betula prospective cohort study. *Alzheimer's & Dementia: The Journal of the Alzheimer's Association*, *11*(11), 1385–1392. https://doi.org/10.1016/j.jalz.2014.11.006

Rosenberg, P. B., Mielke, M. M., Appleby, B. S., Oh, E. S., Geda, Y. E., & Lyketsos, C. G. (2013). The Association of Neuropsychiatric Symptoms in MCI with Incident Dementia and Alzheimer Disease. *The American Journal of Geriatric Psychiatry*, *21*(7), 685–695. https://doi.org/10.1016/j.jagp.2013.01.006

Rossetti, Z. L., & Carboni, S. (2005). Noradrenaline and Dopamine Elevations in the Rat Prefrontal Cortex in Spatial Working Memory. *Journal of Neuroscience*, *25*(9), 2322–2329. https://doi.org/10.1523/JNEUROSCI.3038-04.2005

Rowe, C. C., Ellis, K. A., Rimajova, M., Bourgeat, P., Pike, K. E., Jones, G., Fripp, J., Tochon-Danguy, H., Morandeau, L., O'Keefe, G., Price, R., Raniga, P., Robins, P., Acosta, O., Lenzo, N., Szoeke, C., Salvado, O., Head, R., Martins, R., … Villemagne, V. L. (2010). Amyloid imaging results from the Australian Imaging, Biomarkers and Lifestyle (AIBL) study of aging. *Neurobiology of Aging*, *31*(8), 1275–1283. https://doi.org/10.1016/j.neurobiolaging.2010.04.007

Royston, M. C., Mann, D., Pickering-Brown, S., Owen, F., Perry, R., Raghavan, R., Khin-Nu, C., Tyrer, S., Day, K., & Crook, R. (1994). Apolipoprotein E epsilon 2 allele promotes longevity and protects patients with Down's syndrome from dementia. *Neuroreport*, *5*(18), 2583–2585. https://doi.org/10.1097/00001756-199412000-00044

Rusanen, M., Kivipelto, M., Quesenberry, C. P., Zhou, J., & Whitmer, R. A. (2011). Heavy smoking in midlife and long-term risk of Alzheimer disease and vascular dementia. *Archives of Internal Medicine*, *171*(4), 333–339. https://doi.org/10.1001/archinternmed.2010.393

S

Sabbagh, M. N., Lue, L.-F., Fayard, D., & Shi, J. (2017). Increasing Precision of Clinical Diagnosis of Alzheimer's Disease Using a Combined Algorithm Incorporating Clinical and Novel Biomarker Data. *Neurology and Therapy*, *6*(1), 83–95. https://doi.org/10.1007/s40120-017-0069-5

Saeed, A., Lopez, O., Cohen, A., & Reis, S. E. (2023). Cardiovascular Disease and Alzheimer's Disease: The Heart–Brain Axis. *Journal of the American Heart Association*, *12*(21), e030780. https://doi.org/10.1161/JAHA.123.030780

Saito, T., Matsuba, Y., Mihira, N., Takano, J., Nilsson, P., Itohara, S., Iwata, N., & Saido, T. C. (2014). Single App knock-in mouse models of Alzheimer's disease. *Nature Neuroscience*, *17*(5), 661–663. https://doi.org/10.1038/nn.3697

Saito, T., Mihira, N., Matsuba, Y., Sasaguri, H., Hashimoto, S., Narasimhan, S., Zhang, B., Murayama, S., Higuchi, M., Lee, V. M. Y., Trojanowski, J. Q., & Saido, T. C. (2019). Humanization of the entire murine Mapt gene provides a murine model of pathological human tau propagation. *Journal of Biological Chemistry*, *294*(34), 12754–12765. https://doi.org/10.1074/jbc.RA119.009487

Sakakibara, Y., Hirota, Y., Ibaraki, K., Takei, K., Chikamatsu, S., Tsubokawa, Y., Saito, T., Saido, T. C., Sekiya, M., & Iijima, K. M. (2021). Widespread Reduced Density of Noradrenergic Locus Coeruleus Axons in the App Knock-In Mouse Model of Amyloid-β Amyloidosis. *Journal of Alzheimer's Disease*, *82*(4), 1513. https://doi.org/10.3233/JAD-210385

Sakakibara, Y., Sekiya, M., Saito, T., Saido, T. C., & Iijima, K. M. (2018). Cognitive and emotional alterations in App knock-in mouse models of Aβ amyloidosis. *BMC Neuroscience*, *19*(1), 46. https://doi.org/10.1186/s12868-018-0446-8

Sakono, M., & Zako, T. (2010). Amyloid oligomers: Formation and toxicity of Aβ oligomers. *The FEBS Journal*, *277*(6), 1348–1358. https://doi.org/10.1111/j.1742-4658.2010.07568.x

Salbaum, J. M., & Ruddle, F. H. (1994). Embryonic expression pattern of amyloid protein precursor suggests a role in differentiation of specific subsets of neurons. *Journal of Experimental Zoology*, *269*(2), 116–127. https://doi.org/10.1002/jez.1402690205

Sanz Perl, Y., Bocaccio, H., Pallavicini, C., Pérez-Ipiña, I., Laureys, S., Laufs, H., Kringelbach, M., Deco, G., & Tagliazucchi, E. (2021). Nonequilibrium brain dynamics as a signature of consciousness. *Physical Review E*, *104*(1), 014411. https://doi.org/10.1103/PhysRevE.104.014411

Sara, S. J., & Bouret, S. (2012). Orienting and Reorienting: The Locus Coeruleus Mediates Cognition through Arousal. *Neuron*, *76*(1), 130–141. https://doi.org/10.1016/j.neuron.2012.09.011

Sarasso, S., Boly, M., Napolitani, M., Gosseries, O., Charland-Verville, V., Casarotto, S., Rosanova, M., Casali, A. G., Brichant, J.-F., Boveroux, P., Rex, S., Tononi, G., Laureys, S., & Massimini, M. (2015). Consciousness and Complexity during Unresponsiveness Induced by Propofol, Xenon, and Ketamine. *Current Biology*, *25*(23), 3099–3105. https://doi.org/10.1016/j.cub.2015.10.014

Sarfati, R., Hayes, J. C., & Peleg, O. (2021). Self-organization in natural swarms of Photinus carolinus synchronous fireflies. *Science Advances*, *7*(28), eabg9259. https://doi.org/10.1126/sciadv.abg9259

Scheuner, D., Eckman, C., Jensen, M., Song, X., Citron, M., Suzuki, N., Bird, T. D., Hardy, J., Hutton, M., Kukull, W., Larson, E., Levy-Lahad, L., Viitanen, M., Peskind, E., Poorkaj, P., Schellenberg, G., Tanzi, R., Wasco, W., Lannfelt, L., … Younkin, S. (1996). Secreted amyloid β–protein similar to that in the senile plaques of Alzheimer's disease is increased in vivo by the presenilin 1 and 2 and APP mutations linked to familial Alzheimer's disease. *Nature Medicine*, *2*(8), 864–870. https://doi.org/10.1038/nm0896-864

Schneider, M., Tzanou, A., Uran, C., & Vinck, M. (2023). Cell-type-specific propagation of visual flicker. *Cell Reports*, *42*(5), 112492. https://doi.org/10.1016/j.celrep.2023.112492

Schomburg, E. W., Fernández-Ruiz, A., Mizuseki, K., Berényi, A., Anastassiou, C. A., Koch, C., & Buzsáki, G. (2014). Theta Phase Segregation of Input-Specific Gamma Patterns in Entorhinal-Hippocampal Networks. *Neuron*, *84*(2), 470–485. https://doi.org/10.1016/j.neuron.2014.08.051

Schrödinger, E. (1929). Die Erfassung der Quantengesetze durch kontinuierliche Funktionen. *Die Naturwissenschaften*, *17*(26), 486–489. https://doi.org/10.1007/BF01505681

Schumacher, J., Peraza, L. R., Firbank, M., Thomas, A. J., Kaiser, M., Gallagher, P., O'Brien, J. T., Blamire, A. M., & Taylor, J.-P. (2019). Dynamic functional connectivity changes in dementia with Lewy bodies and Alzheimer's disease. *NeuroImage: Clinical*, *22*, 101812. https://doi.org/10.1016/j.nicl.2019.101812

Seif, A., Hafezi, M., & Jarzynski, C. (2021). Machine learning the thermodynamic arrow of time. *Nature Physics*, *17*(1), 105–113. https://doi.org/10.1038/s41567-020-1018-2

Selkoe, D. J., & Hardy, J. (2016). The amyloid hypothesis of Alzheimer's disease at 25 years. *EMBO Molecular Medicine*, *8*(6), 595–608. https://doi.org/10.15252/emmm.201606210

Senkowski, D., & Engel, A. K. (2024). Multi-timescale neural dynamics for multisensory integration. *Nature Reviews Neuroscience*, *25*(9), 625–642. https://doi.org/10.1038/s41583-024-00845-7

Shankar, G. M., Bloodgood, B. L., Townsend, M., Walsh, D. M., Selkoe, D. J., & Sabatini, B. L. (2007). Natural Oligomers of the Alzheimer Amyloid-β Protein Induce Reversible Synapse Loss by Modulating an NMDA-Type Glutamate Receptor-Dependent Signaling Pathway. *Journal of Neuroscience*, *27*(11), 2866–2875. https://doi.org/10.1523/JNEUROSCI.4970-06.2007

Shen, Q., Wu, X., Zhang, Z., Zhang, D., Yang, S., & Xing, D. (2022). Gamma frequency light flicker regulates amyloid precursor protein trafficking for reducing β-amyloid load in Alzheimer's disease model. *Aging Cell*, *21*(3), e13573. https://doi.org/10.1111/acel.13573

Sherrington, R., Rogaev, E. I., Liang, Y., Rogaeva, E. A., Levesque, G., Ikeda, M., Chi, H., Lin, C., Li, G., Holman, K., Tsuda, T., Mar, L., Foncin, J.-F., Bruni, A. C., Montesi, M. P., Sorbi, S., Rainero, I., Pinessi, L., Nee, L., … St George-Hyslop, P. H. (1995). Cloning of a gene bearing missense mutations in early-onset familial Alzheimer's disease. *Nature*, *375*(6534), 754–760. https://doi.org/10.1038/375754a0

Shew, W. L., & Plenz, D. (2013). The functional benefits of criticality in the cortex. *The Neuroscientist : A Review Journal Bringing Neurobiology, Neurology and Psychiatry*, *19*(1), 88–100. https://doi.org/10.1177/1073858412445487

Singer, A. C., Martorell, A. J., Douglas, J. M., Abdurrob, F., Attokaren, M. K., Tipton, J., Mathys, H., Adaikkan, C., & Tsai, L.-H. (2018). Noninvasive 40-Hz light flicker to recruit microglia and reduce amyloid beta load. *Nature Protocols*, *13*(8), 1850–1868. https://doi.org/10.1038/s41596-018-0021-x

Siok, C. J., Rogers, J. A., Kocsis, B., & Hajós, M. (2006). Activation of α7 acetylcholine receptors augments stimulation-induced hippocampal theta oscillation. *European Journal of Neuroscience*, *23*(2), 570–574. https://doi.org/10.1111/j.1460-9568.2005.04560.x

Sirota, A., Csicsvari, J., Buhl, D., & Buzsáki, G. (2003). Communication between neocortex and hippocampus during sleep in rodents. *Proceedings of the National Academy of Sciences*, *100*(4), 2065–2069. https://doi.org/10.1073/pnas.0437938100

Sivanandam, T. M., & Thakur, M. K. (2012). Traumatic brain injury: A risk factor for Alzheimer's disease. *Neuroscience & Biobehavioral Reviews*, *36*(5), 1376–1381. https://doi.org/10.1016/j.neubiorev.2012.02.013

Smith, J. B., Lee, A. K., & Jackson, J. (2020). The claustrum. *Current Biology*, *30*(23), R1401–R1406. https://doi.org/10.1016/j.cub.2020.09.069

Smith, M. A., Sayre, L. M., Monnier, V. M., & Perry, G. (1995). Radical AGEing in Alzheimer's disease. *Trends in Neurosciences*, *18*(4), 172–176. https://doi.org/10.1016/0166-2236(95)93897-7

Soto, C. (2003). Unfolding the role of protein misfolding in neurodegenerative diseases. *Nature Reviews Neuroscience*, *4*(1), 49–60. https://doi.org/10.1038/nrn1007

Soula, M., Martín-Ávila, A., Zhang, Y., Dhingra, A., Nitzan, N., Sadowski, M. J., Gan, W.-B., & Buzsáki, G. (2023). Forty-hertz light stimulation does not entrain native gamma oscillations in Alzheimer's disease model mice. *Nature Neuroscience*, *26*(4), 570–578. https://doi.org/10.1038/s41593-023-01270-2

Squire, L. R., Wixted, J. T., & Clark, R. E. (2007). Recognition memory and the medial temporal lobe: A new perspective. *Nature Reviews Neuroscience*, *8*(11), 872–883. https://doi.org/10.1038/nrn2154

Stam, C. J. (2005). Nonlinear dynamical analysis of EEG and MEG: Review of an emerging field. *Clinical Neurophysiology*, *116*(10), 2266–2301. https://doi.org/10.1016/j.clinph.2005.06.011

Steffen, J., Krohn, M., Paarmann, K., Schwitlick, C., Brüning, T., Marreiros, R., Müller-Schiffmann, A., Korth, C., Braun, K., & Pahnke, J. (2016). Revisiting rodent models: Octodon degus as Alzheimer's disease model? *Acta Neuropathologica Communications*, *4*(1), 91. https://doi.org/10.1186/s40478-016-0363-y

Steriade, M. (2006). Grouping of brain rhythms in corticothalamic systems. *Neuroscience*, *137*(4), 1087–1106. https://doi.org/10.1016/j.neuroscience.2005.10.029

Steriade, M., McCormick, D. A., & Sejnowski, T. J. (1993). Thalamocortical Oscillations in the Sleeping and Aroused Brain. *Science*, *262*(5134), 679–685. https://doi.org/10.1126/science.8235588

Stewart, S., Cacucci, F., & Lever, C. (2011). Which Memory Task for My Mouse? A Systematic Review of Spatial Memory Performance in the Tg2576 Alzheimer's Mouse Model. *Journal of Alzheimer's Disease*, *26*(1), 105–126. https://doi.org/10.3233/JAD-2011-101827

Stokes, M. G., Kusunoki, M., Sigala, N., Nili, H., Gaffan, D., & Duncan, J. (2013). Dynamic Coding for Cognitive Control in Prefrontal Cortex. *Neuron*, *78*(2), 364–375. https://doi.org/10.1016/j.neuron.2013.01.039

Strooper, B. D. (2014). Lessons from a Failed γ-Secretase Alzheimer Trial. *Cell*, *159*(4), 721–726. https://doi.org/10.1016/j.cell.2014.10.016

Stulz, S. B., Castro, S., Dumont, G., Gutkin, B., & Battaglia, D. (2024). *Compensating functional connectivity changes due to structural connectivity damage via modifications of local dynamics* (p. 2024.05.31.596792). bioRxiv. https://doi.org/10.1101/2024.05.31.596792

Suk, H.-J., Buie, N., Xu, G., Banerjee, A., Boyden, E. S., & Tsai, L.-H. (2023). Vibrotactile stimulation at gamma frequency mitigates pathology related to neurodegeneration and improves motor function. *Frontiers in Aging Neuroscience*, *15*. https://doi.org/10.3389/fnagi.2023.1129510

Szabo, A. B., Cattaud, V., Bezzina, C., Dard, R. F., Sayegh, F., Gauzin, S., Lejards, C., Valton, L., Rampon, C., Verret, L., & Dahan, L. (2023). Neuronal hyperexcitability in the Tg2576 mouse model of Alzheimer's disease – the influence of sleep and noradrenergic transmission. *Neurobiology of Aging*, *123*, 35–48. https://doi.org/10.1016/j.neurobiolaging.2022.11.017

Szczepanik, A. M., Rampe, D., & Ringheim, G. E. (2001). Amyloid-β peptide fragments p3 and p4 induce pro-inflammatory cytokine and chemokine production in vitro and in vivo. *Journal of Neurochemistry*, *77*(1), 304–317. https://doi.org/10.1046/j.1471-4159.2001.00240.x

T

Tagliazucchi, E., Balenzuela, P., Fraiman, D., & Chialvo, D. R. (2012). Criticality in Large-Scale Brain fMRI Dynamics Unveiled by a Novel Point Process Analysis. *Frontiers in Physiology*, *3*. https://doi.org/10.3389/fphys.2012.00015

Tait, L., Tamagnini, F., Stothart, G., Barvas, E., Monaldini, C., Frusciante, R., Volpini, M., Guttmann, S., Coulthard, E., Brown, J. T., Kazanina, N., & Goodfellow, M. (2020). EEG microstate complexity for aiding early diagnosis of Alzheimer's disease. *Scientific Reports*, *10*(1), 17627. https://doi.org/10.1038/s41598-020-74790-7

Tamura, M., Spellman, T. J., Rosen, A. M., Gogos, J. A., & Gordon, J. A. (2017). Hippocampal-prefrontal theta-gamma coupling during performance of a spatial working

memory task. *Nature Communications*, *8*(1), 2182. https://doi.org/10.1038/s41467-017-02108-9

Thal, D. R., Rüb, U., Orantes, M., & Braak, H. (2002). Phases of Aβ-deposition in the human brain and its relevance for the development of AD. *Neurology*, *58*(12), 1791–1800.

Theofilas, P., Ehrenberg, A. J., Dunlop, S., Di Lorenzo Alho, A. T., Nguy, A., Leite, R. E. P., Rodriguez, R. D., Mejia, M. B., Suemoto, C. K., Ferretti-Rebustini, R. E. D. L., Polichiso, L., Nascimento, C. F., Seeley, W. W., Nitrini, R., Pasqualucci, C. A., Jacob Filho, W., Rueb, U., Neuhaus, J., Heinsen, H., & Grinberg, L. T. (2017). Locus coeruleus volume and cell population changes during Alzheimer's disease progression: A stereological study in human postmortem brains with potential implication for early-stage biomarker discovery. *Alzheimer's & Dementia*, *13*(3), 236–246. https://doi.org/10.1016/j.jalz.2016.06.2362

Therriault, J., Pascoal, T. A., Lussier, F. Z., Tissot, C., Chamoun, M., Bezgin, G., Servaes, S., Benedet, A. L., Ashton, N. J., Karikari, T. K., Lantero-Rodriguez, J., Kunach, P., Wang, Y.-T., Fernandez-Arias, J., Massarweh, G., Vitali, P., Soucy, J.-P., Saha-Chaudhuri, P., Blennow, K., … Rosa-Neto, P. (2022). Biomarker modeling of Alzheimer's disease using PET-based Braak staging. *Nature Aging*, *2*(6), 526–535. https://doi.org/10.1038/s43587-022-00204-0

Tiesinga, P., & Sejnowski, T. J. (2009). Cortical Enlightenment: Are Attentional Gamma Oscillations Driven by ING or PING? *Neuron*, *63*(6), 727–732. https://doi.org/10.1016/j.neuron.2009.09.009

Toker, D., Pappas, I., Lendner, J. D., Frohlich, J., Mateos, D. M., Muthukumaraswamy, S., Carhart-Harris, R., Paff, M., Vespa, P. M., Monti, M. M., Sommer, F. T., Knight, R. T., & D'Esposito, M. (2022). Consciousness is supported by near-critical slow cortical electrodynamics. *Proceedings of the National Academy of Sciences*, *119*(7), e2024455119. https://doi.org/10.1073/pnas.2024455119

Tononi, G., & Cirelli, C. (2014). Sleep and the Price of Plasticity: From Synaptic and Cellular Homeostasis to Memory Consolidation and Integration. *Neuron*, *81*(1), 12–34. https://doi.org/10.1016/j.neuron.2013.12.025

Tononi, G., & Pompeiano, O. (1995). Pharmacology of the Cholinergic System. In A. Kales (Ed.), *The Pharmacology of Sleep* (pp. 143–210). Springer. https://doi.org/10.1007/978-3-642-57836-6_7

Tort, A. B. L., Komorowski, R., Eichenbaum, H., & Kopell, N. (2010). Measuring Phase-Amplitude Coupling Between Neuronal Oscillations of Different Frequencies. *Journal of Neurophysiology*, *104*(2), 1195–1210. https://doi.org/10.1152/jn.00106.2010

Tort, A. B. L., Kramer, M. A., Thorn, C., Gibson, D. J., Kubota, Y., Graybiel, A. M., & Kopell, N. J. (2008). Dynamic cross-frequency couplings of local field potential oscillations in rat striatum and hippocampus during performance of a T-maze task. *Proceedings of the National Academy of Sciences*, *105*(51), 20517–20522. https://doi.org/10.1073/pnas.0810524105

Toyoizumi, T., & Abbott, L. F. (2011). Beyond the edge of chaos: Amplification and temporal integration by recurrent networks in the chaotic regime. *Physical Review E*, *84*(5), 051908. https://doi.org/10.1103/PhysRevE.84.051908

Trapp, B. D., & Hauer, P. E. (1994). Amyloid precursor protein is enriched in radial glia: Implications for neuronal development. *Journal of Neuroscience Research*, *37*(4), 538–550. https://doi.org/10.1002/jnr.490370413

Tromp, D., Dufour, A., Lithfous, S., Pebayle, T., & Després, O. (2015). Episodic memory in normal aging and Alzheimer disease: Insights from imaging and behavioral studies. *Ageing Research Reviews*, *24*, 232–262. https://doi.org/10.1016/j.arr.2015.08.006

Tseng, B. P., Green, K. N., Chan, J. L., Blurton-Jones, M., & LaFerla, F. M. (2008). Aβ inhibits the proteasome and enhances amyloid and tau accumulation. *Neurobiology of Aging*, *29*(11), 1607–1618. https://doi.org/10.1016/j.neurobiolaging.2007.04.014

U

Ungerleider, L. G., Courtney, S. M., & Haxby, J. V. (1998). A neural system for human visual working memory. *Proceedings of the National Academy of Sciences*, *95*(3), 883–890. https://doi.org/10.1073/pnas.95.3.883

V

Valincius, G., Heinrich, F., Budvytyte, R., Vanderah, D. J., McGillivray, D. J., Sokolov, Y., Hall, J. E., & Lösche, M. (2008). Soluble Amyloid β-Oligomers Affect Dielectric Membrane Properties by Bilayer Insertion and Domain Formation: Implications for Cell Toxicity. *Biophysical Journal*, *95*(10), 4845–4861. https://doi.org/10.1529/biophysj.108.130997

Van Cauter, T., Camon, J., Alvernhe, A., Elduayen, C., Sargolini, F., & Save, E. (2013). Distinct Roles of Medial and Lateral Entorhinal Cortex in Spatial Cognition. *Cerebral Cortex*, *23*(2), 451–459. https://doi.org/10.1093/cercor/bhs033

Van De Ville, D., Britz, J., & Michel, C. M. (2010). EEG microstate sequences in healthy humans at rest reveal scale-free dynamics. *Proceedings of the National Academy of Sciences*, *107*(42), 18179–18184. https://doi.org/10.1073/pnas.1007841107

van der Hiele, K., Vein, A. A., Reijntjes, R. H. A. M., Westendorp, R. G. J., Bollen, E. L. E. M., van Buchem, M. A., van Dijk, J. G., & Middelkoop, H. A. M. (2007). EEG correlates in the spectrum of cognitive decline. *Clinical Neurophysiology*, *118*(9), 1931–1939. https://doi.org/10.1016/j.clinph.2007.05.070

Vanni, F., Luković, M., & Grigolini, P. (2011). Criticality and Transmission of Information in a Swarm of Cooperative Units. *Physical Review Letters*, *107*(7), 078103. https://doi.org/10.1103/PhysRevLett.107.078103

Vannimenus, J., & Toulouse, G. (1977). Theory of the frustration effect. II. Ising spins on a square lattice. *Journal of Physics C: Solid State Physics*, *10*(18), L537–L542. https://doi.org/10.1088/0022-3719/10/18/008

Vecchio, I., Sorrentino, L., Paoletti, A., Marra, R., & Arbitrio, M. (2021). The State of The Art on Acetylcholinesterase Inhibitors in the Treatment of Alzheimer's Disease. *Journal of Central Nervous System Disease*, *13*, 11795735211029113. https://doi.org/10.1177/11795735211029113

Verret, L., Mann, E. O., Hang, G. B., Barth, A. M. I., Cobos, I., Ho, K., Devidze, N., Masliah, E., Kreitzer, A. C., Mody, I., Mucke, L., & Palop, J. J. (2012). Inhibitory Interneuron Deficit Links Altered Network Activity and Cognitive Dysfunction in Alzheimer Model. *Cell*, *149*(3), 708–721. https://doi.org/10.1016/j.cell.2012.02.046

Vogel-Ciernia, A., & Wood, M. A. (2014). Examining Object Location and Object Recognition Memory in Mice. *Current Protocols in Neuroscience*, *69*(1). https://doi.org/10.1002/0471142301.ns0831s69

Vossel, K. A., Ranasinghe, K. G., Beagle, A. J., Mizuiri, D., Honma, S. M., Dowling, A. F., Darwish, S. M., Van Berlo, V., Barnes, D. E., Mantle, M., Karydas, A. M., Coppola, G., Roberson, E. D., Miller, B. L., Garcia, P. A., Kirsch, H. E., Mucke, L., & Nagarajan, S. S. (2016). Incidence and impact of subclinical epileptiform activity in Alzheimer's disease. *Annals of Neurology*, *80*(6), 858–870. https://doi.org/10.1002/ana.24794

Vyazovskiy, V. V., Olcese, U., Hanlon, E. C., Nir, Y., Cirelli, C., & Tononi, G. (2011). Local sleep in awake rats. *Nature*, *472*(7344), 443–447. https://doi.org/10.1038/nature10009

W

Wainrib, G., & Touboul, J. (2013). Topological and Dynamical Complexity of Random Neural Networks. *Physical Review Letters*, *110*(11), 118101. https://doi.org/10.1103/PhysRevLett.110.118101

Walker, J. M., Fowler, S. W., Miller, D. K., Sun, A. Y., Weisman, G. A., Wood, W. G., Sun, G. Y., Simonyi, A., & Schachtman, T. R. (2011). Spatial learning and memory impairment and increased locomotion in a transgenic amyloid precursor protein mouse model of Alzheimer's disease. *Behavioural Brain Research*, *222*(1), 169–175. https://doi.org/10.1016/j.bbr.2011.03.049

Walsh, D. M., Klyubin, I., Fadeeva, J. V., Cullen, W. K., Anwyl, R., Wolfe, M. S., Rowan, M. J., & Selkoe, D. J. (2002). Naturally secreted oligomers of amyloid β protein potently inhibit hippocampal long-term potentiation in vivo. *Nature*, *416*(6880), 535–539. https://doi.org/10.1038/416535a

Wan, H., Aggleton, J. P., & Brown, M. W. (1999). Different Contributions of the Hippocampus and Perirhinal Cortex to Recognition Memory. *Journal of Neuroscience*, *19*(3), 1142–1148. https://doi.org/10.1523/JNEUROSCI.19-03-01142.1999

Wang, C., Furlong, T. M., Stratton, P. G., Lee, C. C. Y., Xu, L., Merlin, S., Nolan, C., Arabzadeh, E., Marek, R., & Sah, P. (2021). Hippocampus–Prefrontal Coupling Regulates Recognition Memory for Novelty Discrimination. *Journal of Neuroscience*, *41*(46), 9617–9632. https://doi.org/10.1523/JNEUROSCI.1202-21.2021

Wang, L., Davis, P. B., Volkow, N. D., Berger, N. A., Kaelber, D. C., & Xu, R. (2022). Association of COVID-19 with New-Onset Alzheimer's Disease. *Journal of Alzheimer's Disease: JAD*, *89*(2), 411–414. https://doi.org/10.3233/JAD-220717

Wang, Q., Ng, L., Harris, J. A., Feng, D., Li, Y., Royall, J. J., Oh, S. W., Bernard, A., Sunkin, S. M., Koch, C., & Zeng, H. (2017). Organization of the connections between claustrum and cortex in the mouse. *Journal of Comparative Neurology*, *525*(6), 1317–1346. https://doi.org/10.1002/cne.24047

Wang, Q., Wang, Y., Kuo, H.-C., Xie, P., Kuang, X., Hirokawa, K. E., Naeemi, M., Yao, S., Mallory, M., Ouellette, B., Lesnar, P., Li, Y., Ye, M., Chen, C., Xiong, W., Ahmadinia, L., El-Hifnawi, L., Cetin, A., Sorensen, S. A., … Koch, C. (2023). Regional and cell-type-specific afferent and efferent projections of the mouse claustrum. *Cell Reports*, *42*(2). https://doi.org/10.1016/j.celrep.2023.112118

Wang, R., Wang, B., He, W., & Zheng, H. (2006). Wild-type Presenilin 1 Protects against Alzheimer Disease Mutation-induced Amyloid Pathology *. *Journal of Biological Chemistry*, *281*(22), 15330–15336. https://doi.org/10.1074/jbc.M512574200

Wang, T., Chen, Y., Zou, Y., Pang, Y., He, X., Chen, Y., Liu, Y., Feng, W., Zhang, Y., Li, Q., Shi, J., Ding, F., Marshall, C., Gao, J., & Xiao, M. (2022). Locomotor Hyperactivity in the Early-Stage Alzheimer's Disease-like Pathology of APP/PS1 Mice: Associated with Impaired Polarization of Astrocyte Aquaporin 4. *Aging and Disease*, *13*(5), 1504. https://doi.org/10.14336/AD.2022.0219

Wang, X., Huang, W., Su, L., Xing, Y., Jessen, F., Sun, Y., Shu, N., & Han, Y. (2020). Neuroimaging advances regarding subjective cognitive decline in preclinical Alzheimer's disease. *Molecular Neurodegeneration*, *15*(1), 55. https://doi.org/10.1186/s13024-020-00395-3

Wang, X.-J. (2010). Neurophysiological and Computational Principles of Cortical Rhythms in Cognition. *Physiological Reviews*, *90*(3), 1195–1268. https://doi.org/10.1152/physrev.00035.2008

Warburton, E. C., & Brown, M. W. (2015). Neural circuitry for rat recognition memory. *Behavioural Brain Research*, *285*, 131–139. https://doi.org/10.1016/j.bbr.2014.09.050

Watanabe, T., Hirose, S., Wada, H., Imai, Y., Machida, T., Shirouzu, I., Konishi, S., Miyashita, Y., & Masuda, N. (2014). Energy landscapes of resting-state brain networks. *Frontiers in Neuroinformatics*, *8*. https://doi.org/10.3389/fninf.2014.00012

Wei, W., Norton, D. D., Wang, X., & Kusiak, J. W. (2002). Aβ 17–42 in Alzheimer's disease activates JNK and caspase-8 leading to neuronal apoptosis. *Brain*, *125*(9), 2036–2043. https://doi.org/10.1093/brain/awf205

Willem, M., Tahirovic, S., Busche, M. A., Ovsepian, S. V., Chafai, M., Kootar, S., Hornburg, D., Evans, L. D. B., Moore, S., Daria, A., Hampel, H., Müller, V., Giudici, C., Nuscher, B., Wenninger-Weinzierl, A., Kremmer, E., Heneka, M. T., Thal, D. R., Giedraitis, V., … Haass, C. (2015). η-Secretase processing of APP inhibits neuronal activity in the hippocampus. *Nature*, *526*(7573), 443–447. https://doi.org/10.1038/nature14864

Williamson, J. D. (2023). SPRINT MIND: Implications of Recents Findings for New Trials Focused on ADRD Prevention Through Vascular Pathways. *Alzheimer's & Dementia*, *19*(S23), e079428. https://doi.org/10.1002/alz.079428

Wilson, D. I. G., Langston, R. F., Schlesiger, M. I., Wagner, M., Watanabe, S., & Ainge, J. A. (2013). Lateral entorhinal cortex is critical for novel object-context recognition. *Hippocampus*, *23*(5), 352–366. https://doi.org/10.1002/hipo.22095

Wilson, M. A., & McNaughton, B. L. (1994). Reactivation of Hippocampal Ensemble Memories During Sleep. *Science*, *265*(5172), 676–679. https://doi.org/10.1126/science.8036517

Wilson, R. S., Krueger, K. R., Arnold, S. E., Schneider, J. A., Kelly, J. F., Barnes, L. L., Tang, Y., & Bennett, D. A. (2007). Loneliness and Risk of Alzheimer Disease. *Archives of General Psychiatry*, *64*(2), 234–240. https://doi.org/10.1001/archpsyc.64.2.234

Winters, B. D., & Bussey, T. J. (2005a). Glutamate Receptors in Perirhinal Cortex Mediate Encoding, Retrieval, and Consolidation of Object Recognition Memory. *Journal of Neuroscience*, *25*(17), 4243–4251. https://doi.org/10.1523/JNEUROSCI.0480-05.2005

Winters, B. D., & Bussey, T. J. (2005b). Removal of cholinergic input to perirhinal cortex disrupts object recognition but not spatial working memory in the rat. *European Journal of Neuroscience*, *21*(8), 2263–2270. https://doi.org/10.1111/j.1460-9568.2005.04055.x

Winters, B. D., & Bussey, T. J. (2005c). Transient Inactivation of Perirhinal Cortex Disrupts Encoding, Retrieval, and Consolidation of Object Recognition Memory. *Journal of Neuroscience*, *25*(1), 52–61. https://doi.org/10.1523/JNEUROSCI.3827-04.2005

Winters, B. D., Forwood, S. E., Cowell, R. A., Saksida, L. M., & Bussey, T. J. (2004). Double Dissociation between the Effects of Peri-Postrhinal Cortex and Hippocampal Lesions on Tests of Object Recognition and Spatial Memory: Heterogeneity of Function within the Temporal Lobe. *Journal of Neuroscience*, *24*(26), 5901–5908. https://doi.org/10.1523/JNEUROSCI.1346-04.2004

Wolf, A., Swift, J. B., Swinney, H. L., & Vastano, J. A. (1985). Determining Lyapunov exponents from a time series. *Physica D: Nonlinear Phenomena*, *16*(3), 285–317. https://doi.org/10.1016/0167-2789(85)90011-9

Wong, T. P., Debeir, T., Duff, K., & Cuello, A. C. (1999). Reorganization of Cholinergic Terminals in the Cerebral Cortex and Hippocampus in Transgenic Mice Carrying Mutated Presenilin-1 and Amyloid Precursor Protein Transgenes. *Journal of Neuroscience*, *19*(7), 2706–2716. https://doi.org/10.1523/JNEUROSCI.19-07-02706.1999

Wright, A. L., Zinn, R., Hohensinn, B., Konen, L. M., Beynon, S. B., Tan, R. P., Clark, I. A., Abdipranoto, A., & Vissel, B. (2013). Neuroinflammation and Neuronal Loss Precede Aβ Plaque Deposition in the hAPP-J20 Mouse Model of Alzheimer's Disease. *PLOS ONE*, *8*(4), e59586. https://doi.org/10.1371/journal.pone.0059586

Wu, L., He, Y., Jiang, B., Liu, M., Wang, J., Yang, S., & Wang, Y. (2016). The association between the prevalence, treatment and control of hypertension and the risk of mild cognitive impairment in an elderly urban population in China. *Hypertension Research*, *39*(5), 367–375. https://doi.org/10.1038/hr.2015.146

Wu, Y., Ma, Y., Liu, Z., Geng, Q., Chen, Z., & Zhang, Y. (2017). Alterations of myelin morphology and oligodendrocyte development in early stage of Alzheimer's disease mouse model. *Neuroscience Letters*, *642*, 102–106. https://doi.org/10.1016/j.neulet.2017.02.007

X

Xu, L., Feng, J., & Yu, L. (2022). Avalanche criticality in individuals, fluid intelligence, and working memory. *Human Brain Mapping*, *43*(8), 2534–2553. https://doi.org/10.1002/hbm.25802

Y

Yamamoto, N., Matsubara, E., Maeda, S., Minagawa, H., Takashima, A., Maruyama, W., Michikawa, M., & Yanagisawa, K. (2007). A Ganglioside-induced Toxic Soluble Aβ Assembly: ITS ENHANCED FORMATION FROM AβBEARING THE ARCTIC MUTATION *. *Journal of Biological Chemistry*, *282*(4), 2646–2655. https://doi.org/10.1074/jbc.M606202200

Yan, H., Deng, X., Wang, Y., Wu, S., Jun, D., Yu, M., Liu, B., Wang, H., Pan, Y., Zhang, Z., Chen, J., Wang, Y., Walker, T., Bartlett, P., Ju, J., & Hou, S.-T. (2024). *Enhancement of spatial learning by 40 Hz visual stimulation requires parvalbumin interneuron-dependent hippocampal neurogenesis*. https://doi.org/10.1101/2024.04.28.591481

Yang, F., Chen, L., Yu, Y., Xu, T., Chen, L., Yang, W., Wu, Q., & Han, Y. (2022). Alzheimer's disease and epilepsy: An increasingly recognized comorbidity. *Frontiers in Aging Neuroscience*, *14*. https://doi.org/10.3389/fnagi.2022.940515

Yang, J.-T., Wang, Z.-J., Cai, H.-Y., Yuan, L., Hu, M.-M., Wu, M.-N., & Qi, J.-S. (2018). Sex Differences in Neuropathology and Cognitive Behavior in APP/PS1/tau Triple-Transgenic Mouse Model of Alzheimer's Disease. *Neuroscience Bulletin*, *34*(5), 736–746. https://doi.org/10.1007/s12264-018-0268-9

Yang, Y. L., & Lai, T. W. (2023). Chronic Visual Stimulation with LED Light Flickering at 24, 40, or 80 Hz Failed to Reduce Amyloid β Load in the 5XFAD Alzheimer's Disease Mouse Model. *Eneuro*, *10*(8), ENEURO.0189-23.2023. https://doi.org/10.1523/ENEURO.0189-23.2023

Young, D., Lawlor, P. A., Leone, P., Dragunow, M., & During, M. J. (1999). Environmental enrichment inhibits spontaneous apoptosis, prevents seizures and is neuroprotective. *Nature Medicine*, *5*(4), 448–453. https://doi.org/10.1038/7449

Z

Zanin, M., Güntekin, B., Aktürk, T., Hanoğlu, L., & Papo, D. (2020). Time Irreversibility of Resting-State Activity in the Healthy Brain and Pathology. *Frontiers in Physiology*, *10*, 1619. https://doi.org/10.3389/fphys.2019.01619

Zarahn, E., Aguirre, G., & D'Esposito, M. (2000). Replication and further studies of neural mechanisms of spatial mnemonic processing in humans. *Cognitive Brain Research*, *9*(1), 1–17. https://doi.org/10.1016/S0926-6410(99)00033-6

Zarow, C., Lyness, S. A., Mortimer, J. A., & Chui, H. C. (2003). Neuronal Loss Is Greater in the Locus Coeruleus Than Nucleus Basalis and Substantia Nigra in Alzheimer and Parkinson Diseases. *Archives of Neurology*, *60*(3), 337. https://doi.org/10.1001/archneur.60.3.337

Zempel, H., Thies, E., Mandelkow, E., & Mandelkow, E.-M. (2010). Aβ Oligomers Cause Localized Ca2+ Elevation, Missorting of Endogenous Tau into Dendrites, Tau Phosphorylation, and Destruction of Microtubules and Spines. *Journal of Neuroscience*, *30*(36), 11938–11950. https://doi.org/10.1523/JNEUROSCI.2357-10.2010

Zhang, F., Zhong, R., Li, S., Fu, Z., Wang, R., Wang, T., Huang, Z., & Le, W. (2019). Alteration in sleep architecture and electroencephalogram as an early sign of Alzheimer's disease preceding the disease pathology and cognitive decline. *Alzheimer's & Dementia*, *15*(4), 590–597. https://doi.org/10.1016/j.jalz.2018.12.004

Zhang, W., Bai, M., Xi, Y., Hao, J., Liu, L., Mao, N., Su, C., Miao, J., & Li, Z. (2012). Early memory deficits precede plaque deposition in APPswe/PS1dE9 mice: Involvement of oxidative stress and cholinergic dysfunction. *Free Radical Biology and Medicine*, *52*(8), 1443–1452. https://doi.org/10.1016/j.freeradbiomed.2012.01.023

Zhang, X., Zhong, W., Brankačk, J., Weyer, S. W., Müller, U. C., Tort, A. B. L., & Draguhn, A. (2016). Impaired theta-gamma coupling in APP-deficient mice. *Scientific Reports*, *6*(1), 21948. https://doi.org/10.1038/srep21948

Zhang, Y., McLaughlin, R., Goodyer, C., & LeBlanc, A. (2002). Selective cytotoxicity of intracellular amyloid β peptide1–42 through p53 and Bax in cultured primary human neurons. *Journal of Cell Biology*, *156*(3), 519–529. https://doi.org/10.1083/jcb.200110119

Zhang, Y., Thompson, R., Zhang, H., & Xu, H. (2011). APP processing in Alzheimer's disease. *Molecular Brain*, *4*(1), 3. https://doi.org/10.1186/1756-6606-4-3

Zhang, Y., Zhang, Z., Luo, L., Tong, H., Chen, F., & Hou, S.-T. (2021). 40 Hz Light Flicker Alters Human Brain Electroencephalography Microstates and Complexity Implicated in Brain Diseases. *Frontiers in Neuroscience*, *15*, 777183. https://doi.org/10.3389/fnins.2021.777183

Zheng, L., Yu, M., Lin, R., Wang, Y., Zhuo, Z., Cheng, N., Wang, M., Tang, Y., Wang, L., & Hou, S.-T. (2020). Rhythmic light flicker rescues hippocampal low gamma and protects ischemic neurons by enhancing presynaptic plasticity. *Nature Communications*, *11*(1), Article 1. https://doi.org/10.1038/s41467-020-16826-0

Zhou, J., Yu, J.-T., Wang, H.-F., Meng, X.-F., Tan, C.-C., Wang, J., Wang, C., & Tan, L. (2015). Association between Stroke and Alzheimer's Disease: Systematic Review and Meta-Analysis. *Journal of Alzheimer's Disease*, *43*(2), 479–489. https://doi.org/10.3233/JAD-140666

Zingg, B., Dong, H.-W., Tao, H. W., & Zhang, L. I. (2018). Input–output organization of the mouse claustrum. *Journal of Comparative Neurology*, *526*(15), 2428–2443. https://doi.org/10.1002/cne.24502

Zuckerman, S. L., Brett, B. L., Jeckell, A., Yengo-Kahn, A. M., & Solomon, G. S. (2018). Chronic Traumatic Encephalopathy and Neurodegeneration in Contact Sports and American Football. *Journal of Alzheimer's Disease: JAD*, *66*(1), 37–55. https://doi.org/10.3233/JAD-180218

Zvěřová, M. (2019). Clinical aspects of Alzheimer's disease. *Clinical Biochemistry*, *72*, 3–6. https://doi.org/10.1016/j.clinbiochem.2019.04.015

Annexes

Review published: How many gammas? Redefining Hippocampal Theta-Gamma Dynamic During Spatial Learning

During my thesis, I had the opportunity to write a mini-review on the hippocampal theta-gamma coupling dynamics during spatial learning.
This mini-review was published in February 2022 and can be found here:

Aguilera M, Douchamps V, Battaglia D and Goutagny R (2022) How Many Gammas? Redefining Hippocampal Theta-Gamma Dynamic During Spatial Learning. *Front. Behav. Neurosci.* 16:811278. doi: 10.3389/fnbeh.2022.811278

I join here the article.

frontiers in Behavioral Neuroscience

MINI REVIEW
published: 01 February 2022
doi: 10.3389/fnbeh.2022.811278

How Many Gammas? Redefining Hippocampal Theta-Gamma Dynamic During Spatial Learning

*Matthieu Aguilera[1], Vincent Douchamps[1], Demian Battaglia[2,3] and Romain Goutagny[1]**

[1] Laboratoire de Neurosciences Cognitives et Adaptatives (LNCA), Faculté de Psychologie, Université de Strasbourg, Strasbourg, France, [2] Institut de Neurosciences des Systèmes, CNRS, Aix-Marseille Université, Marseille, France, [3] University of Strasbourg Institute for Advanced Study (USIAS), Strasbourg, France

The hippocampal formation is one of the brain systems in which the functional roles of coordinated oscillations in information representation and communication are better studied. Within this circuit, neuronal oscillations are conceived as a mechanism to precisely coordinate upstream and downstream neuronal ensembles, underlying dynamic exchange of information. Within a global reference framework provided by theta (θ) oscillations, different gamma-frequency (γ) carriers would temporally segregate information originating from different sources, thereby allowing networks to disambiguate convergent inputs. Two γ sub-bands were thus defined according to their frequency (slow γ, 30–80 Hz; medium γ, 60–120 Hz) and differential power distribution across CA1 dendritic layers. According to this prevalent model, layer-specific γ oscillations in CA1 would reliably identify the temporal dynamics of afferent inputs and may therefore aid in identifying specific memory processes (encoding for medium γ vs. retrieval for slow γ). However, this influential view, derived from time-averages of either specific γ sub-bands or different projection methods, might not capture the complexity of CA1 θ-γ interactions. Recent studies investigating γ oscillations at the θ cycle timescale have revealed a more dynamic and diverse landscape of θ-γ motifs, with many θ cycles containing multiple γ bouts of various frequencies. To properly capture the hippocampal oscillatory complexity, we have argued in this review that we should consider the entirety of the data and its multidimensional complexity. This will call for a revision of the actual model and will require the use of new tools allowing the description of individual γ bouts in their full complexity.

Keywords: hippocampus, oscillations, spatial cognition, navigation, complexity, spatial learning

OPEN ACCESS

Edited by:
Gabrielle Girardeau, INSERM U839 Institut du Fer à Moulin (IFM), France

Reviewed by:
Antonio Fernández-Ruiz, New York University, United States

***Correspondence:**
Romain Goutagny
goutagny@unistra.fr

Specialty section:
This article was submitted to Learning and Memory, a section of the journal Frontiers in Behavioral Neuroscience

Received: *08 November 2021*
Accepted: *03 January 2022*
Published: *01 February 2022*

Citation:
Aguilera M, Douchamps V, Battaglia D and Goutagny R (2022) How Many Gammas? Redefining Hippocampal Theta-Gamma Dynamic During Spatial Learning. Front. Behav. Neurosci. 16:811278. doi: 10.3389/fnbeh.2022.811278

INTRODUCTION

The ability to represent the surrounding space is crucial for most evolved animals and is at the core of the ability to navigate in the environment, looking out for food, shelter, or other behaviorally relevant locations. For an organism to effectively navigate, it should possess the cognitive representations of critical regions in their environment (e.g., nest locations and food locations), to recall these regions when the need arises, and the means to exploit relations between such regions and their immediate position. In other words, the navigating agent constantly needs to

compare current sensory inputs (i.e., encoding of current information) with stored memories (i.e., retrieval of past information). These two seemingly opposed processes (encoding vs. retrieval) are thought to be mediated by two segregated areas of the medial temporal lobe: the hippocampal CA3 region and the entorhinal cortex (EC). Hippocampal CA3, through its massive recurrent network, would support retrieval of past memories (Rolls, 2018), whereas the EC (and more precisely its medial part; MEC) would support encoding of current sensory information (Brun et al., 2002, 2008; Fyhn et al., 2004; Hafting et al., 2005). These two regions in turn project to hippocampal region CA1, which is thought to act as a comparator to determine if ongoing sensory inputs represent new information that needs to be stored (Hasselmo et al., 2002). How does CA1 integrate these different inputs while minimizing interference? Current hypotheses suggest a critical role for brain oscillations in the selective routing of information (Fries, 2009). During spatial navigation, the hippocampus mainly exhibits theta (θ) and gamma (γ) oscillations. It is now accepted that hippocampal γ oscillations can be segregated into slow and medium (or fast, depending on the authors) γ rhythms, each originating from different brain regions and subserving different cognitive functions (Colgin et al., 2009; Schomburg et al., 2014). More recently, studies refining the time scale of analysis have shown that this model might be too simplistic, with a greater variability than initially expected. By putting in perspective these different studies, we have argued in this review that tackling this variability is needed to fully characterize the hippocampal θ-γ dynamic.

THE γ SUB-BANDS MODEL: A SUITABLE FRAMEWORK TO UNDERSTAND HIPPOCAMPAL COMPUTATION

Excellent reviews on the cellular mechanisms responsible for hippocampal θ (Buzsáki, 2002) and γ oscillations (Buzśaki and Wang, 2012) have already been published and fell outside the scope of the present review (see also Wang, 2010, for a comprehensive survey of the modeling literature).

Neuronal oscillations are conceived as a mechanism to precisely coordinate upstream and downstream neuronal ensembles, underlying the dynamic exchange of information (Fries, 2009). In the medial temporal lobe, it is proposed that, within a global reference framework provided by θ oscillations, different γ-frequency carriers would temporally segregate information originating from different sources, thereby allowing a target "reader" area to disambiguate convergent inputs (Buzsáki, 2010). As such, hippocampal CA1 γ oscillations, although initially described as forming a single wide frequency band (40–100 Hz; Bragin et al., 1995), were later dissociated into two sub-bands according to their frequency (i.e., slow γ, 25–55 Hz; fast γ, 65–140 Hz), and their phase of appearance related to pyramidal layer θ oscillations (i.e., early phase of the descending part for slow γ and trough for fast γ; Colgin et al., 2009). The fact that bursts of slow γ were associated with increased coherence between CA3 and CA1, whereas fast γ was associated with increased coherence between the MEC and CA1, prompted the authors to suggest that these two independent γ rhythms would selectively "route information" in the hippocampal entorhinal network (Colgin et al., 2009). Building on this framework and on the proposed specific role of CA3 and the MEC in memory processes, the same authors further proposed that these two γ rhythms in CA1 might subserve different cognitive operations, i.e., slow γ would be important for memory retrieval, whereas fast γ would support memory encoding (Colgin and Moser, 2010). While appealing in its simplicity, this model nevertheless carries some caveats. First, while the phase separation of inputs relative to θ oscillation would indeed allow for a separation of the information (Fries, 2009), the reported phase of fast γ does not fit with the "separate phases of encoding and retrieval (SPEAR)" model proposed by Hasselmo et al. (2002). Second, by using single-site recording in the CA1 pyramidal layer, Colgin et al. (2009) were not able to isolate the source of the slow- and fast-γ oscillations. Indeed, one should expect slow γ to be prominent in the CA1 *stratum radiatum* (str.rad), the input of CA3 through the Schaffer collaterals, and fast γ in the CA1 *stratum lacunosum-moleculare* (str.lm), the inputs of the MEC layer 3 through the temporo-ammonic pathway. Finally, while slow and fast γ differentially modulate place cells sequences according to the purported role of each γ rhythm (prospective vs. retrospective coding; Bieri et al., 2014), the authors never actually performed navigation task requiring allocentric memory [open field in Colgin et al. (2009) and linear track in Bieri et al. (2014)].

To fill these gaps, Schomburg et al. (2014) performed high-density multisite recording covering most layers of CA1 to CA3 and dentate gyrus (DG) regions along the transverse axis of the hippocampus in rats navigating in a linear track, a T maze, or an open field. Using a powerful source separation technique and focusing on the hippocampal CA1 area (independent component analysis; Fernández-Ruiz and Herreras, 2013), they were able to identify three γ independent components (ICs). The first component with a strong current sink was localized in the str.rad (termed rad IC), exhibiting slow-γ oscillations (30–80 Hz), phase-locked to the descending phase of CA1 pyramidal θ. The second γ component with a strong current sink was localized to the str.lm (termed lm IC), exhibiting mid-γ oscillations (60–120 Hz), phase-locked to the peak of CA1 pyramidal θ. Finally, the third component with a current source was localized in the CA1 pyramidal layer (termed CA1 pyr IC), exhibiting fast γ (>140 Hz), phase-locked to the through of CA1 pyramidal θ. Based on the location of the current sink/sources and single-unit recordings (in CA1, CA3, and the MEC), the authors proposed that slow γ would represent a communication channel between CA3 and CA1, whereas mid-γ would aid communication between the MEC and CA1. Importantly, there is a clear difference in the θ phase between the mid-γ reported by Schomburg et al. (2014) and the corresponding fast γ reported by Colgin et al. (2009), which can be due in part to the lack of source localization in the study by Colgin et al. Nevertheless, the relative phase of slow and medium γ in the Schomburg et al. (2014) study is coherent with the SPEAR model (Hasselmo et al., 2002). Do these different γ components subserve different cognitive operations? To answer this question, Schomburg and

colleagues characterized the dynamics of the γ components during different phases of a T-maze task. They showed that the θ-γ coupling strength of the rad IC selectively increased in the center arm of the maze, a place where memory recall is expected (i.e., in order to guide subsequent behavior). Recently, Fernández-Ruiz et al. (2021) extended this concept to the DG. Using the same decomposition method, they characterized three independent components, namely, a slow-γ IC (30–50 Hz) in the outer molecular layer of the DG, a mid-γ IC (60–80 Hz) in the inner molecular layer of the DG, and a fast-γ IC (100–150 Hz) in the middle molecular layer of the DG, coming from lateral EC associational and/or commissural, and MEC inputs, respectively. During spatial learning, fast-γ oscillations synchronize the MEC and DG, while during object learning, slow-γ oscillations synchronize the LEC and DG. To assess causality, the authors performed γ-frequency optogenetic perturbation of MEC and LEC. This led to reduced DG layer-specific fast- and slow-γ sub-bands and to learning impairments in a spatial and object learning task, respectively.

Altogether, these seminal studies set the stage for what we decided to call the "sub-bands model." The premise of this model is that if there are different rhythms generated by different brain regions, they must subserve different cognitive operations. However, a problem with influential models is that they tend to inform research in the field, biasing the interpretation of results and narrowing the spectrum of hypotheses that could be considered, e.g., to explain disruptions of function in pathology. For example, a decrease in hippocampal slow-γ power observed in several rodent models of Alzheimer's disease (Gillespie et al., 2016; Iaccarino et al., 2016; Mably et al., 2017) was linked to retrieval impairment (Mably and Colgin, 2018; Etter et al., 2019) in accordance to the purported role of those oscillations in memory retrieval.

A SUITABLE MODEL, BUT SURELY TOO RESTRICTIVE

As stated in the "Introduction" section, a navigating agent constantly needs to compare current sensory inputs (i.e., encoding of current information) with stored memories (i.e., retrieval of past information). To gain a better temporal resolution, one can study γ dynamic at the θ time-scale level (Dvorak et al., 2018; Lopes-dos-Santos et al., 2018; Zhang et al., 2019), a proposed unit of computation (Lisman, 2005; Lisman and Buzsáki, 2008). By using various methods of γ detection in a θ cycle by cycle manner (γ detector reported by Dvorak et al., 2018, Ensemble Empirical Mode Decomposition of a γ signal reported by Lopes-dos-Santos et al., 2018 and unsupervised clustering reported by Zhang et al., 2019), these studies showed a more complex landscape than initially proposed (with an increasing number of θ-γ motifs, with up to 5 prototypic motifs reported by Lopes-dos-Santos et al., 2018; **Figure 1**). Overall, all the studies agreed on the presence of at least three different γ oscillations, similar to the definition put forward by Schomburg et al. (2014) (**Figure 1**). Collectively, they support the concept that different γ frequencies subserve different cognitive operations by channeling information in specific pathways (refer to Zhou et al., 2019, for a critical view on the existence of a "real" slow-γ oscillation in the hippocampal network). At the first sight, they seem to consolidate the current γ sub-bands model. However, they also all report high diversity of coupling patterns across θ cycles, with most of the cycle containing multiple γ events. In other words, each θ cycle can simultaneously contain slow- and medium-γ events (**Figure 1**). This diversity was always mentioned, but surprisingly not properly studied, as they all acknowledge restricting analyses to either the highest amplitude γ events (Dvorak et al., 2018) or the one fitting the best canonical clustered results (Lopes-dos-Santos et al., 2018; Zhang et al., 2019). As such, they analyzed only a part of the available landscape of θ-γ motif (36% of all θ cycles reported by Lopes-dos-Santos et al., 2018). What does that imply in terms of local computation? It was indeed assumed that each θ cycle would subserve a specific function based on the associated dominant γ oscillation: in CA1, θ cycles with slow γ would be "retrieval cycles," whereas cycles with mid-γ would be "encoding cycles" (Colgin et al., 2009; Bieri et al., 2014; Schomburg et al., 2014). The fact that θ cycles mostly contain multiple, low-amplitude, different γ events complexifies this hypothesis (Bagur and Benchenane, 2018). What is the role of a θ cycle with concomitant, same-amplitude slow and medium γ? Can one θ cycle promote different cognitive operations? As an example of possible complexity, Lopes-dos-Santos and colleagues have shown that each θ-nested spectral component (tSC, equivalent of a specific θ-γ motif) represents a distinct spiking dynamic of distinguishable cell ensembles (Lopes-dos-Santos et al., 2018). Since each θ cycle does not present a single tSC but a weighted combination of multiple tSC, what will be the output of such θ cycles (e.g., multiple assemblies co-firing and sequential ordering of different assemblies).

Most, if not all, of the aforementioned studies have focused on the interaction between multiple γ and single θ oscillations (CA1 pyramidal θ). However, it was recently shown that θ oscillations themselves in the dorsal hippocampus are not a unitary process. Using ICA decomposition, López-Madrona et al. (2020) identified three independent θ ICs contributed by different synaptic pathways, namely, the first in the str.rad, the second in the str.lm, and the third in the mid-molecular layer of the DG. Thus, as there are multiple γ, there may also be multiple θ, opening the way to a potential combinatorial explosion of the number of possible θ-γ configurations.

As a concluding, near tautological, remark, we would like to stress that any method for the unsupervised extraction of classes of oscillatory events will end up finding them. The exact number of identified patterns will depend on the specificities of the experimental dataset and algorithm used but will always nevertheless remain a discrete integer number as the applied methods are designed to do so. In front of the inflation of the number of possibly relevant θ-γ patterns exhibited by the recent literature, and the diversity of γ sub-bands definition across aforementioned studies (see Zhou et al., 2019), it may be legitimate to wonder whether the paradigm of looking for discrete classes of events is well-grounded. From a complex dynamics perspective, a neural circuit with recurrent excitatory and inhibitory interconnections

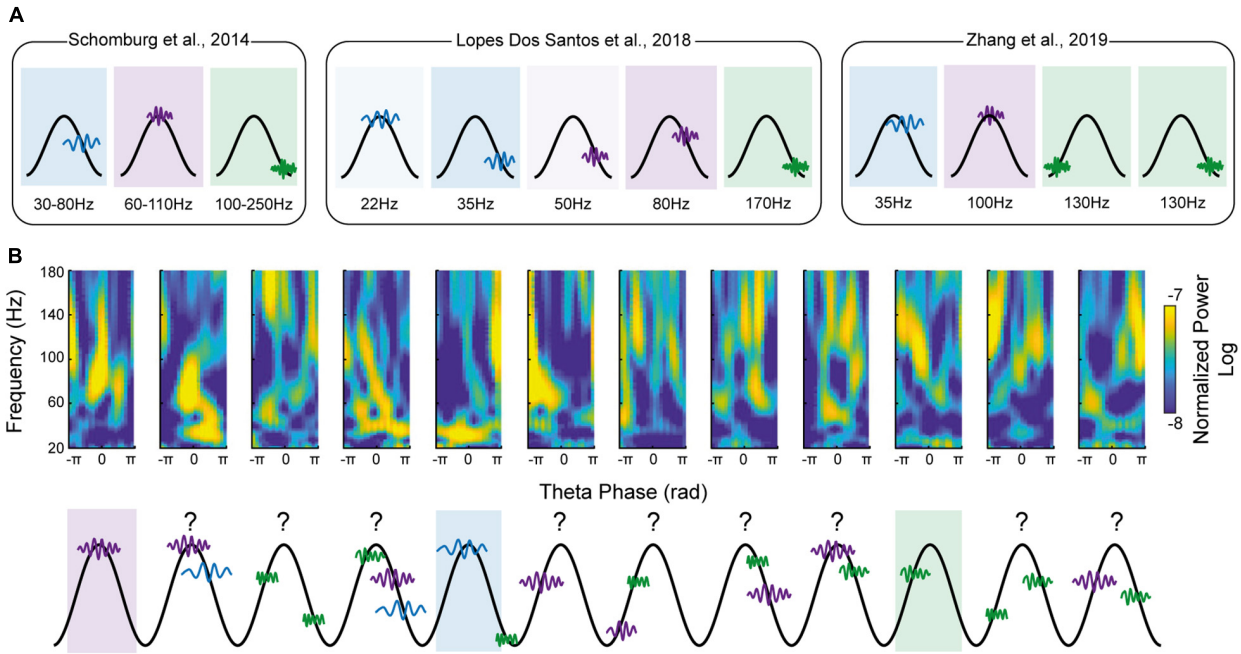

FIGURE 1 | Decomposing theta-gamma oscillations in discrete motifs do not capture the full gamma diversity. **(A)** Schematic representations of the main theta-gamma motifs found in the literature. Gamma frequency is color-coded (blue corresponding to slow-gamma, purple to mid-gamma and green to fast-gamma). Note the inflation of the different motifs since the initial proposal by Colgin et al. (2009) (from 2 in Colgin et al., 2009 to 5 in Lopes-dos-Santos et al., 2018). **(B)** Top: Raw example of theta-gamma motifs found in hippocampal CA1 pyramidal layer (reproduced from Figure 1B of Zhang et al., 2019 https://doi.org/10.7554/eLife.44320.002). Bottom: Schematic representation of the above theta-gamma motifs. Note that only few theta cycles present a prototypic motif as described in **(A)**. In fact, most of the theta cycles can be described as a weighted combination of the different prototypic motifs.

is supposed to give rise to oscillations that are not well-behaved and tuned metronomes but can fluctuate in frequency as a function of noisy background inputs (Brunel and Wang, 2003; Brunel and Hansel, 2006). Such stochastic-like oscillations, despite their highly transient and irregular nature, can still be fit for functions as selective information routing, thanks to emergent self-organization mechanisms (Palmigiano et al., 2017). It may thus be that the diversity of θ-γ oscillatory patterns displayed by neural recordings is not the manifestation of the coexistence of multiple, discrete generation mechanisms or sources, but instead the unique, diverse output of a common underlying circuit dynamics, non-linear and complex in nature.

It is noted that a similar debate has also occurred in the literature concerning the diversity of cortical interneurons, that may exist as a large number of discrete types with different functions (Markram et al., 2004; Burkhalter, 2008) and form an interneuron continuum (Parra et al., 1998) or a structured continuum with smooth tendencies (Battaglia et al., 2013).

CONCLUSION AND PERSPECTIVES: IS θ-γ LANDSCAPE RANDOM OR COMPLEX?

In this review, we have argued that the current model of hippocampal θ-γ oscillations might not capture the complexity of CA1 θ-γ interactions despite the evident appeal of its simplicity and the functional link to memory processes. Indeed, rather than containing a given γ event, most of the θ cycles contain multiple, low-amplitude, γ bouts. Furthermore, many of the observed γ frequencies do not fit well into a classification involving only a few discrete γ types. Should these low-amplitude events be dismissed as noise? To properly describe hippocampal oscillatory complexity, we believe the entirety of the data should be taken into consideration (without assuming that the strongest γ events are the only ones carrying information). This will require the use of new tools that do not assume *a priori* that certain classes of γ rhythms exist but instead enable the description of individual γ bouts in their full complexity. Individual oscillatory events may have wildly fluctuating frequency, amplitude, and phase with respect to ongoing θ. However, these fluctuations could still be correlated to behavior and memory processing but in a collective and synergistic manner. Individual features of oscillatory activity may be only weakly informative about behavior because of their apparent randomness. However, multiple features taken together may still carry relevant information that individual features do not (Wibral et al., 2017). Such a situation may occur if the observed oscillatory events do not arise in all theoretically possible configurations of features but are sampled on a low-dimensional manifold in state space (Chaudhuri and Fiete, 2016). This representation would constrain dynamic trajectories, creating interdependencies between them, possibly modulated by context. In such a view, there would not be discrete classes

of oscillatory events but a lower-dimensional space of possible modes of oscillation that the system can smoothly explore along time, possibly under the biasing influence of the exogenous or endogenous input drive. Machine learning approaches could then be used to learn these manifolds without fully determining oscillatory modes and their relations to behavior so as to decode and extract the complex information hidden in the apparent stochasticity of the observed activity time-series.

AUTHOR CONTRIBUTIONS

MA, RG, and DB wrote the manuscript. VD provided critical inputs. All authors contributed to the article and approved the submitted version.

FUNDING

This work was supported by the Agence Nationale de la Recherche (ANR JCC: ANR-17-CE37-0002 to RG), the University of Strasbourg Institute for Advanced Study (USIAS 2020 fellowship to DB), the Fondation pour la Recherche Medicale (FRM, Ph.D. fellowship to MA), and the University of Strasbourg and the Centre National de la Recherche Scientifique (CNRS).

ACKNOWLEDGMENTS

The authors wish to thank all the intern students who worked on this project across the years. They are extremely grateful to Jesse Jackson for critical comments on this review.

REFERENCES

Bagur, S., and Benchenane, K. (2018). The Theta rhythm mixes and matches gamma oscillations cycle by cycle. *Neuron* 100, 768–771. doi: 10.1016/j.neuron.2018.11.008

Battaglia, D., Karagiannis, A., Gallopin, T., Gutch, H. W., and Cauli, B. (2013). Beyond the frontiers of neuronal types. *Front. Neural Circuits* 7:13. doi: 10.3389/fncir.2013.00013

Bieri, K. W., Bobbitt, K. N., and Colgin, L. L. (2014). Slow and fast gamma rhythms coordinate different spatial coding modes in hippocampal place cells. *Neuron* 82, 670–681. doi: 10.1016/j.neuron.2014.03.013

Bragin, A., Jando, G., Nadasdy, Z., Hetke, J., Wise, K., and Buzsaki, G. (1995). Gamma (40-100 Hz) oscillation in the hippocampus of the behaving rat. *J. Neurosci.* 15, 47–60. doi: 10.1523/jneurosci.15-01-00047.1995

Brun, V. H., Leutgeb, S., Wu, H.-Q., Schwarcz, R., Witter, M. P., Moser, E. I., et al. (2008). Impaired spatial representation in CA1 after lesion of direct input from entorhinal cortex. *Neuron* 57, 290–302. doi: 10.1016/j.neuron.2007.11.034

Brun, V. H., Otnæss, M. K., Molden, S., Steffenach, H. A., Witter, M. P., Moser, M. B., et al. (2002). Place cells and place recognition maintained by direct entorhinal-hippocampal circuitry. *Science* 296, 2243–2246. doi: 10.1126/science.1071089

Brunel, N., and Hansel, D. (2006). How noise affects the synchronization properties of recurrent networks of inhibitory neurons. *Neural Comput.* 18, 1066–1110. doi: 10.1162/neco.2006.18.5.1066

Brunel, N., and Wang, X. J. (2003). What determines the frequency of fast network oscillations with irregular neural discharges? I. Synaptic dynamics and excitation-inhibition balance. *J. Neurophysiol.* 90, 415–430. doi: 10.1152/jn.01095.2002

Burkhalter, A. (2008). Many specialists for suppressing cortical excitation. *Front. Neurosci.* 2:155–167. doi: 10.3389/neuro.01.026.2008

Buzsáki, G. (2002). Theta oscillations in the hippocampus. *Neuron* 33, 325–340. doi: 10.1016/S0896-6273(02)00586-X

Buzsáki, G. (2010). Neural syntax: cell assemblies, synapsembles, and readers. *Neuron* 68, 362–385. doi: 10.1016/j.neuron.2010.09.023

Buzśaki, G., and Wang, X. J. (2012). Mechanisms of gamma oscillations. *Annu. Rev. Neurosci.* 35, 203–225. doi: 10.1146/annurev-neuro-062111-150444

Chaudhuri, R., and Fiete, I. (2016). Computational principles of memory. *Nat. Neurosci.* 19, 394–403. doi: 10.1038/nn.4237

Colgin, L. L., and Moser, E. I. (2010). Gamma oscillations in the hippocampus. *Physiology* 25, 319–329. doi: 10.1152/physiol.00021.2010

Colgin, L. L., Denninger, T., Fyhn, M., Hafting, T., Bonnevie, T., Jensen, O., et al. (2009). Frequency of gamma oscillations routes flow of information in the hippocampus. *Nature* 462, 353–357. doi: 10.1038/nature08573

Dvorak, D., Radwan, B., Sparks, F., Talbot, Z. N., and Fenton, A. (2018). Control of recollection by slow gamma dominating mid-frequency gamma in hippocampus CA1. *PLoS Biol.* 16:e2003354. doi: 10.1371/journal.pbio.2003354

Etter, G., van der Veldt, S., Manseau, F., Zarrinkoub, I., Trillaud-Doppia, E., and Williams, S. (2019). Optogenetic gamma stimulation rescues memory impairments in an Alzheimer's disease mouse model. *Nat. Commun.* 10:5322. doi: 10.1038/s41467-019-13260-9

Fernández-Ruiz, A., and Herreras, O. (2013). Identifying the synaptic origin of ongoing neuronal oscillations through spatial discrimination of electric fields. *Front. Comput. Neurosci.* 7:5. doi: 10.3389/fncom.2013.00005

Fernández-Ruiz, A., Oliva, A., Soula, M., Rocha-Almeida, F., Nagy, G. A., Martin-Vazquez, G., et al. (2021). Gamma rhythm communication between entorhinal cortex and dentate gyrus neuronal assemblies. *Science* 372:eabf3119. doi: 10.1126/science.abf3119

Fries, P. (2009). Neuronal gamma-band synchronization as a fundamental process in cortical computation. *Annu. Rev. Neurosci.* 32, 209–224. doi: 10.1146/annurev.neuro.051508.135603

Fyhn, M., Molden, S., Witter, M. P., Moser, E. I., and Moser, M. B. (2004). Spatial representation in the entorhinal cortex. *Science* 305, 1258–1264. doi: 10.1126/science.1099901

Gillespie, A. K., Jones, E. A., Lin, Y. H., Karlsson, M. P., Kay, K., Yoon, S. Y., et al. (2016). Apolipoprotein E4 causes age-dependent disruption of slow gamma oscillations during hippocampal sharp-wave ripples. *Neuron* 90, 740–751. doi: 10.1016/j.neuron.2016.04.009

Hafting, T., Fyhn, M., Molden, S., Moser, M. B., and Moser, E. I. (2005). Microstructure of a spatial map in the entorhinal cortex. *Nature* 436, 801–806. doi: 10.1038/nature03721

Hasselmo, M. E., Bodelón, C., and Wyble, B. P. (2002). A proposed function for hippocampal theta rhythm: separate phases of encoding and retrieval enhance reversal of prior learning. *Neural Comput.* 14, 793–817. doi: 10.1162/089976602317318965

Iaccarino, H. F., Singer, A. C., Martorell, A. J., Rudenko, A., Gao, F., Gillingham, T. Z., et al. (2016). Gamma frequency entrainment attenuates amyloid load and modifies microglia. *Nature* 540, 230–235. doi: 10.1038/nature20587

Lisman, J. (2005). The theta/gamma discrete phase code occuring during the hippocampal phase precession may be a more general brain coding scheme. *Hippocampus* 15, 913–922. doi: 10.1002/hipo.20121

Lisman, J., and Buzsáki, G. (2008). A neural coding scheme formed by the combined function of gamma and theta oscillations. *Schizophr. Bull.* 34, 974–980. doi: 10.1093/schbul/sbn060

Lopes-dos-Santos, V., van de Ven, G. M., Morley, A., Trouche, S., Campo-Urriza, N., and Dupret, D. (2018). Parsing hippocampal theta oscillations by nested spectral components during spatial exploration and memory-guided behavior. *Neuron* 100, 940–952.e7. doi: 10.1016/j.neuron.2018.09.031

López-Madrona, V. J., Pérez-Montoyo, E., Álvarez-Salvado, E., Moratal, D., Herreras, O., Pereda, E., et al. (2020). Different theta frameworks coexist in the rat hippocampus and are coordinated during memory-guided and novelty tasks. *Elife* 9:e57313. doi: 10.7554/eLife.57313

Mably, A. J., and Colgin, L. L. (2018). Gamma oscillations in cognitive disorders. *Curr. Opin. Neurobiol.* 52, 182–187. doi: 10.1016/j.conb.2018.07.009

Mably, A. J., Gereke, B. J., Jones, D. T., and Colgin, L. L. (2017). Impairments in spatial representations and rhythmic coordination of place cells in the 3xTg mouse model of Alzheimer's disease. *Hippocampus* 27, 378–392. doi: 10.1002/hipo.22697

Markram, H., Toledo-Rodriguez, M., Wang, Y., Gupta, A., Silberberg, G., and Wu, C. (2004). Interneurons of the neocortical inhibitory system. *Nat. Rev. Neurosci.* 5, 793–807. doi: 10.1038/nrn1519

Palmigiano, A., Geisel, T., Wolf, F., and Battaglia, D. (2017). Flexible information routing by transient synchrony. *Nat. Neurosci.* 20, 1014–1022. doi: 10.1038/nn.4569

Parra, P., Gulyás, A. I., and Miles, R. (1998). How many subtypes of inhibitory cells in the hippocampus? *Neuron* 20, 983–993. doi: 10.1016/S0896-6273(00)80479-1

Rolls, E. T. (2018). The storage and recall of memories in the hippocampo-cortical system. *Cell Tissue Res.* 373, 577–604. doi: 10.1007/s00441-017-2744-3

Schomburg, E. W., Fernández-Ruiz, A., Mizuseki, K., Berényi, A., Anastassiou, C. A., Koch, C., et al. (2014). Theta phase segregation of input-specific gamma patterns in entorhinal-hippocampal networks. *Neuron* 84, 470–485. doi: 10.1016/j.neuron.2014.08.051

Wang, X. J. (2010). Neurophysiological and computational principles of cortical rhythms in cognition. *Physiol. Rev.* 90, 1195–1268. doi: 10.1152/physrev.00035.2008

Wibral, M., Priesemann, V., Kay, J. W., Lizier, J. T., and Phillips, W. A. (2017). Partial information decomposition as a unified approach to the specification of neural goal functions. *Brain Cogn.* 112, 25–38. doi: 10.1016/j.bandc.2015.09.004

Zhang, L., Lee, J., Rozell, C., and Singer, A. C. (2019). Sub-second dynamics of theta-gamma coupling in hippocampal CA1. *Elife* 8:e44320. doi: 10.7554/eLife.44320

Zhou, Y., Sheremet, A., Qin, Y., Kennedy, J. P., DiCola, N. M., Burke, S. N., et al. (2019). Methodological considerations on the use of different spectral decomposition algorithms to study hippocampal rhythms. *eNeuro* 6, ENEURO.142–ENEURO.119. doi: 10.1523/ENEURO.0142-19.2019

Conflict of Interest: The authors declare that the research was conducted in the absence of any commercial or financial relationships that could be construed as a potential conflict of interest.

Version française et résumée de la thèse

Afin de réaliser une version résumée de la thèse en francais, différents chapitres de l'introduction, l'article de la partie 1 des résultats et la conclusion générale ont été traduits en français.
Les figures n'ont pas été remises dans cette partie et ont les index pour les figures mises dans la thèse en anglais.

1. La maladie d'Alzheimer

En 1906, le Dr. Alois Alzheimer, un médecin allemand, décrivit pour la première fois le cas d'une patiente, Mme Auguste Deter, une femme de 51 ans, qui présentait des troubles cognitifs, des hallucinations, des délires, des symptômes focaux et une incompétence psychosociale, symptômes collectivement reconnus comme une démence sénile. Après analyse histologique post-mortem du cerveau d'Auguste Deter, le Dr Alzheimer décrivit une accumulation de plaques extracellulaires et d'enchevêtrements neurofibrillaires (Maurer et al., 1997). En 1910, E. Kraepelin nomma officiellement cette condition "maladie d'Alzheimer". Plus d'un siècle plus tard, la maladie d'Alzheimer est devenue l'un des défis médicaux les plus importants auxquels notre société est confrontée. Elle est maintenant reconnue comme une maladie neurodégénérative caractérisée par l'accumulation de plaques amyloïdes, résultant de l'agrégation du peptide β-amyloïde (Aβ), et d'enchevêtrements neurofibrillaires, causés par l'agrégation de la protéine Tau hyperphosphorylée. Ces changements pathologiques conduisent ultimement à la mort neuronale et à la démence.

1.1. La maladie d'Alzheimer en chiffres

La maladie d'Alzheimer (MA) est la première cause de démence dans le monde, représentant plus de 60-70% des 55 millions de personnes atteintes de démence dans le monde (Alzheimer's disease international, 2023), et ce nombre devrait presque doubler tous les 20 ans pour atteindre 139 millions d'ici 2050, l'augmentation affectant principalement les pays à revenu faible et intermédiaire (Alzheimer's disease international, 2015). En France, 3 millions de personnes sont directement (patients) ou indirectement (aidants, famille) concernées par la MA (France Alzheimer, FRM). Sur la base d'une étude épidémiologique française sur les personnes de plus de 65 ans (cohorte PAQUID, Ramaroson et al. 2003) et des données de santé publique françaises, le nombre de personnes de plus de 65 ans atteintes de MA a été évalué à 1 million en 2018 et estimé à 1,8 million en 2050 (Vaincre Alzheimer). L'incidence (le nombre de nouveaux cas de la maladie sur une période donnée) est estimée à 225 000 personnes par an. Cette dernière dépend de l'âge, évoluant de 2‰ pour les individus entre 65 et 69 ans à 70‰ pour les plus de 90 ans, l'âge étant le principal facteur de risque de la maladie. Cependant, ces chiffres tiennent principalement

compte des stades finaux de la maladie, alors que la pathologie d'Alzheimer commence des années avant l'apparition des symptômes. Par conséquent, le nombre de personnes touchées est probablement sous-estimé. En effet, une étude récente a estimé qu'en considérant tous les différents stades de la maladie, depuis le stade prodromal asymptomatique jusqu'à la démence, 416 millions de personnes seraient dans le continuum de la MA dans le monde, représentant 22% des personnes âgées de 50 ans et plus (Gustavsson et al., 2023), soulignant l'importance de la recherche sur cette pathologie.

1.2. Les facteurs de risque de la maladie

Le principal facteur de risque de la MA reste le vieillissement. Cela pourrait s'expliquer d'abord par l'influence de facteurs de vieillissement non spécifiques comme l'augmentation des radicaux libres oxygénés (M. A. Smith et al., 1995), ou la dérégulation hormonale notamment via la ménopause (Mosconi et al., 2021). De plus, les protéinopathies communes associées à la MA — comme les plaques amyloïdes formées par l'accumulation de peptides Aβ ou les enchevêtrements neurofibrillaires résultant de l'agrégation des protéines Tau hyperphosphorylées — ont été liées au vieillissement (Arriagada et al., 1992) et sont même trouvées chez des individus âgés non pathologiques ou asymptomatiques (Iacono et al., 2014; Monsell et al., 2013; Rowe et al., 2010). Outre le vieillissement, d'autres facteurs de risque ont été identifiés notamment en fonction du type de pathologie MA. La forme familiale, représentant moins de 2% des cas de MA (Bekris et al., 2010), est liée à des mutations génétiques héréditaires. En revanche, la MA sporadique, représentant 98% des cas de MA, peut être liée à des facteurs de risque environnementaux.

1.3. Évolution clinique de la maladie

Même si une altération de l'odorat ou hyposmie est l'une des caractéristiques cliniques les plus précoces de la MA (J. M. Peters et al., 2003), il existe un consensus selon lequel la maladie commence cliniquement par des plaintes mnésiques. Des batteries de tests neuropsychologiques, telles que l'examen CERAD (Consortium to Establish a Registry for Alzheimer's Disease), le Mini-Mental State Examination et l'échelle Clinical Dementia Rating, sont couramment utilisées pour évaluer divers domaines cognitifs (Folstein et al., 1975; J. C. Morris, 1993). Les patients atteints de MA

présentent un profil cognitif marqué par des déficits dans plusieurs domaines, qui s'aggravent progressivement au fil du temps (pour revue, voir Peña-Casanova et al. 2012; Tromp et al. 2015). Au début, la mémoire de travail montre un déclin progressif, les patients devenant de plus en plus sensibles aux distractions pendant les tâches de mémoire. Des altérations de la mémoire spatiale et de l'orientation sont également souvent observées comme déficits cognitifs précoces. Les patients peuvent rencontrer des difficultés importantes pour naviguer dans des environnements familiers et se souvenir des relations spatiales, ce qui peut conduire à une désorientation accrue.
Au fur et à mesure que la maladie progresse, les déficits des fonctions exécutives deviennent plus prononcés. Les patients commencent à avoir des difficultés avec les tâches nécessitant de la planification, de la résolution de problèmes ou de la flexibilité cognitive. Il est important de noter que la maladie est maintenant comprise comme ayant une phase préclinique prolongée, commençant souvent des années voire des décennies avant que les symptômes ne deviennent perceptibles. Cette progression étendue a conduit à l'identification de plusieurs stades de la MA, notamment le déclin cognitif subjectif, le trouble cognitif léger (MCI), et finalement la démence. Alors que la recherche se poursuit, une attention croissante sur ces stades précoces aide à cartographier la trajectoire du déclin cognitif et à affiner notre compréhension de la pathologie de la MA.

1.3.1. Déclin Cognitif Subjectif

Le Déclin Cognitif Subjectif (SCD) fait référence aux individus qui rapportent des difficultés de mémoire ou cognitives malgré l'absence de déficits objectifs lors des tests neuropsychologiques (Jessen, Amariglio, et al., 2014). Bien que les évaluations cliniques ne révèlent pas de déficiences, les personnes présentant un SCD montrent souvent des changements pathologiques, tels qu'une connectivité fonctionnelle cérébrale perturbée similaire à celle observée dans le MCI (López-Sanz et al., 2017), une altération du couplage phase-amplitude à l'état de repos (C.-H. Cheng et al., 2023), et des changements structurels dans la matière grise et blanche (X. Wang et al., 2020). Ces altérations, ainsi que le fait que les individus avec SCD présentent un risque plus élevé de développer une démence de type Alzheimer (Jessen, Wolfsgruber, et al., 2014; Reisberg et al., 2010; Rönnlund et al., 2015), positionnent le SCD comme une manifestation clinique potentiellement précoce de la MA. La

détection correcte de ce stade en clinique pourrait donc représenter un moyen de diagnostiquer la MA plus tôt.

1.3.2. Trouble Cognitif Léger

Le Trouble Cognitif Léger (MCI) est un état transitoire entre le vieillissement normal et la démence, caractérisé par une perte de mémoire qui dépasse ce qui est attendu pour l'âge correspondant mais ne répond pas aux critères de la MA (Petersen et al., 2001). En raison de sa définition large et de son hétérogénéité sous-jacente, le MCI est classé en deux sous-types : le MCI amnésique (aMCI), où la perte de mémoire est prédominante, et le MCI non-amnésique (naMCI), qui implique des déficiences dans des domaines cognitifs autres que la mémoire. Les individus atteints d'aMCI ont une probabilité plus élevée de développer une MA, avec un taux de conversion d'environ 12% par an (Campbell et al., 2013). Ce risque accru pourrait être lié à la présence, chez les patients aMCI, d'enchevêtrements neurofibrillaires observés dans les régions critiques pour la mémoire, comme l'hippocampe, le cortex entorhinal et l'amygdale (Markesbery, 2010). Le taux élevé de conversion vers la MA et les similitudes dans la physiopathologie ont conduit à suggérer que l'aMCI pourrait être considéré comme un stade prodromal de la MA. Cependant, il faut rappeler que le MCI ne progresse pas toujours vers la MA et peut également précéder d'autres maladies neurodégénératives, comme la démence à corps de Lewy (Ferman et al., 2013) ou la maladie de Parkinson (J. G. Goldman et al., 2015) et peut même revenir à un état cognitif normal (Koepsell & Monsell, 2012).

1.3.3. Démence

Comme mentionné précédemment, environ 10% des individus atteints de MCI progresseront vers une démence de type Alzheimer, qui peut être considérée comme le stade final de la maladie. Les patients connaissent une aggravation significative des symptômes, notamment des manifestations neuropsychiatriques sévères telles que l'agressivité, les épisodes psychotiques et les hallucinations. Au fur et à mesure que les fonctions cognitives et motrices se détériorent, les individus perdent progressivement la capacité de naviguer dans leur environnement et d'effectuer des mouvements de base, devenant souvent muets et incontinents. Cette immobilité physique augmente le risque de complications telles que la thrombose veineuse

profonde, la malnutrition, les pneumopathies et les infections, qui sont fréquemment les principales causes de décès chez les patients atteints de MA (Zvěřová, 2019).

1.4. Évolution neuropathologique de la maladie

L'évolution neuropathologique de la MA n'est pas aléatoire, elle suit un schéma spécifique, caractérisé pour la première fois par Eva et Heiko Braak grâce à l'analyse histologique post-mortem de cerveaux de patients atteints de MA. Les stades de Braak (Braak & Braak, 1991) décrivent la propagation des enchevêtrements neurofibrillaires de Tau (NFT). Dans les stades I et II, appelés "stades transentorhinaux", les NFT apparaissent dans le cortex transentorhinal et la région CA1 de l'hippocampe. Les stades III et IV, connus comme "stades limbiques", montrent une implication significative des cortex entorhinaux et transentorhinaux, avec une propagation ultérieure à l'hippocampe, l'amygdale, le thalamus, le noyau accumbens et le claustrum. Aux stades V et VI, appelés "stades isocorticaux", l'isocortex est fortement affecté, avec une implication croissante de toutes les régions précédemment mentionnées. Plus tard, Dietmar Thal, un étudiant du groupe de Braak, a cartographié la progression des dépôts d'Aβ (Thal et al., 2002). La phase I est marquée par des plaques diffuses focales dans les couches II, III, IV et V des cortex frontal, temporal, pariétal et occipital. Dans la phase II, l'Aβ se propage au cortex entorhinal, à l'hippocampe et au cortex insulaire. La phase III implique des régions sous-corticales telles que l'amygdale, le thalamus, le striatum et l'hypothalamus. Dans la phase IV, les dépôts d'Aβ apparaissent dans des zones comme la substance noire, le colliculus supérieur, le noyau rouge et la région CA4 de l'hippocampe. Enfin, la phase V montre une implication du cervelet, du locus coeruleus et d'autres régions du tronc cérébral. Selon ces classifications, les dépôts d'Aβ et de Tau suivraient donc deux schémas de progression distincts (Figure 2).

Le développement des techniques de neuroimagerie, en particulier la tomographie par émission de positons (PET-scans ; Ametamey et al., 2008), a permis d'étudier ces stades chez les patients vivants. Le PET-scans permet la visualisation de molécules spécifiques marquées avec des traceurs radioactifs, facilitant l'étude des processus métaboliques et physiologiques. Le marquage longitudinal de l'Aβ a affiné les premiers stades de Thal, révélant que l'accumulation d'Aβ commence en réalité dans le précuneus, le cortex orbitofrontal médian et le cortex cingulaire postérieur, régions intégrales du réseau du mode par défaut (DMN ; Palmqvist et al. 2017). De même,

l'imagerie de Tau a confirmé le stade hiérarchique de Braak de l'agrégation de Tau, montrant que la progression à travers les stades de Braak corrèle avec l'évolution des niveaux de Tau hyperphosphorylée et d'Aβ dans le liquide céphalo-rachindien (LCR ; Therriault et al., 2022). Il est intéressant de noter que, bien que les stades I et II de Braak puissent survenir sans dépôt d'Aβ, la progression au-delà du stade III est exclusivement associée à la présence d'Aβ (Therriault et al., 2022). De plus, les altérations cognitives s'alignent sur les stades de Braak : des déficits subtils de la mémoire sont observés au stade II, conformément à l'accumulation de Tau dans les régions temporales médianes critiques pour la mémoire, tandis que les stades IV et V de Braak sont incompatibles avec une cognition normale (Therriault et al., 2022). Globalement, la classification de Braak de la pathologie tau et les différentes phases de dépôt amyloïde fournissent un cadre solide pour comprendre la progression neuropathologique de la MA, aidant à suivre l'évolution de la maladie tant au niveau des marqueurs moléculaires que du déclin cognitif (Figure 3).

1.5. Diagnostic et traitement

1.5.1. Le défi majeur du diagnostic

Pendant des décennies, le critère pour classer un groupe de symptômes comme "MA définitive" était l'analyse histologique post-mortem, ce qui peut certainement être considéré comme un diagnostic tardif. À cette époque, les stades plus précoces étaient classés comme "MA probable" ou "MA possible" et liés principalement à un trouble amnésique progressif avec démence affectant les fonctions cognitives et exécutives et par l'exclusion d'autres diagnostics (G. McKhann et al., 1984). Les critères diagnostiques ont donc subi une évolution nécessaire. Une réévaluation récente par le Groupe de Travail International a établi des critères pour le phénotypage clinique de la MA, ainsi que pour les stades asymptomatiques et présymptomatiques de la maladie. Ces critères ont été principalement utilisés dans la pratique clinique au cours de la dernière décennie (Dubois et al., 2014). La MA typique serait ainsi décrite comme la présence d'une déficience précoce et significative de la mémoire épisodique survenant progressivement et rapportée par le patient ou l'informateur comme ayant persisté pendant plus de 6 mois. Le patient doit également présenter un syndrome amnésique de type hippocampique, évalué par des performances significativement altérées lors d'un test de mémoire épisodique. De plus, le patient devrait présenter au

moins l'une des preuves in vivo suivantes : une diminution d'$A\beta_{42}$ avec une augmentation de Tau dans le LCR, une augmentation de la rétention du traceur sur le PET amyloïde, ou une mutation autosomique dominante de la MA dans PSEN1, PSEN2 ou APP (mutations impliquées dans les formes familiales de la MA). Les critères pour la MA asymptomatique ou présymptomatique résident principalement dans la présence de l'un des biomarqueurs in vivo ou d'une mutation autosomique dominante de la MA prouvée, respectivement, sans présenter de déficits cognitifs. Malgré une amélioration certaine par rapport à la classification précédente, cette dernière présente encore certaines lacunes. En effet, comme nous l'avons indiqué dans le chapitre précédent, les déficits mnésiques apparaissent après une progression déjà longue de la maladie ; attendre des troubles de la mémoire, et plus encore ceux qui durent déjà depuis 6 mois, signifie détecter la maladie à un stade déjà très avancé. D'un autre côté, nous avons vu précédemment que l'imagerie PET de certains biomarqueurs et le dosage du LCR peuvent montrer des marqueurs pathologiques avant les déficits cognitifs et pourraient donc apparaître comme une solution viable pour détecter les stades plus précoces de la maladie. Cependant, ces techniques sont des procédures invasives - injection intraveineuse d'un traceur radioactif pour les scans PET et ponction lombaire pour l'analyse du LCR - qui peuvent être traumatisantes pour le patient. Par conséquent, la nature invasive de ces procédures limite leur utilisation en l'absence de symptômes cliniques, conduisant à des diagnostics tardifs. En conséquence, les efforts se sont orientés vers une détection plus précoce par des techniques moins invasives. Une approche qui gagne en attention est l'affinement des examens cognitifs, qui pourrait permettre un diagnostic plus précoce en créant des tests plus sensibles et en tenant compte des plaintes cognitives des patients, même lorsqu'aucune déficience objective n'est détectée (comme dans le SCD ; Sabbagh et al. 2017). Outre ces examens cognitifs affinés, trouver un biomarqueur non invasif fiable pour les stades précoces comme le SCD représenterait une avancée majeure dans le diagnostic et la prise en charge de la MA, car cela faciliterait l'implémentation clinique et permettrait le diagnostic avant l'apparition de symptômes significatifs.

1.5.2. Les tentatives de traitement de la MA

À l'heure actuelle, il n'existe toujours pas de traitement pour la MA. Le protocole de traitement actuel vise principalement à maintenir la qualité de vie, à atténuer le fardeau

de la maladie et à ralentir la progression de la déficience cognitive en combinant des inhibiteurs de la cholinestérase et un antagoniste NMDA comme la mémantine (Atri, 2019). Cette combinaison montre en effet certains bénéfices sur les performances cognitives chez les patients atteints de MA, notamment en augmentant les niveaux d'acétylcholine aux synapses centrales (Grutzendler & Morris, 2001; Hampel et al., 2018). Cependant, ces traitements ciblent les symptômes plutôt que la pathologie sous-jacente de la MA.

Au cours des dernières décennies, de nombreux essais cliniques ont été menés pour divers composés, mais la plupart se sont soldés par un échec. Entre 2002 et 2012, 244 composés ont été testés dans 413 essais, avec un taux de succès pour l'approbation par la Food and Drug Administration (FDA) de seulement 0,4% (J. L. Cummings et al., 2014). Les efforts récents se sont concentrés sur de nouvelles approches pharmacologiques, telles que les anticorps qui se lient aux formes solubles d'Aβ (Solanezumab) ou les inhibiteurs de la γ-sécrétase (Semagacestat), qui visent à réduire la production d'Aβ. Malheureusement, aucune de ces approches n'a démontré d'amélioration cognitive (Doody et al., 2013, 2014), et dans certains cas, les inhibiteurs de la γ-sécrétase ont même aggravé les symptômes de la MA (Strooper, 2014). Étant donné les défis des interventions pharmacologiques et les effets secondaires associés à ces traitements, il y a un intérêt croissant pour l'exploration d'approches alternatives non invasives qui pourraient offrir une voie prometteuse pour le développement thérapeutique futur.

1.6. Évaluation de la mémoire chez les rongeurs

Comme mentionné précédemment, les patients atteints de MA présentent des altérations précoces dans plusieurs domaines cognitifs, notamment la mémoire de travail, la flexibilité cognitive et la mémoire spatiale. Dans les modèles de rongeurs de la maladie, différents types de mémoire peuvent également être évalués, fournissant des informations précieuses sur les mécanismes sous-jacents des déficits cognitifs initiaux. Nous allons passer en revue les tests pertinents (dont certains ont été utilisés dans notre travail) et discuter de la façon dont ils sont évalués et affectés par la maladie.

1.6.1. Mémoire de reconnaissance

Les rongeurs sont naturellement curieux et ont tendance à explorer les nouveaux objets dans leur environnement, un comportement qui constitue la base du paradigme de reconnaissance spontanée d'objets (Ennaceur & Delacour, 1988). Dans cette tâche, les rongeurs sont d'abord exposés à deux objets identiques. Après un intervalle inter-essai (ITI) spécifié, ils sont exposés à un objet familier et un objet nouveau. La plupart des rongeurs peuvent faire la distinction entre les deux, passant généralement plus de temps à explorer le nouvel objet, la mémoire de reconnaissance à court et à long terme étant évaluée en faisant varier l'ITI de quelques minutes à plusieurs heures, voire plusieurs jours.

Le cortex périrhinal (PRC) est une région cérébrale clé impliquée dans la mémoire de reconnaissance pour des ITI allant de 5 minutes à 24 heures (Barker et al., 2007; Wan et al., 1999; Winters et al., 2004; Winters & Bussey, 2005a, 2005c, 2005b). Cependant, le rôle de l'hippocampe (HPC) dans la reconnaissance d'objets reste débattu ; certaines études suggèrent que les lésions hippocampiques n'affectent pas la mémoire de reconnaissance (Winters et al., 2004), tandis que d'autres indiquent qu'elles l'affectent (Cohen et al., 2013). La complexité de la tâche peut influencer les contributions du PRC et de l'HPC, les deux régions pouvant potentiellement servir des fonctions complémentaires (Cinalli Jr. et al., 2020; Squire et al., 2007). De plus, l'HPC, le cortex préfrontal (PFC) et le cortex rétrosplénial (RSC) sont impliqués dans la reconnaissance d'objets à long terme lorsque l'ITI s'étend à 24 heures (de Landeta et al., 2020; Preston & Eichenbaum, 2013; Warburton & Brown, 2015).

Des déficits de reconnaissance d'objets sont progressivement observés dans divers modèles de souris de la MA. Différents modèles APP transgéniques simples présentent des déficits à différents âges : les souris tgCRND8 montrent des déficits de reconnaissance d'objets à long terme dès 8 semaines (Francis et al., 2012), les souris tg2576 à 13 semaines (Huang et al., 2006), et les souris J20 à 3 mois (Ameen-Ali et al., 2019). Dans les modèles APP/PS1 double-transgéniques, les déficits apparaissent vers 6 mois (Howlett et al., 2004), et chez les souris 5XFAD, à 4 mois, tous deux avec un ITI de 4 heures (D.-H. Kim et al., 2020). Ces résultats suggèrent que les modèles de souris transgéniques présentent généralement des déficits de reconnaissance d'objets vers 4 mois, avec une plus grande sensibilité pour la mémoire de reconnaissance à long terme. Il est intéressant de noter que les souris dKI AppNL-

F/MAPT ne montrent pas de déficience dans la reconnaissance d'objets à 6 mois, que l'ITI soit de 5 minutes ou de 24 heures (Borcuk et al., 2022).

1.6.2. Mémoire associative

L'exploration spontanée d'objets peut être adaptée pour évaluer des paradigmes de mémoire plus complexes au-delà de la simple reconnaissance d'objets, comme la mémoire associative. Dans les tâches de mémoire associative, les animaux doivent se souvenir de l'association entre différents éléments de la tâche. Un tel paradigme est la tâche Objet-en-Place (OiP), où les animaux rencontrent d'abord deux objets distincts. Après un intervalle inter-essai défini, généralement court, l'un des objets originaux est remplacé par un duplicata de l'autre objet familier. Ce test évalue la capacité de l'animal à détecter l'intrusion d'un objet familier dans la position précédemment occupée par un objet familier différent (Dix & Aggleton, 1999).
Différents réseaux et régions cérébrales sont impliqués selon la difficulté de la tâche. Alors que la version de la tâche avec quatre objets nécessite un réseau complexe qui inclut, sans s'y limiter, le PRC, le PFC, l'HPC et le RSC (Chao et al., 2022), la version à deux objets implique principalement le cortex entorhinal latéral (LEC) et le PFC (Chao et al., 2016; Kuruvilla et al., 2020).
La mémoire associative est notamment affectée précocement dans plusieurs modèles de souris de la MA. Les souris transgéniques simples tgCRND8 montrent des déficits dans les tâches OiP à deux objets dès 2 mois, même avant de présenter des déficits de reconnaissance d'objets ou une formation de plaques amyloïdes (Hamm et al., 2017). De même, les souris double-transgéniques APP/PS1 présentent des déficits dans les tâches OiP à deux objets vers 4 mois (Bonardi et al., 2021, p. 20). Enfin, les déficits dans la tâche OiP à deux objets semblent être les premiers déficits de mémoire détectables dans le modèle de souris dKI AppNL-F/MAPT, commençant à 4 mois d'âge (Borcuk et al., 2022).

2. Dynamiques Cérébrale

Le cerveau traite l'information à travers des motifs dynamiques d'activité neuronale qui se modifient et se réorganisent continuellement. Cette dynamique est fondamentale pour le fonctionnement cérébral, déterminant comment l'information est encodée,

transformée et transmise à travers les circuits neuronaux. Les récentes avancées en biologie, physique, techniques et plus globalement en neurosciences ont permis d'enregistrer l'activité cérébrale dans différents états cérébraux, pendant la réalisation de différentes tâches ou au cours de processus pathologiques, permettant une meilleure compréhension du fonctionnement cérébral dans diverses circonstances. Ces études ont révélé que l'activité cérébrale change selon différents états cérébraux et demandes cognitives, même de subtiles altérations dans la dynamique pouvant perturber le traitement de l'information. Cela souligne l'importance d'étudier la dynamique cérébrale pour comprendre à la fois le fonctionnement cognitif sain et son altération dans les conditions neurologiques.

2.1. Dynamique cérébrale ou la différence entre réseaux structurels et fonctionnels

Il est largement admis que les réseaux fonctionnels du cerveau sont influencés par les réseaux structurels sous-jacents. Cependant, même si les réseaux fonctionnels émergent principalement des réseaux structurels, cette relation n'est pas toujours directe (Mišić et al., 2016). Les réseaux structurels peuvent être cartographiés en utilisant l'IRM de diffusion, qui suit les faisceaux de matière blanche dans le cerveau et aide à construire le réseau anatomique sous-jacent du cerveau (Basser et al., 1994; Hagmann et al., 2007). Les réseaux fonctionnels, quant à eux, peuvent être examinés en utilisant des techniques comme l'EEG, la Magnétoencéphalographie (MEG) ou plus communément l'IRM fonctionnelle (IRMf), qui mesure le signal dépendant du niveau d'oxygène sanguin (BOLD), un indicateur de l'activité neuronale basé sur l'utilisation d'oxygène dans les régions cérébrales (H.-J. Park & Friston, 2013). Les corrélations entre les signaux BOLD à travers différentes régions permettent de calculer la connectivité fonctionnelle.

En combinant l'IRM structurelle et fonctionnelle, ces deux réseaux peuvent être comparés chez un même individu, révélant des résultats intéressants. Les motifs de connectivité fonctionnelle ne reflètent pas toujours l'organisation structurelle du cerveau et peuvent varier selon la tâche cognitive ou l'état de conscience. Par exemple, pendant les états de conscience réduite, la connectivité fonctionnelle s'aligne plus étroitement avec la connectivité structurelle du cerveau (Barttfeld et al., 2015). Ces différences deviennent plus prononcées lors de l'analyse de la connectivité

fonctionnelle sur des échelles de temps plus courtes, qui captent les fluctuations moment par moment des états cérébraux et évitent le moyennage statistique de l'activité dans le temps. Par conséquent, bien que les réseaux structurels fournissent les fondements de l'activité cérébrale, plusieurs réseaux fonctionnels peuvent émerger de cette topologie structurelle fixe, un phénomène appelé multiplicité fonctionnelle (Battaglia, 2014). Ces réseaux fonctionnels s'adapteront dynamiquement pour répondre aux demandes cognitives, des niveaux plus élevés de conscience ou d'engagement conduisant à une augmentation de la dynamique des motifs fonctionnels (Deco et al., 2015; Sarasso et al., 2015).

Cela souligne l'importance d'étudier la dynamique cérébrale. Dans les maladies neurodégénératives, les perturbations dans les motifs fonctionnels dynamiques peuvent précéder les changements détectables dans les réseaux structurels. Inversement, restaurer une dynamique fonctionnelle saine pourrait aider à compenser les dommages structurels, offrant une voie potentielle pour les interventions thérapeutiques (Stulz et al., 2024).

2.2. Dynamiques des systèmes non linéaires

L'activité cérébrale émerge d'interactions complexes entre neurones, régions et réseaux qui ne peuvent pas être totalement comprises à travers de simples relations linéaires. Alors que les systèmes linéaires suivent le principe de superposition, où la réponse à des entrées combinées égale la somme des réponses aux entrées individuelles, la dynamique cérébrale est fondamentalement non linéaire - le tout est différent de la somme de ses parties. Cette non-linéarité permet au cerveau de générer une dynamique riche nécessaire à la cognition, mais rend également l'activité cérébrale plus difficile à analyser et à prédire.

Pour évaluer la dynamique cérébrale non linéaire, nous devons d'abord considérer les séries temporelles de l'activité cérébrale enregistrées dans l'espace des phases. L'espace des phases est un espace mathématique où tous les états possibles d'un système dynamique sont représentés. Pour la dynamique cérébrale, chaque point dans cet espace pourrait représenter une configuration particulière d'activité neuronale à travers plusieurs canaux ou régions cérébrales. L'évolution du système dans le temps trace une trajectoire dans cet espace des phases.

2.2.1. Stabilité et Dimensionnalité

Une des principales caractéristiques pour évaluer la dynamique d'un système réside dans sa stabilité et sa dimensionnalité. Ces mesures permettent de caractériser la forme dynamique du système et s'il s'organise autour d'états dynamiques stables ou instables appelés attracteurs de phase. Le spectre de Lyapunov représente un moyen de caractériser la stabilité du système dynamique en capturant les taux d'expansion ou de contraction le long de différentes directions dans l'espace des phases (Wolf et al., 1985). Chaque exposant de Lyapunov du spectre quantifie la divergence, donc l'instabilité (s'il est positif) ou la convergence, donc la stabilité (s'il est négatif) des trajectoires voisines dans l'espace des phases.

Le spectre de Lyapunov est intimement lié à la dimensionnalité de l'attracteur du système, connue sous le nom de dimension de Lyapunov ou de Kaplan-Yorke. Cette mesure estime le nombre de degrés de liberté gouvernant la dynamique du système. Ces mesures permettent de caractériser le système : des exposants uniquement négatifs dans le spectre de Lyapunov couplés à une faible dimension de l'attracteur décriront un système simple où, de n'importe où dans l'espace des phases, le système sera attiré vers un attracteur stable. D'un autre côté, un exposant positif dans le spectre de Lyapunov couplé à un attracteur de haute dimension décrira un système chaotique qui sera hautement sensible aux conditions initiales. En effet, lorsqu'il y a à la fois des exposants négatifs et positifs dans le spectre de Lyapunov, selon les conditions initiales, la dynamique peut converger vers un attracteur ou les trajectoires dans l'espace des phases peuvent diverger. Certains attracteurs prototypiques peuvent aussi être caractérisés par des exposants nuls et négatifs dans le spectre de Lyapunov, décrivant un attracteur oscillatoire stable. Dans le cerveau, la dynamique EEG semble ne pas montrer de forme non linéaire spécifique, mais ce système montre tout de même des changements de conformation selon les états cérébraux avec une dynamique moins complexe passant à une dimension plus basse et un exposant maximal de Lyapunov plus faible pendant le sommeil profond (Stam, 2005). Ainsi, les caractéristiques non linéaires du système dans l'espace des phases peuvent servir à mesurer la dynamique cérébrale globale en condition saine mais aussi comment elle est impactée par les pathologies, comme cela a été fait pour l'épilepsie (Babloyantz & Destexhe, 1986).

2.2.2. Stabilité et dimensions instantanées

Malgré le fait qu'elles permettent une première caractérisation du système dynamique, les mesures de Lyapunov précédemment mentionnées présentent des limites majeures : elles nécessitent une connaissance complète des équations régissant le système, des données de séries temporelles étendues, et ne sont pas précises dans le temps. Cependant, lors de la réalisation de tâches cognitives, on pourrait s'attendre à ce que le système dynamique puisse basculer entre des conformations stables et instables pour permettre des patterns dynamiques complexes favorisant le traitement de l'information.

Les avancées récentes dans l'analyse des systèmes dynamiques ont introduit des métriques dérivées de la théorie des valeurs extrêmes qui s’affranchissent de ces limitations. Deux métriques clés sont la persistance inverse (θ) et la dimension instantanée. La persistance inverse, mathématiquement liée à l'indice extrémal dans la théorie des valeurs extrêmes, quantifie la fréquence à laquelle un système transite entre différents états. Une valeur θ plus basse indique une stabilité plus élevée (le système reste plus longtemps dans les états), tandis que des valeurs plus élevées suggèrent des transitions d'état plus fréquentes. Cette métrique reflète ainsi la fluidité du système. La dimension instantanée caractérise la densité des états voisins autour d'une configuration donnée, reflétant la prévisibilité locale et la complexité.

Ces métriques sont particulièrement précieuses car elles peuvent être calculées uniquement à partir des données de séries temporelles empiriques, sans nécessiter la connaissance des équations sous-jacentes du système. Bien qu'initialement développées pour étudier les flux atmosphériques et les événements météorologiques extrêmes (Faranda et al., 2017), ces approches sont bien adaptées pour analyser la dynamique cérébrale. Tout comme les flux atmosphériques sont caractérisés par une dynamique chaotique et des motifs récurrents à grande échelle, l'activité cérébrale montre une complexité similaire avec des transitions entre différents états fonctionnels. Lorsqu'on considère le cerveau comme un système dynamique, les premiers stades de la maladie pourraient se manifester par des changements dans ces propriétés instantanées plutôt que par des changements globaux dans le comportement du système. L'évaluation des propriétés instantanées du système comme la persistance (ou son inverse, la fluidité) et la dimension pourrait ainsi représenter une approche prometteuse pour comprendre le fonctionnement cérébral dans des conditions saines

et pathologiques. Dans ce manuscrit de thèse, vous verrez plus loin comment nous avons utilisé la fluidité dynamique instantanée du cerveau pour évaluer la pathologie MA précoce, offrant des perspectives sur la stabilité du système qui pourraient être difficiles à accéder via l'analyse traditionnelle de Lyapunov car les algorithmes classiques (Grassberger & Procaccia, 1983) nécessitent beaucoup plus de données pour converger correctement.

2.2.3. Paysages énergétiques

Les attracteurs peuvent être caractérisés comme précédemment par des mesures de stabilité. Cependant, ils peuvent aussi être vus comme des puits d'énergie. En effet, la dynamique du système peut être représentée comme une balle roulant sur un plan comportant des puits et des collines : si la balle monte une colline, elle en tombera rapidement, au contraire si elle tombe dans un puits, elle y restera très probablement et nécessitera beaucoup d'énergie pour en sortir. Dans ce contexte, les puits représenteront les états dynamiques les plus probables, donc étant des états de basse énergie et étant des attracteurs. Au contraire, les collines représentent des états instables moins probables de haute énergie.

Ces paysages énergétiques peuvent être déterminés en utilisant une approche statistique comme les modèles d'Entropie Maximum qui visent à trouver la distribution présentant l'entropie la plus élevée satisfaisant les contraintes observées, l'énergie ici se réfère à la définition de la théorie de l'information au lieu de celle métabolique et représentera principalement la probabilité d'apparition des états. Ces paysages énergétiques ont été appliqués aux données de réseaux fonctionnels et structurels du cerveau et utilisés pour caractériser les réseaux cérébraux au repos (Watanabe et al., 2014). Ils se sont montrés appropriés pour décrire la dynamique des modules dans le connectome cérébral humain (Ashourvan et al., 2017), et se sont révélés être liés à la connectivité structurelle (S. Gu et al., 2018). Combiner les paysages énergétiques et la fluidité et dimension instantanées précédemment discutées pourrait donc être une approche prometteuse pour caractériser correctement la dynamique du système. Une fluidité réduite résulterait-elle de la création d'un nouveau puits d'énergie ou de l'approfondissement d'un puits existant ? L'examen de ces patterns énergétiques permettrait alors d'identifier les réseaux impliqués dans ces patterns spécifiques d'énergie et de fluidité.

2.3. Dynamique Cérébrale et Mémoire

Puisque la dynamique cérébrale joue un rôle crucial dans le traitement de l'information, elle apparaît donc essentielle pour l'établissement correct des processus de mémoire, qui sont un élément clé de ce manuscrit. Cette section explorera l'implication de la dynamique cérébrale dans divers processus mnésiques bien étudiés.

2.3.1. Mémoire de reconnaissance

La mémoire de reconnaissance représente un exemple de la façon dont la dynamique cérébrale soutient la fonction cognitive à travers de multiples mécanismes complémentaires. Il est proposé que la mémoire de reconnaissance repose sur la dynamique des attracteurs au sein des réseaux neuronaux. Lorsque les souvenirs sont initialement formés, des assemblées spécifiques de neurones s'activent ensemble, renforçant leurs connexions synaptiques par la plasticité hebbienne. Ces connexions renforcées créent des attracteurs stables dans l'espace d'états du réseau, chacun correspondant à une trace mnésique distincte. Lorsqu'un stimulus familier est rencontré, les entrées sensorielles guident l'activité neuronale vers ces attracteurs préétablis. Ce processus dynamique permet non seulement la reconnaissance directe mais soutient également la complétion de motifs (c'est-à-dire la capacité à reconstruire des souvenirs complets à partir d'indices partiels ou dégradés), car même des entrées incomplètes peuvent conduire le système vers le bassin d'attraction approprié (Daelli & Treves, 2010).

Cependant, la mémoire de reconnaissance ne repose pas uniquement sur la dynamique des attracteurs pour détecter la familiarité. Elle dépend aussi de manière critique de la capacité du cerveau à détecter la nouveauté à travers des processus dynamiques distincts. Dans une tâche de NOR, l'HPC présente une augmentation de la puissance des oscillations thêta lors de l'exploration du nouvel objet, signalant potentiellement la détection d'une nouvelle information. Cette réponse à la nouveauté implique une dynamique coordonnée entre l'HPC et le PFC, principalement à travers une synchronisation des oscillations thêta médiée par des projections directes de l'HPC vers le PFC, établissant ainsi un circuit fonctionnel pour le traitement de la nouveauté. L'importance de cette interaction dynamique est soulignée par les résultats

montrant que la perturbation du couplage HPC-PFC en thêta altère les performances dans les tâches de reconnaissance d'objets nouveaux (C. Wang et al., 2021).
Ces processus dynamiques complémentaires, détection de la familiarité basée sur les attracteurs et détection de la nouveauté médiée par les oscillations, travaillent ensemble pour permettre une mémoire de reconnaissance flexible et fiable.

2.3.2. Mémoire de travail

Tous les souvenirs ou événements ne peuvent pas être consolidés pendant le sommeil, car certaines informations doivent être stockées uniquement temporairement pour un rappel rapide. À cette fin, la mémoire de travail est employée, définie comme un système pour maintenir et manipuler l'information sur de courtes périodes (Baddeley, 1986). Une région cérébrale clé impliquée dans la mémoire de travail est le PFC, car il est actif pendant les tâches de mémoire de travail (Funahashi, 2006; Leung et al., 2002; Ungerleider et al., 1998; Zarahn et al., 2000) et ses lésions affectent les performances en mémoire de travail (Goldman-Rakic, 2011; Milner, 1963). Il est important de noter que la mise en tampon de l'information dans le PFC est largement facilitée par des processus dynamiques.
Un processus dynamique clé implique le transfert de la trace mnésique vers le PFC, facilité par des interactions fonctionnelles de longue portée entre l'hippocampe et le PFC. Notamment, ce transfert repose sur un motif dynamique précédemment mentionné : le couplage phase-amplitude (PAC) thêta-gamma. Pendant les tâches de mémoire de travail, un couplage émerge entre l'amplitude des oscillations gamma dans le PFC et la phase des oscillations thêta hippocampiques. Ce couplage s'intensifie avec des périodes de rétention mnésique plus longues, particulièrement lorsque des délais sont introduits dans la tâche ou lorsque les tâches augmentent en complexité (Tamura et al., 2017). On pense que ce PAC thêta-gamma organise l'activité de décharge du PFC en relation avec la dynamique hippocampique.
Il est intéressant de noter que le PFC présente des réseaux d'attracteurs avec des connexions excitatrices récurrentes entre les neurones pyramidaux, permettant à ces réseaux de maintenir des patterns stables d'activité neuronale même après que le stimulus soit retiré, permettant ainsi le maintien de la mémoire à court terme (Deco & Rolls, 2003). Cependant, ce 'maintien de la mémoire' est basé sur une représentation dynamique plutôt que stable, car les décodeurs entraînés à décoder l'identité des stimuli visuels lorsqu'ils sont visibles basés sur l'activité neuronale du PFC étaient

incapables de décoder la mémoire de ce stimulus même après un court délai de 250 ms (Stokes et al., 2013). Enfin, à plus grande échelle, la mémoire de travail semble reposer sur un fonctionnement en régime critique au sein du cerveau. Les individus présentant une activité en avalanche du cerveau entier plus proche de la criticité démontrent une connectivité fonctionnelle plus complexe et de meilleures performances dans les tâches de mémoire de travail (Xu et al., 2022, p. 202).

2.4. Dynamique Cérébrale dans la MA

La MA est caractérisée par des altérations significatives de la dynamique cérébrale, l'un des premiers changements observables dans les réseaux étant l'hyperactivité neuronale. Cette hyperactivité est d'abord notée dans des groupes de neurones hyperactifs situés près des plaques amyloïdes (Busche et al., 2008). Il est intéressant de noter que les signes d'hyperactivité peuvent apparaître plus tôt dans la maladie et sont souvent associés à des symptômes communément observés dans l'épilepsie, une comorbidité majeure chez les patients atteints de MA, particulièrement ceux présentant des formes précoces génétiquement liées (Horváth et al., 2018; Lam et al., 2020; Vossel et al., 2016). Dans la MA, l'hyperexcitabilité est fréquemment indiquée par la présence de pointes intericales pendant le sommeil dans les modèles murins, qui servent de marqueurs d'hypersynchronie pathologique au sein des réseaux neuronaux (Bezzina et al., 2015; Palop et al., 2007; Szabo et al., 2023; Verret et al., 2012). Cette hyperactivité serait due à un dysfonctionnement des interneurones inhibiteurs exprimant la parvalbumine, qui influencent directement l'activité des neurones pyramidaux devenant hyperactifs dans la MA. Ces interneurones sont cruciaux pour la génération des rythmes gamma, qui se sont révélés être diminués à la fois dans les modèles murins de MA et chez les patients (Casula et al., 2022; Hamm et al., 2017; Iaccarino et al., 2016; Verret et al., 2012). Notamment, la restauration du fonctionnement normal des interneurones PV dans un modèle animal de MA s'est avérée améliorer l'activité gamma, réduire l'hyperactivité et améliorer la fonction cognitive (Verret et al., 2012). Ces altérations de l'activité gamma seront un point clé dans le Chapitre III de cette introduction.

Cependant, les réductions des oscillations gamma ne sont pas les seules altérations oscillatoires observées dans la MA. Le PAC entre les oscillations thêta et gamma, crucial pour les processus de mémoire, est perturbé dans l'hippocampe avant l'accumulation d'Aβ (Goutagny et al., 2013).

Cette découverte indique des changements plus larges dans la dynamique fonctionnelle des réseaux oscillatoires dans la MA, caractérisés par ce qu'on appelle un "ralentissement de l'EEG" (Dauwels et al., 2011). Plus précisément, alors que la puissance des rythmes de plus haute fréquence comme le gamma et le bêta est diminuée, il y a une augmentation de la puissance des rythmes plus lents comme le delta et le thêta, résultant en cet effet global de ralentissement (Baker et al., 2008; Claus et al., 1998; Czigler et al., 2008; Moretti et al., 2009; van der Hiele et al., 2007). À plus grande échelle, un ralentissement général de la dynamique est également observé dans la MA. L'analyse des micro-états EEG a montré que les séquences sont moins dynamiques, caractérisées par des durées plus longues des micro-états individuels (Lian et al., 2021; Tait et al., 2020). Comme mentionné précédemment, les altérations dans la durée des micro-états peuvent affecter la dynamique invariante d'échelle de ces séquences (Van De Ville et al., 2010). En fait, les patients atteints de MA présentent non seulement des transitions d'état dynamiques réduites mais aussi moins de séquences complexes de micro-états, comme en témoigne une diminution de la complexité de Lempel-Ziv, suggérant un éloignement du bord du chaos du système (Tait et al., 2020). L'analyse des réseaux cérébraux dynamiques à grande échelle à travers la connectivité fonctionnelle dynamique (dFC) révèle que la MA est associée à des fluctuations spatio-temporelles désordonnées qui sont caractéristiques de la dFC saine (Arbabyazd et al., 2023; Canal-Garcia et al., 2024; Y. Gu et al., 2020; Núñez et al., 2021; Schumacher et al., 2019). Notamment, pendant les états de repos, les patients atteints de MA démontrent une flexibilité de réseau réduite et une intégration accrue entre les régions dans différents réseaux de repos, indiquant une perte de capacité dynamique (Canal-Garcia et al., 2024). De plus, la dynamique cérébrale chez les patients atteints de MA s'est révélée être piégée dans des états hypersynchronisés, conduisant à des altérations de la méta-connectivité et une "frustration" générale au sein du système, qui contribue à un ralentissement de la dynamique (Arbabyazd et al., 2023). Ces observations s'alignent avec la perte de complexité du système précédemment discutée (Tait et al., 2020). En outre, des études utilisant l'IRMf et l'EEG ont montré que la MA est associée à une irréversibilité réduite des signaux neuronaux, corrélée avec le déclin cognitif et l'atrophie (Cruzat et al., 2023).

En résumé, la MA est marquée par des altérations dynamiques à plusieurs échelles, toutes convergeant vers un répertoire diminué de régimes dynamiques et une perte

de complexité. Ces changements impactent négativement le fonctionnement sain des réseaux cérébraux, sapant la capacité à générer des processus cognitifs efficaces.

3. Stimulations sensorielles pour guérir la MA : le GENUS

Récemment, une nouvelle thérapie non invasive consistant en une stimulation multi-sensorielle à une fréquence de 40 Hz appelée Entraînement Gamma Utilisant des Stimuli Sensoriels (GENUS) (Singer et al., 2018) attire de plus en plus l'attention après avoir fourni des résultats étonnamment intéressants dans la MA et d'autres neuropathologies.

3.1. GENUS and AD

GENUS a été développé initialement contre la pathologie MA et est encore aujourd'hui principalement étudié dans le contexte de la pathologie MA.

3.1.1. Pourquoi nous avons commencé à utiliser la lumière clignotante dans la MA ?

Une question importante se pose : comment en sommes-nous venus à utiliser les stimulations lumineuses ou sonores à 40 Hz comme traitement potentiel de la MA ? Bien que cela puisse sembler peu conventionnel à première vue, cette approche est fondée sur des découvertes montrant que les oscillations gamma sont perturbées dans les modèles murins de MA. Si vous vous souvenez de notre discussion dans le chapitre précédent, nous avons souligné comment, dans la MA, les perturbations des oscillations gamma sont liées à une altération de la fonction des interneurones à décharge rapide exprimant la PV. En 2012, Verret et collaborateurs ont démontré que le modèle murin hAPP J20 présente des altérations des interneurones PV, notamment une expression réduite des canaux NaV1.1. Ces canaux sodiques voltage-dépendants, critiques pour la génération de potentiels d'action dans les interneurones PV, soutiennent leur action inhibitrice et aident à réguler l'équilibre excitateur-inhibiteur dans les réseaux corticaux. Dans le modèle hAPP J20, la diminution de NaV1.1 était associée à une diminution des oscillations gamma (gamme 20-80 Hz) et à une altération de la mémoire. Remarquablement, l'augmentation des niveaux de NaV1.1 spécifiquement dans les interneurones PV chez ces souris hAPP J20 a restauré l'activité gamma et réduit les déficits de mémoire (Verret et al., 2012). De plus, il a été

constaté que le modèle de souris 5XFAD présente une activité gamma lente réduite (30-50 Hz) dans l'hippocampe pendant les événements SW-R, ce qui est associé à des niveaux élevés d'Aβ sans accumulation significative de plaques ni preuve de déficit cognitif (Iaccarino et al., 2016). Ensemble, ces résultats indiquent que les altérations des oscillations gamma peuvent servir d'indicateur des perturbations des réseaux corticaux et hippocampiques dans la MA. Ainsi, restaurer l'activité gamma pourrait avoir un impact positif sur la pathologie.

Pour tester cette hypothèse, Iacarrino et ses collaborateurs se sont appuyés sur des découvertes montrant que l'activation optogénétique des interneurones PV à 40 Hz augmente la puissance gamma corticale (Cardin et al., 2009). Ils ont donc stimulé les cellules PV de CA1 à 40 Hz pour moduler les oscillations gamma hippocampiques. Une heure de cette stimulation a effectivement augmenté la puissance LFP à 40 Hz dans CA1, mais plus intriguant encore, elle a également réduit les niveaux des peptides $A\beta_{40}$ et $A\beta_{42}$ dans cette région. Cet effet semblait résulter d'une diminution de la production d'Aβ, car des réductions des sous-produits du clivage de l'APP, tels que les fragments C-terminaux (CTF), ont également été observées après une heure de stimulation. Ces résultats suggèrent que l'activation des cellules PV hippocampiques à 40 Hz (et donc l'augmentation des oscillations gamma) réduit la pathologie amyloïde.

Aussi prometteuse que cette approche puisse être, la stimulation optogénétique de types neuronaux spécifiques n'est pas facilement transférable aux patients humains. Cependant, de nombreuses études ont montré que la stimulation visuelle peut entraîner des oscillations dans la bande de fréquence gamma (Fries et al., 2007; Gray et al., 1989). Ils se sont donc demandé si la stimulation visuelle à 40 Hz pouvait similairement entraîner des oscillations gamma et présenter les mêmes effets bénéfiques. Une heure de clignotement visuel à 40 Hz a réussi à induire des oscillations à 40 Hz dans le cortex visuel et à réduire les niveaux d'$A\beta_{40}$ et Aβ42 solubles et insolubles dans cette zone cérébrale. De manière frappante, l'effet était spécifique au clignotement à 40 Hz car ni la lumière constante ni le clignotement à 20 Hz, 80 Hz ou aléatoire n'ont significativement réduit les niveaux d'Aβ par rapport aux contrôles sombres et lumineux. Enfin, un protocole chronique de sept jours d'une heure quotidienne de stimulation visuelle a réduit la charge en plaques amyloïdes dans le cortex visuel de souris 5XFAD âgées de six mois (Iaccarino et al., 2016).

3.1.2. Effets bénéfiques de GENUS dans la MA

Alors que GENUS a commencé comme un protocole de stimulation visuelle, il a été étendu pour tester plusieurs modalités sensorielles, y compris la stimulation vibrotactile (Suk et al., 2023). Cependant, il a rapidement évolué pour combiner des stimuli visuels et auditifs, qui ont montré des résultats supérieurs (Martorell et al., 2019). Parmi les preuves les plus convaincantes de l'efficacité de GENUS figure l'amélioration constante des performances cognitives à travers plusieurs modèles de souris MA et groupes d'âge. Les études ont démontré la restauration de la mémoire spatiale (Adaikkan et al., 2019; S. Liu et al., 2023; Martorell et al., 2019) et de la mémoire de reconnaissance d'objets (Martorell et al., 2019; Murdock et al., 2024). Cependant, les mécanismes sous-jacents à ces effets bénéfiques restent incomplètement compris, avec plusieurs hypothèses proposées pour expliquer les actions thérapeutiques de GENUS.

3.1.3. Hypothèse de la restauration des oscillations gamma

La stimulation non invasive GENUS s'est révélée capable d'entraîner des oscillations à 40 Hz et de moduler l'activité neuronale dans de multiples régions cérébrales, incluant les cortex auditif, visuel, somatosensoriel et préfrontal, ainsi que l'hippocampe (Adaikkan et al., 2019). Comme mentionné précédemment, les oscillations gamma sont constamment diminuées dans les modèles animaux de la maladie d'Alzheimer et chez les patients humains. Étant donné le rôle présumé des oscillations gamma dans l'organisation des assemblées cellulaires et la facilitation des interactions entre réseaux (Buzsaki, 2006), l'induction d'activité gamma par GENUS pourrait contribuer aux améliorations de la fonction mnésique. En conséquence, des preuves récentes montrent que GENUS peut renforcer la coordination gamma entre les régions CA3 et CA1 de l'hippocampe, contribuant potentiellement à l'amélioration des performances en mémoire spatiale (Paulson et al., 2024).

3.1.4. L'accent sur l'hypothèse amyloïde

Compte tenu des observations initiales des effets de GENUS sur le peptide Aβ et les plaques amyloïdes (Iaccarino et al., 2016) et de la prédominance de l'hypothèse amyloïde dans la recherche sur la MA (Selkoe & Hardy, 2016), les premières études

mécanistiques se sont concentrées sur l'amyloïdopathie comme explication primaire des bénéfices cognitifs de GENUS. La stimulation GENUS non invasive a réduit la neurodégénérescence (Adaikkan et al., 2019) et diminué les concentrations d'$A\beta_{40}$ et $A\beta_{42}$ solubles et insolubles, ainsi que la charge en plaques amyloïdes dans plusieurs régions (S. Liu et al., 2023; Martorell et al., 2019; Shen et al., 2022). Bien que les premières preuves suggéraient que la réduction des niveaux d'Aβ pourrait provenir d'une diminution de la production, spécifiquement, par une réduction du clivage amyloïdogénique de l'APP par la β-sécrétase et une amélioration des voies non-amyloïdogéniques de l'α-sécrétase (Iaccarino et al., 2016; Shen et al., 2022), les recherches ultérieures ont mis l'accent sur l'amélioration des mécanismes de clairance d'Aβ par de multiples voies. Premièrement, il modifie l'activité microgliale par plusieurs mécanismes : altération de la morphologie microgliale (Iaccarino et al., 2016; Martorell et al., 2019), réduction de la neuroinflammation (Adaikkan et al., 2019), et promotion du regroupement microglial autour des plaques amyloïdes, ce qui augmente la captation d'Aβ (Iaccarino et al., 2016; Martorell et al., 2019). Deuxièmement, GENUS améliore la fonction vasculaire cérébrale en favorisant la pulsatilité artérielle et le flux vasculaire, particulièrement par la modulation astrocytaire (Martorell et al., 2019; Murdock et al., 2024). Enfin, il facilite la clairance d'Aβ via le système glymphatique à travers la régulation des canaux Aquaporine 4 (Murdock et al., 2024).

Selon ce cadre centré sur l'amyloïde, le GENUS améliorerait la fonction cognitive principalement en améliorant la clairance cérébrale d'Aβ par les voies microgliales et glymphatiques. Cette réduction des niveaux pathologiques d'Aβ conduirait ensuite à une amélioration de la fonction neuronale et une réduction de la pathologie MA. Cependant, comme nous le verrons plus tard, des études récentes ont remis en question certains aspects de ce mécanisme, indiquant la nécessité d'explorer des cadres explicatifs supplémentaires.

3.1.5. Neuroprotection, Neurogénèse et plasticité synaptique

Au-delà de ses effets sur la pathologie amyloïde, le GENUS démontre de multiples effets bénéfiques qui pourraient contribuer à l'amélioration des résultats dans la MA. L'exposition chronique au GENUS réduit la neurodégénérescence et fournit des bénéfices neuroprotecteurs directs en régulant positivement les protéines cytoprotectrices et en réduisant les dommages à l'ADN (Adaikkan et al., 2019). Cet

effet neuroprotecteur est particulièrement significatif étant donné que la MA est principalement une maladie neurodégénérative.

Les effets protecteurs du GENUS s'étendent au-delà des neurones pour inclure l'intégrité de la matière blanche. Dans la MA, les gaines de myéline produites par les oligodendrocytes subissent des altérations significatives, altérant la transmission des signaux axonaux (Nasrabady et al., 2018; Y. Wu et al., 2017). Des études récentes démontrent que GENUS peut réduire la démyélinisation, prévenir la perte d'oligodendrocytes et stimuler l'oligodendrogenèse dans les modèles de démyélinisation, suggérant un mécanisme potentiel pour maintenir la connectivité neuronale fonctionnelle (Rodrigues-Amorim et al., 2024).

En plus de ses effets protecteurs, le GENUS pourrait également favoriser la génération de nouveaux neurones. Bien que la neurogénèse adulte soit typiquement limitée à des régions cérébrales spécifiques comme le gyrus denté hippocampique ou le bulbe olfactif et produise relativement peu de neurones (Gage, 2019), des études récentes indiquent que le GENUS peut améliorer ce processus. Cet effet neurogénique semble dépendre des interneurones exprimant la parvalbumine et corrèle avec une amélioration de la fonction cognitive (Islam et al., 2024; Yan et al., 2024).

3.2. Trop beau pour être vrai ?

Des études récentes ont soulevé des questions importantes sur plusieurs aspects fondamentaux du GENUS et de ses mécanismes d'action supposés. Un point de débat principal concerne la nature de l'activité oscillatoire induite. Alors que la plupart des études sur le GENUS rapportent une "augmentation de la puissance gamma" pendant la stimulation, une analyse attentive révèle que cette augmentation se manifeste principalement comme un pic aigu dans le spectre de puissance à 40 Hz, directement entraîné par la fréquence de stimulation. Cela a conduit à l'argument que le GENUS pourrait ne pas réellement entraîner des oscillations gamma natives ou des oscillateurs gamma physiologiques, mais plutôt entraîner les régions cérébrales à 40 Hz, suggérant un processus distinct de celui initialement proposé avec des implications mécanistiques différentes (Duecker et al., 2021; Soula et al., 2023).

Un second débat significatif se centre sur l'étendue spatiale des effets du GENUS. Alors que les études initiales rapportaient un entraînement à 40 Hz se propageant à des régions distantes incluant l'hippocampe et le cortex préfrontal (Adaikkan et al., 2019; Martorell et al., 2019), des investigations récentes suggèrent une propagation

spatiale plus limitée. Certaines études rapportent que l'entraînement visuel à 40 Hz s'étend à peine au-delà du cortex visuel et est notamment absent dans l'hippocampe (Schneider et al., 2023; Soula et al., 2023). Il est intéressant de noter que l'entraînement le plus fort apparaît dans les cellules excitatrices du Noyau Géniculé Latéral, tandis que l'activation du cortex visuel cible préférentiellement les interneurones à décharge rapide exprimant la parvalbumine (Schneider et al., 2023).

Le troisième point majeur de contestation concerne les effets du GENUS sur la pathologie amyloïde. Des études récentes n'ont pas réussi à reproduire les réductions rapportées de la charge en plaques amyloïdes suite à la stimulation GENUS (Soula et al., 2023; Y. L. Yang & Lai, 2023). Cependant, il est important de noter que certaines de ces études n'ont employé que des protocoles de stimulation aigus, soulignant l'importance potentielle de la stimulation chronique pour obtenir des effets thérapeutiques.

Notamment, malgré ces remises en question d'aspects mécanistiques spécifiques du GENUS, aucune de ces études n'a directement évalué ce qui pourrait être l'effet le plus crucial : la restauration des performances mnésiques. Ainsi, bien que ces débats nécessitent une réévaluation des mécanismes sous-jacents aux effets du GENUS, ils n'invalident pas le potentiel thérapeutique de l'approche. Ils suggèrent plutôt la nécessité de nouvelles hypothèses concernant son mode d'action qui s'étendent au-delà des explications simples d'entraînement à 40 Hz et centrées sur l'amyloïde.

Résultats : Caractérisation non linéaire des altérations de la dynamique cérébrale globale chez de jeunes souris dKI modèles de MA préclinique et effets d'un protocole vGENUS chronique

40 Hz light stimulation restores early brain dynamics alterations and associative memory in Alzheimer's disease model mice

Matthieu Aguilera[1], Chantal Mathis[1], Karin Herbeaux[1], Amine Isik[1], Davide Faranda[2], Demian Battaglia[1,*] & Romain Goutagny[1,*]

[1] Université de Strasbourg, CNRS, Laboratoire de Neurosciences Cognitives et Adaptatives (LNCA), UMR 7364, F–67000 Strasbourg, France.
[2] Université Paris Saclay, CEA – CNRS – UVSQ, Laboratoire des Sciences du Climat et de l'Environnement (LSCE), F-91191 Gif-sur-Yvette, France
* Demian Battaglia – Romain Goutagny.
Email: dbattaglia@unistra.fr – goutagny@unistra.fr

Author Contributions: M.A. and R.G. performed the experiments and analyzed the data. C.M. provided the animals and gave inputs for behavioral experiments. K.H. performed immunochemistry experiments. A.I. managed the animal breeding and genotyping. D.F. provided code for dynamic fluidity analyses. R.G. and D.B. conceived the experimental and analytical design; M.A., R.G. and D.B. wrote the article.

Competing Interest Statement: The authors declare no competing interests.
Classification: Biological sciences, Neurosciences
Keywords: Alzheimer's disease, EEG, Dynamics, Gamma stimulation, GENUS

Résumé

Les biomarqueurs précoces sont cruciaux pour une intervention rapide dans la maladie d'Alzheimer (MA). Nous avons étudié les altérations de la dynamique cérébrale chez de jeunes souris AppNL-F/MAPT double knock-in (dKI), un modèle de MA précoce, avant l'apparition des plaques amyloïdes. En utilisant des enregistrements EEG haute densité et de nouvelles métriques issues de domaines extérieurs aux neurosciences, nous avons évalué la fluidité de la dynamique cérébrale—une mesure de la capacité du cerveau à transiter entre différents états d'activité. Nous avons révélé que les souris dKI présentent des réductions précoces et spécifiques à l'état d'éveil de la fluidité de la dynamique cérébrale, associées à des déficits cognitifs dans des tâches de mémoire complexes. Pour étudier les interventions potentielles ciblant ces dynamiques cérébrales altérées, nous avons appliqué l'entraînement gamma visuel utilisant des stimuli sensoriels (vGENUS). Des sessions quotidiennes de vGENUS sur deux semaines ont restauré la fluidité de la dynamique cérébrale et corrigé les déficits de mémoire chez les souris dKI. Il est important de noter que ces effets s'accumulent pendant le protocole de stimulation et persistent après la fin de la stimulation, suggérant une modulation à long terme de la fonction cérébrale. Nos résultats identifient l'altération de la dynamique cérébrale comme un marqueur précoce des changements liés à la MA et démontrent que vGENUS est une intervention non pharmacologique prometteuse. Cette étude fournit de nouvelles perspectives sur la physiopathologie précoce de la MA et suggère de nouvelles approches pour le diagnostic précoce et le traitement.

Introduction

La maladie d'Alzheimer (MA) est un trouble neurodégénératif dévastateur et la principale cause de démence dans le monde, définie par la conjonction d'une perte progressive de la mémoire et d'un déclin cognitif avec des changements neuropathologiques spécifiques. Malgré sa prévalence élevée et probablement sous-estimée (1), des traitements efficaces et des outils de diagnostic précoce restent insaisissables. Les caractéristiques pathologiques de la MA incluent les plaques amyloïdes extracellulaires formées par le peptide bêta-amyloïde (Aβ) agrégé, et les

enchevêtrements neurofibrillaires intracellulaires de protéines Tau hyperphosphorylées. Pendant des décennies, l'hypothèse amyloïde a dominé la recherche sur la MA, postulant que l'accumulation d'Aβ et les plaques amyloïdes induisent des dysfonctionnements des réseaux responsables des déficits cognitifs (2). Le diagnostic de la MA nécessite la présence à la fois d'une déficience cognitive et de preuves de pathologie amyloïde qui est détectée soit par l'analyse du liquide céphalo-rachidien (LCR) via ponction lombaire pour mesurer la réduction des niveaux d'Aβ soluble (3), soit par des techniques de neuroimagerie telles que la tomographie par émission de positons (TEP) pour visualiser les dépôts d'Aβ insolubles (4). Cependant, des preuves croissantes remettent en question le moment et la spécificité de ces critères diagnostiques : les déficits de mémoire précèdent souvent la formation détectable de plaques amyloïdes (5-8) et peuvent survenir indépendamment d'Aβ (9). Inversement, les plaques amyloïdes sont parfois présentes chez des individus âgés non pathologiques ou asymptomatiques (10-12). Bien que la voie amyloïde joue indéniablement un rôle dans la MA (2), ces résultats soulignent la nécessité de biomarqueurs précoces alternatifs qui capturent d'autres aspects critiques de la progression de la maladie.

Un indicateur précoce prometteur de la MA, aux côtés des déficits de mémoire, est l'altération de l'activité des réseaux cérébraux, qui peut se manifester avant l'apparition des plaques amyloïdes (9). Les techniques avancées de neuroimagerie telles que l'Imagerie par Résonance Magnétique fonctionnelle (IRMf) et l'Électroencéphalographie (EEG) permettent l'étude de la dynamique cérébrale globale, se concentrant sur les réseaux cérébraux entiers plutôt que sur des changements spécifiques à une région. Ces outils ont révélé que la dynamique cérébrale globale suit des patterns invariants d'échelle (13), ralentit pendant le vieillissement (14), et est altérée dans la MA (15-17). Ainsi, les changements dans la dynamique cérébrale globale pourraient servir de biomarqueur précoce de la MA, ouvrant de nouvelles fenêtres pour le diagnostic précoce et les stratégies d'intervention.

L'absence de traitements efficaces reste un autre défi majeur dans la MA. Alors que de nombreux médicaments ciblant la réduction d'Aβ ont été développés sur la base de l'hypothèse amyloïde, beaucoup ont échoué à inverser les symptômes de la MA et ont été abandonnés en raison d'effets secondaires (18, 19). Dans ce contexte, une nouvelle thérapie non invasive basée sur la stimulation gamma à 40 Hz utilisant des

stimuli sensoriels (GENUS (20)) a montré des bénéfices prometteurs pour la mémoire à la fois dans les modèles murins de MA (21, 22) et chez les patients atteints de MA probable légère (23) (pour revue, voir (24)). Divers mécanismes ont été proposés pour expliquer ces effets, notamment la réduction de la neurodégénérescence et l'amélioration de la mémoire par la diminution de la charge en plaques amyloïdes, principalement via l'activation microgliale et les réponses gliales (21, 22), ou l'amélioration de la clairance cérébrale (25).

Cependant, des études récentes ont remis en question ces idées, questionnant la signification de l'entraînement gamma via les stimulations sensorielles. Certaines rapportent une propagation limitée au-delà du cortex visuel et un manque d'engagement dans des régions clés telles que CA1 hippocampique (26), tandis que d'autres débattent si de véritables oscillations gamma sont même entraînées (27). L'impact de ces stimulations sur les charges en plaques amyloïdes reste également controversé (27, 28). Malgré ces débats en cours, les discussions sur le GENUS sont largement restées focalisées sur ses effets liés à l'hypothèse amyloïde.

Nous proposons une hypothèse alternative : le GENUS pourrait restaurer la mémoire en modulant la dynamique des réseaux cérébraux globaux, qui est altérée précocement dans la MA, plutôt que par des effets spécifiques à 40 Hz. Cette nouvelle perspective est soutenue par des preuves récentes démontrant que le GENUS peut affecter la dynamique cérébrale au-delà de la pathologie MA (29, 30), suggérant des impacts plus larges sur la fonction cérébrale.

Pour tester cette hypothèse, nous avons réalisé des enregistrements EEG haute densité (hdEEG) chez un modèle murin de MA préclinique (souris double knock-in AppNL-F/MAPT (31) ; dKI, n=8, les deux sexes) et des congénères contrôles (n=8, les deux sexes) pendant la réalisation de tâches de mémoire. Notre travail précédent (32) a démontré qu'à 4 mois, les souris dKI maintiennent des performances normales dans les tâches simples (par exemple, la Reconnaissance d'Objet Nouveau à court terme ou la Localisation d'Objet) mais présentent des déficits spécifiques et subtils dans les tâches de mémoire associative plus complexes telles que l'association Objet-Place. Dans cette étude, nous avons évalué les performances mnésiques et la dynamique cérébrale pendant les tâches d'association Objet-Place et de Reconnaissance d'Objet Nouveau à long terme avant et après 2 semaines d'exposition quotidienne au GENUS visuel (vGENUS).

Résultats

Les jeunes souris dKI présentent des déficits de mémoire dans les tâches complexes avant l'apparition des plaques amyloïdes

Nous avons d'abord évalué l'étendue de la pathologie amyloïde chez les souris dKI âgées de 4 mois. Pour cet objectif, nous avons réalisé une immunohistochimie 6E10 sur des sections de cerveau de 4 souris WT et 4 souris dKI (Fig. 1A, B ; 2 mâles et 2 femelles par groupe). Sur 262 coupes cérébrales de souris dKI, nous n'avons détecté qu'une seule plaque, contrastant fortement avec les contrôles positifs dKI de 12 mois (1 mâle, 1 femelle) où nous avons observé plus de 10 plaques par coupe. Ces résultats confirment que les souris dKI de 4 mois ne présentent pas encore de dépôt significatif de plaques amyloïdes.

Nous avons ensuite évalué les performances mnésiques des souris dKI à ce stade pré-plaque. La tâche de Reconnaissance d'Objet Nouveau (NOR) avec un délai de 24 heures, un test standard pour évaluer la mémoire de reconnaissance (33), n'a révélé aucun déficit significatif chez les jeunes souris dKI (Fig. 1C, Fig. S1). Cela indique que la mémoire de reconnaissance à long terme reste intacte à ce stade, contrairement aux modèles murins présentant une pathologie amyloïde établie (34). Cependant, lorsque nous avons employé une tâche de mémoire plus complexe testant la mémoire associative à court terme, la tâche Objet en Place (OiP), nous avons détecté des déficits mnésiques précoces subtils mais significatifs chez les souris dKI (Fig. 1D, Fig. S1).

Ces résultats, cohérents avec notre travail précédent (32), démontrent que les souris dKI de 4 mois présentent des déficits de mémoire mesurables dans les tâches complexes avant le développement d'une pathologie significative des plaques amyloïdes. Cela fournit une fenêtre critique pour étudier les altérations précoces des réseaux cérébraux associées à la MA et pour tester des interventions précoces potentielles avant le développement d'une pathologie substantielle.

La dynamique cérébrale globale des souris dKI est altérée avant l'apparition des plaques amyloïdes

Pour étudier si ces déficits de mémoire précoces étaient associés à des altérations de la dynamique cérébrale globale, nous avons d'abord concentré notre analyse sur la tâche OiP, où nous avons observé des déficits cognitifs. Nous avons enregistré l'EEG haute densité pendant la réalisation de la tâche et caractérisé la dynamique cérébrale globale en utilisant une approche non biaisée. Cette méthode traitait les séries temporelles EEG multivariées comme des trajectoires dans un espace de haute dimension des topographies d'activité cérébrale (30 dimensions, correspondant au nombre de canaux hdEEG). En utilisant t-SNE (35), une méthode d'incorporation non linéaire préservant les distances, nous avons visualisé ces configurations comme des points dans un espace bidimensionnel. Pour chaque point, nous avons calculé la fluidité dynamique locale (36), une métrique liée au temps que le système prend pour quitter un voisinage du point visité dans l'espace des configurations dynamiques (Méthodes). Cette quantité, fondée sur des concepts de la théorie statistique des événements extrêmes (37) et précédemment utilisée dans l'analyse des séries temporelles climatiques (36), offre des avantages importants par rapport aux métriques plus classiques (38) de stabilité dynamique car elle peut être correctement estimée à partir d'une quantité considérablement plus faible de données.

Bien que la forme globale du manifold échantillonné soit similaire entre les génotypes, la distribution moyenne de la fluidité dynamique à travers le manifold était significativement plus basse chez les souris dKI (Fig. 2C Haut ; KS = 0,2283 ± 0,0277, $p < 0,001$). Cette réduction était associée à l'exploration par les souris dKI de configurations dynamiques non observées chez les souris WT, correspondant potentiellement à des états avec une fluidité anormalement basse (Fig. 2B, Haut, où les configurations uniques aux souris dKI apparaissent comme des points noirs dans le graphique de dispersion WT).

Ces résultats suggèrent qu'à l'âge de 4 mois, les souris dKI connaissent des événements où la dynamique cérébrale présente transitoirement une fluidité réduite.

Pour déterminer si ces altérations de la dynamique cérébrale étaient spécifiques aux tâches montrant des déficits cognitifs, nous avons également analysé la fluidité dynamique pendant la réalisation de la tâche NOR. Notamment, la fluidité dynamique était également significativement plus basse chez les dKI (Fig. 2C, Bas ; KS = 0,1626

± 0,0279, p = 0,026), malgré l'absence de déficits de mémoire observables dans cette tâche. Nous n'avons trouvé aucune différence significative de fluidité dynamique entre les deux tâches que ce soit pour les souris WT (KS = 0,0558 ± 0,026, p = 1) ou dKI (KS = 0,1296 ± 0,0263, p = 0,1468). Cela suggère que la réduction de la fluidité dynamique est une caractéristique générale des souris dKI, indépendante des demandes spécifiques à la tâche, et pourrait servir d'indicateur sensible précoce des changements cérébraux liés à la MA.

Pour corroborer ces résultats, nous avons effectué des analyses de micro-états EEG (39). Les micro-états représentent un petit nombre de topographies EEG stéréotypées, extraites via un clustering non supervisé. Les enregistrements continus ont ensuite été convertis en séquences d'étiquettes symboliques indiquant le micro-état le plus proche de la topographie actuelle (Fig. 2A, Bas). À partir de ces séquences, nous avons calculé une mesure équivalente à la fluidité en quantifiant la probabilité inverse de rester dans le même micro-état du temps t à t+1 (Méthodes). Cette mesure a été calculée pour plusieurs micro-états (de 3 à 8) puis moyennée pour générer une seule valeur. La fluidité des micro-états était significativement réduite chez les souris dKI dans les tâches OiP et NOR par rapport aux WT (Fig. 2D, ANOVA bidirectionnelle, $F(1,28) = 6,656$, $p = 0,015$) et montrait une forte corrélation avec la fluidité dynamique précédemment calculée (Fig. 2D, $R^2 = 0,4539$, $p < 0,001$).

De plus, nous avons évalué la complexité des séquences de micro-états en utilisant une approche de longueur de description minimale, qui s'est précédemment révélée être affectée dans la MA (17). En cohérence avec les résultats de fluidité des micro-états, la complexité des séquences de micro-états était significativement réduite chez les souris dKI pendant les tâches OiP et NOR par rapport aux souris WT (Fig. 2E, ANOVA bidirectionnelle, $F(1,28) = 7,522$, $p = 0,011$) et corrélait également fortement avec la fluidité dynamique (Fig. 2E $R^2 = 0,4371$, $p < 0,001$). Ces résultats étaient robustes, restant indépendants du nombre moyen de micro-états extraits (Fig. S2), des auto-répétitions des micro-états (Fig. S2), et ont été confirmés en utilisant une méthode alternative d'extraction des micro-états EEG (Fig. S3).

La dynamique cérébrale globale des souris dKI n'est pas altérée pendant le sommeil

Étant donné que la dynamique cérébrale globale était altérée dans les tâches OiP et NOR, mais que les souris dKI ne montraient des déficits de mémoire que dans la tâche OiP, nous avons cherché à comprendre cette divergence. Nous avons émis l'hypothèse que la différence pourrait être attribuée soit à la complexité de la tâche (NOR étant plus simple que OiP) soit à la différence de délai entre les tâches. Le délai de 24h dans la tâche NOR permet le sommeil pendant l'intervalle inter-essai, permettant potentiellement une consolidation de la mémoire hors ligne. Pour déterminer si la dynamique cérébrale est altérée pendant le sommeil, nous avons analysé la fluidité dynamique pendant le sommeil paradoxal (REM) et le sommeil à ondes lentes (SWS) dans les heures suivant l'apprentissage dans la tâche NOR de 24h (Fig. 3A), car ces états sont critiques pour la consolidation de la mémoire (40, 41). De manière intéressante, nous avons constaté que tant le SWS (KS = 0,0876 ± 0,0273, p = 0,3122) que le REM (KS = 0,0653 ± 0,0232, p = 0,617) présentaient une fluidité dynamique similaire entre les souris dKI et WT (Fig. 3B). Cette fluidité dynamique préservée pendant le sommeil, contrairement à la dynamique altérée pendant l'éveil, pourrait expliquer l'impact différentiel sur le comportement observé entre les deux tâches de mémoire. Plus précisément, alors que la tâche OiP repose sur des processus associatifs en ligne qui peuvent être perturbés par des réductions transitoires de la fluidité dynamique, la tâche NOR de 24h peut bénéficier de la consolidation de la mémoire hors ligne pendant le sommeil. La dynamique intacte pendant le sommeil pourrait donc aider à compenser les erreurs introduites par la dynamique altérée pendant l'éveil.

vGENUS entraîne différentiellement les régions corticales à 40Hz et augmente la dynamique cérébrale chez les souris dKI

Étant donné la fluidité dynamique réduite observée chez les souris dKI, nous avons ensuite étudié si vGENUS pouvait potentiellement moduler cette dynamique cérébrale altérée. Nous avons mené 2 semaines de sessions quotidiennes de vGENUS d'une heure et analysé l'hdEEG pendant 10 minutes durant la stimulation à la fois le premier et le dernier (15ème) jour du protocole pour évaluer les effets immédiats et à long terme de l'intervention.

Tout d'abord, nous avons examiné les effets du vGENUS sur l'activité corticale. Les canaux EEG ont été regroupés par région corticale selon la parcellation du cerveau de souris de l'Institut Allen pour faciliter l'interprétation (Fig. 4A). Un pic à 40Hz dans le spectre de puissance a été observé à travers les régions pour les deux génotypes, avec une proportion plus élevée du spectre de puissance dans les régions occipitales (i.e. visuelles) (Fig. 4B, C). Cependant, la puissance relative à 40Hz pendant la stimulation différait entre les génotypes et entre le Jour 1 et le Jour 15 du protocole de stimulation (Fig. 4D, ANOVA répétée à trois voies, $F(1,84) = 4,619$, $p = 0,034$). Plus précisément, la puissance relative à 40Hz pendant la stimulation était plus faible chez les souris dKI au Jour 1 ($t(84) = 3,265$, $p = 0,009$) mais pas significativement différente des niveaux WT au Jour 15 ($t(84) = 1,975$, $p = 0,309$). Ces résultats suggèrent que la réponse corticale à la stimulation visuelle à 40Hz est initialement réduite chez les jeunes souris dKI mais change au cours du protocole vGENUS de 15 jours.

Étant donné le débat en cours sur la signification de la stimulation à 40Hz, nous avons ensuite évalué si vGENUS impactait la dynamique cérébrale globale au-delà de ses effets sur la puissance à 40Hz. Pour cela, nous avons calculé la fluidité dynamique pendant les périodes de stimulation aux Jours 1 et 15. Au Jour 1, les souris dKI présentaient une fluidité dynamique significativement plus faible par rapport aux souris WT (Fig. 4E, $KS = 0,2548 \pm 0,0284$, $p < 0,001$). Cependant, après 15 jours de stimulation, la fluidité dynamique chez les souris dKI a augmenté ($KS = 0,1587 \pm 0,0275$, $p = 0,03$), atteignant des niveaux comparables aux souris WT ($KS = 0,1459 \pm 0,0266$, $p = 0,066$).

Ces résultats suggèrent que bien que vGENUS ait un effet différentiel immédiat sur la puissance à 40Hz chez les souris dKI, son impact sur la dynamique cérébrale globale ne devient évident qu'après une stimulation prolongée. Cela souligne l'importance de la stimulation chronique dans la promotion des effets de vGENUS sur la fonction cérébrale globale et suggère que les mécanismes sous-jacents à ces effets pourraient impliquer des processus au-delà du simple entraînement des oscillations corticales.

L'augmentation de la dynamique cérébrale chez les souris dKI persiste après la fin de la stimulation et restaure les performances mnésiques.

Puisque les déficits de mémoire chez les jeunes souris dKI étaient probablement liés à une dynamique cérébrale altérée, nous avons examiné si la restauration de la

dynamique cérébrale médiée par vGENUS améliorerait également les performances mnésiques. À la fin des 2 semaines de vGENUS, les tâches NOR et OiP ont été effectuées dans le même ordre qu'avant vGENUS (Fig. 5A). vGENUS n'a pas affecté les performances dans la tâche NOR, car les souris dKI ne montraient pas de déficits de mémoire avant et après vGENUS (Fig. 5B, Gauche, Fig. S4). Cependant, il n'y avait plus de différence significative de fluidité dynamique entre les génotypes (Fig. 5B, Droite, KS = 0,0798 ± 0,0235, p = 0,6405) en raison d'une augmentation significative de la fluidité dynamique chez les souris dKI après vGENUS (KS = 0,2137 ± 0,0293, p = 0,0042).

Ainsi, l'augmentation de la dynamique cérébrale induite par vGENUS semble persister même après les sessions de stimulation, suggérant un changement stable vers une dynamique cérébrale plus physiologique qui pourrait bénéficier aux performances cognitives. En effet, après deux semaines de vGENUS, les souris dKI ne montraient plus de déficits dans la tâche OiP (Fig. 5C, Gauche, Fig. S4). De façon similaire à la tâche NOR, la fluidité de la dynamique cérébrale pendant la tâche OiP ne montrait pas de différence significative entre les génotypes après vGENUS (Fig. 5C, Droite, KS = 0,1298 ± 0,0270, p = 0,0999) en raison d'une augmentation spécifique chez les souris dKI (KS = 0,237 ± 0,0283, p < 0,001).

L'analyse des micro-états discrétisés a confirmé ces résultats, ne montrant aucune différence significative entre les génotypes tant dans la fluidité des micro-états (Fig. 5E, Fig. S5) que dans la complexité des séquences de micro-états (Fig. 5F, Fig. S5) après deux semaines de vGENUS.

Nos résultats démontrent que vGENUS restaure les performances mnésiques dans la tâche OiP en augmentant significativement la fluidité dynamique, même après la fin de la stimulation, spécifiquement chez les souris dKI. En effet, vGENUS semble cibler spécifiquement les états de faible fluidité dynamique précédemment identifiés chez les souris dKI. Cet effet peut être visualisé dans la Fig. 5D, où les configurations présentes chez les souris dKI avant vGENUS mais absentes après le traitement sont montrées en points rouges. En éliminant ces états de faible fluidité, vGENUS "dégèle" efficacement la dynamique cérébrale, la ramenant à un état plus fluide similaire à celui observé chez les souris WT. Il est important de noter que ces effets de vGENUS sur la fluidité de la dynamique cérébrale semblent être spécifiques aux états pathologiques. La dynamique du sommeil, qui n'était pas affectée chez les souris dKI avant le traitement, n'a montré aucune différence de fluidité après vGENUS (Fig. S6),

suggérant que vGENUS cible sélectivement les états cérébraux anormaux d'éveil sans perturber la dynamique normale du sommeil.

Discussion

En utilisant des enregistrements EEG haute densité pendant la réalisation de tâches de mémoire spécifiques dans un modèle murin de MA préclinique et en évaluant la dynamique cérébrale globale à travers de nouvelles métriques initialement employées dans des domaines extérieurs aux neurosciences (36), nous avons démontré que les souris dKI présentent des altérations précoces et spécifiques à l'état d'éveil dans la dynamique cérébrale, associées à des déficits cognitifs dans des tâches de mémoire complexes. Crucialement, ces altérations surviennent avant l'apparition des plaques amyloïdes, remettant en question la vision traditionnelle de la pathologie MA précoce centrée sur l'amyloïde. De plus, nous avons montré que deux semaines de vGENUS augmentaient la dynamique cérébrale entre le premier et le dernier jour du protocole. Cette augmentation de la fluidité de la dynamique cérébrale persistait après la fin des stimulations, pendant la réalisation des tâches de mémoire où les déficits précédemment observés étaient corrigés.

Nos résultats suggèrent que les altérations de la dynamique cérébrale à l'état d'éveil pourraient être une caractéristique précoce de la MA, survenant avant la formation des plaques amyloïdes. La similitude entre les enregistrements hdEEG dans cette étude et ceux typiquement réalisés chez l'humain suggère que la fluidité de la dynamique cérébrale pourrait émerger comme un marqueur diagnostique prometteur. Ceci est soutenu par des découvertes précédentes montrant que la complexité des séquences de micro-états est réduite chez les patients atteints de MA et peut aider à prédire la progression du Trouble Cognitif Léger (MCI) vers la MA (17). De plus, le ralentissement et l'augmentation de la frustration de blocage dans la connectivité fonctionnelle dynamique en IRMf au repos avaient déjà été rapportés dans la Maladie d'Alzheimer (15) ou les modèles de déficits mnésiques précoces par challenge cognitif (42). Étant donné la nature non invasive et l'accessibilité de l'EEG, l'évaluation de la fluidité de la dynamique cérébrale pourrait permettre une détection plus précoce de la MA, potentiellement pendant les stades MCI et de Déclin Cognitif Subjectif (SCD), où les patients rapportent des problèmes cognitifs mais ne montrent pas de déficits dans les

tests neuropsychologiques standards. Un outil diagnostique facilement implémentable pour la MA à un stade précoce pourrait améliorer significativement le moment et l'efficacité des interventions thérapeutiques. La traduction clinique potentielle de cette approche mérite des investigations supplémentaires, incluant des études longitudinales dans des populations humaines pour valider le pouvoir prédictif de la fluidité de la dynamique cérébrale dans la progression de la MA.

Conformément aux études précédentes (21, 22), nous avons constaté que 2 semaines de vGENUS corrigeaient les déficits de mémoire liés à la MA chez les souris dKI. Cependant, comme l'ont souligné des études récentes (27, 28), puisque les souris dKI de 4 mois ne présentent pas de plaques amyloïdes, il est improbable que vGENUS cible directement la pathologie amyloïde, ou du moins pas exclusivement ni principalement. Au lieu de cela, nos données suggèrent que vGENUS restaure une fluidité de la dynamique cérébrale saine, un effet qui persiste même après la fin de la stimulation. Cette découverte indique un impact plus large de vGENUS sur la dynamique cérébrale au-delà de l'entraînement à 40Hz, qui a été débattu dans la littérature récente (26, 27). Notamment, la restauration de la dynamique cérébrale globale n'était pas immédiate mais nécessitait un protocole chronique de 2 semaines, indiquant que des processus à long terme plutôt qu'un entraînement cérébral immédiat conduisent probablement ces changements.

Une explication potentielle des effets observés pourrait être la réorganisation métabolique des réseaux cérébraux. En effet, il a été démontré que vGENUS entraîne des réactions vasculaires dans le cerveau, notamment en augmentant le diamètre des vaisseaux sanguins (22, 25) et a déjà démontré des effets bénéfiques dans des modèles murins d'accident vasculaire cérébral (43). Étant donné que l'hypoperfusion cérébrale a été liée au développement de la MA (44) et que les dysfonctionnements cérébrovasculaires sont associés à des déficits cognitifs (45), l'augmentation du flux sanguin cérébral induite par vGENUS pourrait améliorer le métabolisme cérébral et, par conséquent, la dynamique cérébrale.

Une autre possibilité est que vGENUS module des systèmes neuromodulateurs spécifiques, particulièrement étant donné que la réduction de la fluidité de la dynamique cérébrale observée chez les souris dKI est spécifique à l'état d'éveil. vGENUS n'a montré aucun effet sur la dynamique cérébrale pendant le sommeil, suggérant que le mécanisme pourrait impliquer des neuromodulateurs spécifiques à l'éveil tels que le système noradrénergique, qui est à la fois une cible précoce dans la

pathologie MA (46) et connu pour affecter la dynamique cérébrale à grande échelle (47). Des recherches futures seront nécessaires pour clarifier les mécanismes précis par lesquels vGENUS exerce ses effets. Cependant, nos résultats, ainsi que les découvertes précédentes, convergent pour suggérer que les effets bénéfiques de vGENUS sur la dynamique cérébrale globale ne sont pas spécifiques à la MA, car il a également montré des bénéfices chez les patients épileptiques (30). Cela suggère que vGENUS pourrait représenter une option de traitement non invasif prometteuse pour une variété de troubles neurologiques en ciblant et en modulant la dynamique cérébrale à grande échelle. Plus précisément, il pourrait déclencher des mécanismes endogènes pour compenser les dysfonctionnements précoces des circuits via une "reprogrammation" du point de fonctionnement de l'opération dynamique des réseaux cérébraux (48, 49).

Bien que notre étude fournisse de nouvelles perspectives sur la physiopathologie précoce de la MA et les interventions potentielles, il est important de garder à l'esprit que l'utilisation d'un modèle murin, tout en permettant un contrôle et une manipulation précis, pourrait ne pas récapituler complètement la pathologie MA humaine. De plus, les effets à long terme de vGENUS au-delà de la période de deux semaines étudiée ici restent à explorer.

En conclusion, notre étude révèle l'altération de la dynamique cérébrale comme un marqueur précoce des changements liés à la MA, détectable avant la formation significative de plaques amyloïdes et corrélant avec des déficits cognitifs subtils. Nous démontrons que vGENUS peut restaurer cette dynamique altérée et améliorer les déficits de mémoire associés. Ces résultats ne fournissent pas seulement de nouvelles perspectives sur la physiopathologie précoce de la MA, mais suggèrent également de nouvelles approches pour le diagnostic précoce et l'intervention dans la MA et potentiellement d'autres troubles neurologiques caractérisés par une dynamique cérébrale perturbée.

Conclusion générale

Dans cette thèse, nous démontrons que le modèle murin dKI AppNL-F/MAPT de la pathologie précoce de la MA présente des déficits précoces de la mémoire dans une tâche subtile de mémoire associative, parallèlement à des altérations de la dynamique cérébrale globale. Ces altérations révèlent que la dynamique cérébrale est plus lente ou moins fluide chez les souris dKI, avec l'émergence d'états pathologiques de faible fluidité avant l'apparition des marqueurs biologiques classiques de la maladie. Nous avons identifié ces changements en utilisant des enregistrements EEG du scalp - une technique non invasive et cliniquement accessible - soulignant le potentiel de la fluidité de la dynamique cérébrale basée sur l'EEG comme outil diagnostique prometteur pour détecter la MA aux stades précliniques. Cela serait particulièrement précieux pour les cas de SCD, où les options diagnostiques actuelles, telles que les scans PET ou les mesures d'Aβ dans le LCR, sont limitées en raison de leur caractère invasif.

Dans notre étude, deux semaines de stimulation lumineuse quotidienne d'une heure à 40 Hz (vGENUS) ont réussi à restaurer la fonction mnésique chez les souris dKI et à normaliser la dynamique cérébrale à un état sain. Notamment, ces bénéfices sont survenus avant l'apparition des biomarqueurs traditionnels de la MA et sans corriger les oscillations gamma corticales altérées, soulignant les effets neuroprotecteurs étendus de cette intervention non invasive pendant les stades précoces de la maladie - même avant un développement pathologique significatif. En raison du caractère non invasif et de la facilité de mise en œuvre de ce protocole, il pourrait être adopté de manière réalisable dans les contextes cliniques, fournissant une intervention sûre et sans effets secondaires pour les individus présentant des signes précoces de déclin cognitif, ralentissant potentiellement la progression de la maladie.

Ensemble, nos résultats proposent une double approche pour la MA : une méthode non invasive de détection précoce couplée à une stratégie d'intervention non invasive qui est efficace même aux stades précoces de la maladie. Cela pourrait contribuer à réduire la prévalence future de la démence liée à la MA, atténuer les augmentations prévues des cas de MA, et finalement améliorer la qualité de vie des individus touchés et de leurs familles.

Université de Strasbourg

École doctorale
Sciences de la vie
et de la santé | ED 414
Université de Strasbourg

Matthieu AGUILERA

The Light at the End of the Tunnel: Study of Early-Stage Brain Dynamics Alterations in Alzheimer's Disease and Beneficial Effects of Light Stimulation in the App^{NL-F}/MAPT Mouse Model.

Résumé

La maladie d'Alzheimer (MA), première cause de démence dans le monde, reste un défi majeur en raison de son diagnostic tardif et de l'absence de traitements efficaces. Alors que le diagnostic actuel repose sur la détection à travers des méthodes invasives de marqueurs pathologiques classiques tels que les plaques amyloïdes après l'apparition des symptômes cognitifs, de nombreuses études suggèrent que les changements pathologiques débutent des décennies avant ces manifestations cliniques. Le bon fonctionnement cérébral dépend d'une activité dynamique complexe, permettant des transitions flexibles entre différents réseaux fonctionnels. Ces dynamiques cérébrales, observables par EEG ou IRM fonctionnel, sont altérées dans plusieurs troubles neurologiques, dont la MA. Compte tenu de l'importance de la dynamique cérébrale pour les fonctions cognitives, une approche thérapeutique récente, appelée GENUS, utilise des stimulations sensorielles à 40 Hz pour moduler les oscillations neuronales. Cette approche a des effets prometteurs dans la MA malgré des mécanismes encore mal connus. En utilisant des enregistrements EEG haute densité dans un modèle préclinique de la MA, nous avons démontré des altérations de la dynamique cérébrale avant la formation des plaques amyloïdes, avec une fluidité réduite durant l'éveil associée à des déficits cognitifs subtils. Deux semaines de GENUS ont permis de restaurer à la fois les performances mnésiques et la dynamique cérébrale avant la formation des plaques amyloïdes, suggérant des bénéfices au-delà des effets du GENUS précédemment rapportés sur la pathologie amyloïde. Ce travail de thèse propose ainsi un outil de diagnostic précoce prometteur basé sur des mesures EEG non invasives, et démontre l'efficacité d'une intervention thérapeutique simple, facilement applicable en clinique, offrant de nouvelles perspectives pour la détection et le traitement précoces de la MA.

Mots-clés : Maladie d'Alzheimer, EEG, Dynamique cérébrale, stimulations gamma, GENUS

Summary

Alzheimer's disease (AD), the leading cause of dementia worldwide, remains a major healthcare challenge due to late diagnosis and lack of effective treatments. While current diagnosis relies on invasive detection of classic amyloid and tau pathological hallmarks after cognitive symptoms appear, mounting evidence suggests that pathological changes begin decades before these clinical manifestations. Proper brain function depends on complex dynamic activity, allowing flexible transitions between different functional networks. These brain dynamics, assessable through EEG or functional MRI, are altered in various neurological conditions, including AD. Given their importance in cognitive function, a recent therapeutic approach called GENUS uses 40Hz sensory stimulation to modulate neural oscillations, showing promising effects in AD despite debated mechanisms. Using high-density EEG recordings in a preclinical AD mouse model, we demonstrated altered brain dynamics before amyloid plaque formation, showing reduced fluidity during wakefulness concurrent with subtle cognitive deficits. Two weeks of visual GENUS restored both memory performance and brain dynamics before amyloid plaque formation, suggesting benefits beyond previously reported effects on amyloid pathology. This thesis work presents both a promising early diagnostic tool based on non-invasive EEG measurements and demonstrates the efficacy of a simple therapeutic intervention readily implementable in clinical settings, offering new perspectives for early AD detection and treatment.

Keywords: Alzheimer's disease, EEG, Brain dynamics, Gamma stimulations, GENUS